Thesis for the degree of Doctor of Philosophy

Synthesis and Applications of Novel Azolium Salts

Andrea Dallas B.Sc.

Dublin City University

School of Chemical Sciences

September 2003

Supervisor: Dr. Kieran Nolan

Declaration

I hereby certify that this material, which I now submit for assessment on the programme of study leading to the award of Doctor of Philosophy is entirely my own work and has not been taken from the work of others save and to the extent that such work has been cited and acknowledged within the text of my work.

Signed: A. Dallas ID No.: 97971184

Andrea Dallas

Date: 16/9/03

Abbrevations

ATP	Adenosine triphosphate
BuLi	*n*-Butyl lithium
Bu	Butyl
Bzim	Benzimidazole/benzimidazolium
n-Bu	*normal*-Butyl
cat.	Catalyst
Cp	Cyclopentadiene
CV	Cyclic voltammetry
DAB	1,4-Diazobutadiene
DCM	Dichloromethane
dba	Dibenzylideneacetone
DME	Dimethoxyethane
DMF	*N*,*N*-Dimethylformamide
DMSO	Dimethyl sulfoxide
DNA	Deoxyribonucleic acid
dpim	1-Methylimidazol-2-yldiphenylphosphine
dppf	Bis(diphenylphosphino)ferrocene
ee	Enantiomeric excess
Et	Ethyl
Fc	Ferrocene
fc	1,1′-Disubstituted ferrocene
Fc-DAB	*N*,*N*′-Diferrocenyl-1,4-diaza-1,3-butadiene
HCN	*N*-Heterocyclic carbene
Im	Imidazole/imidazolium

IR	Infrared
Me	Methyl
MeCN	Acetonitrile
MeOH	Methanol
m.p.	Melting point
NMR	Nuclear magnetic resonance
PBP	Phosphate binding protein
PET	Photoinduced electron transfer
PPFA	*R*,S_p-*N*,*N*-Dimethyl-1-[(2-diphenylphosphino)ferrocene]ethylamine
Ph	Phenyl
Pr	Propyl
RT	Room temperature
SCE	Saturated calomel electrode
THF	Tetrahydrofuran
t.l.c.	Thin layer chromatography
TMEDA	*N*,*N*,*N'*,*N'*-Tetramethyl-1,2-ethanediamine
VOC	Volatile organic compounds

Publications

The following paper was published as part of the work contained within this thesis:

[1] J. Howarth, A. Dallas, *Molecules*, 5 (2000) 851.

The following presentations were presented as part of the work contained within this thesis:

[1] A. Dallas, J. Howarth, 'Synthesis of Novel Ferrocenyl–azole Compounds', 13th International Conference on Organic Synthesis (ICOS-13), Warsaw, Poland, 1–5 July, 2000. Poster.

[2] A. Dallas, J. Howarth, '(1-Methylferrocenyl)imidazolium Iodide Salts: Synthesis and Characterisation', 51th Irish Chemistry Colloquium, Cork, Republic of Ireland, 14–15 May, 2001. Presentation.

Abstract

The application of azole and azolium compounds is of widespread interest both industrially and academically. There are many lively and diverse research areas employing these compounds, including organometallic processes, molecular recognition and biological research. Thus, the objective of this research was the preparation novel azolium salts and their application in some of these areas. Ferrocenyl–imidazole and ferrocenyl–benzimidazole compounds and their respective salts were prepared and their catalytic, chemoreceptor and biological properties studied.

Monosubstituted ferrocenyl–azolium salts (1-ferrocenylmethy-3-alkylazolium halides), acyclic bisazolium–ferrocenyl salts {1-[(1-ferrocenylmethyl-3-butyl)azolium]-3-ferrocenylmethylazolium diiodides and 1,1′-bis(1-methyl-3-methylbenzimidazolium) ferrocenyl iodides} were synthesised. In addition, a very interesting macrocyclic benzimidazolium–ferrocenyl cyclophane was prepared – bis{1-[(1,1′-ferrocenylmethyl-3-butyl)benzimidazolium]-3-ferrocenylmethyl}benzimidazolium tetraiodide.

The action of these ferrocenyl–azolium salts as highly effective auxiliary ligands in transition metal-mediated catalysis was shown through catalytic studies using the Heck reaction. Furthermore, different catalytic efficiencies of benzimidazolium vs. imidazolium salts in the Heck reaction depending on the system was demonstrated in a comparitive study. In addition, 1-butyl-3-methylimidazollium hexafluorophosphate was successfully employed as a recyclable, highly efficient solvent in the Heck reaction compared to DMF.

Potential biological applications of these compounds include molecular recognition and antimicrobial studies. Coupling the redox active ferrocenyl unit with the cationic azolium nucleus allowed them to be realised as ionophores. Acyclic ferrocenyl–azolium salts demonstrated evidence of anion co-ordination in ^{1}H NMR anion titration experiments. Also screening of a range of ferrocenyl–azole/azolium compounds against *P. aeruginosa* and *C. albicans* showed that azolium compounds with two ferrocene units in their structure had highly effective antifungal properties.

Furthermore, a second co-ordination functionality was introduced into the ferrocenyl–azolium system. Thus, the preparation of a 1,1′-disubstituted ferrocenyl salt system with an imidazolium nucleus on one Cp ring and a diphenyl(sulphido)phosphine entity on the second Cp ring and a series of 1-ferrocenylmethylazole–diphenylphosphine functionalised compounds was carried out. Thus, developing a range of compounds that show great potential as ligands.

Acknowledgements

Firstly, I would like to thank my supervisor Dr. Kieran Nolan for his very valuable help and encouragement with this project. Without him I definitely would not have got this far. I would also like to thank my initial supervisor Dr. Joshua Howarth for commencement of this research and Dr. Petr Štěpnicka for his help and allowing me work in his laboratory in Prague. The academic staff and technical staff of DCU must also be thanked with special thanks to Dr. John Gallagher for his X-ray crystallography, Dr Dermot Brougham for his molecular modelling experiments, Dr Alan Farrell and Dr Brid Quilty for conducting the antimicrobial screening, Mick Burke for his technical support and Dr. Paraic James.

Thanks also to the many people I have worked with over the years from my first lab with the A115 lads – Keith, Cathal, Jay, Davey, Donal, John-Luc, Kev and Podraig; the latest lab with Darragh, Dave, Steve, Paula, Ger, Mariead, Ben, Moss, Robbie, Ray, Neil, Ji-Feng, Noel, Frankie and Colom (past and present); the lab in Prague with Tomaš and Libor and finally to my group (in yet another lab) – Rachel, Ian, Yang, Steve, Shane, Pauline and Carol. Special thanks go to Kathleen, Mary Ann, Dec, Paddy, Darren, Kieran and to Paul especially for keeping me sane with pints, various holidays, laughs and listening to me moan over the years!

Finally, a million thanks to my parents and family for their love and support: mum and dad (Tom and Sue), Helen, Sonja, Graeme, grandma and grandad (Rose and Tom) and finally my aunt and uncle Chris and Bill.

Table of Contents

Chapter 1

Azole Derivatives and Their Applications in Catalysis and Anion Recognition

1.1 Azoles – an introduction

The azole system arguably represents one of the most ubiquitous classes of heterocyclic species. Their many wide-ranging applications vary from medicinal use as pharmaceuticals to actually being some of the building blocks necessary for life. They are also used in numerous more technical applications, such as electrolytes, components in supramolecular structures and in polymers [1].

The azoles can be defined as five-membered heterocycles with more than one heteroatom that are formally derived from pyrrole (**1**), furan (**2**) and thiophene (**3**), where a CH unit is replaced with an sp^2 hydribised nitrogen atom. Of the nitrogen containing azoles, the preferred nomenclature gives them names ending in -azole. There are two classes of diazoles – pyrazole (**4**) and imidazole (**5**); two classes of triazoles – 1,2,3-triazole (**6**) and 1,2,4-triazole (**7**) and one tetrazole (**8**).

The azoles also have benzo-analogues, where a benzene ring is fused to the azole ring, sharing a double bond. The parent compound for the nitrogen-based benzoazoles is indole (**9**), from which indazole (**10**), benzimidazole (**11**) and benzotriazole (**12**) are derived. The parent compounds and resulting nitrogen azoles are shown in Figure 1.1.

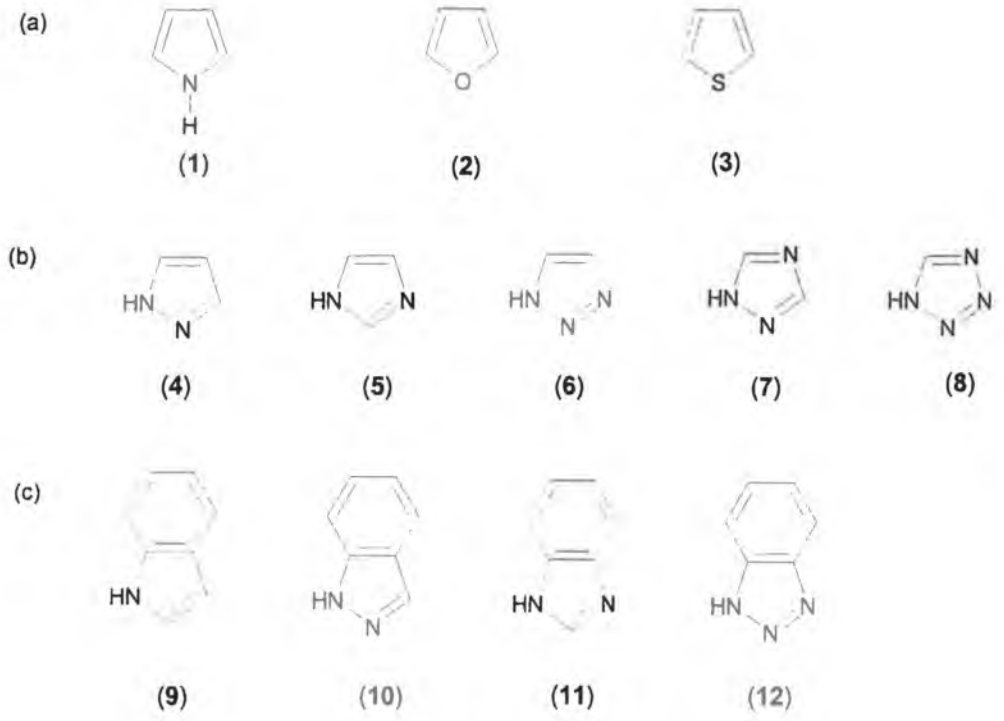

Figure 1.1. *(a)The five-membered parent compounds of the azoles, (b) the five-membered nitrogen-based azoles and (c) their benzo-analogues.*

The azoles have a wide variety of applications with the emphasis being on their roles in agriculture and medicine, as they have been shown to have a wide-range of biologically active properties, including being bacteriostats, bacteriocides, insecticides, fungicides, sedatives, anticarcinogens and psychopharmacological agents.

Here is a brief illustration of the great diversity of properties and applications that the azoles have been used for: Pyrroles have traditionally been employed for drug, dye and anaesthetic uses, with growing interest in applying reduced pyrroles (pyrazolines) as chemical bleaching agents and luminescent and fluorescent substances. The imidazole moiety has been found in a number of naturally occurring compounds, such as histamine (**13**) [the decarboxylation product of the essential amino acid histidine

(**14**)], allantoin (**15**) [the end product of the nitrogen metabolism in some animals] and pilocarpine (**16**) [an imidazole alkaloid] (see Figure 1.2). The triazoles have been employed as light-stabilisers, optical brightening agents, herbicides, adhesives and as precursors of other biologically active agents, such as azapurines, while the tetrazoles have also found applications as antibacterial agents.

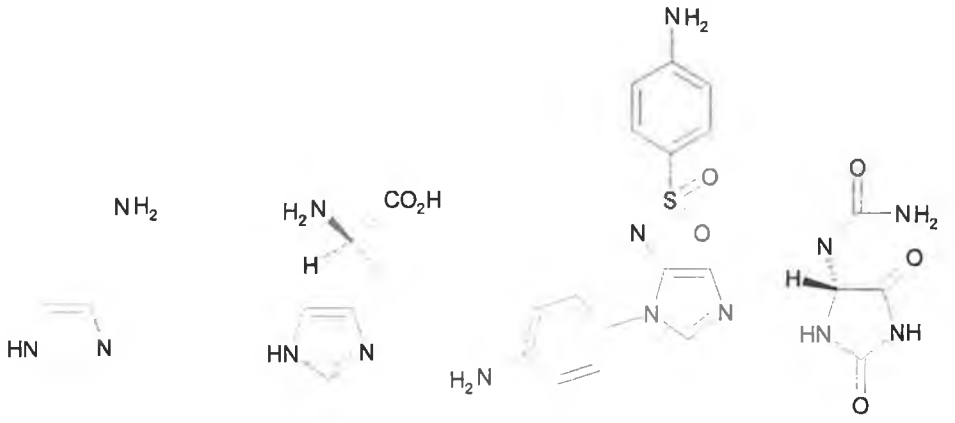

Figure 1.2. *Some naturally occurring compounds where the imidazole nucleus has been found.*

Imidazole is a 1,3-diazole, and can be essentially thought of as being a pyrrole structure with a pyridine-like nitrogen replacing a CH group at the 3-position (Figure 1.3a). The 'pyrrole' nitrogen has two π-electrons delocalised in the aromatic sextet, while the 'pyridine' nitrogen is holding its lone pair of electrons in an sp^2 orbital outside the ring. This addition of a pyridine nitrogen drastically affects the properties of the pyrrole-derived compound. Imidazole has an aromatic character, as evidenced by its ^1H NMR spectrum. The protons are not all equivalent as in benzene, but resonate in the aromatic region of the spectrum, showing that a ring current must be present. However, it also has some interesting different characteristics from its two parent compounds, such as increased hydrogen bonding and amphoteric properties.

The parent compound of benzimidazole is indole, where again the 3-CH has been replaced with a nitrogen. It is a ten π-electron aromatic system that holds a lone pair of electrons outside the ring on the nitrogen and shows aromaticity with a ring current, as illustrated by its ^{1}H NMR resonances. Figure 1.3 shows the electron density and resulting ^{1}H NMR shifts in both compounds.

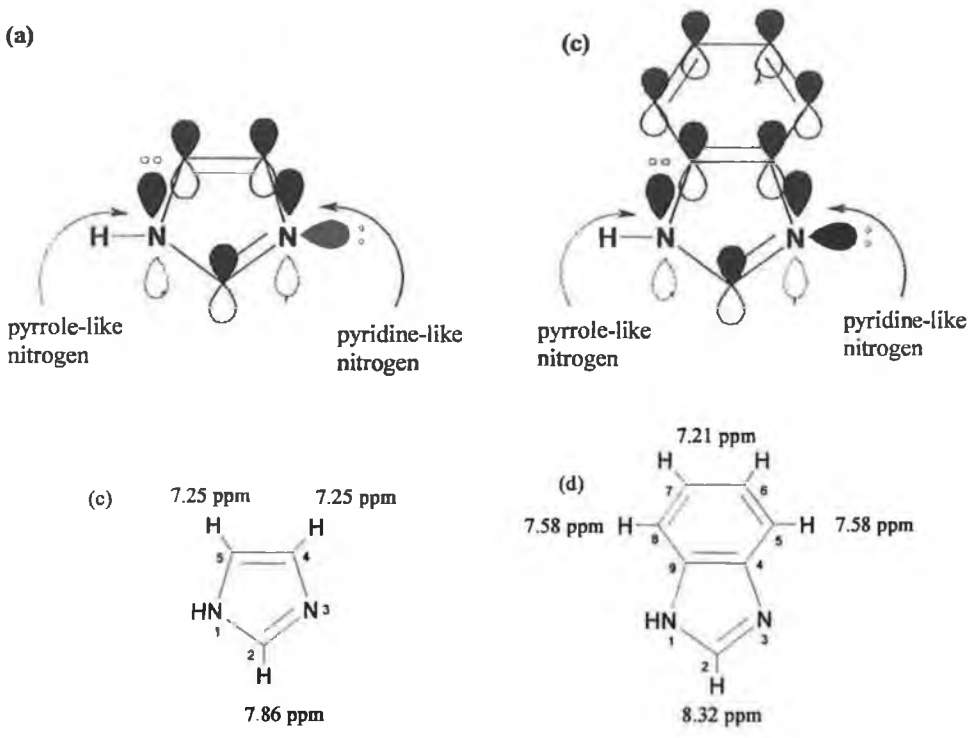

Figure 1.3. *The distribution of electron density in the unsubstituted (a) imidazole and (b) benzimidazole rings. ^{1}H NMR chemical shifts for (c) imidazole ($CDCl_3$) and (d) benzimidazole (DMSO–d_6), demonstrating aromaticity.*

1.2 Applications of azoles

1.2.1 Biological applications

Imidazole and benzimidazole show hydrogen-bonding properties not seen in other azoles, display amphoteric properties and in general have varied chemical properties, hence leading to their many different applications. As it is such a large of class of

compounds, this review will focus on the imidazole/imidazolium systems together with their benzo-analogues.

The imidazole/imidazolium systems have been of interest as potential therapeutic agents due to their biological activities. Imidazole, in particular, is found a great deal in nature. Its amphoteric, nucleophilic, electrophilic and solubility properties means that it can perform a variety of different functions in various biological pathways, hence it is used in enzyme reactions and other various biological processes. An example of this is histidine, which is found at the active sites of ribonuclease and several other enzymes. At physiological pH (~7.4), it is present in both its protonated and deprotonated forms, and as such in some enzymes its function is for proton transfer catalysis. For benzimidazole, indole is within the skeleton of the amino acid tryptophan and the indole alkaloids (biologically active compounds from plants, such as strychnine and LSD). Therefore, imidazoles and benzimidazoles have been the starting point for many therapeutic and biologically active compounds.

1.2.2 The use of azoles in transition metal catalysis

One particular area where the application of azoles – in particular imidazoles – has been expanding is that of transition metal catalysis. Transition metal-catalysed cross-coupling processes have become some of the most important tools in organic synthesis. Carbon–carbon bond formation is arguably one of the most important synthetic procedures in organic chemistry, as it is often one of the key steps in the building of complex carbon skeletons. While in the past 50–100 years, chemists had an array of techniques for the building of C–C bonds between saturated sp^3 carbons, direct methods for the coupling together of unsaturated sp^2 or sp carbons were very

rare. However, in the 1970s transition metal-mediated cross-coupling reactions were discovered, and since then a wide variety of methodologies have been developed to the point where these transition metal catalysed cross-coupling is one of the most essential techniques in modern synthesis.

There is one generalised pathway for transition metal-mediated catalytic cycles – that of oxidative addition/reductive elimination, which is obviously subject to minor variations depending on the reaction. All cross-coupling reactions have a metal nucleus that is able to vary its oxidation state, co-ordination numbers, reaction partners (an electrophile and a nucleophile) and ligands co-ordinated to the metal centre. The catalysts work by co-ordination of the reaction partners with the metal centre, and thus can accelerate the reaction in one or more of the following ways: bringing the reaction partners into close proximity, activating a reaction partner and/or facilitating nucleophilic attack. The simplified catalytic cycle of a transition metal-mediated reaction is outlined in Scheme 1.1.

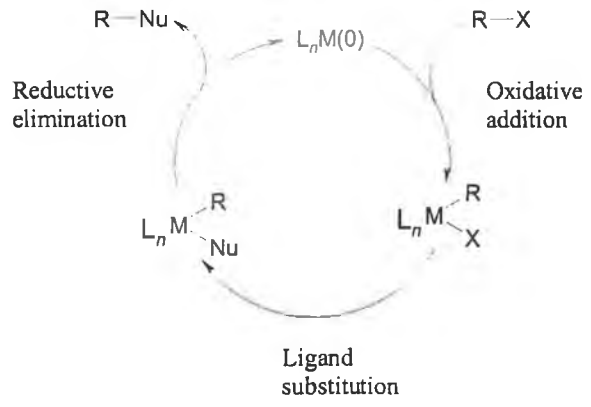

Reaction	E^+
Kumada	RMgX
Negishi	RZnX
Negishi	RZr
Suzkui-Miyaura	RBX_2
Stille	$RSnR_3$
Buchwald-Hartwig	R_2NH
Buchwald-Hartwig	ROH
Buchwald-Hartwig	RSH
Heck	RC=CR

Scheme 1.1. *Generalised catalytic cycle for transition metal-mediated reactions.*

Here the metal centre enters the cycle in an oxidation state of 0 [stabilised by ligand(s)], whereupon oxidative addition of the electrophile into the complex causes the oxidation state to increase to +2. The electrophile is nearly always an organohalide or triflate. Aryl, vinyl, allyl and benzyl groups can all be used as substrates. The ligand substitution/transmetallation/migration steps are unique to each reaction but generally the nucleophile will enter the cycle with some change in the geometry of the intermediate complex and replacement of the halide/triflate. On reductive elimination, the two organo species are coupled together (therefore they must be *cis* in the intermediate complex) allowing the release of the product and regeneration of the catalyst in the 0 oxidation state.

The metal centre must be able to exist in a variety of oxidative states, especially a co-ordinatively unsaturated state. The late transition metals (d^8, d^{10}) show a greater ability to do this. Therefore, Ru, Co, Ni, Pd and Pt are the most important metal centres used in cross-coupling catalysis, with palladium and nickel being the most commonly used.

However, it is the ligand that aids the metal in its co-ordination properties and, thus, really determines the catalytic efficiency of the complex. Through ligand variation, a high specificity of the metal centre towards the incoming reaction partners can be tailored. Furthermore, the ligand should be able to stabilise the different co-ordination states and activate the zerovalent metal centre towards the oxidative addition of the electrophile. Therefore, control of product selectivity can be achieved by careful selection of the ligand.

Traditionally triarylphosphines have been used as ligands. These ligands are both electron rich and sterically demanding. It has been shown that the electron-donating ability of the phosphines, together with their bulk increases their catalytic efficiency [2,3]. The combination of these electronic and steric effects has made the phosphines the most popular choice for organometallic catalysis. They are able to stabilise the zerovalent metal centres, while allowing competing ligands to co-ordinate to the metal [4].

However, the alkylphosphines have certain drawbacks: they can be expensive and time-consuming to prepare, they require air and moisture free environments to prevent ligand oxidation and, most importantly, they suffer from P–C bond degradation at elevated temperatures, leading to deactivation of the catalyst. Thus, work is ongoing in the design of cheaper, air-stable ligands, of which carbene ligands are proving to be the most promising.

1.2.2.1 Azoles as N-Heterocyclic carbene ligands in co-ordination compounds

Carbenes are defined as neutral organic species where the carbon atom has only six electrons in its valence shell and has a valence of two. In organic chemistry, carbenes are highly reactive electrophilic transient intermediates that are very rarely isolated due to their electron deficiency. However, it was realised in the early 1960s by Wanzlick [5–11] that if electron-donating substituents were placed adjacent to the carbene centre then the species maybe stabilised. This led to the development of azolylidene units as carbene ligands in co-ordination chemistry. For example, complexes (**17**) and (**18**) were reported, which were obtained from imidazolium salts

and metal compounds containing ligands of sufficient basicity to deprotonate the imidazolium 2-CH and produce the carbene *in situ* (Scheme 1.2).

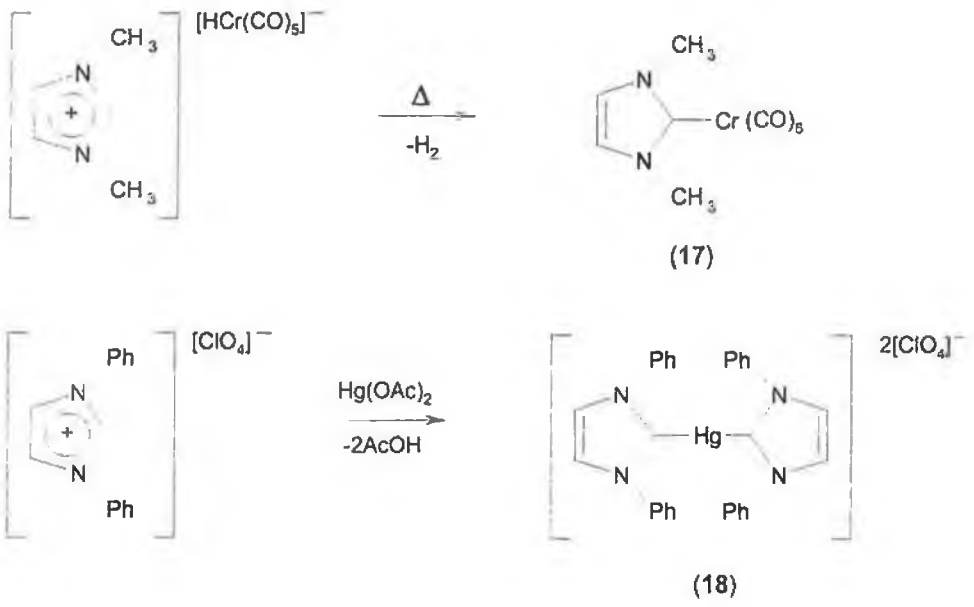

Scheme 1.2. *Examples of the first N-heterocyclic ligands prepared by Wanzlick.*

It was not until the early 1990s, though, that the first free *N*-heterocyclic carbenes using imidazolium precursors were characterised. Ardunego et al. [12] in 1991 successfully prepared and isolated 1,3-di-1-adamantylimidazolylidene (19) (Scheme 1.3). Its characterisation led to a renaissance in the preparation of *N*-heterocyclic carbenes with the imidazolium salt systems being the foremost investigated.

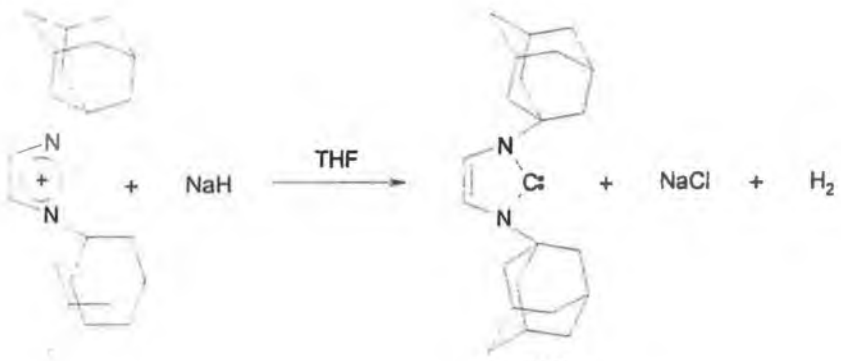

(19)

Scheme 1.3. *The first isolated imidazolylidene carbene prepared by Ardunego et al.*

In these nucleophilic carbene systems, the two non-bonded electrons may either be paired (singlet state) or unpaired (triplet state). The singlet carbenes have a filled and a vacant orbital, whereas the triplet carbene has two singly occupied orbitals and is regarded as a diradical (Figure 1.4a). If the groups adjacent to the carbene centre are electron-donating, they can interact with the vacant *p*-orbital of the singlet state via electronic mesomeric effects and stabilise the singlet state with respect to the triplet state. Also the *N*-heterocyclic carbenes possess an electron-withdrawing inductive effect, yielding a 'push–pull' effect [13,14] that ensures that all *N*-heterocyclic carbenes are nucleophilic singlet carbenes. Thus, the azole moieties make very good precursors for carbenes due to their electronic structures.

The chemical properties of these nucleophilic ligands have been investigated by many researchers, the most prominent of which include Herrmann et al. [15 and Refs. therein], Öfele et al. [16], Kuhn et al. [17–21], Enders et al. [22–25], Teles et al. [26] and others [27–32]. These studies have focused on using the *N*-heterocyclic carbenes as ligands in co-ordination complexes and their application in transition metal catalysis. Furthermore, studies on their stability and electronic structure have also been reported [33–36]. The *N*-heterocyclic azole carbenes that have been prepared and employed as ligands for transition metals are shown in Figure 1.4.

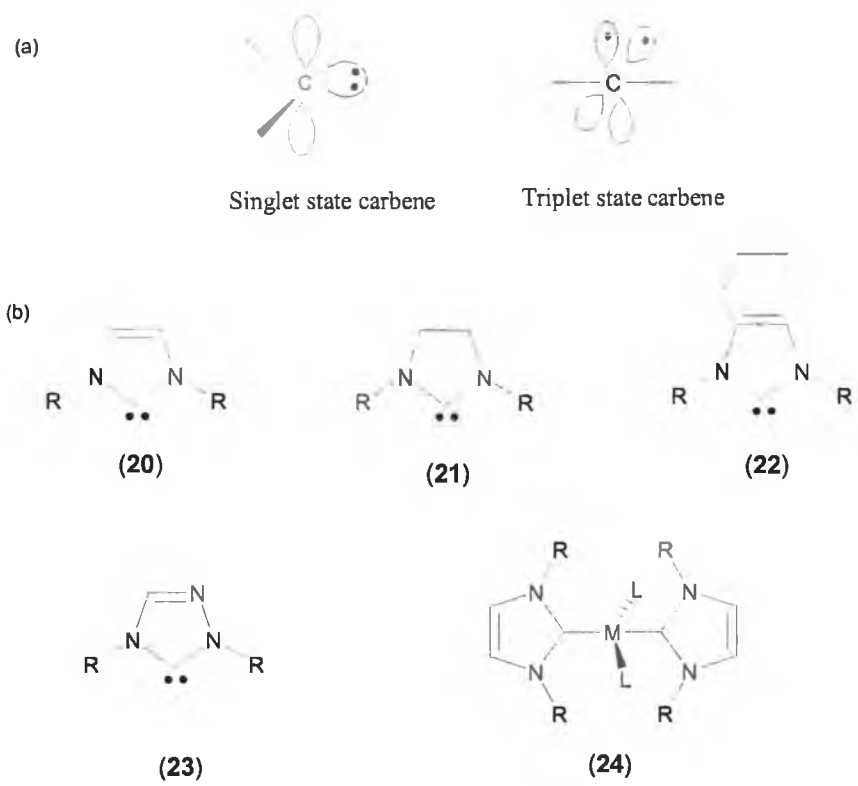

Figure 1.4. *(a) Singlet and triplet state carbenes. (b) Free azole carbenes: imidazolylidenes (20), imidazolinylidenes (21), benzimidazolylidenes (22) and triazolylidenes (23). A typical azolylidene complex (24).*

The method for generating these carbenes involves deprotonation of the dialkylazolium salt usually using potassium *t*-butoxide in tetrahydrofuran (THF) (Scheme 1.4).

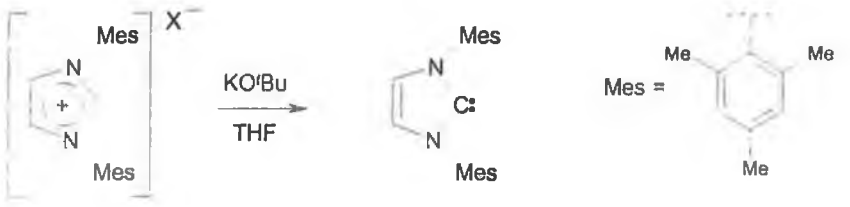

Scheme 1.4. *Typical formation of an imidazolylidene carbene from a 1,3-dialklyimidazolium salt.*

However, apart from physical studies on the imidazolylidenes, these free carbenes are very rarely generated and isolated, instead they are usually converted directly into the desired complex. This is achieved in two ways. The first involves the generation of the carbene using potassium *t*-butoxide in the presence of a metal complex (it has been found that free carbenes can easily replace several different types of ligands, e.g. halides, alkenes, carbonyls, arenes and phosphines [37]) (Scheme 1.5a). The second involves reaction of the precursor azolium salt with a metal complex containing basic ligands, e.g. the acetate anion (Scheme 1.5b).

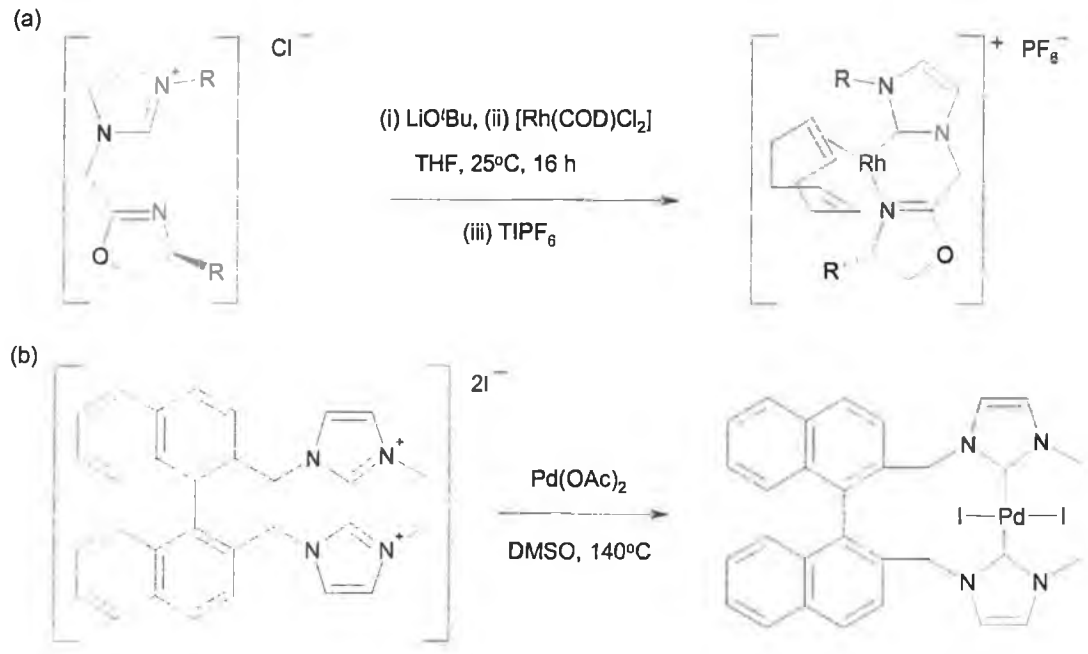

Scheme 1.5. *Formation of N-heterocyclic carbene ligands.*

As expected these carbenes act as neutral two electron donor ligands. They exhibit strong σ-bonding tendencies with no significant π-backbonding. Thus, it has been found that they are better electron donors than the phosphine ligands [38–40]. It was perceived that they could not only act as phosphine mimics but could actually outperform them in transition metal catalysis.

These azolylidene ligands have shown great promise as auxiliary ligands. Due to the excellent σ-bonds formed between the metal and carbon, they have shown great thermal stability [41,42], appear to be strong co-ordinating ligands that undergo little to no dissociation to the metal in solution [43] and act as non-participating ligands that are not consumed in the catalytic process [44,45]. Therefore, they compare favourably in all aspects to the phosphines. Furthermore, due to the nature of the azole entity various substituents can be introduced that can affect the electronic properties,

steric demands and chirality of the ligand. Thus, the azolylidene carbenes satisfy the criteria of being efficient catalytic ligands in organometallic cross-coupling reactions.

The following reactions give an idea of how the azolylidene ligands have been applied in transition metal-mediated cross-coupling reactions: Sukuzi coupling [46,47], aryl amination [48], amide α-amination [49], hydrosilylation [50], ethylene/carbon monoxide copolymerisation [51], Kumada coupling [52,53], the Stille coupling [54], furan synthesis and alkyne coupling [55], olefin cyclopropanation [56], arlyation and alkenylation of aldehydes [57], reduction of aryl halides [58] and in asymmetric catalysis [40]. It should be noted that while co-ordination compounds of the imidazolylidenes, imidazolinylidenes, benzimidazolylidenes and triazolylidenes have been prepared, so far in the vast majority of cases it is imidazolylidenes that have been applied to organometallic catalysis.

1.2.2.2 Heck reaction

The Heck reaction (Scheme 1.6) is the palladium-catalysed arylation of alkenes that is now one of the most versatile tools in organic synthesis for the creation of C–C bonds. It was first pioneered by both Heck [59] and Mizoroki [60] independently in the late 1960s, and through much further investigation of its scope, it is now one of the simplest methods of synthesising various substituted olefins, dienes and other unsaturated compounds.

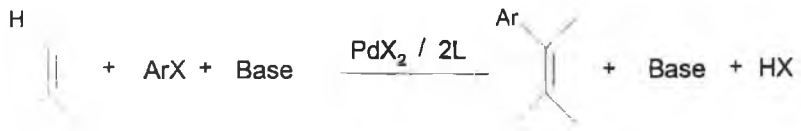

Scheme 1.6. *The Heck reaction.*

In the Heck reaction the electrophile can be an aryl, heterocyclic, benzylic or a vinylic halide/triflate. A Pd(II) compound, such as palladium dichloride or palladium acetate is the most widely employed type of catalyst. Although the reaction can be carried out using just the Pd(II) salt, it has been shown the reaction will proceed far more effectively if specific ligands are employed. The most generally used ligands are the triarylphosphines. However, as the Heck reaction is so wide ranging the tailoring of ligands to particular reaction partners and conditions is sometimes either desirable or necessary.

In the Heck reaction, the nucleophiles are usually mono- or 1,1-disubstituted alkenes as they are more reactive. Generally as the substitution number in the alkene increases the reactivity decreases, to the point where there are only a few limited examples of trisubstituted alkenes undergoing cross-coupling [61]. Aprotic solvents, such as *N*,*N*-dimethylformamide (DMF), dimethyl sulfoxide (DMSO) or acetonitrile, are typically used. Finally, a base is essential in the catalytic cycle and is either a secondary or tertiary amine or a sodium/potassium acetate, carbonate or bicarbonate salt.

The mechanism of the Heck reaction (Figure 1.5) can be divided into four main steps: the preactivation, oxidative addition, ligand substitution, migratory insertion and reductive elimination.

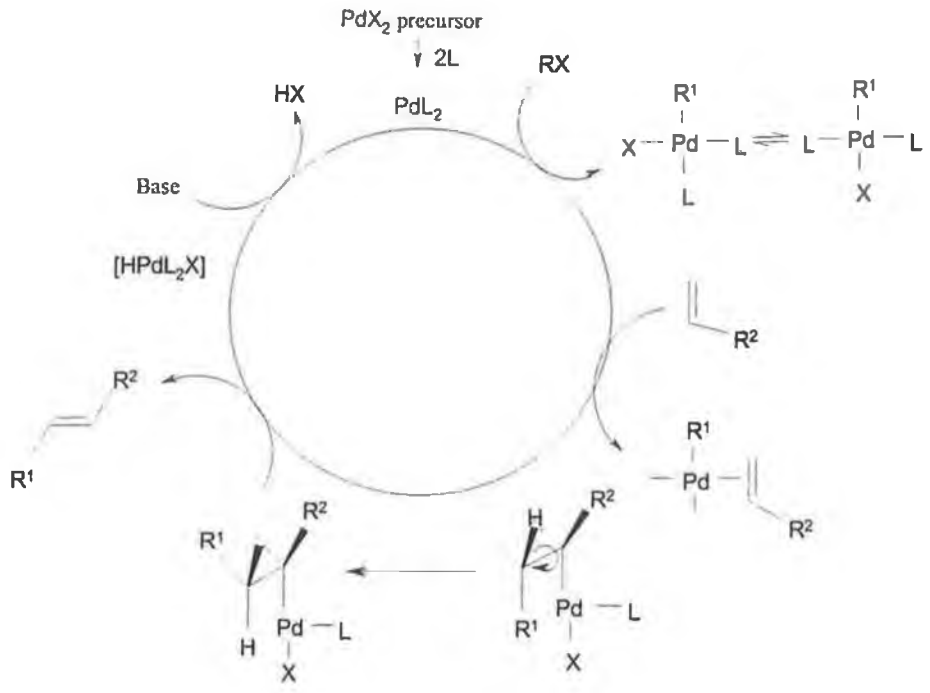

Figure 1.5. *The mechanism of the Heck reaction.*

1.2.2.3 Azolium/palladium systems in the Heck reaction

The Heck reaction was one of the first transition metal-mediated reactions to which the novel *N*-heterocyclic carbene co-ordination compounds were applied. Herrmann et al. showed that complexes (**25**) and (**26**) were able to couple aryl bromides and aryl chlorides to alkenes in yields of 99% [62]. Furthermore, it was shown that the precursor to (**25**) – 1,3,dimethylimidazolium iodide (**27**) – could be introduced into the reaction and generate the coupled product in comparable yields to **25** and **26**, thus eliminating the need to prepare the palladium complexes (**25** and **26**) beforehand (Scheme 1.7).

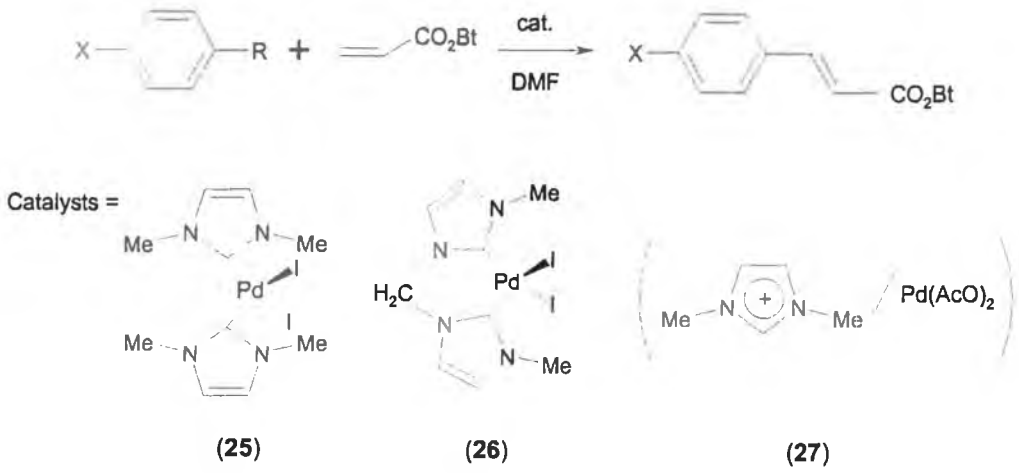

Scheme 1.7. *First use of imidazolylidene complexes in the Heck reaction.*

Other groups have also employed imidazolylidene ligands in the catalysis of the Heck reaction. Nolan et al. employed very facile imidazolium salt/palladium systems to the Heck reaction (Scheme 1.8) [62,63]. This group has shown that it is not necessary to prepare the carbene co-ordination compound beforehand. They also found that bulkier imidazolium chlorides possessing *N*-aryl *ortho*-substitutents displayed the best constant activity when used with palladium acetate. Imidazolium precursors (**28a**)–(**31a**) were tested along with their imidazolinylidene analogues (**28b**)–(**31b**) (Scheme 1.8). It was found that 2,4,6-trimethylbenzene imidazolium salt (**30a**) yielded the best overall catalytic system [63] when used for the coupling of arylbromides.

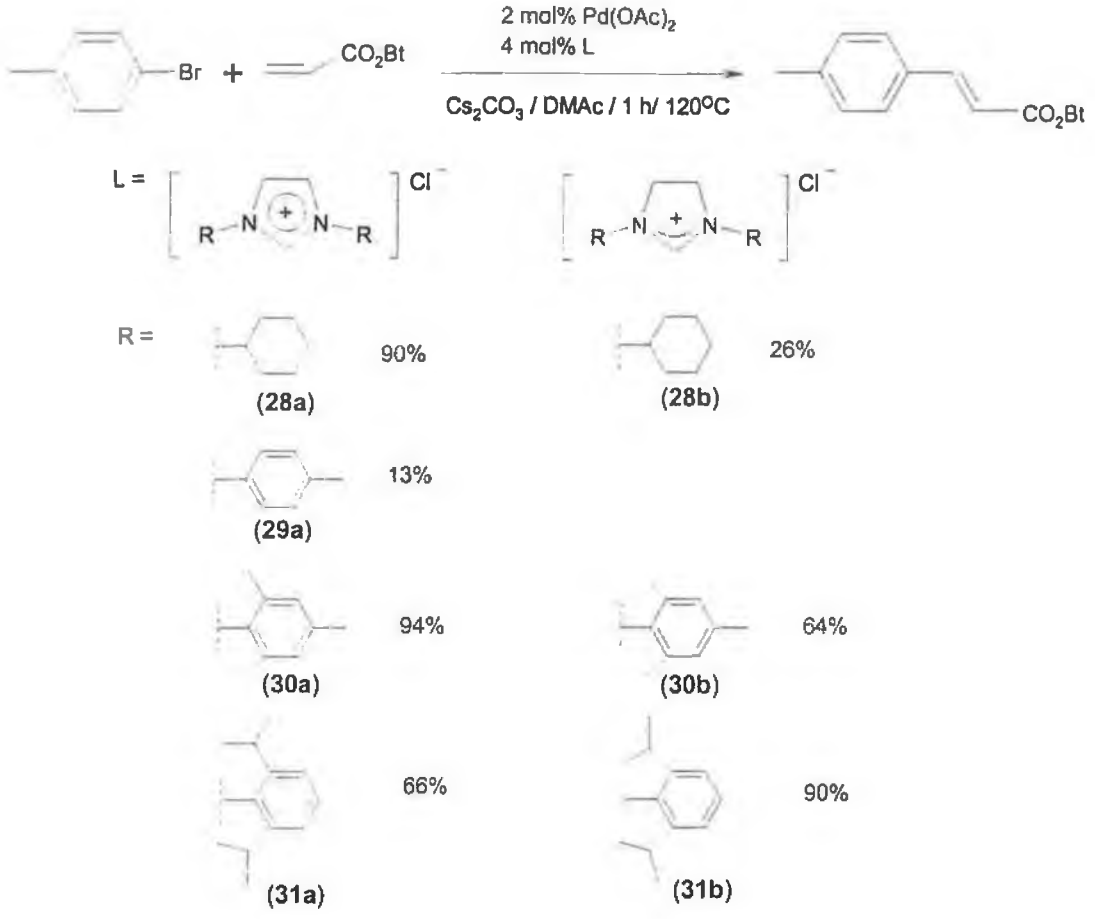

Scheme 1.8. *The investigation of Nolan et al. in the electronic and steric effect of the imidazolium precursor on reaction rate.*

A number of reports are given in the literature about the application of the imidazolylidene complexes and the imidazolium salts to the Heck reaction. There have been comparisons of mono, bi and tridentate carbene systems (e.g. **32**) and mixed carbene/nitrogen donor systems (e.g. **33**) [46,64,65] (Figure 1.6).

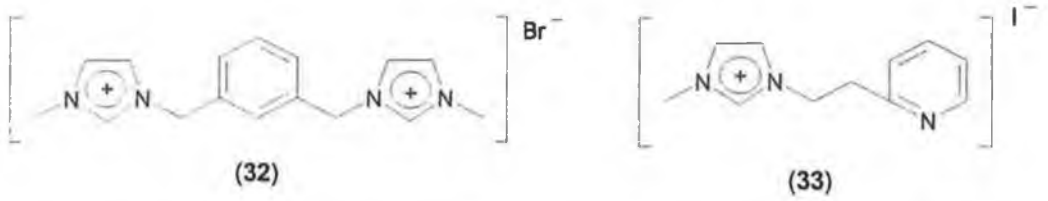

(32) (33)

Figure 1.6. Chelate imidazolium and mixed carbene/nitrogen donor systems that have been applied to the Heck reaction.

Nolan et al. [62] prepared a mixed carbene/phosphine imidazolium chloride that showed comparable results to the monodentate imidazolium chloride salts employed (Figure 1.7).

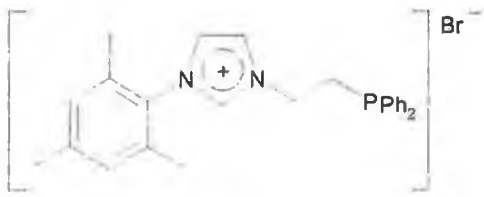

(34)

Figure 1.7. The mixed phosphine/carbene system (34) used by Nolan et al.

1.2.3 Azoles as solvents in organic processes

1.2.3.1 Ionic liquids

Chemistry is dominated by the study of species in solution. Any refinement or improvement upon the existing range of solvents used in synthetic techniques is of much interest to chemists. So the discovery of ionic compounds that have melting points at or below 298 K (fused salts) – the so-called 'ionic liquids' – has created a very lively avenue of research, as they have the potential to create new solvent systems for the many varied preparative reactions that are used commercially (for fully comprehensive reviews see Refs. [66,67]).

They offer many advantages over traditionally used organic solvents. They are:

- Non-volatile – no measurable vapour pressure, so product recovery by distillation is possible, which may not be the case with some organic solvents used commercially. Also there is no evaporation with ionic liquids, so there would be no release of volatile organic compounds (VOCs) as is associated with organic solvents.
- Wide liquid range – they are thermally stable up to 400°C, so distillation of compounds is possible at high temperature.
- Chemically stable – no special conditions need be applied to due chemical sensitivities.
- Ability to dissolve a wide range of organic, organometallic and inorganic compounds – so a wide range of possible reactions can be carried out, including catalytic systems.
- Immiscibility with a wide range of organic solvents – allows biphasic systems to be set up.

- Controllable physical properties – melting point, density, viscosity, liquidus range, miscibility with other solvents, polarity and co-ordination properties can all be fine-tuned with careful selection and adjustment of anion and cation.

Ionic liquids are typically composed of an organic salt. As they are fused salts (i.e. liquids that are composed solely of ions), they resemble ionic melts, but whereas very high-temperatures are required to produce melts (800°C for NaCl), ionic liquids remain liquid at room temperature and below – even to –96°C.

There are four types of ionic liquids grouped according to the cation (Figure 1.8). Generally they are based on a bulky cation coupled with a wide variety of anions (e.g. PF_6^-, NO_3^-, $AlCl_4^-$).

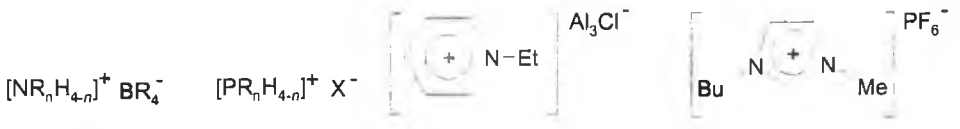

(35) **(36)** **(37)** **(38)**

Figure 1.8. *The four types of salts that form ionic liquids: **(35)** alkylammonium, **(36)** alkyphosphonium, **(37)** N-pyridinium and **(38)** 1,3-dialkylimidazolium salts.*

The alkylammonium and alkyphosphonium have been shown to be hydrophobic and have limited applications due to their low conductivity, instability and difficulty of preparation [68,69], while the ionic liquids based on 1-methylimidazole are becoming the most commonly used systems.

1.2.3.1.1 Ionic liquid development

Ambient temperature fused salts have been know since 1913, for example $[EtNH_3][NO_3]$, which has a melting point of 12°C [70]. However, it was in the 1950s that they became something of a chemical curiosity with the study of alkylpyridinium chloroaluminate-based ionic liquids (**37**). Then it was in the 1980s with the discovery of the room temperature imidazolium-based chloroaluminates, with their wider liquidus range and high conductivity, that the ionic liquids became a serious research interest.

1.2.3.1.1.1 Chloroaluminates(III)

Aluminium chloride–*N*-ethylpyridinium bromide ([*N*-etpy]Br·$AlCl_3$) (**37**) was the first chloroaluminate to be discovered as a molten salt at room temperature [71]. The range of aluminium chloride–*N*-alkylpyridinium halides was then extended with the synthesis of aluminium chloride–*N*-butylpyridinium chloride ([*N*-bupy]Cl·$AlCl_3$) (**38**), one of the most extensively investigated ionic liquids [72]. In the 1980s, a series of 1,3-dialkylimidazolium ionic liquids were developed that were found to have a wider liquidus range, higher conductivity and were easier to prepare. Of these aluminium chloride–1-ethyl-3-methylimidazolium ([EMIM]Cl·$AlCl_3$) (**39**) and aluminium chloride–1-butyl-3-methylimidazolium ([BMIM]Cl·$AlCl_2Et$) (**40**) have been the most widely studied systems (Figure 1.9).

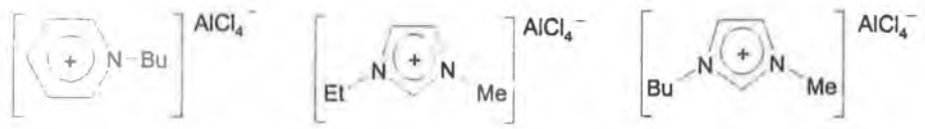

(38) (39) (40)

Figure 1.9. *The most studied chloroaluminate ionic liquids.*

It was thought that the adjustable acid–base properties of the room-temperature chloroaluminates would make them attractive solvents for acid–base dependent chemical processes. However, the 1,3-dialkylimidazolium chloroaluminate(III) species are extremely air and moisture sensitive and so must be protected rigorously from moisture and other oxide impurities [66]. Also there is a tendency of many substrates to react with halometallates, presenting further problems. Thus, their application to organic synthesis was limited.

1.2.3.1.1.2 Air and moisture stable azolium ionic liquids

The area of ionic liquid chemistry was renewed in 1992 by the discovery of Wilkes et al. [73] and Fuller et al. [74] of the air and moisture stable ionic liquids. These were initially based on the 1-ethyl-3-methylimidazolium ($[EMIM]^+$) cation. The inert salts that were produced were shown to have low melting points, with the $[EMIM]PF_6$ salt having a melting point range of 58–60°C, while the BF_4^- and CH_3COO^- salts had melting points of 15 and –45°C, respectively.

The $[BMIM]^+$-based BF_4^- and PF_6^- salts then followed from Suarez et al. in 1995 [75], and then in 1996 Bonhôte et al. [68] synthesised a series of 1,3-dialkylimidazolium salts. A great variety of cations with different alkyl groups at the C(2), C(4) and C(5) positions of imidazole were combined with a variety of inorganic

anions, such as CF_3COO^-, $CF_3SO_3^-$, $C_4F_9\ SO_3^-$ and $(CF_3SO_2)_2N^-$. They all possess melting points below room temperature, furthermore, they possess low viscosities, were air and moisture stable and were inexpensive to prepare. These characteristics coupled with the fact that they could solubilise a wide range of organic and inorganic compounds, meant that their applicability to classical organic chemistry could be realised.

The specific properties of the moisture stable imidazolium ionic liquids that make them so suitable as solvents for organic processes are:

i. their high degree of thermal stability up to 400°C [76];
ii. their chemical stability – they are non-flammable, stable against strong reducing metals, such as sodium and lithium, and have shown great inertness to organic reagents in synthesis;
iii. have controllable miscibility with organic reagents [68,77,78];
iv. are polar compounds, thus are able to dissolve inorganic compounds (i.e. catalysts).

1.2.3.2 Synthetic applications of the ionic liquids

The ionic liquids can be applied for use in (i) classical organic synthesis and (ii) biphasic catalysis. The most important application of the ionic liquids is the employment of the neutral, moisture stable ionic liquids for biphasic catalysis.

1.2.3.2.1 Classical organic synthesis

The chloroaluminates, of which the acidic [EMIM]Cl·$AlCl_3$ is the most widely used, are employed as solvents for reactions that are typically catalysed by $AlCl_3$.

The Friedel–Crafts acylation was the first reaction to be thoroughly investigated in the chloroaluminate ionic liquids. Wilkes et al. successfully used the acidic [EMIM]Cl·$AlCl_3$ system for the Friedel–Crafts alkylation and acylation of simple benzene derivatives [66]. More recently, it has been shown that Friedel–Crafts acylation in ionic liquids can be applied to organometallic compounds in [EMIM]I·$AlCl_3$, with ferrocene being acetylated with either acid anhydrides or acid chlorides and the rate of reaction and selectivity (mono or bis substitution) being controlled by the $AlCl_3$ concentration in the melt [79] (see Scheme 1.9).

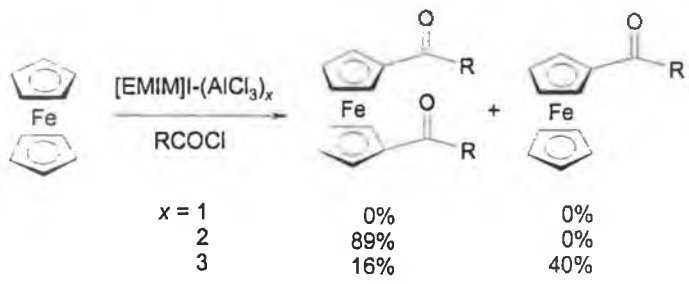

Scheme 1.9. *Friedel–Crafts acylation of ferrocene.*

The acylative cleavage of ethers, in which a variety of cyclic and acyclic ethers were cleaved using benzoyl chloride to give difunctionalised iodobenzoate adducts [80] (see Scheme 1.10), was carried out in [EMIM]Cl·$AlCl_3$.

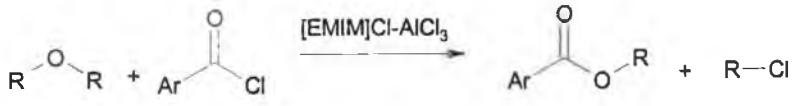

Scheme 1.10. *The acylative cleavage of cyclic and acyclic ethers in chloroaluminate melt.*

The use of the moisture stable ionic liquids has grown rapidly in recent years, as due to the ease of their handling, it appears that they can be applied to any synthetic

procedure. One of the most important classical organic reactions in which they have shown to be excellent solvents is the Diels–Alder reaction. The reaction between cyclopentadiene and methyl acrylate was shown to proceed well in $[EtNH_3]NO_3$, $[BMIM]BF_4$, $[BMIM]ClO_4$, $[EMIM]CF_3SO_3$, $[EMIM]NO_3$ and $[EMIM]PF_6$ [81–83]. These ionic liquids gave a high *endo* selectivity and reactions proceeded at a faster rate compared to non-polar solvents.

Furthermore, in the only instance where the ionic liquids have been used purely for their Lewis acidity, rather as solvents, they were used as recyclable Lewis acid catalysts for the Diels–Alder reaction [84]. Using cyclopentadiene and either methacrolein or crotonaldehyde, the imidazolium salts were added to the system in catalytic quantities (0.2 eqs.) in dicholoromethane (with no other Lewis acid present) and were found to catalyse the reaction, demonstrating that even the simple, neutral imidazolium-based ionic liquids were able to act as Lewis acids (see Scheme 1.11).

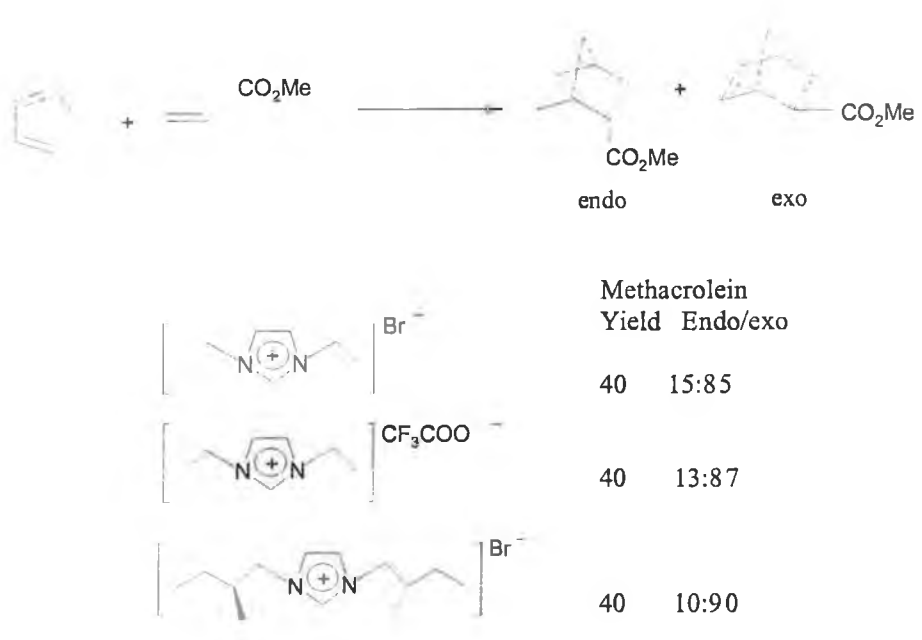

Scheme 1.11. *Calalysis of Diels–Alder reaction using 1,3-dialkylimidazolium salts.*

1.2.3.2.2 Biphasic catalysis

Biphasic catalysis is usually based on the transposition of known reactions from a one-phase homogenous system (solvent phase) to a two-phase homogenous system (ionic liquid and solvent/reagents phases). With the catalyst dissolved in the ionic liquid phase and the reactants forming an organic phase to be collected by decantation, extraction or distillation.

One of the best investigated applications of the ionic liquids to transition-metal catalysis and the development of a two-phase homogenous system from a one-phase system using ionic liquids is the nickel-catalysed oligmerisation of short chain alkenes in the chloroaluminate melts. Industrially, these reactions are used for the synthesis of polyethylene co-monomers or intermediates for the preparation of detergents, plasticisers and lubricating oils. However, the processes involved suffer from expensive catalysts, poor catalyst isolation and recovery leading to high operational and environmental costs.

In 1990, Chauvin et al. carried out the dimerisation of propene to hexenes using various organochloroaluminate salts, such as [BMIM]Cl·$AlCl_3$ and [bupy]Cl·$AlCl_3$, as the solvent and various NiX_2L_2 (L=methylallyl or phosphine ligands) complexes as the catalyst [85]. This reaction has been extended to the oligmerisation of ethylene [86] and butene [87,88].

One of the most impressive examples of the oligomerisation of alkenes in chloroaluminate solvents was the use of the nickel catalyst [(cod)Ni(hfacac)] (cod=cyclooct-4-ene-1-yl) in acidic [*N*-bupy]·$AlCl_3$ with the addition of an organic

buffer such as *N*-methylpyrrole. These conditions yielded the linear dimerisation of 1-butene in a 98% selectivity [89] (Scheme 1.12). It was also found that the catalyst remained contained in the ionic liquid to be reused.

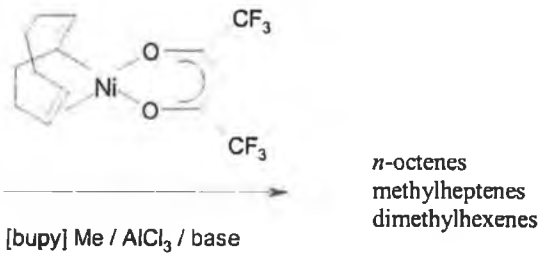

Scheme 1.12. *Oligomerisation of 1-butene in a chloroaluminate melt.*

In biphasic catalysis, often the Lewis acid properties of the moisture/air sensitive organochloroaluminate salts are not required and actually can prove problematic. As a result the moisture stable neutral ionic liquids are becoming ever more popular. As such a wide variety of different transition metal-mediated reactions have been carried out in these neutral (i.e. non-acidic) ionic liquids.

An example to illustrate the use of the moisture stable imidazolium salts in biphasic catalysis is their application to hydrogenation reactions. It was shown that these ionic liquids could be reused as the products could be simply isolated by filtration and that negligible leaching of the catalyst from the ionic liquid phase into the organic layer occurred. Thus, the catalyst could be immobilised in the ionic liquid without specially designed ligands, as was previously required, and the catalyst could be recycled for further use.

De Souza and Dupont et al. first showed this in 1995 using the Wilkinson's complex $[RhCl(PPh_3)]$ to hydrogenate cyclohexane in $[BMIM]BF_4$ and $[BMIM]PF_6$ [75]

(Scheme 1.13). Although there was no noticeable difference in the reaction rate compared to conventional solvents, the ease of product isolation by simple decantation and recycling of the catalyst was shown.

Scheme 1.13. *Selective hydrogenation of methyl sorbate.*

This has been extended, with all of the classical Ru, Rh, Co and Pd catalytic systems having been successfully carried out in the ionic liquid–organic system for the hydrogenation of simple olefins, conjugated dienes and arenes, such as benzene, toluene and cumene, [90] in the 1-butyl-3-methylimidazolium ($[BMIM]^+$) salt systems. Furthermore, asymmetric hydrogenations with the hydrogenation of 2-arylacrylic acids using the chiral Ru-BINAP catalyst in $[BMIM]BF_4$ was successfully carried out with enantiomeric excesses of 86% [91]. Also (*S*)-Naproxen (**41**) was synthesised in this procedure in 80% e.e. (Scheme 1.14).

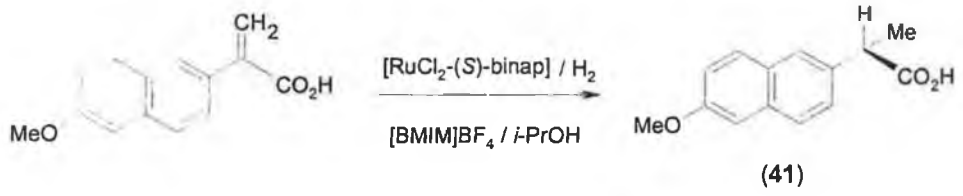

Scheme 1.14. *Formation of (S)-naproxen in an ionic liquid.*

Other transition metal-mediated processes utilising a biphasic ionic liquid system as a means of immobilising the catalyst include, for example, hydroformylations and

oligomerisations. See Ref. [92] for a comprehensive review of ionic liquids in catalytic processes with an emphasis on industrial application.

1.3 Anion recognition

1.3.1 Electrochemical sensing of anions

In order for a sensing device to be realised, the exploitation of a host–guest interaction is necessary, where upon this can be converted into a measurable signal – *transduction*. Therefore, for molecular sensing, a molecule that will undergo some physical or chemical transformation on interaction with an incoming (guest) species is required. For practical application of the compound in sensor technology, it is essential that the host molecule is selective for one species, while being unresponsive to others, and that the binding interaction is reversible.

Another important essential consideration in a sensor may include the immobilisation of the host into a polymer membrane. Thus, there have been various approaches towards the development of novel molecules capable of detecting small molecular guests. There are two main transduction modes used in molecular recognition: electrochemical and optical methods [93].

In the electrochemical methods, usually a transition or lanthanide metal is used in an organometallic compound or an inorganic complex for both guest binding and electrochemical signalling through changes in the metal redox potential on anion–receptor complexation.

In the optical methods, molecular recognition occurs when the proximal association of the guest and host molecules causes either a quenching or enhancement of a chromophore's absorption or a fluorophore's fluorescence.

The most popular technique is that of electrochemical sensing based on the shift of metal redox potential as measured by cyclic voltammetry. The most common design of a chemoreceptor has a metal redox centre coupled to organic appendages capable of the selective co-ordination with molecular guest species (Figure 1.10). This brings the guest into close proximity to the redox centre perturbing its electrochemical properties and producing a measurable shift in redox potential. The host–guest co-ordination is usually through electrostatic interactions, hydrogen bonding and/or ion–dipole attractions.

Figure 1.10. *The production of an electrochemical response generated from the reversible receptor guest–host interaction.*

To achieve specificity in designing a host, guest/host functional group topology in the binding site needs to be considered. It has been shown that acyclic host molecules can conform to a three-dimensional structure, sometimes being able to wrap around a guest (Figure 1.11). However, macrocyclic hosts have shown superior selectivity being able to discriminate between guests due to the set geometry of the cavity [94,95].

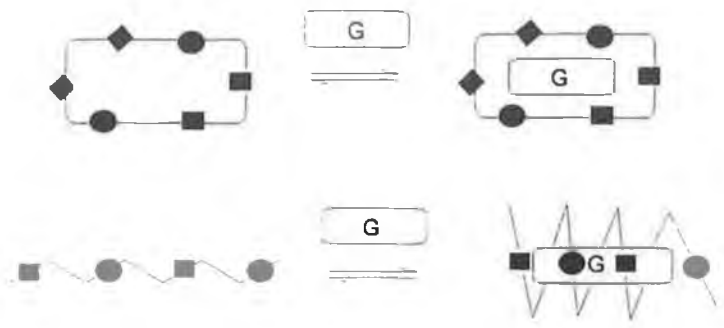

Figure 1.11. *Fixed form versus free form of host–guest recognition.*

While the field of cation recognition has long been established, the corresponding area of anion recognition has lagged behind. Although the first synthetic host receptor was first developed in the 1960s, it has only been over the last decade that the co-ordination chemistry of anions to host molecules has became such a lively area of research. This is perhaps surprising considering the ubiquitous roles that anions play in numerous biological and chemical processes and their importance in medicine and the environment.

For example,

- In chemical processes – anions act as catalysts, bases, redox mediators and reagents. The use of receptors could alter their chemical reactivity, aid mixture separation or stabilise unstable species
- In biological processes – anions are essential in many metabolic systems and also carry genetic information, e.g. DNA is a polyanion and the majority of enzyme substrates and co-factors are anionic.
- In medicine – anions are of great importance in pathological pathways. For example, cystic fibrosis is caused by a misregulation of chloride channels [96] and Alzheimers has been linked to anion-binding enzymes [97].

- In the environment – anions pose a large pollution problem. Pollutants such as nitrates and phosphates in soil water have been linked to the eutrophication of rivers

Therefore, there is a clear need for anions to be monitored, detected and extracted. So consequently, the selective binding and sensing of anions is necessary.

As has already been seen in nature, a complementary relationship between host and guest is essential. An example of this in nature is the phosphate binding protein (PBP) that transports phosphate ions into bacteria cells. The precise positions of the hydrogen bond donor groups in the active site of PBP match the hydrogen bonding oxygen atoms of the tetrahedral phosphate ion and do not allow binding with other anions. For the PBP–phosphate complex, the dissociation constant K_d=1×10^{-6} M at pH 8.3.

By bringing together of many different binding elements, such as geometry, functional group topology, exact dipoles and hydrogen bonding, a system can achieve high specificity. The design of synthetic macrocycles should aim to match the selectivity of naturally occurring supramolecules. Therefore, some of the most selective anion receptors that have been prepared have been macrocyclic with clefts or cavities allowing only a guest with a very specific geometry access.

1.3.2 Design of anion receptors

The design of ionophores capable of anionic recognition has always been regarded as a challenge, and the various factors that must be considered in the design of these molecules include:

- Anions are larger than isoelectronic cations, so will have a lower charge to radius ratio, meaning that electrostatic binding interactions will be less effective.
- Anions have a variety of structures – such as spherical (e.g. Hal^-), linear (e.g. CN^-), triagonal planar (e.g. NO_3^-), tetrahedral (e.g. SO_4^-), octahedral (PF_6^-) and complex geometries (e.g. DNA double helix) – that must be catered for.
- Many anions are typically pH sensitive (e.g. PO_4, F^-), as they have a tendency to become protonated at low pH values losing their negative charge. So a receptor must function within the pH window of the target anion.
- Solvent effects play a crucial role in the control of the binding strength and selectivity of an anion. A receptor is effectively competing with the solvent environment for electrostatic/hydrogen bonding interactions with the anion.

While the design of anion receptors is in its relative infancy and has more inherent difficulties than that of the well-established field of cation receptor technology, there have been various approaches to their design. The variety of these approaches arises from the different possible interaction modes between the host molecule and the guest anion. These interactions can be:

(i) purely electrostatic as in the macrocyclic quaternary mmonium hosts (**42**) and (**43**) [98–103] (Figure 1.12).

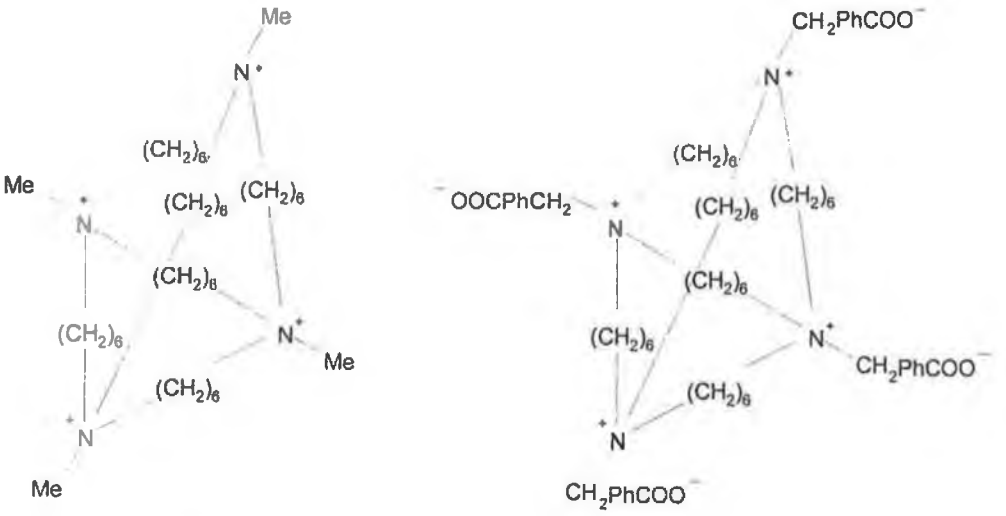

(**42**) (**43**)

Figure 1.12. *The anion host molecules relying on electrostatic attraction only.*

(ii) based on hydrogen bonding, such as the first hydrogen bonding amide anion receptor (**44**) [104] (Figure 1.13). Therefore, good hydrogen bond donors, such as simple amide, urea and thiourea, have made very effective anion receptors [105].

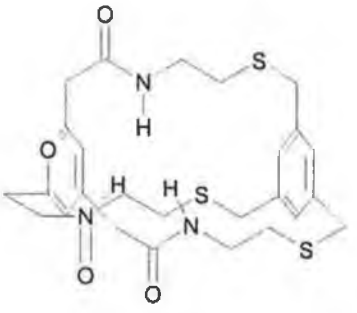

(**44**)

Figure 1.13. *An amide-based anion receptor using only hydrogen bonding for anion co-ordination.*

(iii) or can be a combination of both hydrogen bonding and electrostatic interactions. In fact in many of the nitrogen-based anion receptors both hydrogen bonding and electrostatic interactions are involved, especially with heterocycle based receptors.

(iv) alternatively, electron deficient Lewis acidic centres have been employed for anion co-ordination. There are many novel receptors containing atoms such as boron, mercury, silicon, germanium and tin. The preparation and anion recognition studies of tin macrocycles (**45**) and (**46**) provide an example (Figure 1.14) [106].

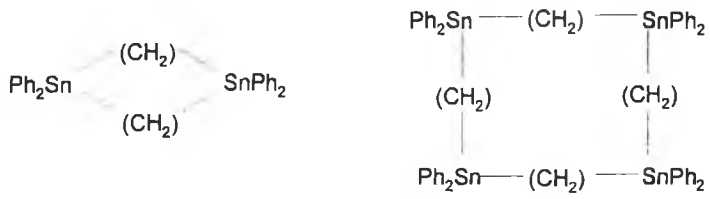

Figure 1.14. *The incorporation of tin atoms into macrocycles for anion receptors based on Lewis acid co-ordination.*

Therefore in the design of an efficient ionophore, the mode of host–anion co-ordination is an important point to consider. While effective receptor systems have been based on the electrostatic interaction model, this does suffer the drawback of the host's counterions interfering in the recognition or in fact simple anion exchange maybe the phenonmen that is being observed. Hydrogen bonds are directional, and thus, allow the possibility of designing host molecules with receptor cavities with specific topologies so that anions with differing geometries and functionality's can be selected for.

1.3.3 1,3-Dialkylazolium compounds as anion receptors

These systems have only very recently begun to be investigated as potential anion receptors. In 1999, Sato et al. recognised that 1,3-dialkylimidazolium salts could act as an alternative to the ammonium and guanidinium groups that were being used as binding sites for anions in receptor molecules. These two groups form stable host–guest complexes through both electrostatic force and hydrogen bonding (Figure 1.15).

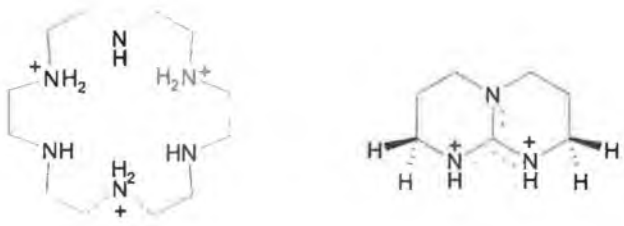

(47)

(48)

Figure 1.15. *(a) An ammonium receptor (47) for NAD^+ and a guanidinium receptor (48).*

As has been established through the structural studies of 1-ethyl-3-methylimidazolium salts [107], the imidazolium cation is capable of both electrostatic interaction and hydrogen bonding with anions. Thus, Sato et al. performed initial ^1H NMR binding studies on 1-methyl-3-methylimidazolium hexafluorophosphate (**49**), which showed significant downfield shifts of the imidazolium 2-H in deuterated acetonitrile. They then prepared dipodal and tripodal systems (**50**) and (**51**), which contain a potential binding cavity [108] (Figure 1.16). Through ^1H NMR titration studies, ESI-MS and molecular modelling, it was shown that these compounds bind strongly to chloride, bromide and iodide anions.

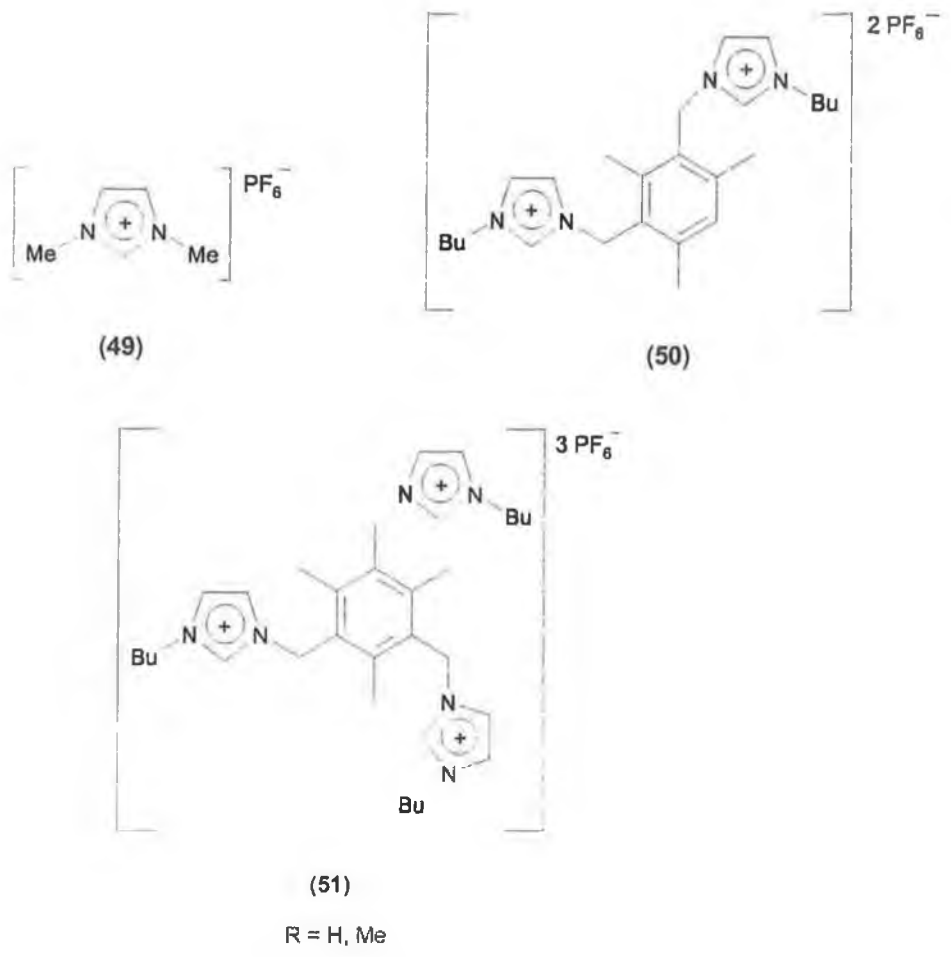

Figure 1.16. *The imidazolium systems (49)–(51) employed by Sato et al. showing anion recognition properties.*

Howarth et al. [109] took this tripodal system and introduced chiral substituents. This homochiral tripodal imidazolium salt **(52)** (Figure 1.17) was then shown to be able to distinguish between anionic enantiomers. Using ^{1}H NMR spectroscopy, it was shown that **52** formed a complex with (*R*)-2-aminopropionate when added to a racemic mixture of sodium 2-aminopropionate. A downfield shift in the α-proton of the proponiate was observed, while there was no shift in that of the (*S*) enantiomer. Thus, leading to the conclusion that this system was able to differentiate between enantiomers.

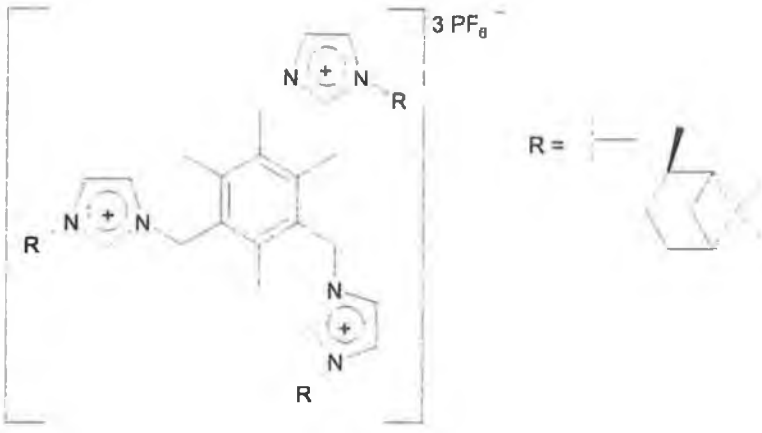

(52)

Figure 1.17. *Homochiral tripodal imiazolium salt (52) capable of differently binding between (R)-2-aminopropionate and (S)-2-aminopropionate.*

Macrocyclic imidazolium cyclophanes, although not a recent discovery, have only just begun to be applied to anion recognition. In 1998, Alcalde et al. prepared the imidazolium cyclophane (**53**) and reported that the introduction of different tetrabutylammonium salts caused significantly varying downfield shifts for the imidazolium 2-H in the order $H_2PO_4^->F^->CH_3COO^->CN^->Cl^-$ [110]. This was extended by Yuan et al. who prepared imidazolium and benzimidazolium cyclophanes [111]. Compound **54** was found to be able to bind selectively to chloride (Figure 1.18). Using UV–Vis spectroscopic titration measurements along with ^1H NMR titration experiments, it was shown that the binding constant for chloride was $4.06\times10^4\ M^{-1}$, which was 2, 5 and 2000 times that of bromide, fluoride and iodide, respectively.

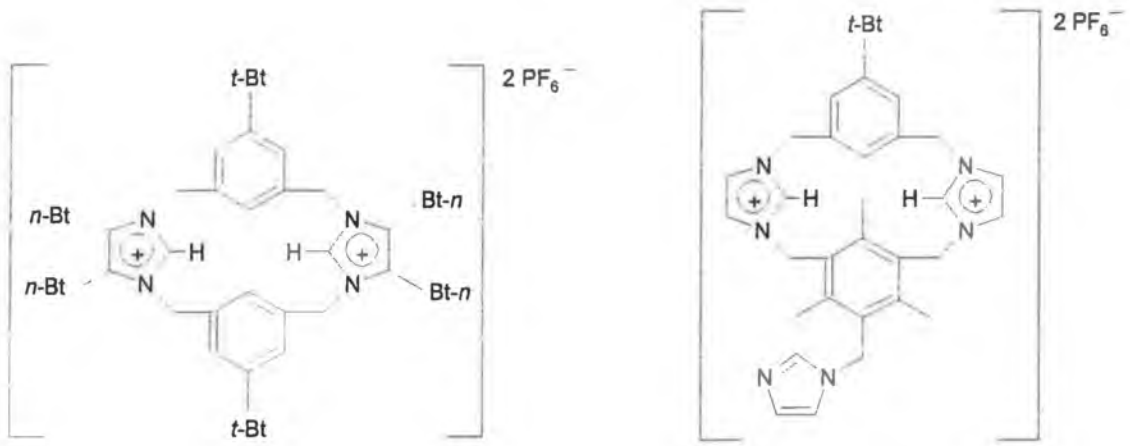

(53) (54)

Figure 1.18. *Imidazolium cyclophanes studied for selective anion recognition.*

1.3.4 Metallocene-based anion receptors

The classical sandwich metallocene has the formula $M(\eta^5\text{-}C_5H_5)_2$. The structure is held together by a highly efficient overlap between the π-electrons of the filled *p*-orbitals of the cyclopentadiene (Cp) rings and the vacant *d*-orbitals of the metal centre (in the case of ferrocene $Fe^{2+}=d^6$). Slight back-bonding from the metal to the π^* orbitals of the Cp rings also occurs (Figure 1.19).

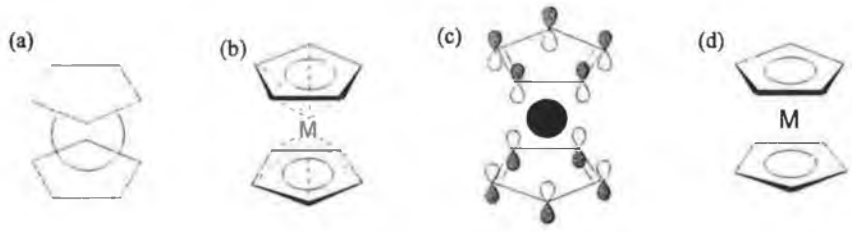

Figure 1.19. *(a) The sandwich structure of a metallocene devised by Wilkinson, (b) p-complexation, (c) p-orbitals of the Cp rings and (d) the generally used representation in the literature.*

One of the most interesting properties of the metallocenes comes from their redox active metal centres. Ferrocene and cobaltocene are particularly attractive in this aspect both undergoing one electron reduction/oxidation processes. Ferrocene can be reversibly oxidised from ferrocene (Fe^{2+}) to the ferrocenium ion (Fe^{3+}). Whereas, cobaltocene is most stable in its oxidised (Co^{3+}) form and will undergo a facile reduction to Co(II) (Figure 1.20). These ferrocene/ferrocenium and cobaltocenium/cobaltocene redox couples can be achieved electrochemically, photochemically or through the use of oxidising agents. Often these metallocenes are introduced into a structure simply to exploit their redox properties in one of these ways. The most popular of these is their application in electrochemistry.

However, out of the two metallocenes ferrocene has been shown to be the most robust, stable and practical. It possesses stronger covalent bonding between the Cp rings and metal, is able to undergo electrophilic aromatic-type substitution reactions more easily, is soluble in most organic solvents, is inexpensive and is available from commercial sources.

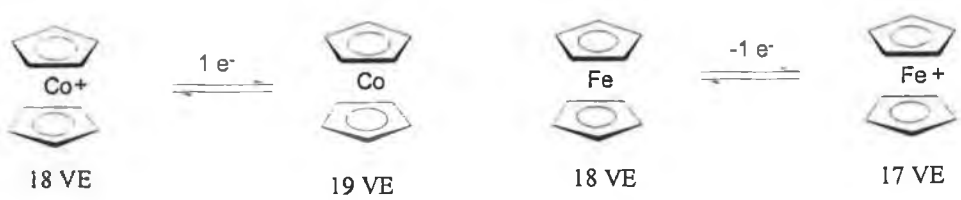

E_o=+0.90 V vs. SCE (CH_3CN)

E_o=+0.31 V vs. SCE (CH_3CN)

Figure 1.20. *Electrochemical redox couples of cobaltocenium/colbalt and ferrocene/ ferrocenium.*

The oxidation is reversible and the potential applied is a function of the substitutents on the Cp units. For example, alkyl groups tend to aid oxidation whereas aryl groups will hinder oxidation. Furthermore, if the substituents bring a guest species into close proximity to the redox centre then the electrochemistry will be affected. So ferrocene and colbaltocenium have been incorporated in many different types of molecules, e.g. macrocycles, cryptands and cavitands, with a view to developing molecular receptors capable of electrochemical transduction. The traditional concept of recognition for ferrocene compounds is shown in Figure 1.21.

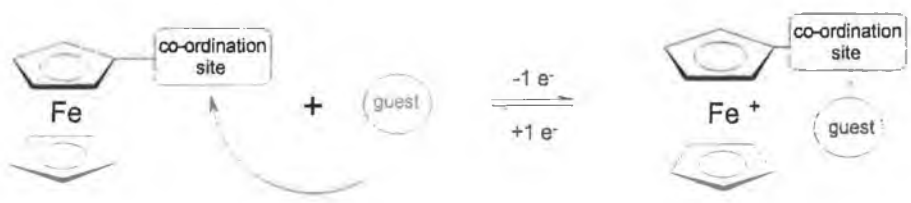

Figure 1.21. *Diagram of the principle of electrochemical recognition.*

If the substituents attached to the metallocene are capable of selectively binding to the guest – through electrostatic attractions, hydrogen bonding, Van der Waals interactions, etc. – the potential needed to oxidise the metallocene unit will then become indicative of the guest species.

1.3.4.1 Cobaltocenium anion receptors

Beer et al. [112] prepared the first redox-responsive metallocene anion receptor, which was based on the cobaltocenium moiety. Macrocyclic (**55**) was shown to be capable of the electrochemical signaling of bromide anions (Figure 1.22). Since then ferrocene has also been employed as the redox centre and a whole plethora of

metallocene-based anion receptors has been developed. Acyclic, macrocyclic and calixarene cobaltocenium- and ferrocene-based host molecules have been prepared.

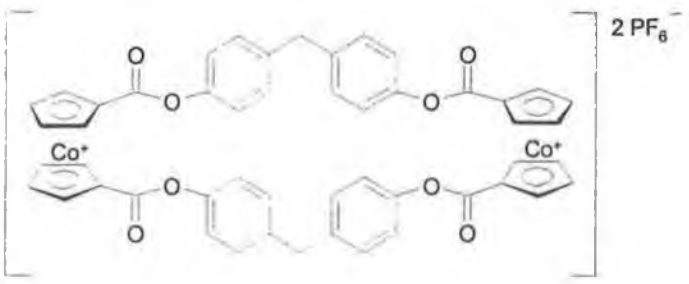

(55)

Figure 1.22. *The first metallocene-based anion receptor capable of the sensing of anions.*

The first cobaltocenium-based receptor molecule only employed electrostatic interactions between the host and guest. The design of these molecules has been extended so that hydrogen bond donors, such as amide functionalities, have been used to co-ordinate the anion, and increasingly complex three-dimensional structures have been created to increase selectivity (Figure 1.23).

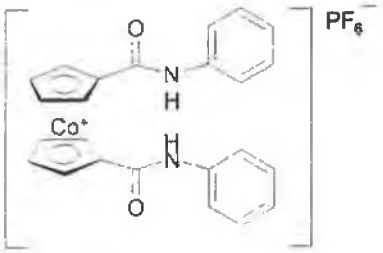

(56)

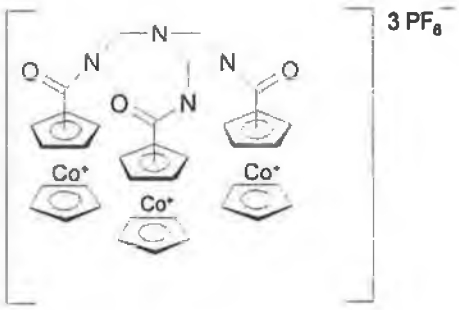

(57)

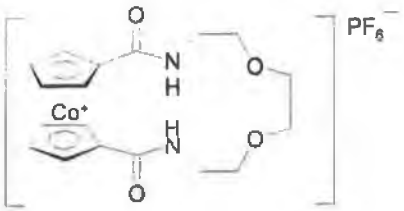

(58)

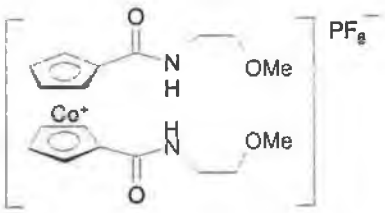

(59)

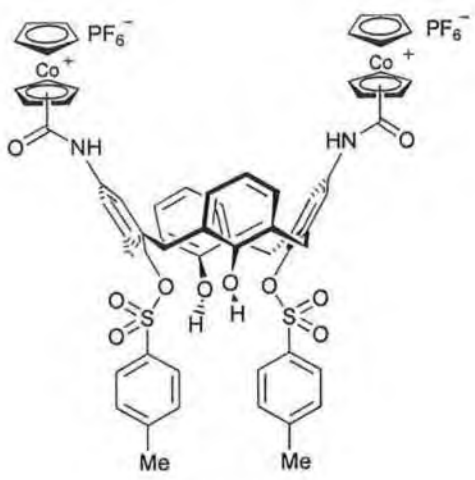

(60)

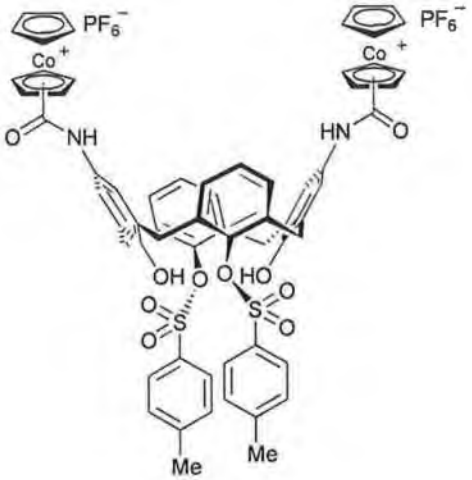

(61)

Figure 1.23. *Acyclic, marcocylic and calixarene derived cobaltocenium receptor molecules (56)–(61).*

Amide functionalised receptors (**56**) and (**57**) demonstrated selective anion co-ordination [113,114]. ^{1}H NMR experiments showed downfield shifts of the receptor protons, especially the amide protons, indicating strong hydrogen bonding between the host and guest. Cyclic voltammetry experiments showed significant cathodic shifts of the reversible $CpCo^+/CpCo$ redox couple for $H_2PO_4^-$ of 200 and 240 mV compared to 30 and 85 mV for Cl^- anions. Receptors (**58**) and (**59**) demonstrated a macrocyclic effect in the complexation with anions [115]. Macrocycle (**58**) was found to have a stability constant with chloride of K=250 M^{-1} in DMSO compared to acyclic receptor (**59**) where K=20^{-1} M.

The coupling of cobaltocenium to the calixarene systems (**60** and **61**) was performed to exploit the topolgical advantage offered by the macrocycle in order to improve anion selectivity (**60**)] [116]. It has been found that it is the degree of preorganization on the upper rim of the calixarene that determines the anion–host co-ordination. Receptors (**60**) and (**61**), for example, show strong selectivity depending on the position of the toysl group on the lower rim. Receptor (**60**) binds CH_3COO^- much better than $H_2PO_4^-$, while the opposite is true in receptor (**61**) [117,118].

1.3.4.2 Ferrocene anion receptors

The initial prototype ferrocene-based anion receptors were often analogous to that of the cobaltocenium receptors. However, one of the main differences is that ferrocene is neutral and, thus, does not interact directly with the anion until it is 'switched on' by being oxidised to ferrocenium. So the stability constants for ferrocene are lower than for cobaltocenium. Now a vast array of different classes of ferrocene receptor molecules exists. There are simple amide functionalised systems, amide–phosphine

systems, calixarene derivatives, ferroceneamines, ferrocenylboronic acid and its derivatives, polyaza and aza-oxo compounds, ferrocene–isophthalimides and –disulphonamides and calixpyrrole derivatives. In Figure 1.24, examples of these different classes of ferrocene-based receptors are given.

(a)

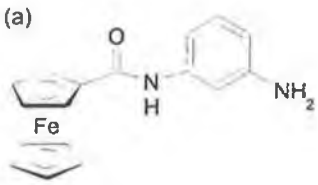

(62)

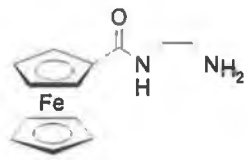

(63)

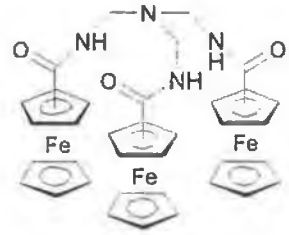

(64)

(b)

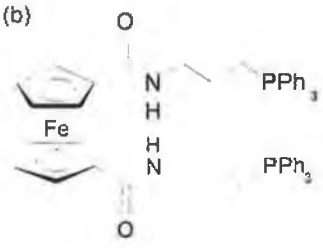

(65)

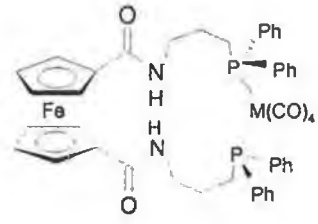

M = Mo, Co

(66)

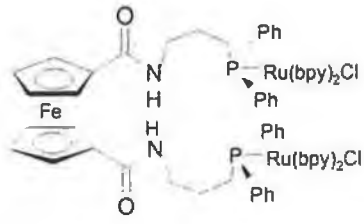

(67)

(c)

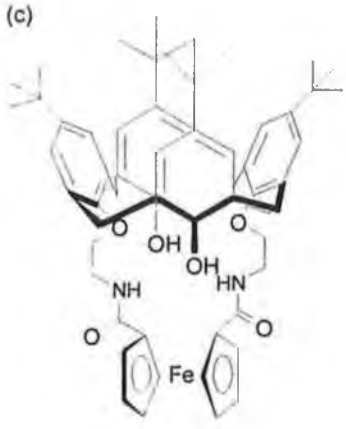

(68)

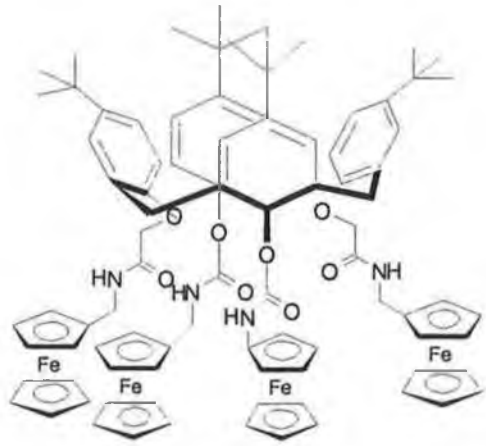

(69)

(d)

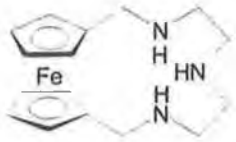

(70)

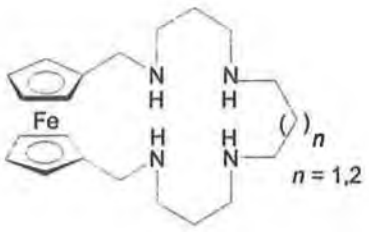

(71)

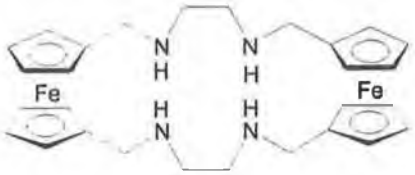

(72)

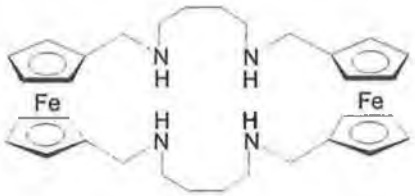

(73)

(e)

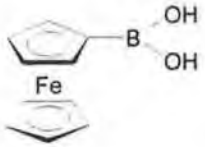

(74)

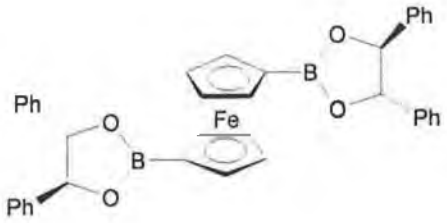

(75)

(f)

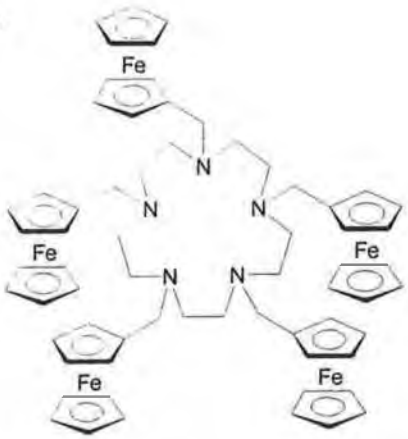

(73)

(74)

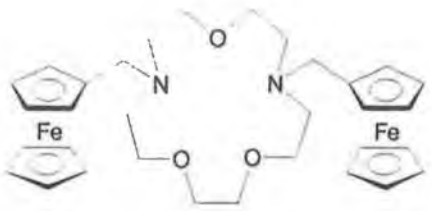

(78)

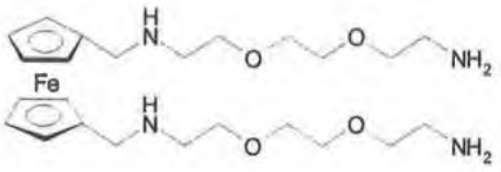

(79)

(g)

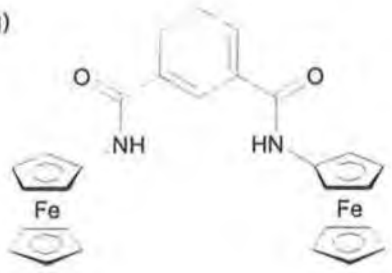

(80)

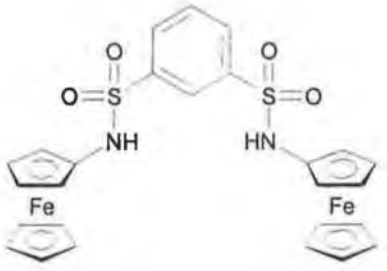

(81)

(h)

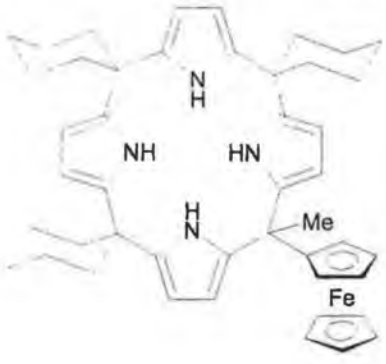

(82)

Figure 1.24. *Examples from the different classes of ferrocene anion receptors prepared. (a) Amide functionalised systems, (b) amide–phosphine systems, (c) calixarene derivatives, (d) ferroceneamines, (e) ferrocenylboronic acid derivatives, (f) polyaza and aza-oxo compounds, (g) isophthalimide and disulphonamide and (h) calixpyrrole derivatives.*

All of these classes of ferrocene system have been shown to be capable of co-ordination with anions. Of particular interest are the amide functionlised receptors (**62**)–(**64**), which were among the first to be prepared. They are able to detect $H_2PO_4^-$ anions, inducing cathodic shifts of up to 240 mV in the presence of a ten-fold excess of hydrogen sulphate and chloride ions [118]. However, the lack of inherent electrostatic attractive forces gives them lower stability constants, as determined by ^1H NMR, than the analogous cobaltocenium compounds. Receptor (**63**) was able to selectively bind HSO_4^- ions in the presence of $H_2PO_4^-$ ions [119]. Protonation of the amine by the acidic sulphate ion causes the receptor to become positively charged, which then binds strongly to the sulphate ion, as shown by the electrochemical response.

Like in the analogous cobaltocenium receptors the ferrocene–calixarene derivatives (**68**) and (**69**) showed increased selectivity for $H_2PO_4^-$ ions. The ferroceneamine compounds (**70**)–(**73**) selectively bind and electrochemically detect phosphate ions, sulphate ions and nucleotides in water [120–122]. The selectivity of the ferroceneamines depends on the pH, hence they are the so-called dual purpose pH dependent receptors with the potential to act as prototype ampherometric sensors.

However, the most selective ferrocenyl chemoreceptor is ferrocenylboric acid (**74**) [123]. It showed excellent selectivity for fluoride ions in the presence of other halide ions, SCN^-, SO_4^- and $H_2PO_4^-$. For fluoride, K_{ox}=1000 M^{-1} in $MeOH/H_2O$, whereas for chloride and bromide the K_{ox} values were less than 2 M^{-1}. So from this simple

molecule other derivatives have been prepared (e.g. **75**), which have been shown so far to bind saccharides at neutral pH [124].

A range of pH stable ferrocenyl–imidazolium and ferrocenyl–benzimidazolium salts (**83**)–(**87**) were prepared by Thomas et al. [125] and Hanlon [126] (Figure 1.25). It was shown that they bind through a possible combination of C–H···X^- hydrogen bonding and electrostatic attraction between the electron deficient Lewis acidic azolium centre and the anion. However, the ^1H NMR studies that were conducted using Cl^-, Br^-, I^-, NO_3^- and HSO_4^- anions did not shown any selectivity of these compounds towards any particular anion.

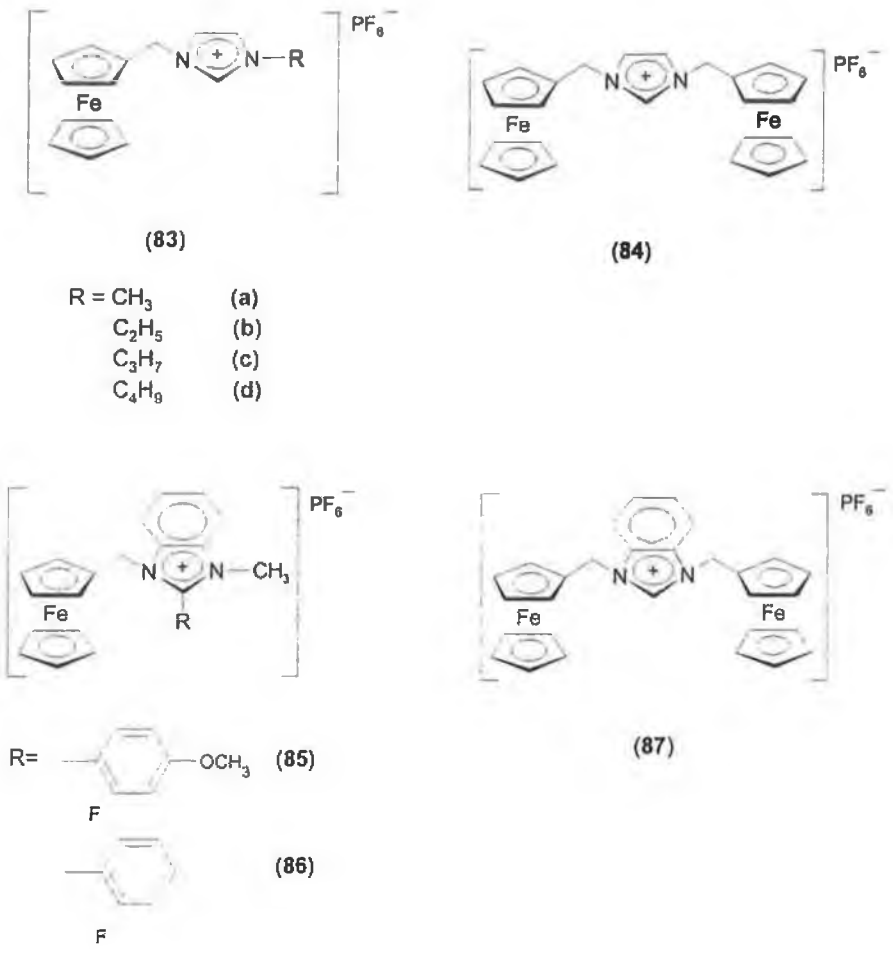

Figure 1.25. *The 1-ferrocenylmethyl-3-alklyazolium salts (83)–(87) in anion recognition ^{1}H NMR titration experiments by Thomas et al. and Hanlon.*

1.4 Functionalisation of azole systems

1.4.1 Ferrocenyl–azolium systems

1.4.1.1 Synthesis

It was Benito et al. in 1995 [127], who first linked a ferrocenyl moiety with an azole by preparing 1-ferrocenylmethyl-2-ferrocenylbenzimidazole (**88**) and 2-ferrocenylbenzimidazole (**89**) by the reaction of ferrocenecarboxaldehyde and *o*-phenylenediamine in the presence of toluenesulfonic acid (see Scheme 1.15).

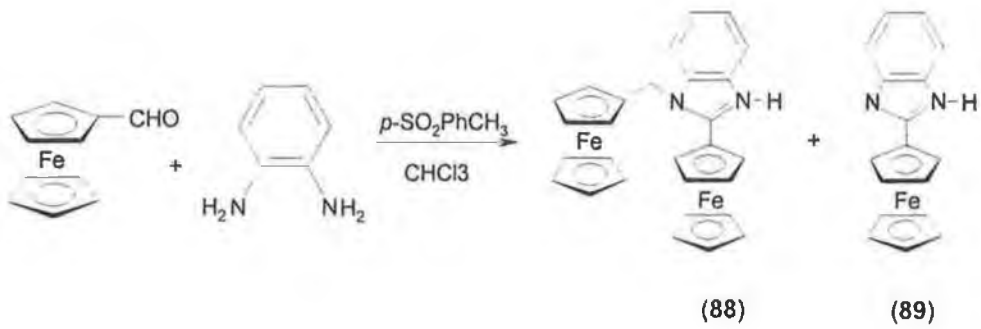

(88) (89)

Scheme 1.15. *Synthesis of 1-ferrocenylmethyl-2-ferrocenylbenzimidazole and 2-ferrocenylbenzimidazole.*

Since then Babin et al. [128–130] has prepared various ferrocenyl–azolium systems with a view to using them as anti-tumour agents, including benzotriazolium, benzimidazolium and imidazolium ferrocenylmethyl derivatives, both as the monosubstituted and disubstituted isomers (Figure 1.26).

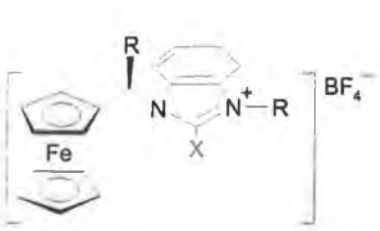

R = H, CH_3
X = CF_3, CF_2CHF_2, $CHFCF_3$

(90)

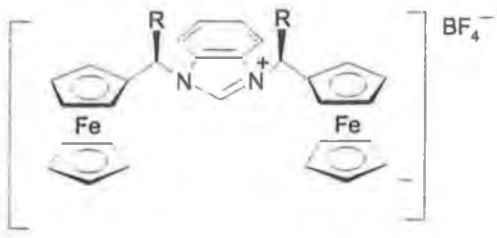

R = H, CH_3

(91)

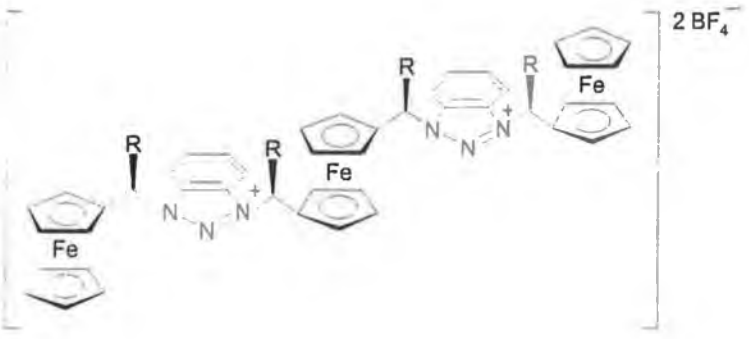

R = H, CH_3

(92)

Figure 1.26. *The ferrocenyl–benzimidazolium tetrafluoroborate salts prepared by Babin et al., e.g. ferrocenylpolyfluorobenzimidazoles (**90**), 1,1′-bis[(1-ferrocenylmethylbenzotriazolium)ethyl]ferrocene bistetrafluoroborates (**91**) and 1,3-bis(ferrocenylmethyl)-2-methyl benzimidazolium tetrafluoroborate (**92**).*

The general method used to prepare these compounds involved the acidic nucleophilic displacement of a ferrocenyl alcohol compound, such as 1-hydroxyethylferrocene, 1-hydroxymethylferrocene (**93**) or 1,1′-bis(hydroxyethyl)ferrocene, using tetrafluoroboric acid and the appropriate azole compound (Scheme 1.16).

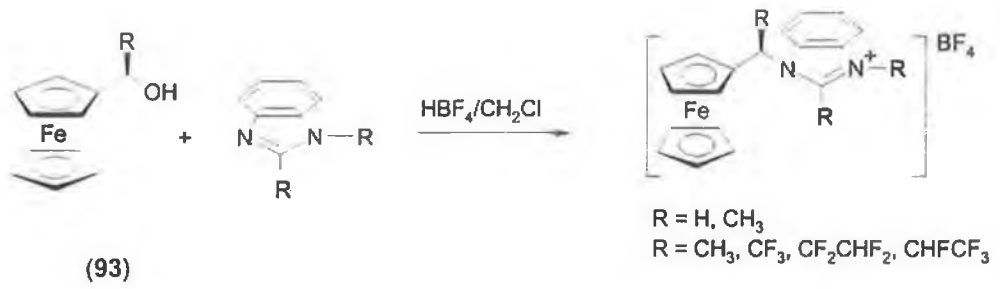

(93)

Scheme 1.16. *Use of tetrafluoroboric acid to couple ferrocenylhydroxy compounds to benzimidazole (Babin et al).*

With an interest in developing novel carbene precursors, Bildstein et al. [131–133] also prepared ferrocene–azolium derivatives. They were interested in the preparation of monosubstituted ferrocenyl azolium systems and have successfully synthesised ferrocenyl–benzimidazolium derivatives with a methylene spacer, ethylene spacer and no spacer functionalities, such as (**94**)–(**96**). The preparations from (trimethylammonium)methylferrocene iodide and 2-bromoethylferrocene are outlined in Scheme 1.17.

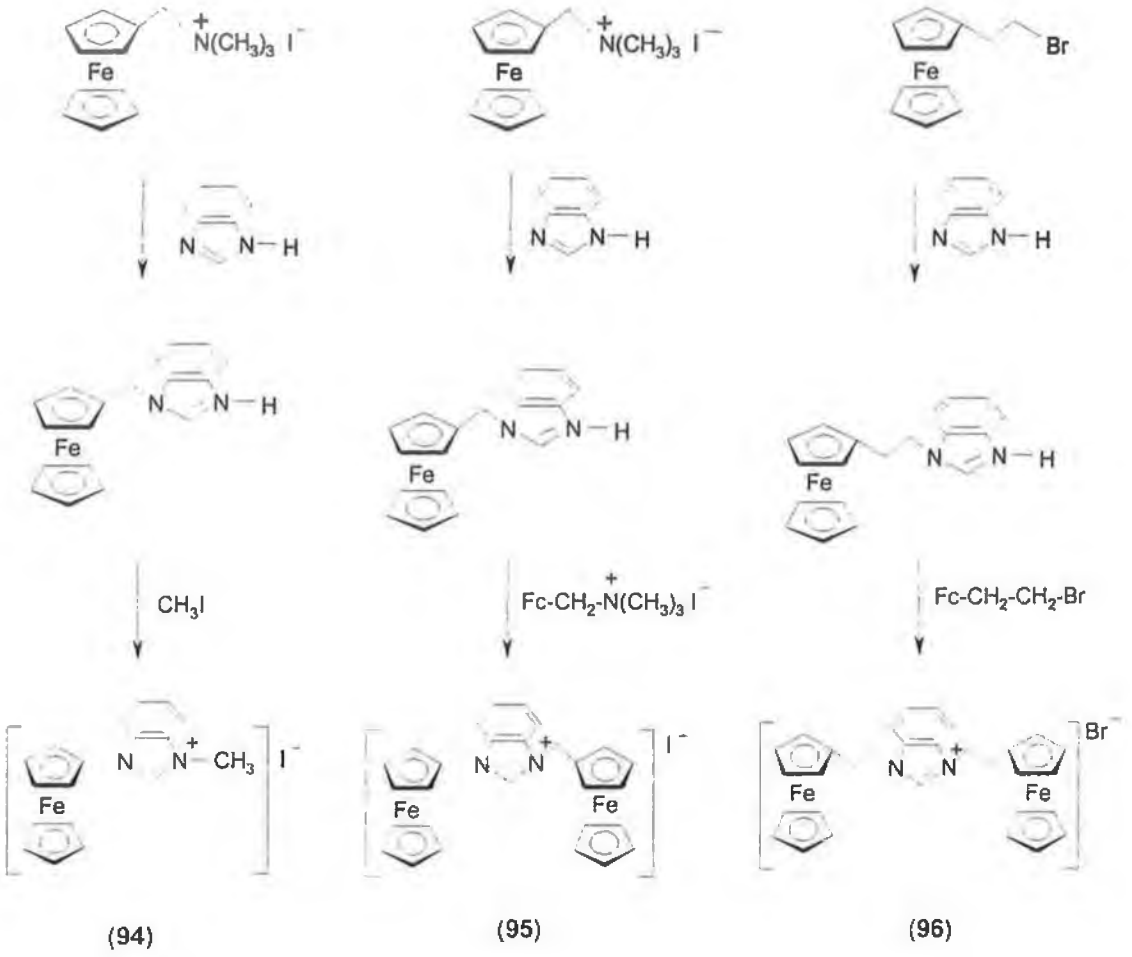

Scheme 1.17. *Pathways taken by Bildstein et al. to ferrocenyl–benzimidazoles.*

Other couplings of the imidazolium and ferrocenyl units have been reported. These include the facile introduction of the imdiazole unit by treatment of a ferrocenyl alcohol with *N,N'*-carbonydiimidazole (CDI) (**97**) (Scheme 1.18) [134]. A variety of chiral and achiral ferrocenylethylimidazoles (**98**)–(**102**) were produced in this way for biological applications.

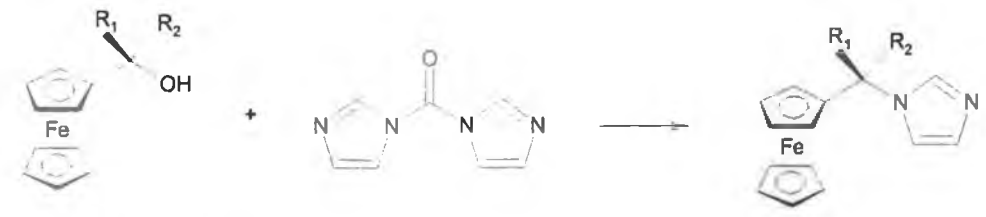

	R_1	R_2
(98)	H	H
(99)	H	CH_3
(100)	H	C_3H_7
(101)	H	C_6H_5
(102)	CH_3	CH_3

Scheme 1.18. *Use of CDI to couple ferrocenyl alcohols to imidazole.*

This technique was also used in the introduction of an imidazole entity into the first ferrocenyl–imidazole system with planar chirality (**103**). Starting from (*S*)-*S*-ferrocenyl-*S*-4-tolyl sulphoxide, going via an alcohol intermediate that was treated with CDI, a planar chiral ferrocenyl–imidazole was prepared. This was then converted with methyl iodide into the corresponding imidazolium salt (**104**) (Scheme 1.19) [135].

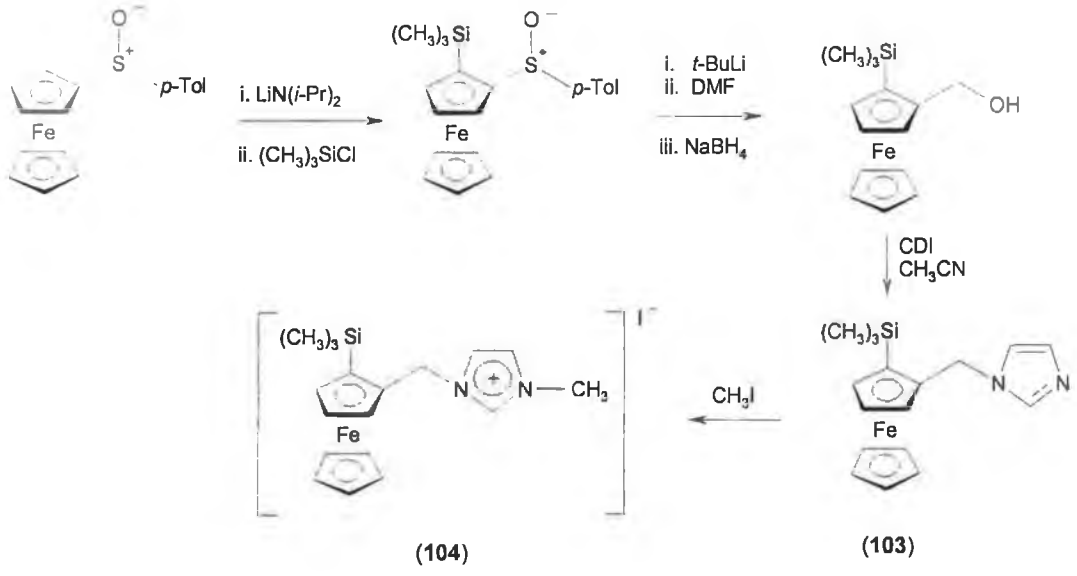

Scheme 1.19. *Synthesis of the first planar chiral ferrocene-imidazole.*

1.4.1.2 Ferrocenyl–azolium systems as carbene ligands

Bildstein et al. then employed the ferrocenyl–azolium salt systems that were synthesised by his group as *N*-heterocyclic carbene derivatives [136] (Scheme 1.20).

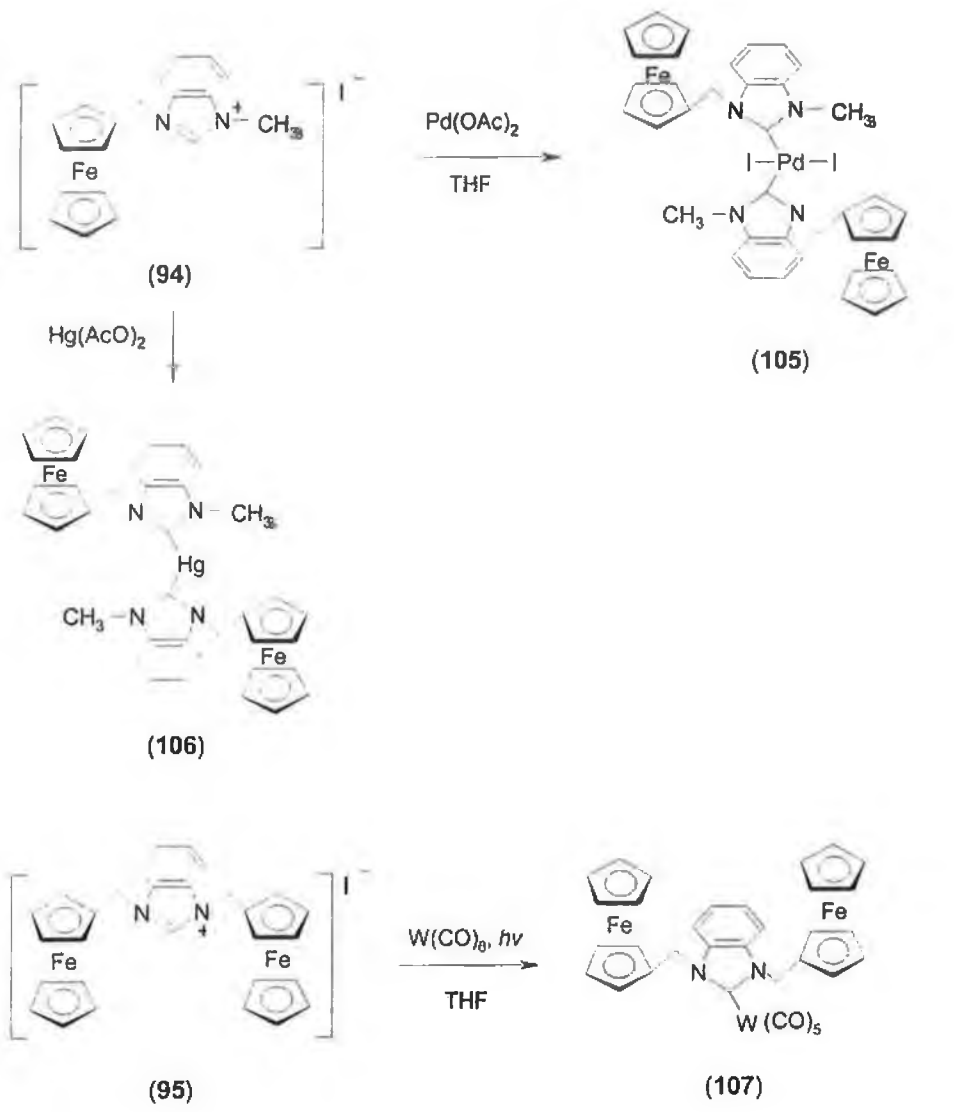

Scheme 1.20. The preparation of ferrocenyl–azolylidene complexes by Bildstein et al.

1-Methyl-3-(ferrocenylmethyl)benzimidazolium (**94**), 1,3-dimethylferrocenyl benzimidazolium (**95**) and 1,3-diethylferrocenylbenzimidazolium salts (**96**) were deprotonated in situ in the presence of metal acetate salts to the give the respective palladium, tungsten and mercury carbene complexes.

Also using 1,3-diferrocenylbenzimidazolium iodide (**108**), a silver complex (**109**) was prepared, although it was found that the preparation of palladium and mercury complexes was not possible. This was presumably due to the steric interaction of the ferrocenyl substituent and the insufficient basicity of the acetate anion preventing the palladium(II) planar geometry (Scheme 1.21).

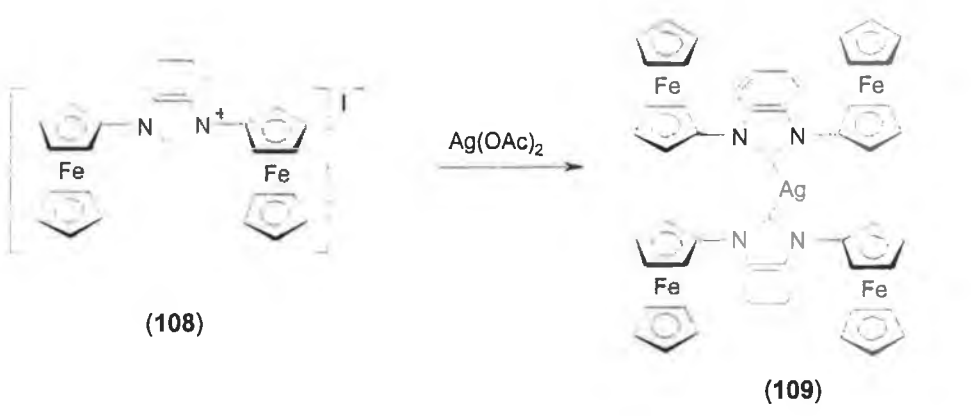

Scheme 1.21. *Preparation of a silver carbene complex (**109**) with a ferrocenyl–azolylidene ligand (**108**).*

A planar chiral carbene complex was prepared by Simenel et al. [135]. The planar chiral ferrocenyl–imidazolium salt (**104**) was employed as a carbene precursor for chromium (**110**) and rhodium (**111**) complexes (Scheme 1.22).

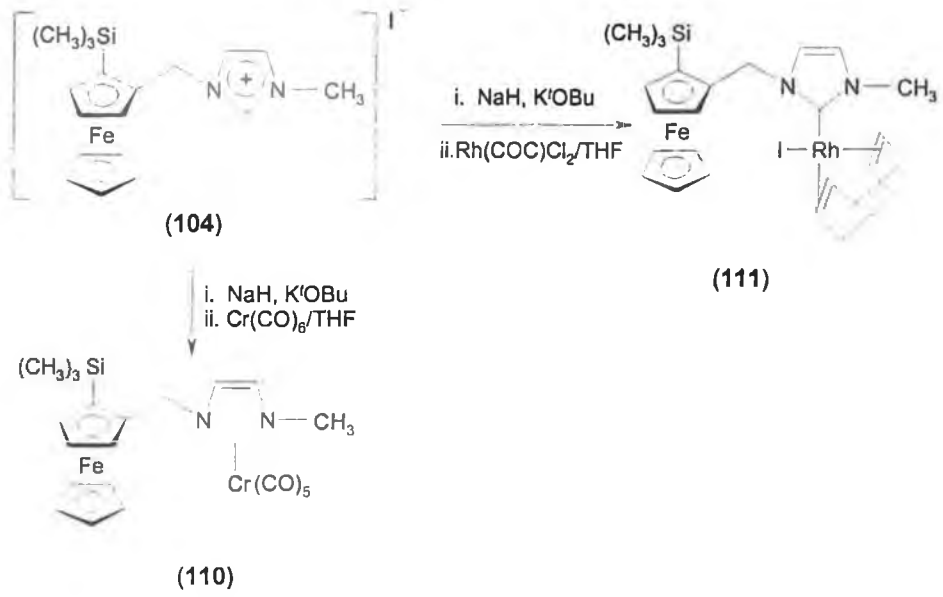

Scheme 1.22. *Chiral chromium and rhodium ferrocenyl–imidazolium complexes.*

1.4.2 Azole–phosphine compounds

1.4.2.1 P, N compounds as mixed ligands for catalysis

Bisphosphine chelate ligands have been employed very successfully in catalysis, however, it is of interest to investigate the effects of a mixed chelate system and the possible advantages it can offer in terms of improving catalyst efficiency. A ligand that employs both phosphorous and nitrogen atoms for co-ordination offers one of the most accessible and viable mixed ligand systems. P,N mixed ligands have a soft phosphorous donor and a hard nitrogen donor, and as such are classified as hemilabile ligands. The differing chelating properties of the two donor atoms means that hemilabile ligands offer a great potential for use in catalysis.

The phosphorous acts as a π-acceptor that can stabilize a metal center in a low oxidation state, whereas the nitrogen uses σ-donation, making the metal susceptible to oxidative addition reactions. Furthermore, the nature of the ligand can be modified

through the extensive substitution chemistry of the phosphorous atom, so that the reactivity of the particular system involved can be controlled. For example, phosphine sulphides and phosphine oxides can be obtained through the sulphonation and oxidation of phosphines.

Due to the hemilability of these mixed ligands, they can stabilize metals in a variety of co-ordination modes, geometries and oxidation states. It is this that leads to their usefulness in catalysis. Firstly, in an otherwise stable complex one end of the ligand, depending on the donor atom and the metal center, can dissociate allowing co-ordination of the organic substrate and the subsequent transformation can be carried out. Secondly, the additional stability associated with chelates ensures that the complex will still be stable in the absence of a substrate. Thirdly, as the P,N-ligands can act as bridging, bidentate or monodentate ligands, a variety of geometries and the stabilization of metal centers in different oxidation states are possible. This means that hemilabile ligands can stabilize the various oxidation states and geometries that can occur during a transition metal catalytic cycle.

So therefore, one approach to the design of a ligand for transition metal catalysis is where there are two different sites for co-ordination, leading to a complex where there is an inherently weaker bond. This then provides a point of preferential reactivity. Also a hemilabile ligand can often increase the reactivity of a catalyst compared to an inert diphosphine system. In some instances, a very weak chelate is needed to activate a transition metal to act in a catalytic system. But on the other hand, a strong bidentate ligand is needed in asymmetric catalysis so as not to allow unselective monodentate ligands to compete and reduce the enantioselectivity of the catalyst.

Furthermore, for the catalytic system to be effective and robust, the precursor should be stable to the inherent degradation processes in the cycle, but able to provide a high level of reactivity by offering a good supply of the intermediate reactive species. The stronger metal–ligand bond promotes the stability of the system by tethering the metal to the ligand as a monodentate ligand, keeping it in close proximity for the recovery step and minimizing entropy effects.

The coupling together of an azole or azolium moiety together with a phosphine functionality would provide a hemilabile system where there is a phosphorous atom available for co-ordination and then either a nitrogen or a carbene. Azole/azolium–phosphorous systems are relatively rare in organic synthesis and only a few such molecules exist. Typically, these two are employed as mixed ligands in co-ordination chemistry. However, there have been very few linkages of an azole heterocyclic ring with a phosphorous to create a novel mixed donor ligand.

It is the substitution of the phosphine functionality at the 2-position on the imidazole ring that has been the popular linkage so far. This group divides into two types: monoazol-2-yldiphenylphosphines and bis- and trisazol-2-yl(phenyl)phosphines. The latter group will be discussed first.

1.4.2.2 Bisazol-2-ylphenyl phosphines and trisazol-2-yl phosphines

A variety of heterocycles, e.g. furan, thiophene and pyridine and also pyrimidine, substituted with a phosphine entity have been reported [137–139], but the first synthesis of a 2-imidazolylphosphine was by Curtis and Browne in 1980 [140] – tris(4,5-dimethylimidazol-2-yl)phosphine (**112**). This was prepared by lithiation of imidazole and subsequent treatment with PCl_3, creating a triheteroarylsubsitituted tertiary phosphine.

Moore and Whitesides a little later in 1982 [141], prepared a range of heterocyclic tertiary phosphines, including tris(1-methylimidazol-2-yl)phosphine (**113**), (1-methylbenzimidazol-2-yl)diphenylphosphine (**114**) and bis(1-methylbenzimidazol-2-yl)phenylphosphine (**115**), and some of which were co-ordinated to platinum (1,5-cyclooctadiene)dimethylplatinum(II), (COD)Pt(CH_3). *Cis*-dimethylbisphosphine platinum(II) complexes (e.g. **116**) were yielded where the ligands were found to act exclusively as monodentate ligands, binding through the phosphorous atom (Figure 1.27).

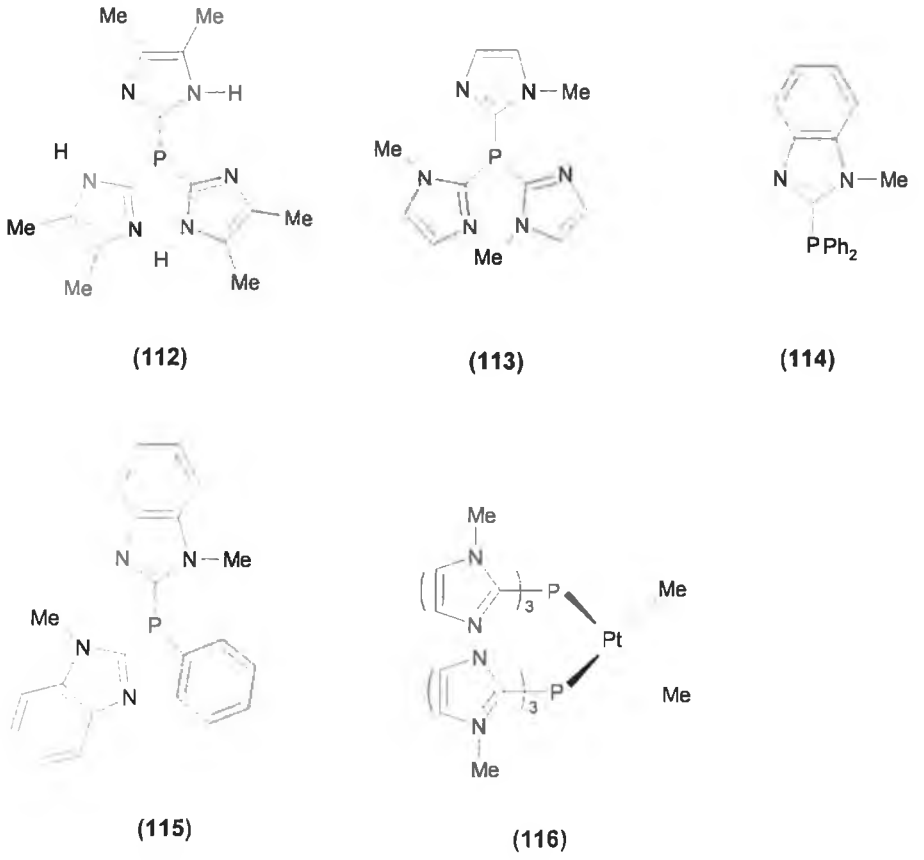

Figure 1.27. *Azole tertiary phosphines.*

Other tris(imidazol-2-yl)phosphines have been prepared and then employed as ligands (Figure 1.28). However, in contrast to the findings of Moore and Whitesides it has been seen that these ligands usually act as tridentate N-donors (**117**) and as such have been used as biomimics of the active site of enzymes whose active sites are lined by histidine residues. Tris[2-(1-*iso*-propyl-4-*tert.*-butylimidazol-2-yl)]phosphine ($Pim^{^{i}Pr,\ ^{t}Bu}$) (**118**) represents a very good structural model of the enzyme carbonic anhydrase. The active site of this enzyme contains three histidine residues that bind a zinc cation in a tridentate manner, and the $([Pim^{^{i}Pr,\ ^{t}Bu}]Zn[OH])^{+}$ complex (**119**) reproduces this environment very well, allowing the evaluation of the coordination abilities of the enzyme's active site [142]. To this end, several studies have been performed on this

system, where other zinc, cadium [143] and cobalt [142,144] complexes have also been employed as the central metal, e.g. $[(Pim^{iPr,\ tBu})Cd(OH_2)(OClO_3)]ClO_4$ (**120**) and $(Pim^{iPr,\ tBu})M(NO_3)$ (M=Zn, Co) [144].

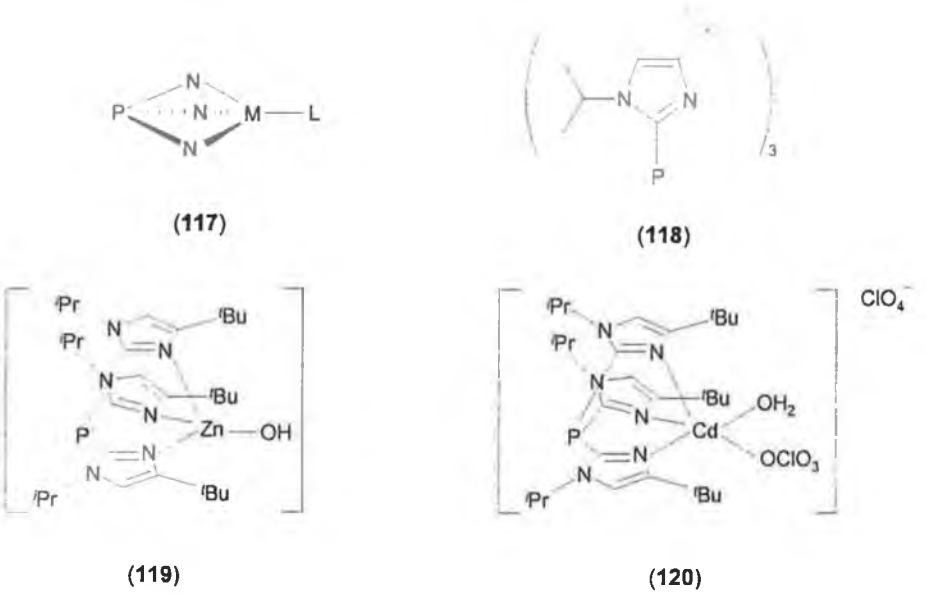

Figure 1.28. *Tris(imidazol-2-yl)phosphines.*

Imidazol-2-ylphosphines have also been used as mimics for hemocyanin, which has a dicopper active site where each copper Cu(I) center is coordinated to three histidine moieties. Complexes of the type [Cu(T1Et4RIP)L]X, where T1Et4RIP=tris(1-ethyl-4-R-imidazol-2-yl)phosphine, R=Me and ^{i}Pr, L=MeCN and O_2 and X=PF_6, ClO_4 and CF_3SO_3, were prepared and it was seen that the imidazolylphosphine ligand acted as a tridentate N-donor system [145].

A group of enzymes have been isolated that contain diiron active sites, including hemerythrin, ribonucleotide reductase and pseudocatalase, all of which have five histidine residues in the active site. Kurtz et al. [146] employed the phosphine–imidazole ligands in order to investigate the structural and physical

properties of these enzymes. Iron and manganese cluster compounds were assembled, yielding (μ-oxo/hydroxo)bis(μ-carboxylato)diiron(III) and dimanganese(III) complexes that used tris(imidazo-2-yl)phosphines as tridentate capping ligands – $[Fe_2O(L)(TMIP)_2](ClO_4)_2$, where L=acetato or hydroxyl and TMIP=tris(1-methylimidazol-2-yl)phosphine.

1.4.2.2 Monoazol-2-yldiphenylphosphines

The synthesis and subsequent use of monoazol-2-yldiphenylphosphines as ligands for uses other than as enzyme active site mimics has been very limited. The synthesis of bis(2-diphenylphosphinoimidazol-1-yl)methane (**121**) [147] and various alkylimidazolium phosphines (**122**) [148] have been reported (Figure 1.29). The 2-imidazolium phosphines were successfully employed as ligands in the Rh-catalysed hydroformylation of 1-octene in basic conditions.

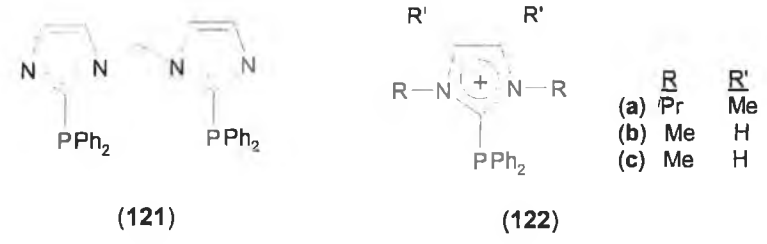

Figure 1.29. *Monoazol-2-yldiphenylphosphines.*

1-Methylimidazol-2-yldiphenylphosphine (dpim) (**123**) has been effectively used as a monodentate ligand for Pd (**124**) and a novel type of P–N bridging ligand for binuclear Pd (**125**), Ag(I) (**126**) and Cu(I) (**127**) complexes [149] (Figure 1.30). In the case of the mononuclear palladium(II) complex, dpim acted as a monodentate P-donor ligand, which in solution exists in the *cis* and *trans* forms. This was obtained by

treatment of $PdCl_2(PhCN)_2$ with the ligand producing $[Pd_2Cl_2(dpim)_2]$ (**124**), which by further treatment with $Pd(dba)_2$ (dba=dibenzylideneacetone) yielded the bridged dinuclear $[Pd_2Cl_2(dpim)_2]$ complex (**125**). Here, though, dpim acts as a bidentate P,N-donor ligand.

Complex **126** was characterized as a nitrate-bridged polymeric silver(I) complex. A stoichiometric reaction of dpim with silver nitrate in methanol gave a complex with an eight-membered annular core with the formula $[Ag_2(\mu\text{-dpim})(NO_3)]NO_2$ (**126**). Again, the dpim acting as both a P and N-donor, with two ligands bridging the silver metal centers in a head-to-tail configuration.

On reaction of $[Cu(MeCN)_4]ClO_4$ with dpim, a rare type of triply-bridged Cu(I) complex was yielded – $[Cu_2(\mu\text{-dpim})_3(MeCN)]ClO_4$ (**127**). It was seen that the dpim ligand used both the nitrogen and phosphorous in its co-ordination. Its geometry was such that one copper center had a distorted tetrahedral co-ordination, using two phosphorous atoms and one nitrogen with MeCN also acting as a ligand and the second copper center was triply co-ordinated with two nitrogens and one phosphorous.

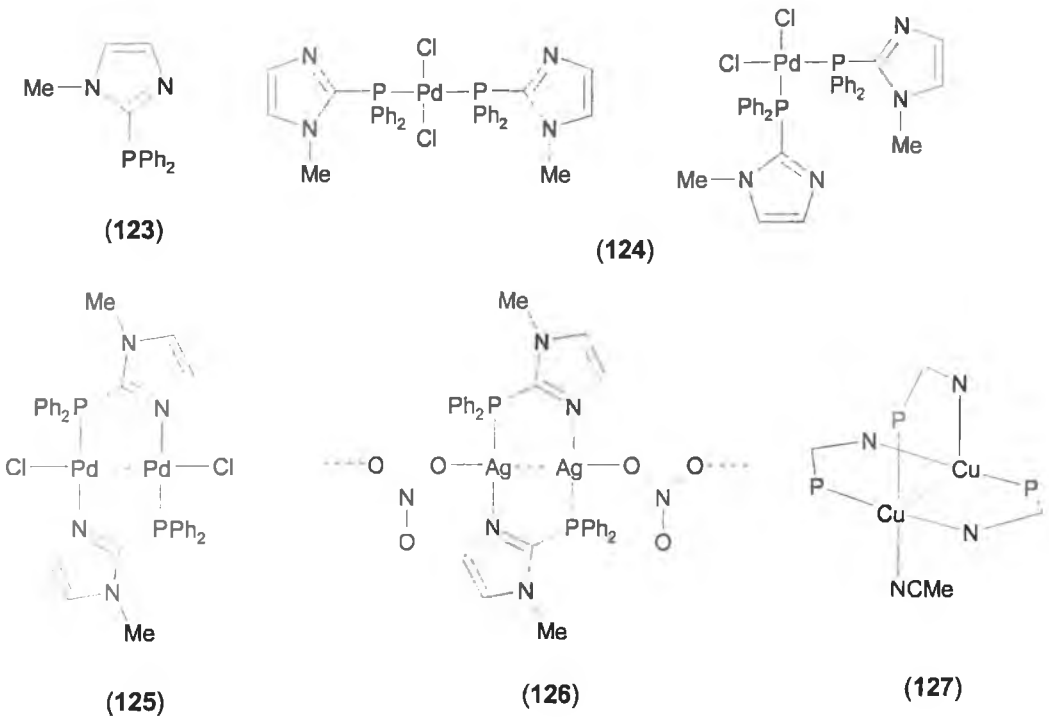

Figure 1.30. *Dpim (123) and its use as a monodentate and P–N bridging ligand for Pd, Ag and Cu.*

1.4.2.3 Other phosphine–azole compounds

Very few compounds with linkages between azole and phosphine moieties have been reported. Wasserscheid et al. [150] have prepared compounds with a phosphine as an *N*-terminal attachment with alkyl or aryl spacer groups (**128–130**) as part of research into ionic liquids (Figure 1.31). However, so far these compounds have not been applied as chelate ligands or to catalysis.

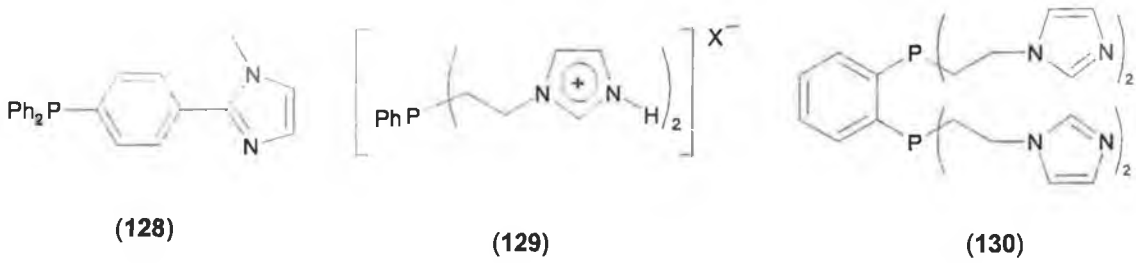

Figure 1.31. *Phosphine–azole systems prepared by Wasserscheid et al.*

1.5 Ferrocenyl–phosphine systems

1.5.1 Ferrocenyl diphosphines

Ferrocene–phosphorous chemistry has been a very widely investigated area for many years, and of which ferrocenyl diphosphine compounds are among the most intensively studied species. In the late 1970s, Kumada et al. synthesised 1,1′-bis(diphenylphosphino)ferrocene (dppf) (**131**) (Figure 1.32) and discovered that it was an excellent catalyst for the coupling of Grignard reagents and alkyl halides and alcohols [151,152], leading to considerable research attention focusing primarily on the use of dppf compounds as ligands in catalysis.

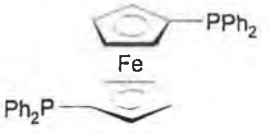

(**131**)

Figure 1.32. *Dppf.*

A vast array of co-ordination compounds have been prepared using dppf as a chelate ligand due to the various co-ordination modes it employs [153]. The skeletal flexibility of the ferrocene backbone, variations in metal geometry and the bonding modes of co-ligands leads to many diverse and unpredictable structures being produced. Shown in Figure 1.33 are some of the co-ordination compounds prepared employing dppf as a ligand (**132**)–(**135**) [153–157].

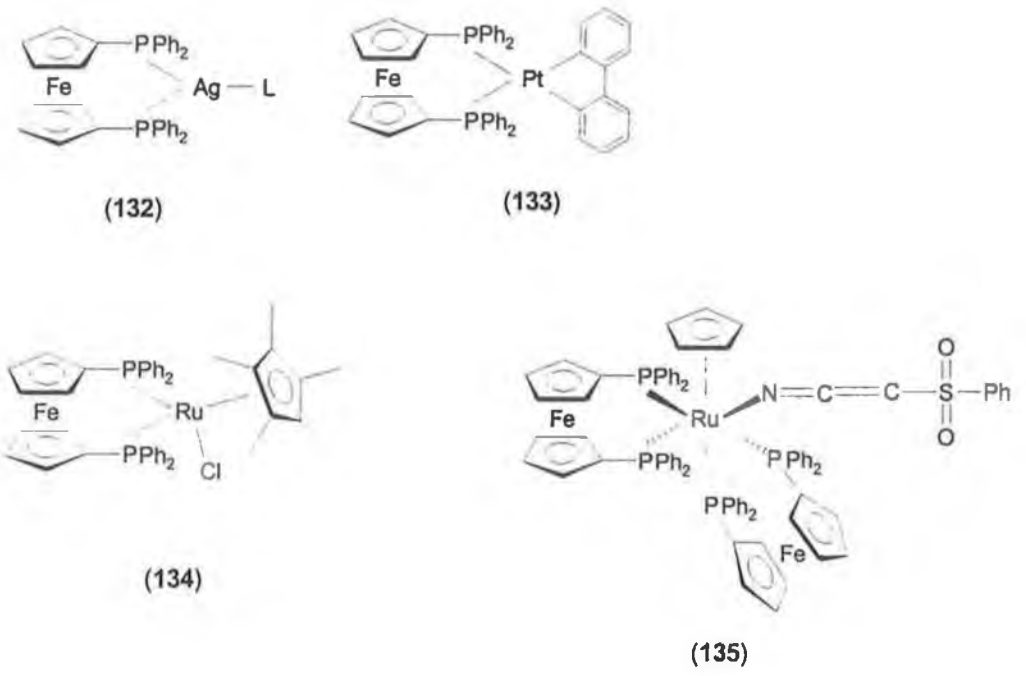

Figure 1.33. *Some of the co-ordination compounds formed using dppf as a ligand (132)–(135).*

The most closely related compounds to the ferrocenyl diphosphines include the analogous alkyl 1,1′-ferrocenyl alkylphosphines (**136**) [158,159], 1,1′-bis[(diphenylphosphino)methyl] ferrocene (dpmf) (**137**) [160] and monosubstituted ferrocenyl dialkylphosphines [161] (Figure 1.34).

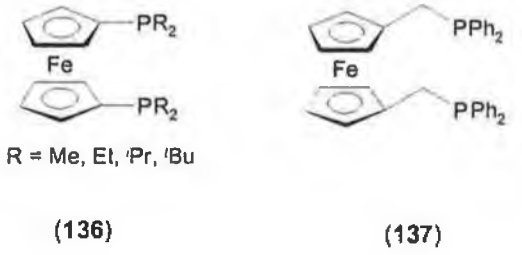

Figure 1.34. *1,1′-Ferrocenyl alkylphosphines (136) and (137).*

Another important class of ferrocenylphosphines are the [1]phosphaferrocenophanes, having the structural formula FcPR (Fc=ferrocene). In 1980, Seyferth prepared the first ferrocene compound internally bridged by phosphorous, (1,1′-ferrocenediyl)phenyl phosphine (**138**) [162] (Figure 1.35). Full structural analysis [163] showed the two Cp rings tilting inwards to accommodate the phosphorous bridge.

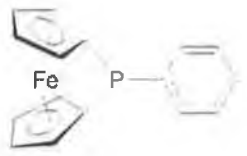

(138)

Figure 1.35. *First prepared and characterised [1]phosphaferrocenophane (**138**).*

1.5.2 Chiral ferrocenyl–phosphines

Ferrocene, when it was first discovered, was treated very much as an organometallic aromatic species analogous to benzene; however, it was soon observed that it could give rise to planar chirality as well as atom-centered chirality. An asymmetrical 1,2-relationship between the substituents on the same Cp ring will create enantiomers based on a plane of symmetry running through the molecule (Figure 1.36). This stereoisomeric feature of ferrocene is one of the principal reasons for the large amount of interest in using ferrocene as a ligand. Chiral ferrocene molecules have been employed very successfully in asymmetric transition metal catalysis.

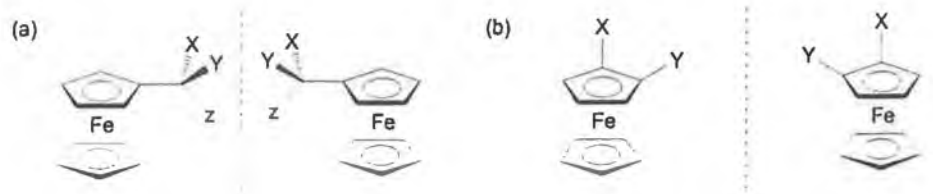

Figure 1.36. *Enantiomers of ferrocene resulting from (a) atom-centred chirality and (b) planar chirality.*

The first chiral ferrocenyl phosphine reported was prepared by Hayashi in 1974, R,S_p-*N,N*-dimethyl-1-[(2-diphenylphosphino)ferrocene]ethylamine (PPFA) (**139**) [164]. The synthesis of which is shown in Scheme 1.23. The chiral auxiliary ensures that *ortho*-lithiation occurs and is highly diastereoselective, through chelation of the lithium by the amine nitrogen. Reaction then with an electrophile gives a 1,2-disubstituted ferrocene.

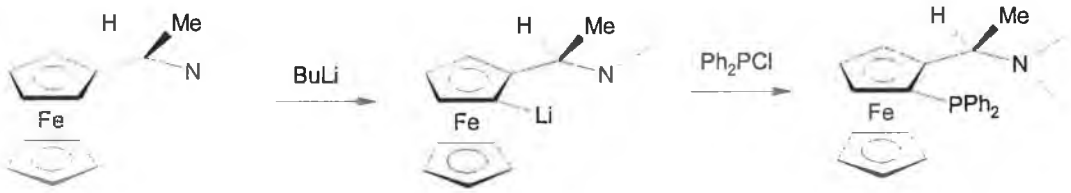

(139)

Scheme 1.23. *The synthesis of (R,S_p)-N,N-dimethyl-1-[(2-diphenylphosphino) ferrocene]ethylamine.*

This technique has led to many planar ferrocenylphosphines based on *N,N*-dimethyl-1-ferrocenylethylamines as the chiral auxiliary. In addition, racemic mixtures of chiral ferrocenes have been prepared that have been separated by the classical technique of resolution using an enantiomerically pure base to prepare diastereoisomers that can be separated by chromatography.

1.5.3 Use of ferrocenyl–phosphines in catalysis

1.5.3.1 Dppf

Since Kumada et al. first employed dppf as a ligand in the catalysis of Grignard cross-coupling between organic bromides [165] and allylic alcohols [152] with $PdCl_2$, there has been an expanding catalogue of transition metal catalysed reactions in which it has been successfully used as a ligand.

So far it has been its use in palladium complexes that has created most of the interest. Some recent developments in this ever-expanding area of research are given in Figure 1.37 as an indication of the scope of applications of dppf as a ligand in transition metal catalysis [166–170].

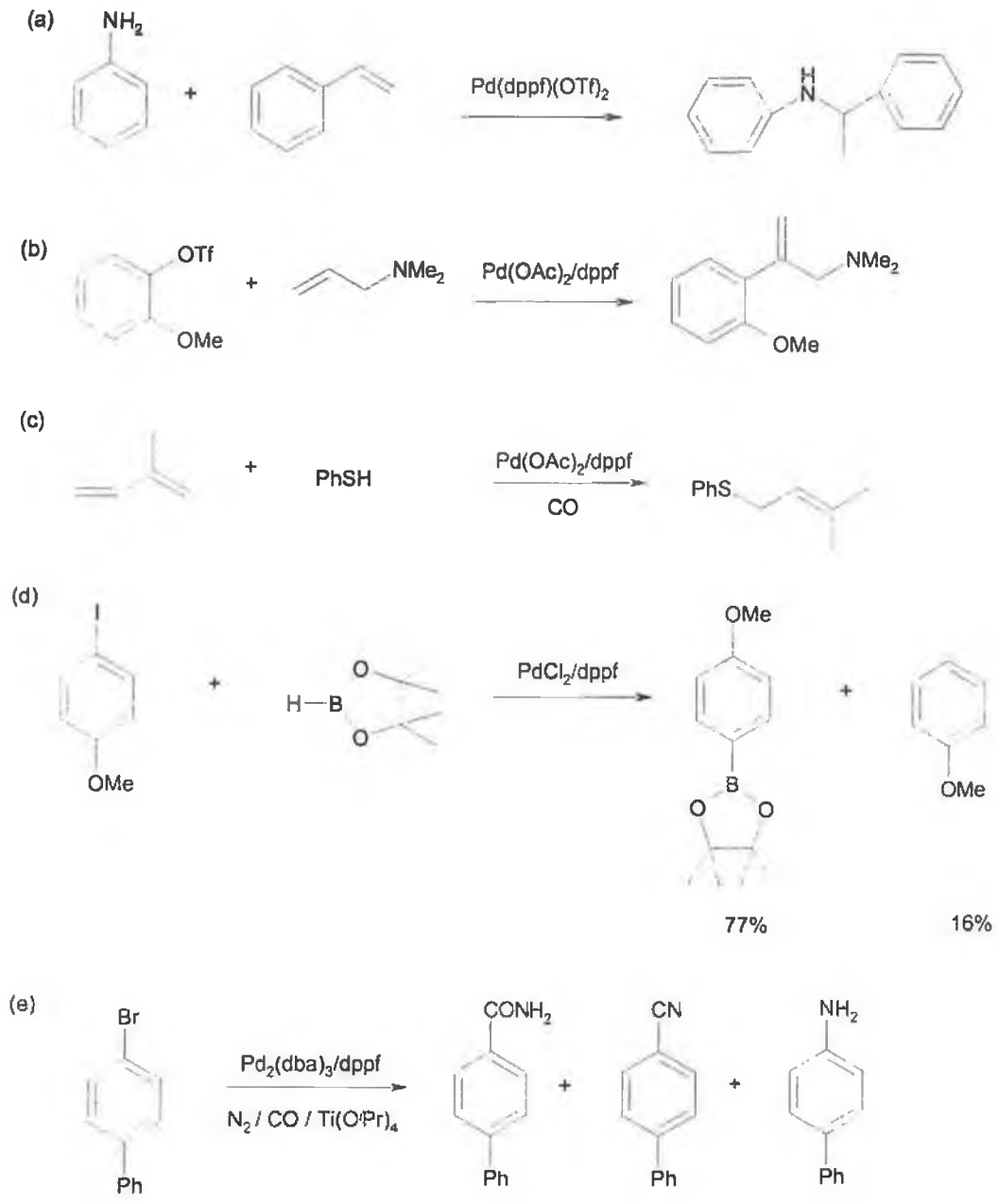

Figure 1.37. The use of dppf as a ligand in palladium-catalysed organic reactions. (a) Hydroamination [166], (b) benzyne/alkene insertion [167], (c) thiocarbonylation [168], (d) borylation [169], (e) carbonylation and nitrogenation [170].

However, there has been limited use of other transition metals, such as rhodium in the coupling of arylboronic acids and carbonyl compounds [169,171], cobalt and nickel [170] (Scheme 1.24).

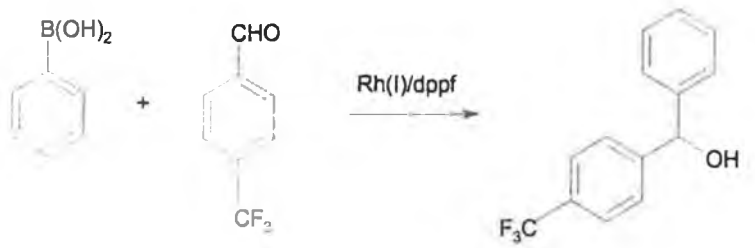

Scheme 1.24. *Rhodium-catalysed cross-coupling using dppf.*

1.5.3.1 Chiral ferrocenyl–phosphines

The driving force behind the area of chiral ferrocenyl phosphines has been their use in catalysis. For asymmetric catalysis, these compounds have several features that make them attractive. Firstly, planar chiral systems, such as ferrocene, never undergo racemisation. Secondly, ferrocene, due to having two Cp rings, can act either as a mono or bidentate ligand, and the chelating entities can either be the same or mixed. Therefore a great variety in bonding modes is possible. Finally, in the case of ferrocenylphosphines having both planar and central chirality, the atom-centered chiral side-chain can participate in the reaction site, aiding the asymmetric selectivity of the product (Figure 1.38).

These factors give the chiral ferrocenylphosphines a major advantage in that they are very flexible with regard to the side-chains and the phosphine groups, meaning that there is a huge potential for modification and hence fine-tuning of the ligand for specific catalytic tasks.

A few examples include the synthesis of (+)-biotin [171], asymmetric hydrogenation of ketoesters [172], asymmetric aminolysis [173], Grignard cross-coupling [174], asymmetric allylations [175] and hydrosilylation [176], and are shown in Figure 1.38.

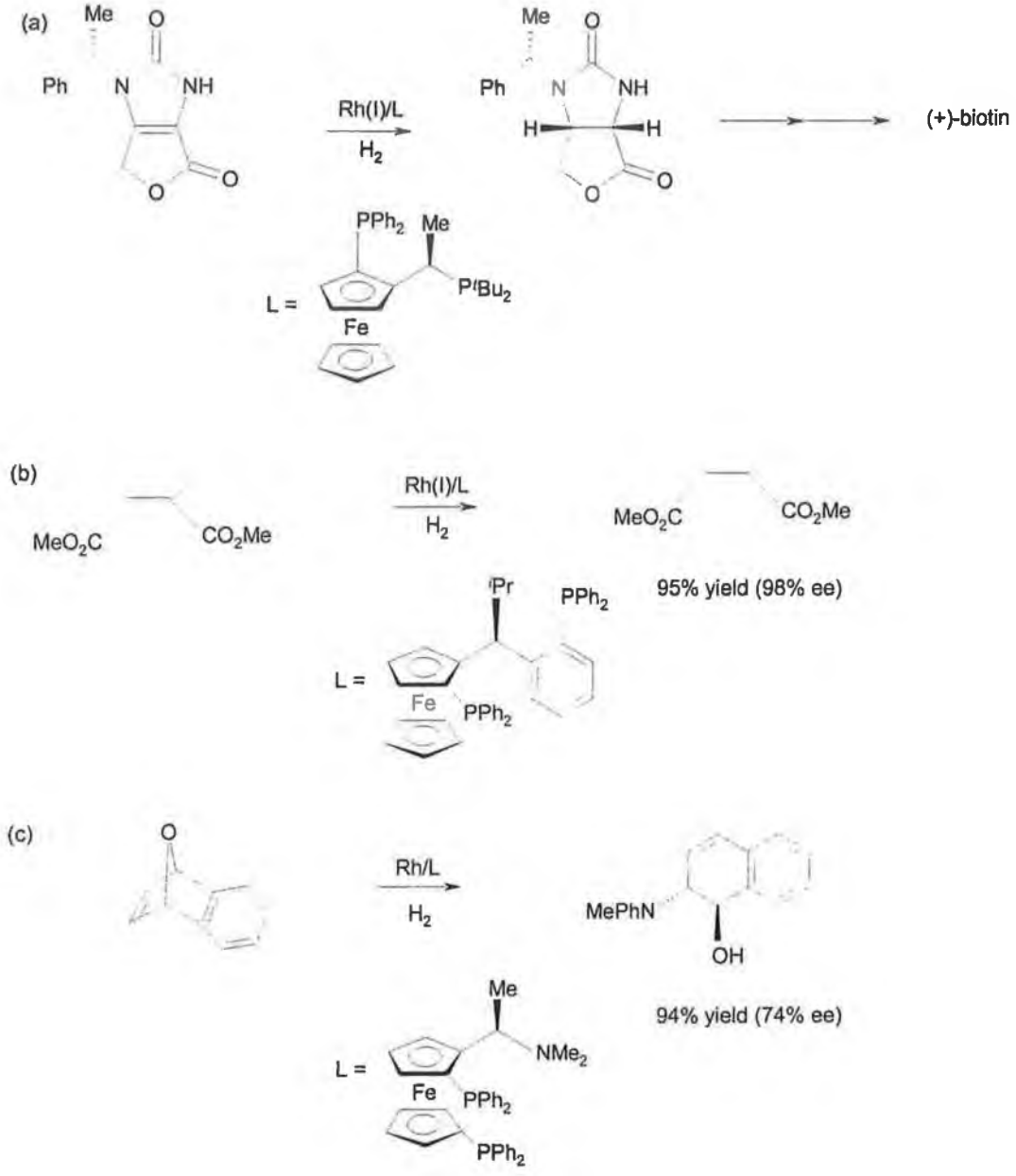
(a)
Me
O
Ph
N
NH
O
O
Rh(I)/L
H2
Me
O
Ph
N
NH
H
H
O
O
(+)-biotin
PPh2
Me
L =
PtBu2
Fe
(b)
MeO2C
CO2Me
Rh(I)/L
H2
MeO2C
CO2Me
95% yield (98% ee)
iPr
PPh2
L =
Fe
PPh2
(c)
O
Rh/L
H2
MePhN
OH
94% yield (74% ee)
Me
NMe2
L =
Fe
PPh2
PPh2

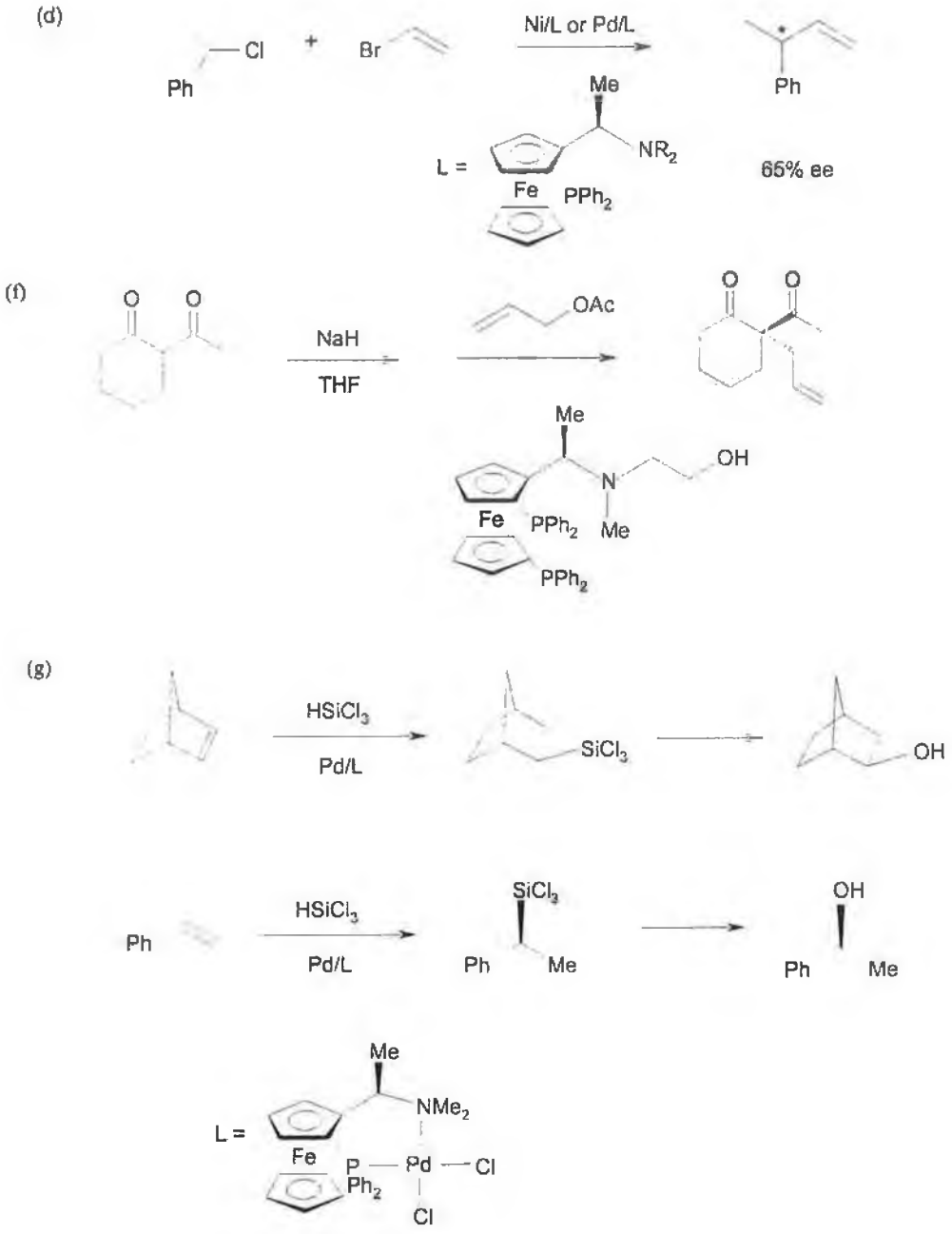

Figure 1.38. *The use of chiral ferrocenylphosphines in asymmetric catalysis.*

1.6 Design of ferrocenyl–azolium salts

As discussed, the azole/azolium system has a lot of potential applications and as such our compounds were designed with two main purposes in mind: as auxiliary ligands in transition metal catalysis and as chemoreceptors for anion recognition. It was proposed to couple together an azolium moiety together with a ferrocene unit. This offers the novelty in both applications, as ferrocene has not been employed as appendage to an azolium system in transition metal-mediated catalysis and the azolium system was only very recently discovered as a promising ligand for use in the electrochemical detection of substrates.

1.6.1 For application as auxiliary ligands in transition metal cross-coupling reactions

In the 1,3-disubstitutedimidazolium salts applied as auxiliary ligands in organometallic cross-coupling reactions, as discussed in Section 1.2.2, a variety of different R substituents have already been employed. However, one substituent that has not been used though is the metallocene unit ferrocene. Thus, the rationale behind applying the proposed ferrocenyl–azolium systems to transition metal catalysis was to investigate the effect of this organometallic species on a specific transition metal-mediated reaction.

Ferrocene has the well-known property of being able to stabilize adjacent electron deficient centers. The stabilization of simple carbenium ions R_2FcC^+ is achieved by delocalisation of the positive charge via a η^6-fulvene-η^5-cyclopentadienyl-Fe(II) (**140**) resonance structure with an exocyclic bent fulvenoid double bond (Scheme 1.25) [41].

(140)

Scheme 1.25. *Stabilisation of a ferrocenylcarbenium ion via the resonance structure (140).*

It was thought that the ferrocenyl unit may be able to effectively stabilize a generated carbene center. It has also been shown that more sterically demanding R groups in the imidazolium structures were able to increase the reaction rates in these catalytic reactions [63]. To this end, substituted phenyl rings had been incorporated in the 1,3-dialkylimidazolium salts [62,63], but so far a ferrocenyl substituent – which would offer a comparitive bulk – had not be utilized.

Therefore, as ferrocenyl–imidazolium salts had previously been prepared (**83** and **84**) for anion recognition studies [125,126] (Figure 1.25), it was decided to extend the application of these compounds to transition metal-mediated synthesis. Also, as no studies had been carried out on the application of benzimidazolium salt systems as auxiliary ligands for cross-coupling reactions, we decided to prepare a series of ferrocenyl–benzimidazolium compounds (**141**) of the type outlined in Figure 1.39.

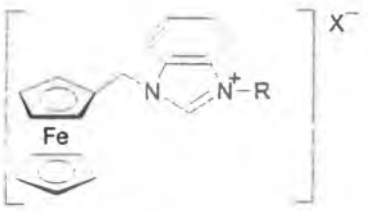

(141)

Figure 1.39. *The proposed ferrocenyl–benzimidazolium salts.*

Furthermore, ferrocene offers the possibility of inducing planar chirality into the system. Although a range of chiral imidazolylidene complexes have been reported and applied to asymmetric transition metal catalysed cross-coupling processes [40], no chiral ferrocenyl–azolylidene complexes have been employed in catalysis. The introduction of central chirality can be easily accomplished in azolium salts, which can then be applied to asymmetric cross-coupling reactions, as has already been shown. However, it was thought a novel pathway to a chiral azolium compound could be achieved by incorporating planar chirality via the ferrocene unit (Figure 1.40) (**142**). Planar chirality offers the clear advantage that racemisation of the compound never occurs, thus, extending the lifetime of the catalyst.

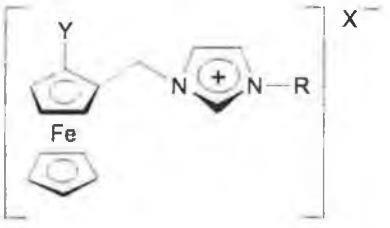

(142)

Figure 1.40. *Proposed ferrocenyl–imidazolium salt (142) with planar chirality.*

1.6.2 For application as chemoreceptors for anion recognition

For the anion recognition application of the ferrocenyl–azolium system, it was envisaged that ferrocene could be used to provide a redox centre capable of the electrochemical recognition of anions. The pendant imidazolium salt moieties would be able to co-ordinate to the anions and, hence bring them into close proximity for transduction to occur at the ferrocene metal centre.

The application of ferrocenyl–azolium hexafluorophosphate salt systems (**83**)–(**87**) to anion recognition has already been shown by Thomas et al. and Hanlon [125,126] (Section 1.3.4.2), but these monosubstituted ferrocenyl–azolium systems did not show any selectivity. A novel type of molecule is therefore required to induce selective anion binding. Macrocyclic ferrocenyl–azolium systems of the two types – (**143**) and (**144**) – shown in Figure 1.41 were proposed.

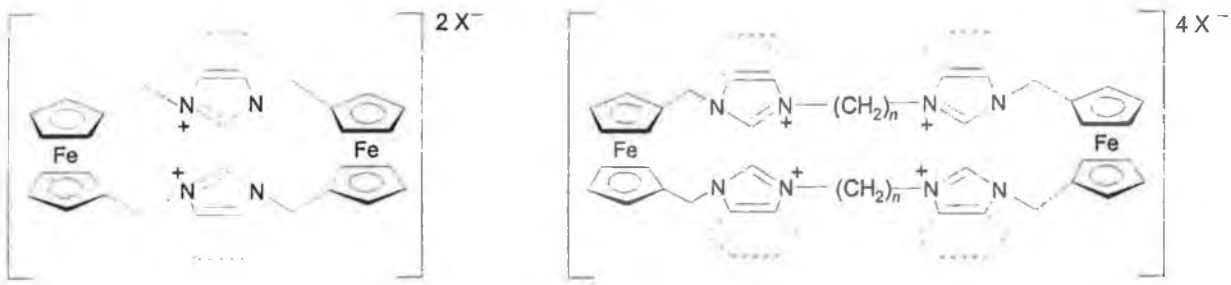

(143) **(144)**

Figure 1.41. *Proposed macrocyclic ferrocenyl–azolium structures.*

A cavity is present in both systems that may aid selective anion binding. In structure **143**, the cavity is more rigid and has two azolium functionalities present, in structure

144 there are four azolium centres with linking alkyl chains that are capable of allowing the system to be more flexible. In both cases, the orientation of the azolium rings and, thus, the direction of the hydrogen bonds will need to be considered in the topology of the cavity and, thus, will be important in the co-ordination of anions and any possible selectivity.

1.6.3 Synthesis

While a synthetic route to the monosubstituted ferrocenyl–azolium salts has been established [125,126], a novel synthetic procedure for these macrocyclic systems was required. Thus, it was proposed that the 1,1′-bis(1-methylazole)ferrocene (**145**) would be the key starting point from which the macrocycles could be prepared. This would then allow the preparation of 1,1′-bis(1-alkyl-3-methylazolium)ferrocenyl salts (**146**), which could also be employed as novel *N*-heterocyclic carbene ligands and novel bidentate auxiliary ligands for transition metal-mediated catalysis (Figure 1.42).

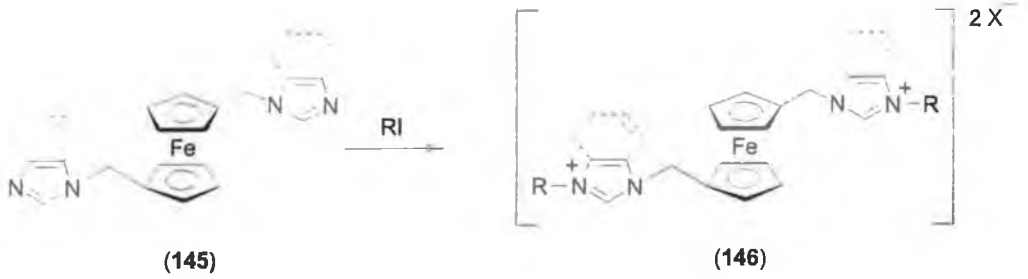

Figure 1.42. *1,1′-Bis(1-methylazole)ferrocene (**145**) as a starting point for the macrocycles (**143**) and (**144**) and 1,1′-bis(1-alkyl-3-methylazolium)ferrocenyl salts (**146**).*

We also proposed the preparation of a linear bisazolium–ferrocenyl system (Figure 1.43) that could be applied both as a bidentate ligand and a possible anion receptor. It would enable a comparative study against the 1,1′-(bisazolium)ferrocenyl salt compounds (**146**). In the case of its application as an *N*-heterocyclic carbene ligand, it can be compared to **146** to determine what effect the spacer unit between the two carbene moieties would have on the efficiency of the bisazolium systems as chelates. For the anion recognition studies, it would be interesting to observe it as an acyclic analogue of marcocycle (**144**) and if it could confer any selectivity as a receptor, possibly by wrapping around the anion. Thus, the preparation of the bridged monosubstituted unit – [1-(1-ferrocenylmethyl)-3-alkylazolium]-3-(1-ferrocenylmethyl)azolium salt (**147**) – was envisaged.

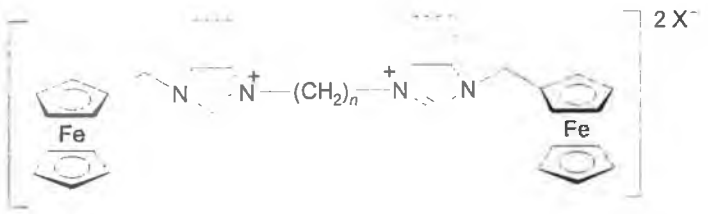

(145)

Figure 1.43. *The proposed linear bisazolium–ferrocenyl system.*

Chapter 2

Synthesis of Ferrocenyl–Azolium Salts

2.1 Introduction

As outlined in Section 1.6, a range of monosubstituted ferrocenyl–imidazolium and ferrocenyl-benzimidazolium salts would be prepared along with 1,1′-bis(azolium)ferrocenyl (**146**) and linear bisazolium–ferrocenyl (**147**) salts. Also the preparation of macrocyclic systems (**143**) and (**144**) would be attempted.

2.2 Results and discussion

2.2.1 Monosubstituted ferrocenyl–azolium salts

2.2.1.1 1-Ferrocenylmethylazoles

The initial aim was the extension of the already prepared ferrocenyl–azolium systems. 1,3-Disubstituted imidazolium salts can be prepared by a few different methods: (i) via preparation of a 1,4-diazobutadiene (DAB) from the condensation of an amine with a glyoxal followed by treatment of the DAB with *para*-formaldehyde and HCl [177]; (ii) one-pot condensation of amines, *para*-formaldehyde and glyoxal under acidic conditions [178] or (iii) by alkylating 1-substitutedazoles with an alkyl halide (usually iodoalkanes) [68] (Scheme 2.1).

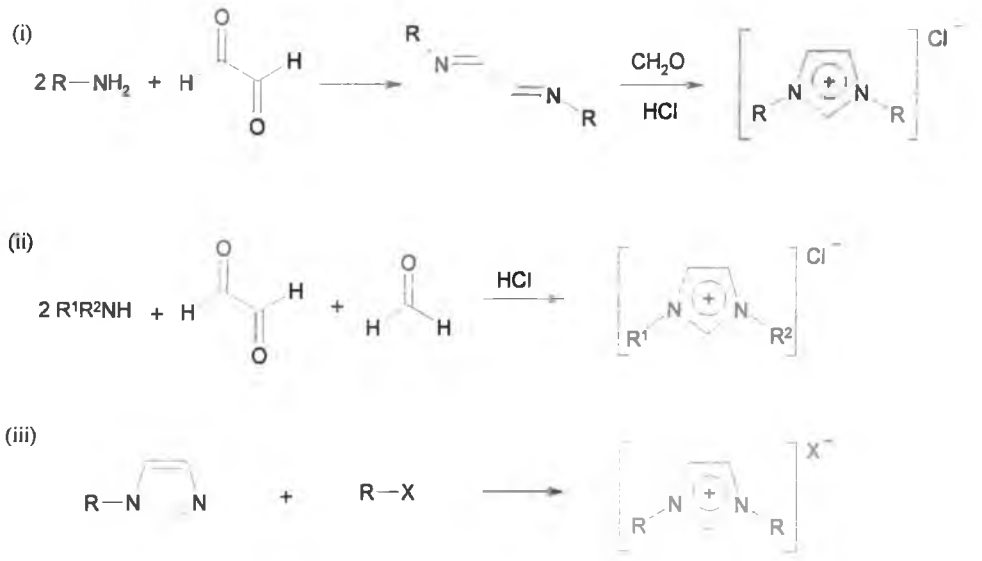

Scheme 2.1. *Methods for imidazolium salt synthesis.*

Following the synthetic route taken by Thomas and Hanlon [125,126] a ferrocenyl–imidazole system was prepared initially, which would then be quarternised by alkylation [method (iii)], yielding ferrocenyl–imidazolium iodides. So the starting point for the synthesis of the ferrocenyl–azolium salts was 1-ferrocenylmethylimidazole (**148**), along with the benzimidazole analogue, 1-ferrocenylmethylbenzimidazole (**149**) (Figure 2.1).

(148) **(149)**

Figure 2.1. *The key intermediates – 1-ferrocenymethylazoles (148) and (149).*

In coupling the ferrocene and azole unit in a facile and high-yielding manner, (ferrocenylmethyl)trimethylammonium iodide (**150**) had proved an ideal starting

material. This compound is an excellent electrophile due to the well-known leaving group properties of the trimethylamine entity, and it can be produced in a convenient route almost directly from ferrocene via an adaptation of the Mannich reaction (Scheme 2.2).

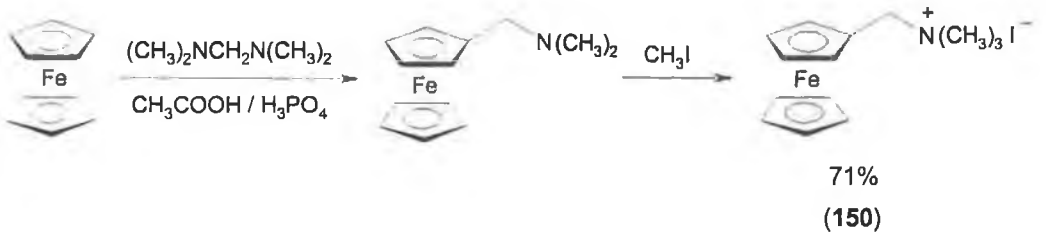

71%

(150)

Scheme 2.2. *Synthesis of* ***150****.*

The azole unit is then employed as the nucleophile. For the electrophilic attack of the ring-nitrogens in the azoles, there are two possible pathways: The first is the electrophilic attack of the neutral azole entity and the second is the electrophilic attack of the azolide anion.

Following the S_E2' mechanism, the classical imidazole alkylation illustrates the first pathway. The imidazole and alkyl halide are reacted together; here, the pyridine-like nitrogen will attack the alkyl halide, generating a positively charged ion that will lose the pyrrole-hydrogen to become neutral (Scheme 2.3). This pathway often leads to loss of product through quaternary salt formation.

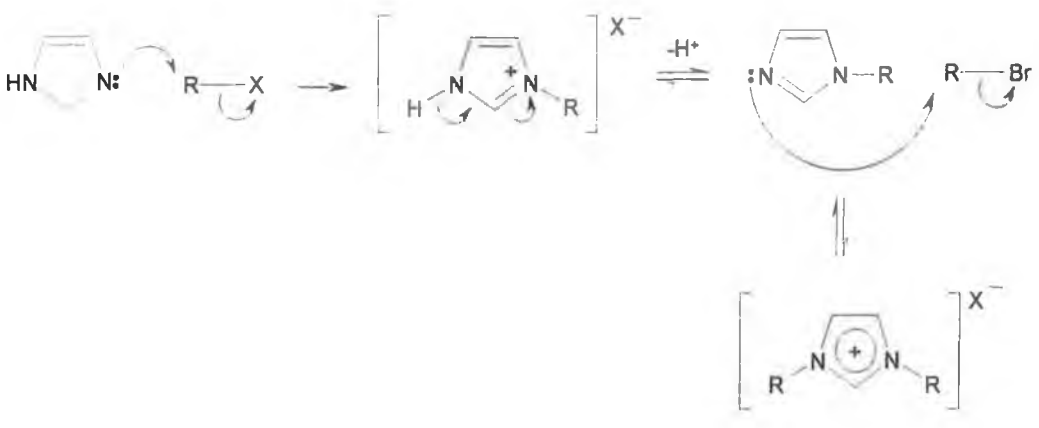

Scheme 2.3. *S_E2' mechanism of imidazole alklyation.*

However, if a base is employed and the azolide anion is generated then high yields of 1-substituted imidazoles are yielded (Scheme 2.4), with little or no quartnerisation occurring.

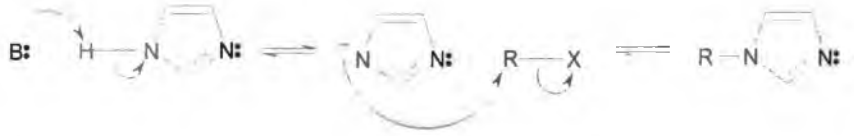

Scheme 2.4. *S_E2cB mechanism of imidazole alklyation, in basic media.*

So rather than using the neutral imidazole, the sodium imidazolide salt was employed. Salt **150** was heated to reflux with the sodium imidazolium salt for 12 h, which yielded **148** in an 69% yield after a simple work-up and purification on silica gel using dichloromethane (DCM)–methanol (95:5). Later **150** was heated to reflux with imidazole and sodium/potassium carbonate in acetonitrile, with the imidazolium anion being generated in situ, producing **148** in a yield of 72%. This second method was then extended to the synthesis of **149**, avoiding the necessity of prior preparation of

the benzimidazolide anion, with a yield of 81% (Scheme 2.5). It was observed that the benzimidazole compound was prepared in a higher yield than the imidazole compound. However, as both **148** and **149** could be produced easily in good yields both compounds were used to generate the respective ferrocenyl–imidazolium and –benzimidazolium salts.

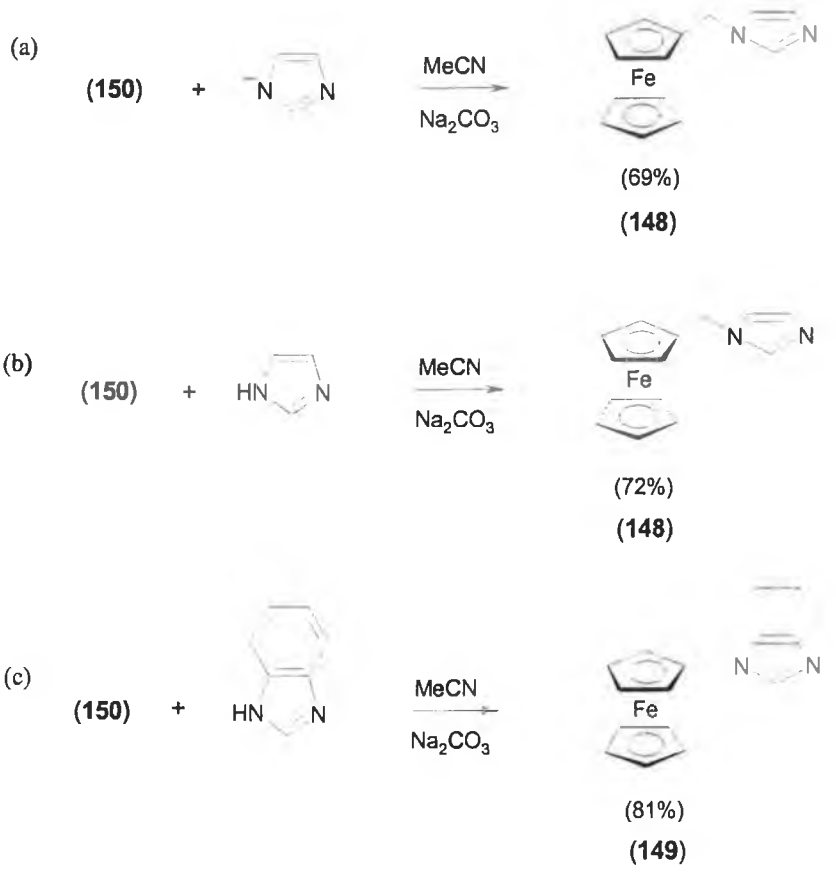

Scheme 2.5. *Synthesis of 1-ferrocenylmethylazole intermediates (148) and (149).*

Predictably, the NMR data for these two compounds are very similar (Figure 2.2). From the ^{1}H NMR ($CDCl_3$) spectra it can be seen that (ignoring the obvious additional phenyl signals for **149**), the characteristic signals for the Fc Cp ring hydrogens, the methylene linker and the 2-H of the azoles are very similar. The

ferrocene peaks are at ~4.10–4.13 ppm for **148** and ~4.16–4.25 ppm for **149**, Fc–C$\underline{H}_2$– resonates at 4.80 (**148**) and 5.07 (**149**) ppm and the 2-azole H resonates at 7.42 and 7.86 ppm for **148** and **149**, respectively. In comparison with the unsubstituted ferrocene (4.18 ppm) and the unsubstituted azoles [imidazole ($CDCl_3$): 7.25 (4,5-H), 7.86 (2-H) ppm], it seems to suggest that while the azole substituent does not exert a large influence on the ferrocenyl unit, the ferrocenyl substituent acts as an electron-donating group towards the azole causing an upfield shift in the azole proton resonances. If the ^{1}H NMR data of the 1-methylimidazole are examined, it is seen that the chemical shifts are almost identical [1-methylimidazole ($CDCl_3$): 6.88 (5-H), 7.08 (4-H), 7.47 (2-H) ppm cf. **148** ($CDCl_3$) 6.85 (5-im H), 6.95 (4-im H), 7.42 (2-im H) ppm]. From the ^{13}C NMR spectra, again the significant peaks are the 2-$\underline{C}$H of the azole rings resonating at 122.77 (**148**) and 143.70 (**149**) ppm and the Fc–$\underline{C}H_2$– resonating at 44.72 and 44.67 ppm, respectively for **148** and **149**.

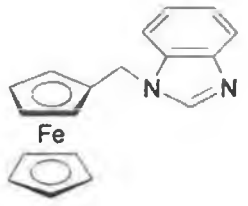

(149)

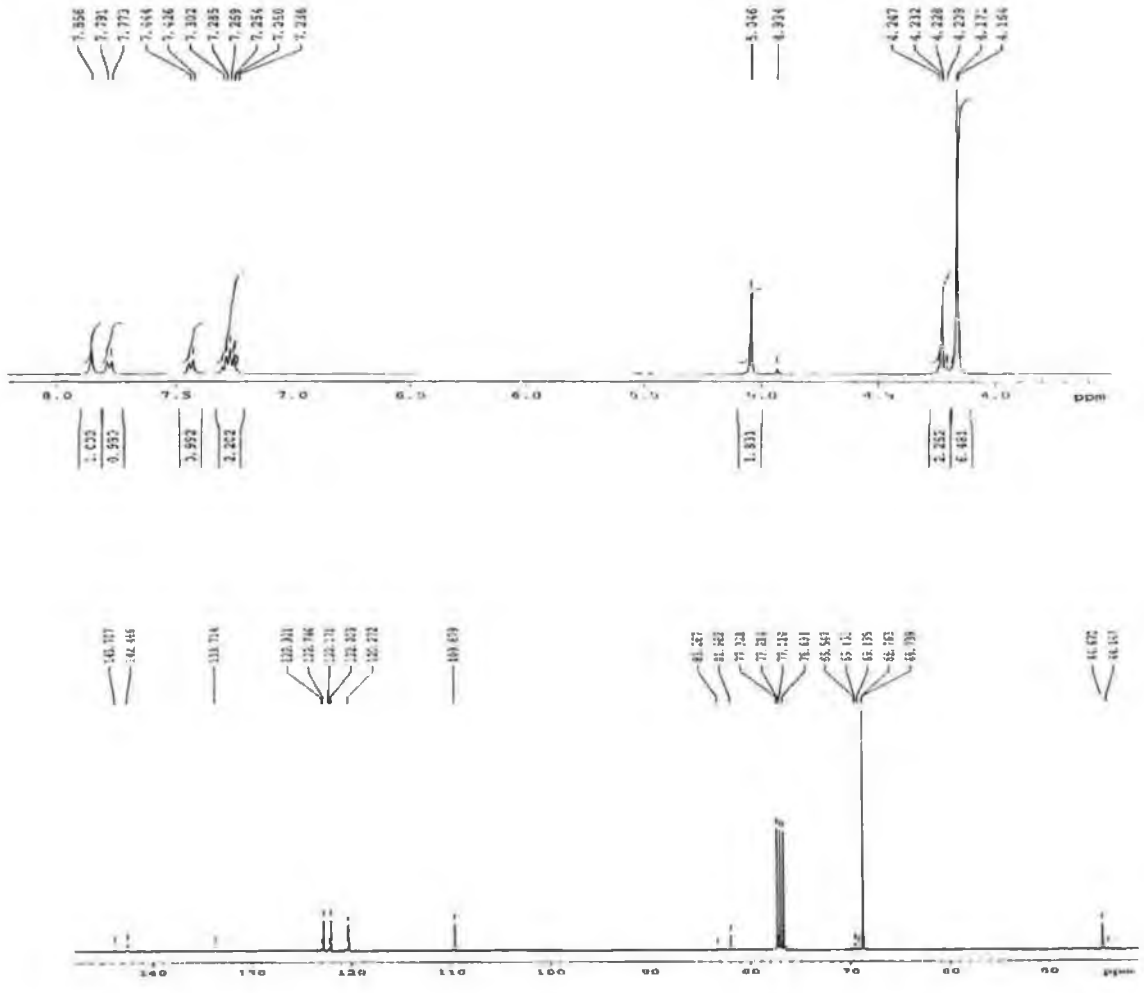

Figure 2.2. *The* ^{1}H *and* ^{13}C *NMR spectra for* ***149****.*

2.2.1.2 1-Ferrocenylmethyl-3-alkylazolium salts

The imidazolium cation centre was then generated in two ways (Schemes 2.6 and 2.7): Firstly, **148** was treated with the appropriate alkyl halide thereby quarternising the neutral imidazole into the imidazolium centre via the mechanism discussed in Scheme 2.1c. The alkyl iodides were employed due to the better leaving group properties of the iodide anion (Scheme 2.6), yielding 1-ferrocenylmethyl-3-alkylimidazolium iodides (**151**)–(**154**). In the case of 1-ferrocenylmethyl-3-benzylimidazolium chloride (**155**), benzyl chloride was used instead due to availability.

(148) **(151)**

Scheme 2.6. *Quarternising of the neutral imidazole into the imidazolium salt, e.g., preparation of 1-ferrocenylmethyl-3-methylimidazolium iodide (**151**).*

Several experimental techniques were employed for the generation of these salts. In the first case, the alkyl iodide and **148** were heated to reflux in acetonitrile for 1–3 h, and the reaction was monitored by thin layer chromatography (t.l.c.), worked up and the product isolated by column chromatography. Another variation of this was the addition of **148** and the alkyl halide together in the minimum amount of acetonitrile. This was left overnight at room temperature and a large volume of diethyl ether added, with crystals forming after 48 h.

In the second approach, **150** was used as the starting material and was treated with the appropriate 1-alkylimidazole (Scheme 2.7). The two reactants were heated to reflux in acetonitrile and the 1-ferrocenylmethyl-3-alkylimidazolium iodide salt was collected by column chromatography. The 1-alkylated imidazoles were prepared according to the procedure of Bônhote et al. [68] or bought commercially. This method allowed the intermediate step of the preparation of **148** to be left out, which makes the overall synthesis from ferrocene to the 1-ferrocenylmethyl-3-imidazolium salts more efficient (Table 2.1). However, in the case of more varied alkyl substituents these could not be bought commercially so an extra synthetic step involving the preparation of the 1-alkylimidazole by the method of Bônhote et al. [68] was required.

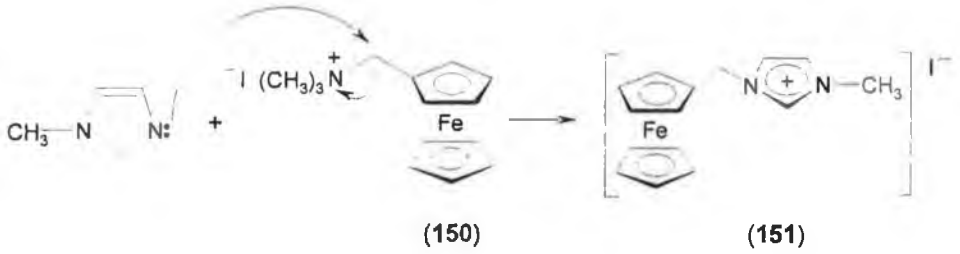

Scheme 2.7. *Nucleophilic substitution of **150** by 1-alkylimidazoles, e.g., **151**.*

In Table 2.1, the different compounds prepared and their respective yields are given, showing a comparison of the different techniques used. Using **150** as the starting material proved the most efficient as regards to yields. However, the preparation of the 1-alkylimidazoles proved to be more demanding practically as they are liquids and so are more difficult to purify than the solid **150**. Therefore, the salt being generated and time considerations generally dictated which technique was used.

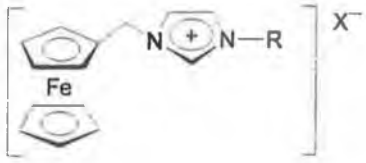

R	Anion	Compound no.	Method of preparation	Yield from ferrocene (%)[a]
$-CH_3$	I^-	**151**	(a)	40
			(b)	36
			(c)	50
$-C_2H_5$	I^-	**152**	(a)	42
			(c)	48
$-C_3H_7$	I^-	**153**	(c)	48
$-C_4H_9$	I^-	**154**	(a)	48
			(c)	58
$-CH_2C_6H_6$	Cl^-	**155**	(b)	40

[a]The yield of **150** from ferrocene was 71% and the yield of **148** from **150** and ferrocene was 69 and 49%, respectively.

Table 2.1. *Comparison of methods used to generate 1-ferrocenylmethyl-3-alkylimidazolium salts: (a) reflux of **148** with an alkyl halide in acetonitrile, column chromatography; (b) treatment of **148** in acetonitrile with an alkyl halide at RT, crystallisation; (c) reflux of **150** with a 1-alkylimidazole in acetonitrile, column chromatography .*

For the preparation of 1-ferrocenylmethyl-3-alkylbenzimidazolium salts, the most convenient method was found to be heating **149** with the appropriate alkyl halide in

acetonitrile and collecting the product by column chromatography. [1-Alkylbenzimidazoles are not commercially available and it was thought unnecessary to have to prepare them.] It was found that the yields of the benzimidazolium salts from the 1-methylferrocenylazole intermediate were lower than those of the corresponding imidazolium salts (Scheme 2.8).

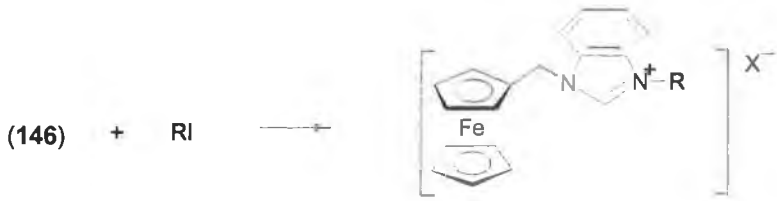

R	X		Yield (%)
CH_3	I	(**156**)	95
C_2H_5	I	(**157**)	42
C_3H_7	I	(**158**)	51
C_4H_9	I	(**159**)	42
$CH_2C_6H_5$	Cl	(**160**)	48

Scheme 2.8. *Preparation (156)–(160).*

Imidazolium and benzimidazolium 'claw'-type structures were also prepared where the azole entity was *N*-substituted by two methylferrocene units (Scheme 2.9). These 1,3-di(ferrocenylmethyl)azolium iodide salts – 1,3-di(ferrocenylmethyl)imidazolium iodide (**161**) and 1,3-di(ferrocenylmethyl)benzimidazolium iodide (**162**) – were prepared according to the procedure of Thomas et al. and Hanlon [125,126] (Scheme 2.9): The starting material (**150**) was heated to reflux with intermediates **148** and **149** in dry acetonitrile for 18 h. Compounds **161** and **162** were obtained after column chromatography and with yields of 80 and 57%, respectively.

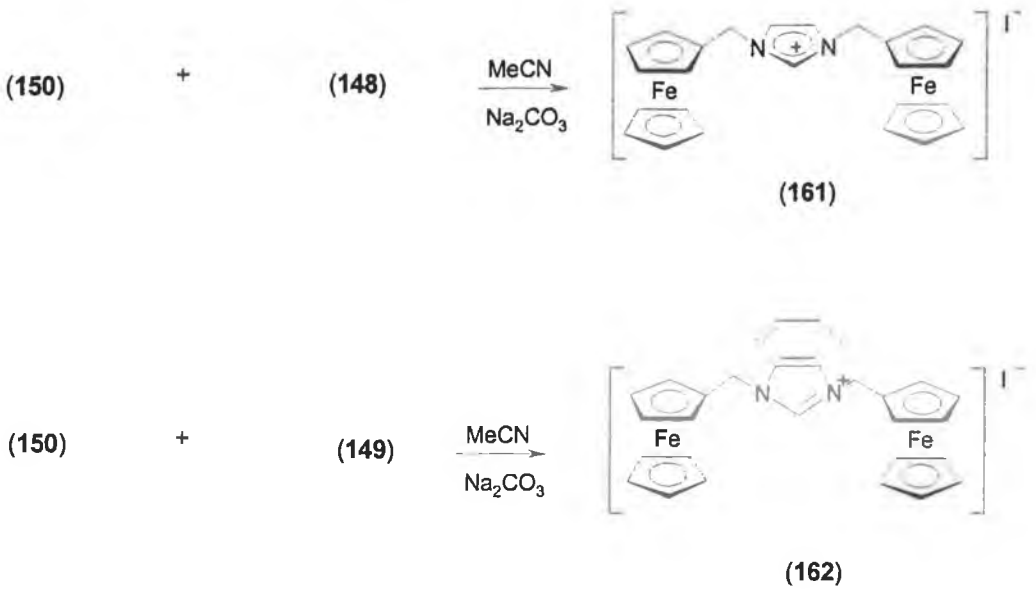

Scheme 2.9. *Preparation of 1,3-di(ferrocenylmethyl)imidazolium iodide (**161**) and 1,3-di(ferrocenylmethyl)benzimidazolium iodide (**162**).*

The diversity of these salts in varying the R substitutent and the central azolium moiety meant that it would be possible to see if there would be any effect on the lipophilicity of the compounds for their application in anion recognition studies, bioactivity studies and catalytic studies.

As a new substituent is added to the pyridine-like nitrogen, the 3-nitrogen develops a positive charge. This means that the ring is now a positively charged aromatic heterocyclic ring (Figure 2.3a). As a result, the ^{1}H NMR signals are shifted downfield (Figure 2.3b) compared to that of the neutral azole compounds. This is most markedly seen at the 2-CH position. In Figure 2.3b, 1,3-dimethylimidazole is given as an illustration.

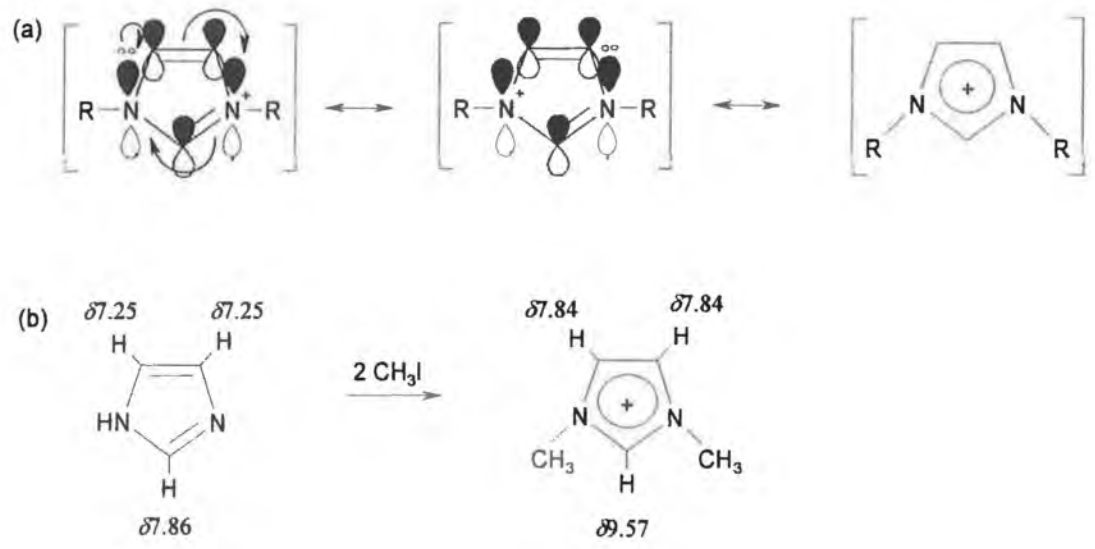

Figure 2.3. *Effect of quarnerisation on (a) the electronic structure of imidazole and (b) the ^{1}H NMR chemical shifts ($CDCl_3$) of imidazole.*

In general, for the ferrocenyl–azolium salts it was seen that the ferrocenyl Cp hydrogens resonated downfield of the unsubstituted ferrocene and the ferrocenylmethylimidazole at ~4.25–4.50 ppm. This suggests that there maybe some delocalisation of the electron density in the Cp rings to stabilise the positively-charged azolium ring, as previously discussed, or an electron-withdrawing effect due to the increased electronegetivity of the nitrogen atoms in the rings. The methylene spacer unit also shifted downfield from 4.72 ppm for the imidazolium salts and 4.94 ppm for the benzimidazolium salts to ~5.4 and 5.6 ppm, respectively, reflecting the increased electron-withdrawing effect of the now positively charged, aromatic azole ring. However, the most significant shift in the ^{1}H NMR signals came from the 2-azole H from 7.41 ppm for the imidazolium derivative and 7.77 ppm for the benzimidazolium derivative to ~10 ppm for both types of salts. This too was observed in the ^{13}C NMR spectra with the 2-C shifting from 82.49 ppm [in the 1-ferrocenylmethyl-3-alkylimidazolium] and 143.70 ppm in the [1-ferrocenylmethyl-3-alkylbenzimidazolium salts] to ~135 and 210 ppm, respectively. The signals for alkyl

chain protons for the different derivatives generally appear at approximately 4.00–4.50 ppm if they are directly adjacent to azolium ring, but then will be observed at 0.95–2.00 ppm depending on their position in the chain. the In Figure 2.4, the ^1H spectra of **156** is shown.

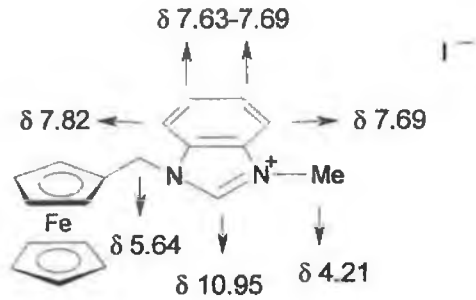

(156)

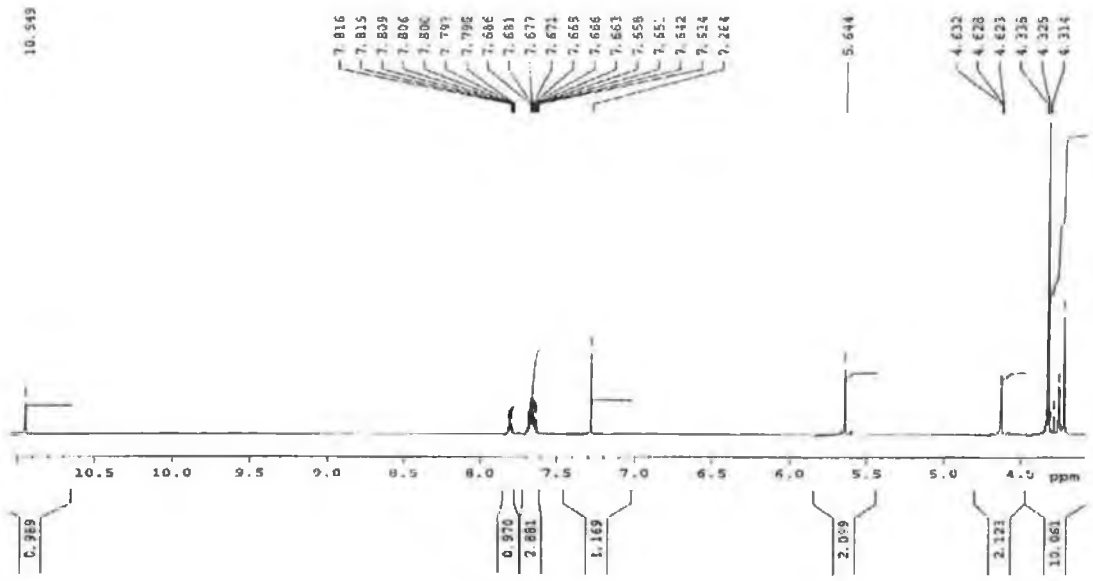

Figure 2.4. *^1H NMR spectra for* ***156*** *($CDCl_3$).*

2.2.2 Bisazolium–ferrocenyl salts

Having prepared the monosubstituted ferrocenyl–azolium salts that could potentially act as monodentate *N*-heterocyclic carbene ligands or as anion chemoreceptors (see Chapters 3 and 4), it was of interest to prepare other ferrocenyl–azolium systems that would contain two azolium centres in a molecule. Molecules with two azolium nuclei could be used as bidentate *N*-heterocyclic ligands or chemoreceptors that may provide greater specificity than the previously prepared monosubstituted ferrocenyl–azolium systems.

So far only a few examples of bidentate ligands being employed in transition metal catalysis have been reported [42–54], so it was thought that it would be interesting to compare the monodentate ferrocenyl–azolium precursors for *N*-heterocyclic carbene ligands with the proposed chelate ligands. Furthermore, a comparative study against the 1,1′-(bisazolium)ferrocenyl salt compounds (**146**), which contain a ferrocene unit as a spacer unit, to the alkyl spacer group in the linear bridged system (**147**) could be carried out to compare any subsequent effect on catalyst efficiency (see Figure 2.5). Furthermore, it was proposed to employ these compounds as chemoreceptors to see if they are able to selectively co-ordinate with anions.

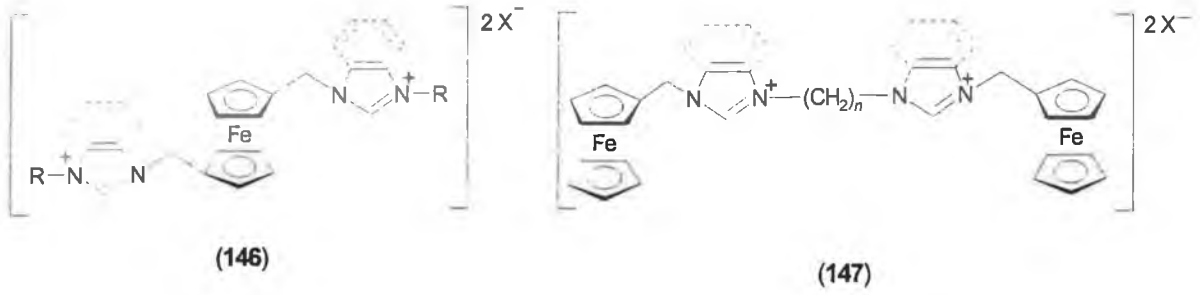

Figure 2.5. *Two possible structures of ferrocenyl-bisazolium salts.*

2.2.2.1 Bridged bisazolium–ferrocenyl salts

A facile way of introducing two azolium centres was the linking together of two monosubstituted ferrocenyl–azole systems to a create a [1-(1-ferrocenylmethyl)-3-alkylazolium]-3-(1-ferrocenylmethyl)azolium salt (**147**) (Figure 2.5). The linker group chosen was a four atom spacer (an *n*-butyl group) and the synthesis involved treating **148** and 1,4-diidobutane to obtain the corresponding 1-(1-ferrocenylmethyl)-3-(4-iodobutyl)imidazolium iodide (**163**). This was collected and heated to reflux with the corresponding aliquot of **148,** yielding the bridged bisazolium–ferrocenyl iodide salt system – 1-[(1-ferrocenylmethyl-3-butyl)imidazolium]-3-ferrocenylmethylimidazolium diiodide (**164**). The benzimidazolium analogue was prepared by the same method, with **149** and 1,4-diidobutane being heated to reflux, obtaining 1-(1-ferrocenylmethyl)-3-(4-iodobutyl)benzimidazolium iodide (**165**). Then further treatment of **165** with **149** produced 1-[(1-ferrocenylmethyl-3-butyl)benzimidazolium]-3-ferrocenylmethylbenzimidazolium diiodide (**166**) (Scheme 2.10).

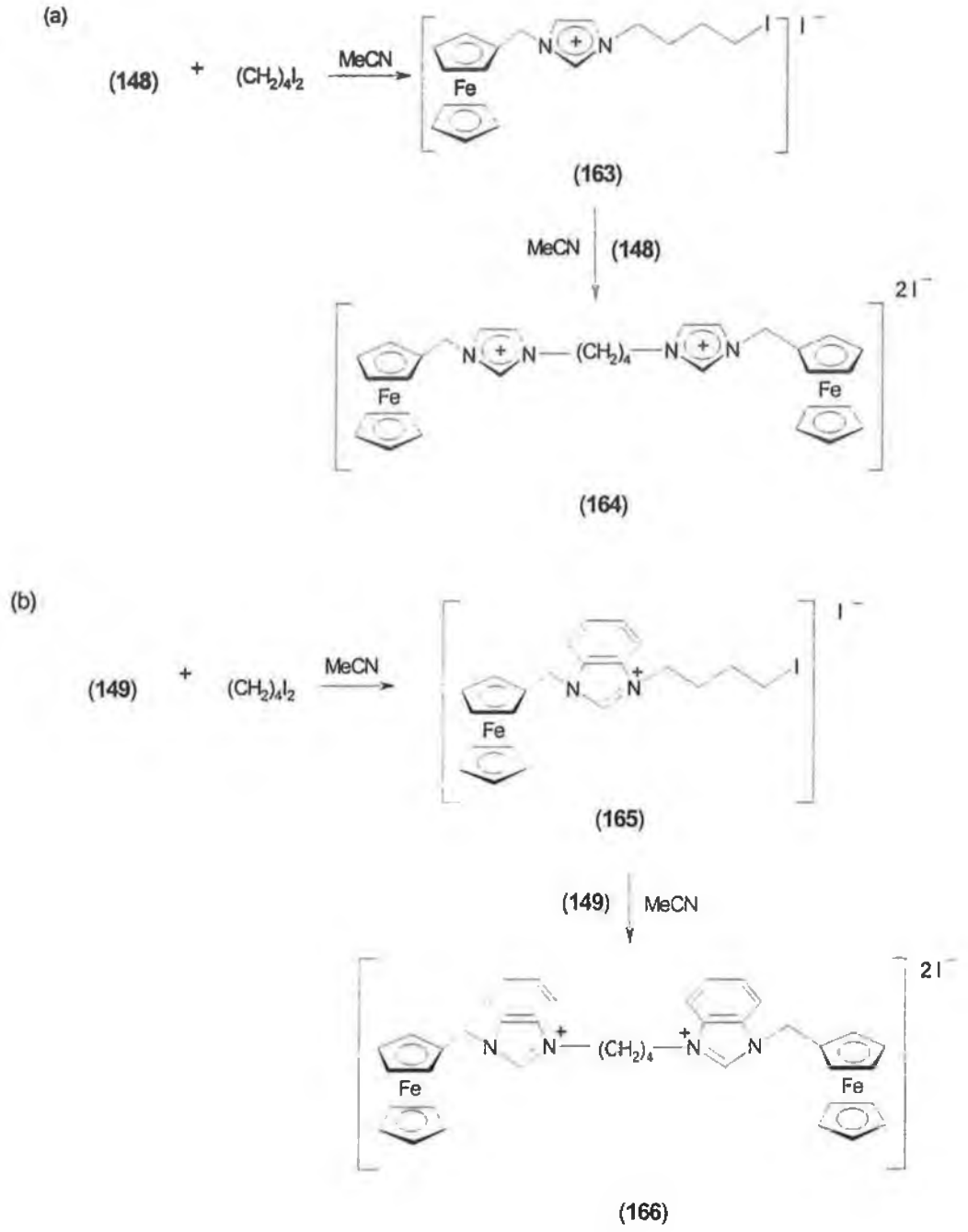

Scheme 2.10. The synthesis of bridged bisazolium–ferrocenyl iodide structures 165 and 166.

The syntheses were simple and high-yielding. For the imidazolium derivatives, the yields were 74% for **163** and 50% for **165**, whereas for the benzimidazolium salts, yields of 79% for the intermediate **164** and 55% for the bridged product (**166**) were

obtained. However, it should be noted that purification of these salts proved to be more difficult than with the monosubstituted ferrocenyl–azolium salts. The solubility of these salts is such that salts **164** was sparingly soluble in chloroform and acetonitrile, while **166** was totally insoluble in dichloromethane, methanol, acetonitrile and other commonly used polar solvents. Thus, they could not be purified by column chromatography. However, both compounds were shown to have a high purity by microanalysis, although some slight impurities remained.

On examination of the ^{1}H NMR spectra of **163–166** (Figure 2.6), it is seen that there is a downfield shift in the methylene linker group and the imidazolium protons as would be expected when an azolium centre is generated. In the imidazolium compounds, the 2-H of the imidazolium unit resonates at 9.21 and 9.74 ppm for **163** and **164**, respectively. A comparison between 1-methylferrocenyl-3-*n*-butylimidazolium iodide (**154**) and **163** shows that the terminal $-CH_3$ group in **154** appears at 0.88 ppm, while the protons on the carbon adjacent (C_4) to the iodo group are shifted much more downfield to 4.45 ppm for **163**. In the butyl chain, protons 1,2,3 show signals at 5.20, 1.74 and 1.22 ppm for **154** and at 5.19, 1.88 and 1.75 ppm for **163**. The bridged product **165** is symmetrical and as such only two resonances are seen for the butyl spacer group, one in the upfield region of the spectrum at 4.21 ppm, reflecting its proximity to the imidazolium centre, and the other at 2.12 ppm.

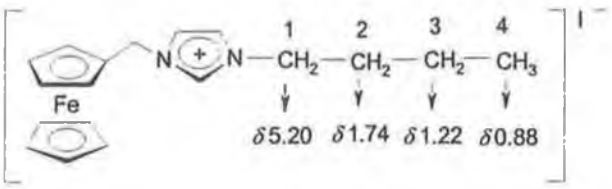

(154)

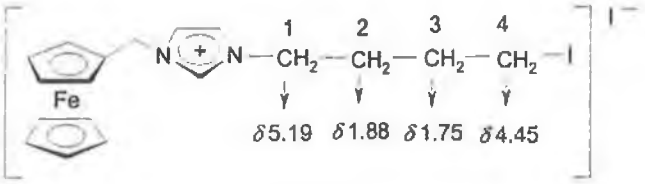

(163)

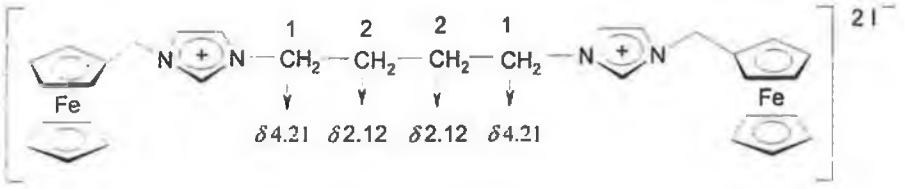

(164)

Figure 2.6. *A comparison of the ^{1}H NMR shifts for the butyl chain in compounds* ***154****,* ***163*** *and* ***164*** *($CDCl_3$).*

2.2.2.2 1,1′-Bisazolium ferrocenyl salts

2.2.2.2.1 1,1'-(1-Methylazole)ferrocenes

The second route to introducing two azolium centres into the ferrocenyl–azolium system was the preparation of a 1,1′-disubstituted ferrocene (Figure 2.7).

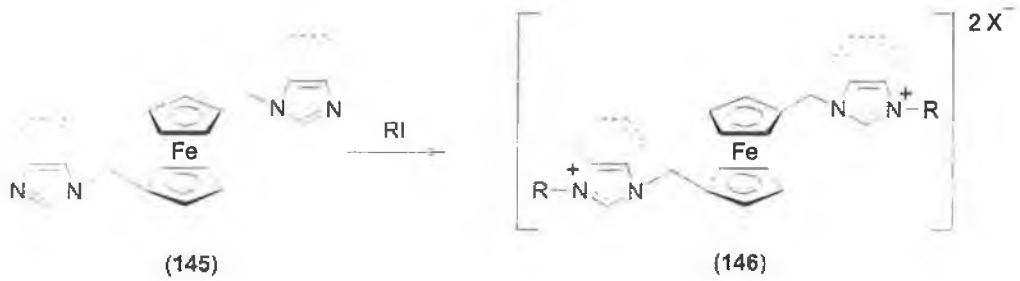

Figure 2.7. The proposed neutral 1,1′-disubstituted ferrocene–azole (145) and 1,1′-disubstituted ferrocenyl–azolium salt (146).

Two approaches to preparing these compounds were available. Again, as it had proven successful with the monosubstituted ferrocenyl–azoles, it was decided to first prepare the neutral ferrocenyl–azole compound (**145**), which could then later be converted into the quarternary salt via alkylation with a haloalkane (Figure 2.7). However, the synthesis of these compounds proved not to be as facile as the monosubstituted ferrocenyl–azoles. A couple of different routes were explored before a satisfactory pathway was found.

The first route employed 1,1′-ferrocenyldicarboxaldehyde (**167**) as the starting material (Scheme 2.11). This was prepared from 1,1′-lithiated ferrocene treated with DMF and then reduced in methanol using sodium borohydride to form 1,1′-ferrocenyldimethanol (**168**). Treatment with phosphorus trichloride and pyridine in acetonitrile formed the chloro- derivative – 1,1′-bis(chloromethyl)ferrocene (**169**) – in situ. In a one-pot procedure, the chloro groups were displaced with imidazole in THF using sodium carbonate to generate the imidazolium anion. 1,1′-Bis(1-methylimidazole)ferrocene (**170**) was afforded as a yellow powder after column chromatography on silica gel using DCM/methanol (50:50).

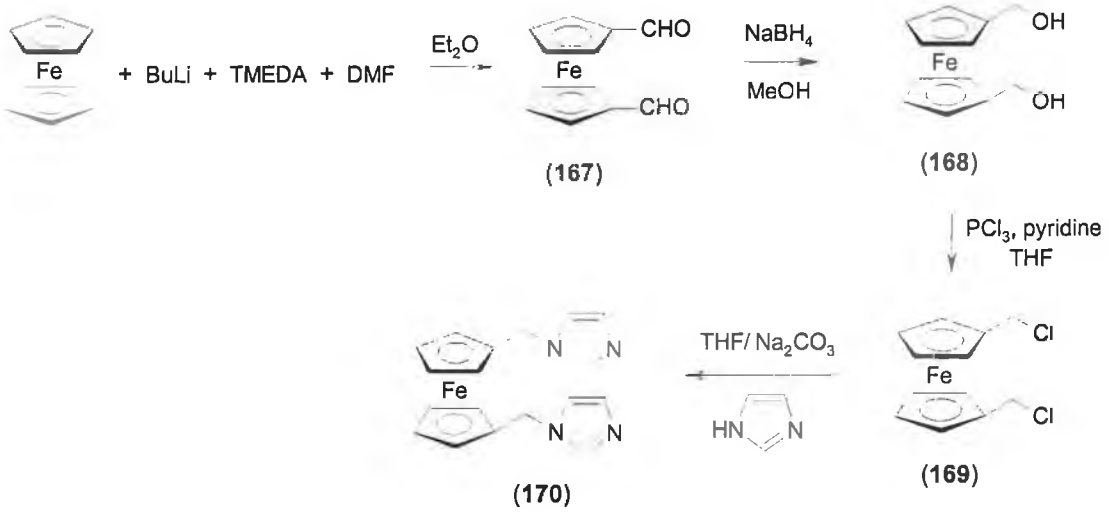

Scheme 2.11. *Synthesis of 1,1′-(1-methylimidazole)ferrocene (**170**) from 1,1′-ferrocenyldicarboxaldehyde (**167**) via a dichloromethyl derivative (**169**).*

As the yield for the last step was very poor (5%), it was envisaged that a tosylate group would be a better leaving group than the chloro group and so improve the efficiency of the imidazole substitution. (1,1′-Ferrocenylmethyl)-*p*-toluene sulphonate (**171**) was prepared from the alcohol intermediate, *p*-toluenesulphonyl chloride and

pyridine in chloroform (which had been purified and dried to remove any ethanol and water) affording a brown gum. However, it did not prove possible to displace the tosylate with the imidazole nucleophile (Scheme 2.12).

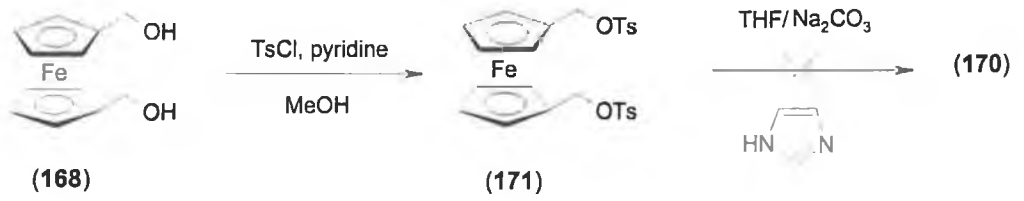

Scheme 2.12. *Attempt use of a tosylate derivative to prepare 170.*

Overall, this general route proved to be lengthy, inconvenient and inefficient, so a different method of introducing the azole functionality into the ferrocene system was required.

It had recently been reported in the literature that ferrocenyl alcohols can be linked to imidazoles using *N,N'*-carbonyldiimidazole (CDI) as the reagent [134,135]. Njar [179] extended the previously known, albeit very low-yielding, use of CDI to convert alcohols to imidazole functionalities by simply changing the solvent from DCM to acetonitrile. It was shown that nearly all types of alcohols, apart from tertiary alcohols, (i.e., primary, secondary, allylic, homoallylic, enolic, benzylic and phenolic alcohols) could be transformed into the desired imidazole or triazole in near quantitative yields. Simenel et al. [135] were able to prepare substituted ferrocenyl imidazoles by the treatment of the precursor ferrocenyl alcohols with CDI (Chapter 1, Section 1.4.1.1). Therefore, it was decided to treat **168** with CDI, preparing **170** in a yield of 71%. The reaction was carried out by heating to reflux all reagents for 4 h in acetonitrile under nitrogen. The product was then isolated by column

chromatography, using DCM/methanol (50:50). This provided a very simple, high-yielding pathway from ferrocene to the desired bisimidazole product (**170**) (Scheme 2.13).

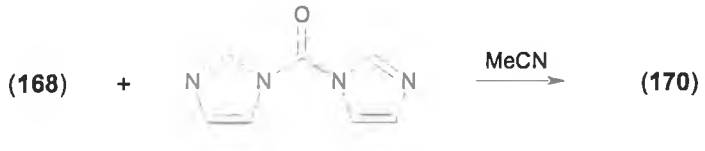

Scheme 2.13. *The synthesis of 1,1'-bis(1-methylimidazole)ferrocene (170) from 1,1'-ferrocenedimethanol (168) using CDI.*

However, this route could not be used for the benzimidazole derivative. Therefore, an alternative route rather than using **168** as the key intermediate was needed. In an analogous pathway to the preparation of the monosubstituted ferrocenyl–azoles from the ferrocenyl–methiodide salt (**150**) as the starting material, a procedure for the convenient synthesis of the bis derivative was found [180].

Glidewell et al. treated 1,1′-dilithiated ferrocene with Eschenmoser's salt – *N,N*-dimethylmethyleneammonium iodide. However, due to commercial problems obtaining Eschenmoser's salt, we used the chloride Schiff base – *N,N*-dimethylmethyleneammonium chloride (**172**), prepared by the procedure of Dimmock et al. [181] – producing exactly comparable results, and yielding 1,1′-bis(*N,N*-dimethylaminomethyl)ferrocene (**173**). This was methylated to the corresponding methiodide salt – ferrocene-1′-diylbis-(methyltrimethylammonium iodide) (**174**). Compound **174** was prepared in an overall yield of 57% from ferrocene. (Scheme 2.14).

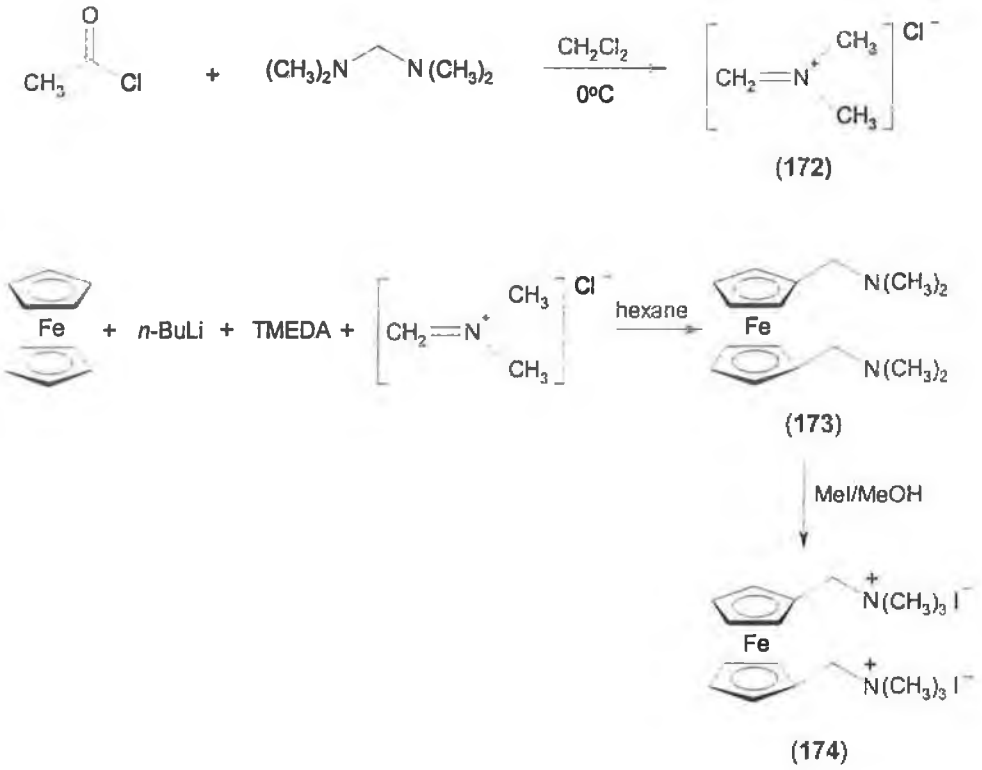

Scheme 2.14. *Synthesis of ferrocene-1'-diylbis-(methyltrimethylammonium iodide) (174), using an adaptation of the procedure of Glidewell et al.*

The preparation of **74** enabled us to use the same procedure as that for the monosubstituted ferrocenyl–azoles, where the azole could be substituted into the ferrocene unit by replacement of the methiodide groups (Scheme 2.15).

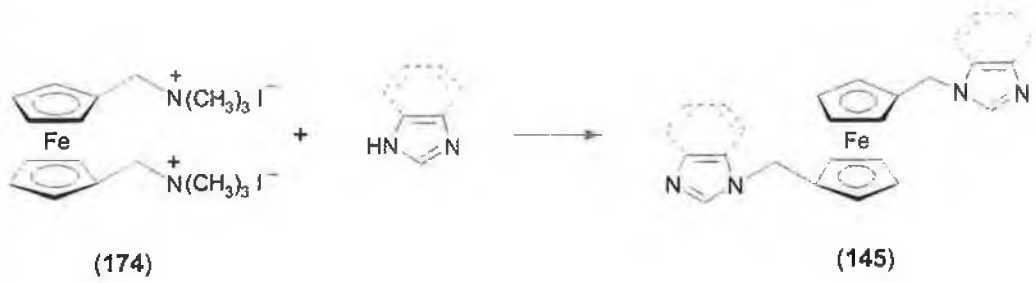

Scheme 2.15. *The proposed use of ferrocene-1'-diylbis-(methyltrimethylammonium iodide) (174) for the preparation of 1,1'-(1-methylazole)ferrocenes (145).*

In an analogous procedure to the synthesis of the monosubstituted ferrocenyl–azole salts, the 1,1′-disubstituted ferrocenyl–azoles were prepared (Scheme 2.16). Compound **174**, the desired azole and potassium carbonate in acetonitrile were heated to reflux and then purified by column chromatography. However, while the reaction was an overnight reaction for the monosubstituted ferrocenyl–azoles, 1 week was required to produced the 1,1′-disubstituted ferrocenyl–azoles. Both the imidazole and benzimidazole analogues – **170** and 1,1′-bis-(1-methylbenzimidazole)ferrocene (**175**) – were produced in yields of 12 and 20%. This shows that the while this is a useful route to the synthesis of the benzimidazole derivative, the reaction was too low-yielding to be of synthetic value for the imidazole derivative as compared to the CDI method. As can be seen from Table 2.2, the most efficient route proved to be via employment of CDI for the synthesis of **170**.

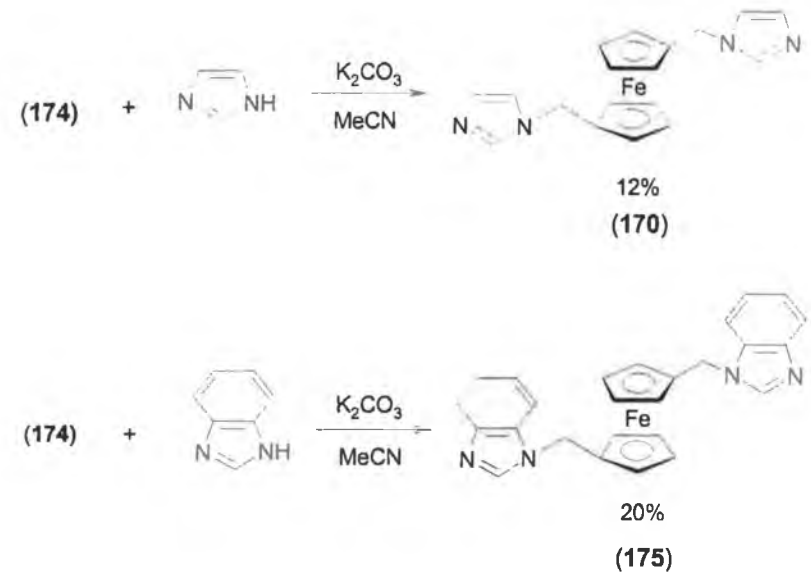

Scheme 2.16. *Preparation of 1,1′-(1-methylazole)ferrocenes (145) – (170) and (175) –from intermediate (174).*

Compound	Compound no.	Method	Yield from ferrocene (%)[a]
fc–CH_2–im[b]	**170**	via **169**	2
		via **168** and CDI	28
		via **174**	7
fc–CH_2–bzim[b]	**175**	via **174**	12

[a]Based on yields of **167**=45%, **168**=39% and **174**=58% from ferrocene.

[b]fc=1,1′-Disubstituted ferrocene (as compared to Fc for 1-monosubstituted ferrocene).

Table 2.2. *A comparison of the different methods employed to prepare the 1,1′-(1-methylazole)ferrocenes (**145**).*

As to be expected the NMR data of the monosubstituted ferrocenyl–azoles and the 1,1′-(1-methylazole)ferrocenes correlate very closely. For the ferrocenyl–imidazole compounds, **148** and **170**, and the ferrocene–benzimidazole compounds, **149** and **175**, almost identical shifts are seen in the key functionalities of the ferrocene Cp rings, the methylene linker and the 2-CH group of the azole ring. As expected the most significant difference between the mono and disubstituted ferrocene–azoles are the integrations recorded. For example, the key integrations in the monosubstituted 1-methylferrocenylazoles (e.g., **149**) are 9:2:1 for the Cp:–CH_2–:2-Az protons compared to 8:4:2 for the 1,1′-(1-methylazole)ferrocenes (e.g., **175**, Figure 2.8)

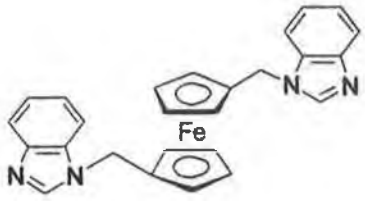

(175)

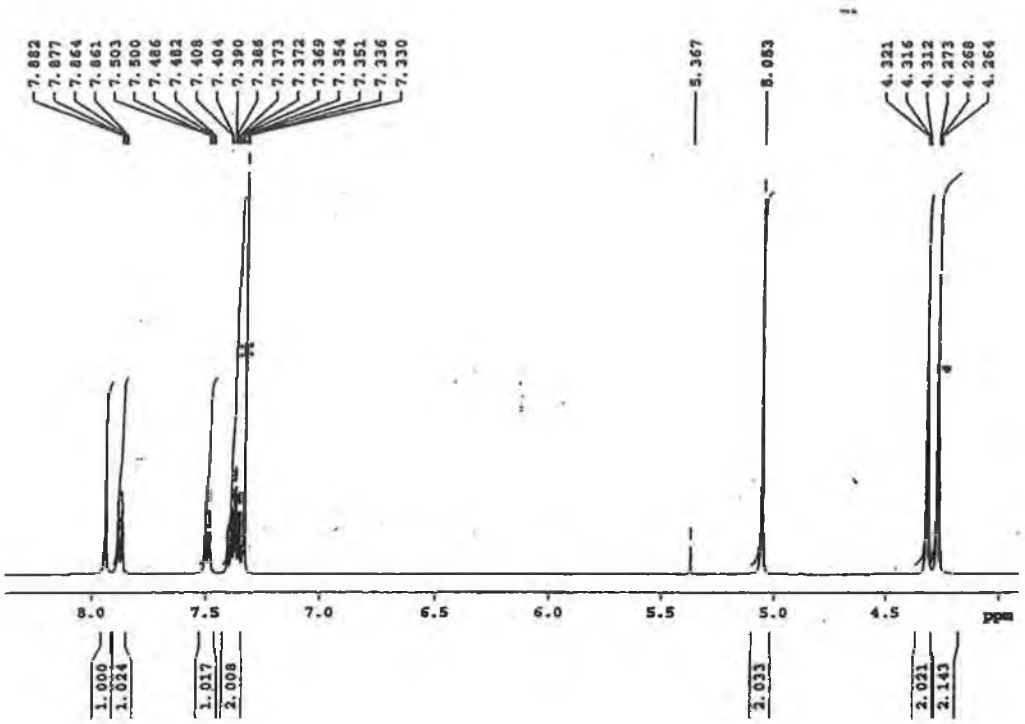

Figure 2.8. *The* ^{1}H *NMR spectra of 175* ($CDCl_3$).

2.2.2.2.2 1,1′-Bis(1-alkyl-3-methylazolium) ferrocenyl salts

The quarternisation of these compounds was achieved in the same way as with the monosubstituted compounds. The bisazole–ferrocenyl systems were heated to reflux in acetonitrile with the appropriate haloalkane. The compounds produced by this procedure are shown in Scheme 2.17. It was decided to concentrate on benzimidazolium salts as they were the most easily prepared.

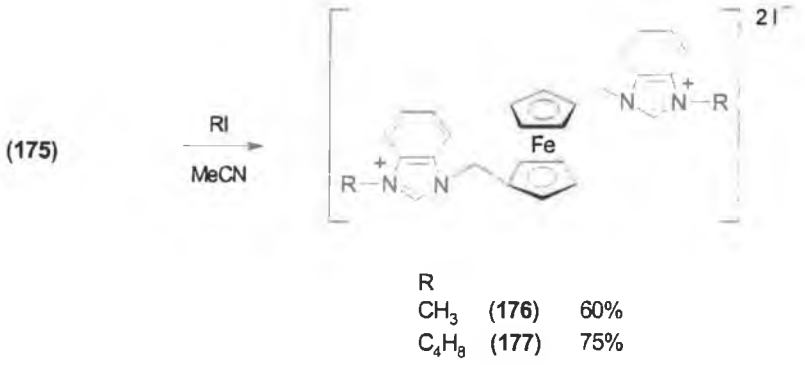

R		
CH_3	**(176)**	60%
C_4H_8	**(177)**	75%

Scheme 2.17. *The preparation of 1,1′-bis(1-alkyl-3-methylazolium)ferrocenyl salts (176) and (177).*

The methyl and *n*-butyl salts were produced. The product precipitated out of the reaction mixture and was collected by filtration. Further purification was carried out by column chromatography. NMR analysis showed that the product had been prepared (Figures 2.9 and 2.10). However, microanalysis showed that some impurities remained that could not be removed by chromatography or crystallisation. Thus, it was concluded that the bisazolium salts – both the bridged and 1,1′-bisazolium ferrocenyl derivatives – were harder to isolate as completely pure products than the monosubstituted analogues.

Again, analogous to the monosubstituted compounds, the trimethylammonium iodide salt, **174**, was treated with a 1-alkylimidazole to see if the 1,1′-bis(1-methyl-3-methylimidazolium)ferrocenyl diiodide could be prepared without the ferrocenyl–azole intermediate (**170**) (Scheme 2.18). However, after heating **174** with 1-methylimidazole in acetonitrile for 7 days no product was formed, showing that this

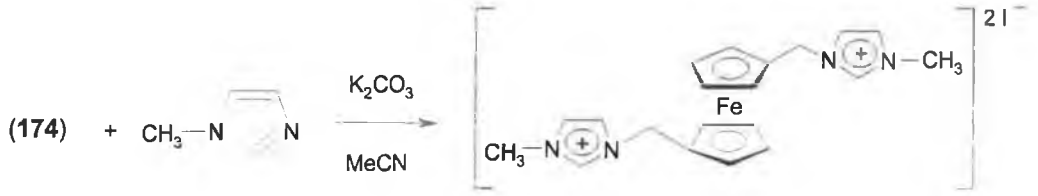

(178)

is not a viable method for the preparation of 1,1′-bis(1-alkyl-3-methylazolium)ferrocenyl salts.

Scheme 2.18. *Treatment of 174 with 1-methylimidazole as an alternative route to 1,1′-bis(1-alkyl-3-methylimidazolium)ferrocenyl salts.*

On formation of the azolium centre, as in the monosubstituted ferrocenyl–azolium compounds, salts **176** and **177** showed a large shift in the signal for the 2-CH of the azolium moiety and a significant shift of the methylene linker resonance compared to the neutral intermediates, **170** and **175**. For compounds **175** and **176**, 2-CH resonates at 9.46 ppm, compared to 7.80 ppm, and Cp–CH_2– resonates at 5.40 vs. 4.92 ppm, respectively, in the ^{1}H NMR spectra. A comparison of the ferrocenyl–benzimidazole/benzimidazolium compounds is given in Figure 2.9 and the ^{1}H spectra for **176** are given in Figure 2.10.

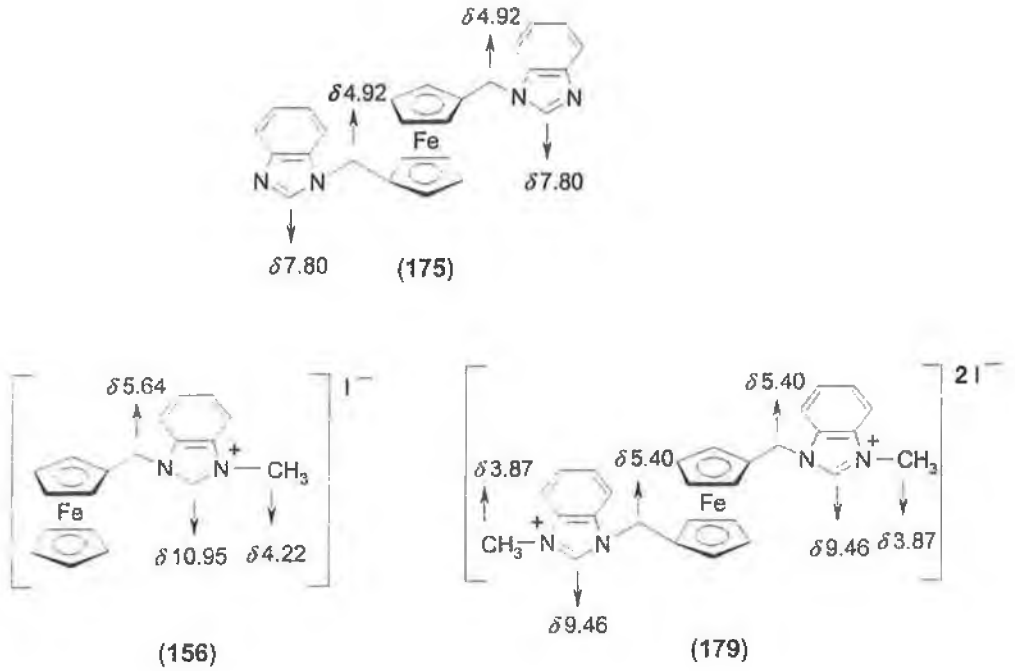

Figure 2.9. The key ^{1}H NMR resonances for 175, 156 and 179.

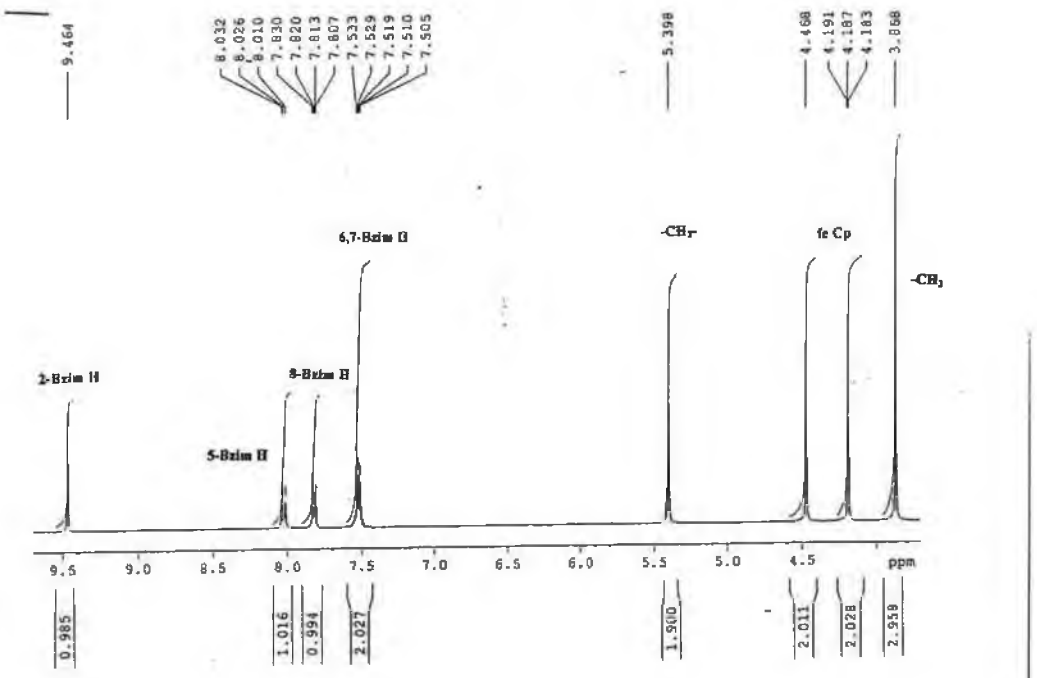

Figure 2.10. ^{1}H NMR spectra of 167.

2.2.3 Ferrocenylcyclophanes

2.2.3.1 1,1'-Ferrocenediazole systems

The preparation of 1,1′-ferrocenediazole systems where the azole and ferrocene units are directly linked (without any bridging $-CH_2-$ spacer group) was attempted, with the same initial aim as with the 1,1'-(1-methylazole)ferrocene systems (**145**): to prepare a neutral (1,1′-ferrocene)diazole compound (**180**) as a building block for a cyclophane structure, such as (**179**) or (**180**) (Figure 2.11).

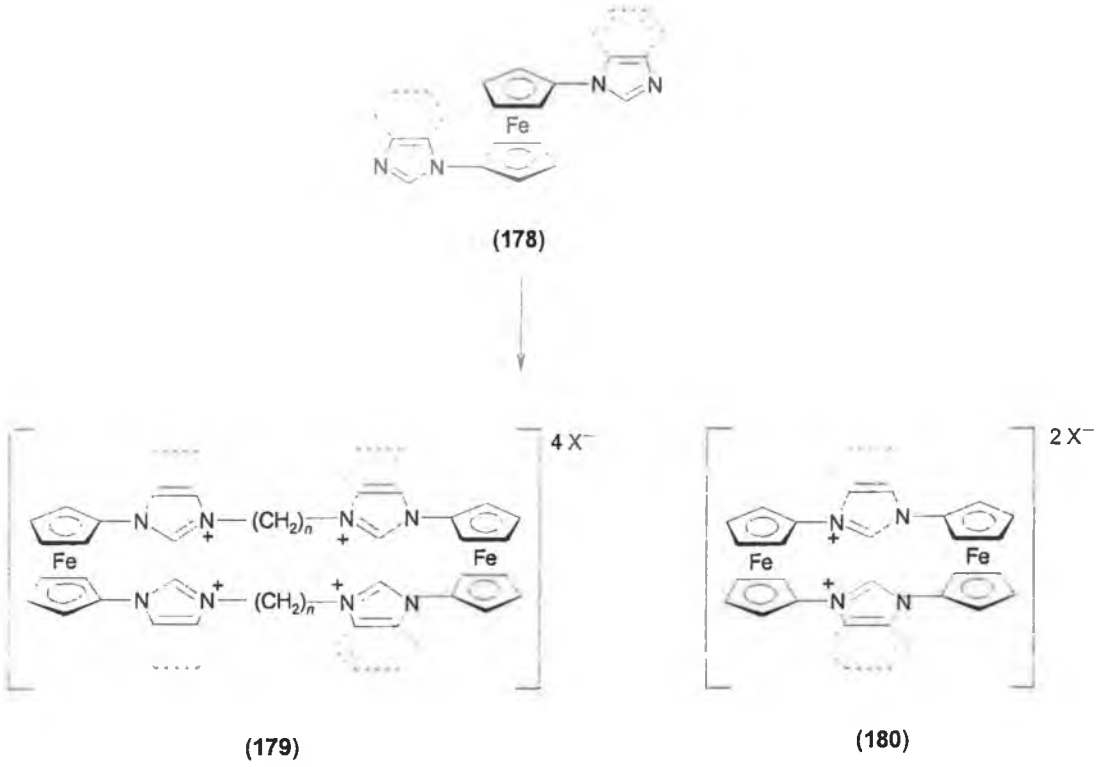

Figure 2.11. *Proposed macrocyclic ferrocenyl–azolium systems (179) and (180) and intermediate (178).*

The proposed method of preparation of **178** was based on copper-catalysed aromatic nucleophilic substitution. It has been well-recorded that nitrogen nucleophiles will readily undergo nucleophilic aromatic substitution if an appropriate copper catalyst is

used, e.g., the Rosenmund–von Braun reaction and the Ullman condensation [182,183]. Sato and Ebine, were able to perform the Gabriel synthesis using 1,1′-dibromoferrocene (**181**) to produce 1,1′-bis(phthalimido)ferrocene (**182**) in moderate yields [184] (Scheme 2.19) using this approach.

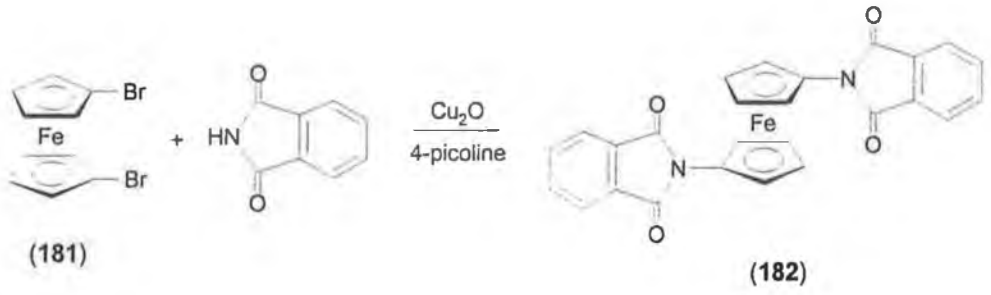

Scheme 2.19. *Preparation of 1,1′-bis(phthalimido)ferrocene (**182**) from 1,1′-dibromoferrocene (**181**) via the Gabriel synthesis.*

The Gabriel synthesis of mono(phthalimido)ferrocene has also been performed using 1-ferrocenylboronic acid, 'copper phthalimide' (derived from the metathesis of potassium phthalimide) and dry acetone as the solvent [185]. Both of these investigations show that ferrocene is capable of undergoing nucleophilic aromatic copper-catalysed substitution with a nitrogen nucleophile. This work suggests that 1,1′-ferrocenyldihalides (X=Br, **181**) and (X=I, **183**) could be used as substrate molecules for copper-catalysed nucleophilic substitution with azole compounds (Scheme 2.20).

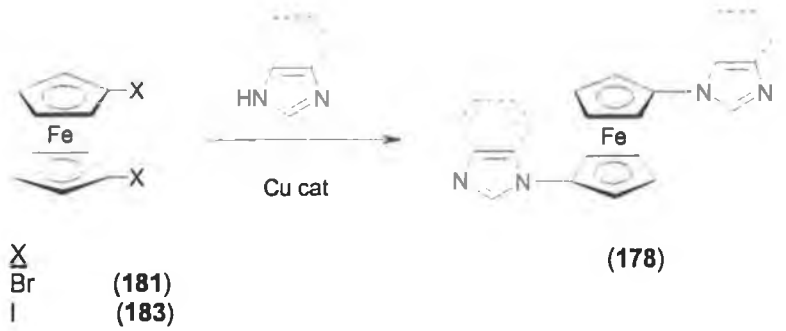

Scheme 2.20. *The proposed method for the synthesis of 1,1'-ferrocenediazoles (**180**).*

This basic reaction was tried many times, using 1,1′-dibromoferrocene (**181**) and 1,1′-diiodoferrocene (**183**) as the substrates in various solvents (DMF, water, DCM and pyridine) with copper acetate, copper(I) oxide, 'copper imidazole' and 'copper benzimidazolium' (obtained by metathesis of sodium imidazolium) as sources of copper and with benzimidazole, imidazole, sodium imidazolium and benzimidazolium as the azole nucleophiles.

These attempts proved unsuccessful in preparing the target compounds (**178**). Thus, it was concluded that copper catalysed nucleophilic substitution of azole entities into the ferrocene structure via bromo or iodo intermediates was not viable. Possibly steric factors could be responsible. The approach of two azoles to the relatively small ferrocene molecule to displace two halo groups may be difficult. Also the halo groups may not have been sufficiently electron withdrawing for the activation of ferrocene to nucleophilic displacement.

Therefore, attention was concentrated on realising the proposed series of 1-ferrocenylmethylazolium and 1,1′-bis(1-alkyl-3-methylazolium)ferrocenyl salt systems, which contain a $-CH_2-$ spacer (**179** and **180**).

2.2.3.2 Macrocyclic tetraazolium–ferrocenyl salts

Thus far, the acyclic linear bridged bisazolium–ferrocenyl salts (**164**) and (**165**), 1,1′-bisazolium–ferrocenyl salts (**176** and **177**) and the 'claw'-type 1,3-di(ferrocenylmethyl)azolium salts (**161**) and (**162**) had been prepared. The next step was extending these systems to produce a macrocycle.

Chemoreceptors with a cavity have shown superior selectivity, being able to discriminate between guests due to the set geometry of the cavity. So while the acyclic ferrocenyl–azolium systems were able to co-ordinate with anions [125,126], a ferrocenyl–azolium salt with a cleft of a specific geometry and topology may be able to offer greater selectivity with regard to anion recognition. The two target macrocycles are shown in Figure 2.12. The targets, **143** and **144**, contain two different types of cavities, with two and four azolium centres, respectively. Compound **143** possesses a more rigid cleft, whereas **144** could have more flexibility. Therefore, it was of interest to prepare the two and then compare their respective ionophore properties.

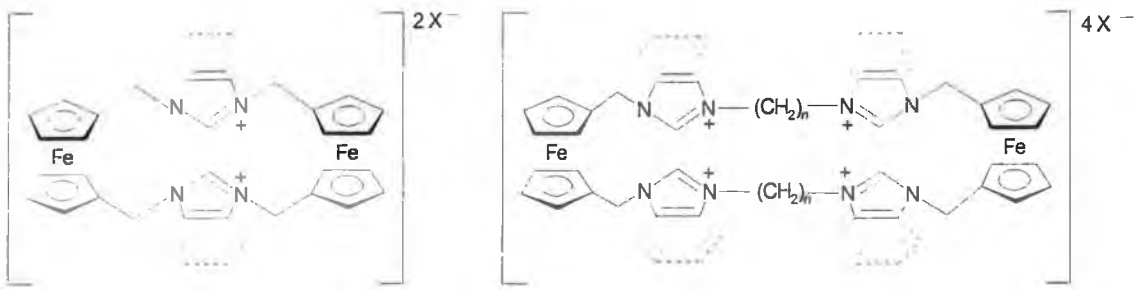

(143) **(144)**

Figure 2.12. *Proposed ferrocenyl–azolium macrocycles (143) and (144).*

Compound **143** was to be prepared in a similar manner to the 1,3-di(ferrocenylmethyl)azolium iodides (**161**) and (**162**). Compounds **161** and **162** were prepared by the reaction of the intermediate 1-ferrocenylmethylazole (**148**) and (**149**) with the mono-substituted ferrocenyl methiodide salt (**150**) in a 1:1 stoichiometry. In order to prepare compound **143**, the 1,1′-bis-(1-methylbenzimidazole)ferrocene (**175**) was treated with the disubstituted ferrocenyl methiodide salt (**174**) in an analogous method: heating to reflux in acetonitrile (Scheme 2.21). However, this reaction was not successful. After nearly 2 weeks of heating, with constant monitoring of the reaction by t.l.c., no new product could be observed.

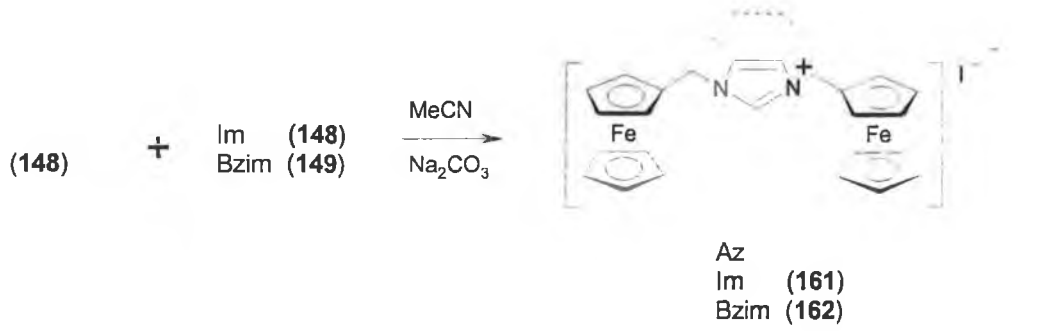

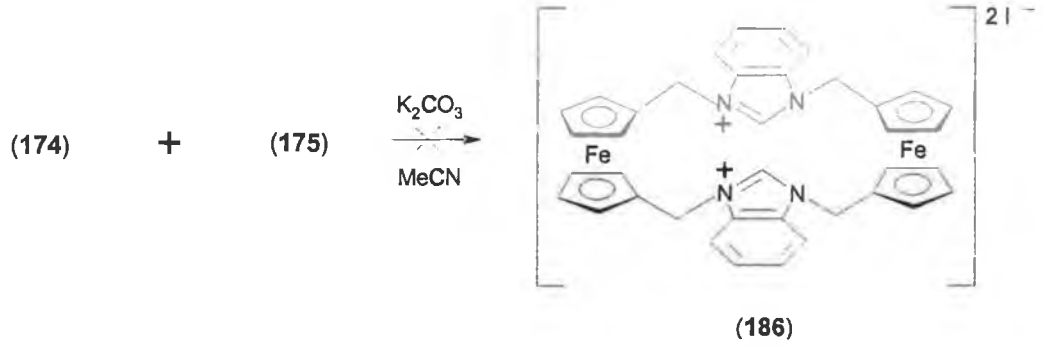

Scheme 2.21. *Attempted synthesis of a 'cage'-type macrocycle from 174 and 175.*

Therefore, it was concluded that this reaction may not work or would be too time-consuming or low-yielding to be of practical use. It was seen that reaction of the monosubstituted ferrocenyl methiodide salt (**150**) with the 1-methylferrocenylazole requires much longer reaction times than that of the reaction of the 1-methylferrocenylazoles with alkyl halides. Furthermore, the preparation of the 1,1′-bis(methylazole)ferrocenes from the bis ferrocenyl methiodide salt (**174**) is much more low yielding than the corresponding preparation of the 1-methylferrocenylazoles from **150**. It appears that as the substitution on the ferrocene compound increases, the approach of an incoming nucleophile is hindered, especially in this case as the nucleophile is a 1,1′-bis(methylazole)ferrocene, which is also subject to being anchored by the ferrocene skeleton, further restricting any freedom of movement. The preferred conformation of **175** is thought to be with the two benzimidazole rings on opposite sides of the ferrocene unit. In order to form the macrocycle **186**, **175** would have to have the two benzimidazole rings orientated on the same side of the ring, and so obviously would be more unstable due to repulsive steric effects (Figure 2.13). So it could be concluded that there is too much steric hindrance for this reaction to proceed.

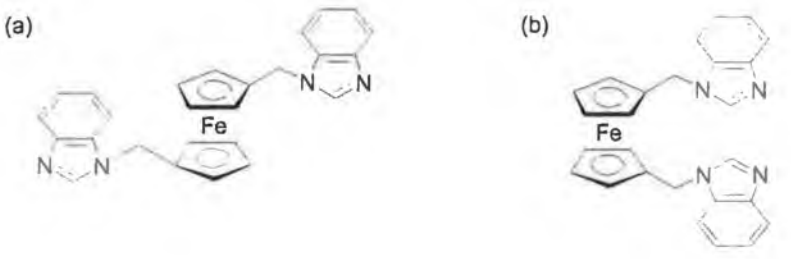

Figure 2.13. *The (a) preferred conformation of 175 and (b) more unstable form.*

However, the preparation of the macrocyclic structure **144** with four azolium centres linking two ferrocene units was successfully carried out. The same synthetic route used to prepare the linear bisazolium–ferrocenyl salts (**164**) and (**166**) was employed. 1,4-Diidobutane was again chosen as the spacer group, which was used to treat 1,1′-bis(1-methylbenzimidazole)ferrocene (**175**) to obtain the iodo- intermediate bis[1-(1,1′-ferrocenylmethyl)-3-(4-iodobutyl)]benzimidazolium iodide (**185**). Reaction of this compound with a further aliquot of **175** gave the final macrocycle – bis{1-[(1,1′-ferrocenylmethyl-3-butyl)benzimidazolium]-3-ferrocenylmethyl}benzimidazolium tetraiodide (**186**) (Scheme 2.22).

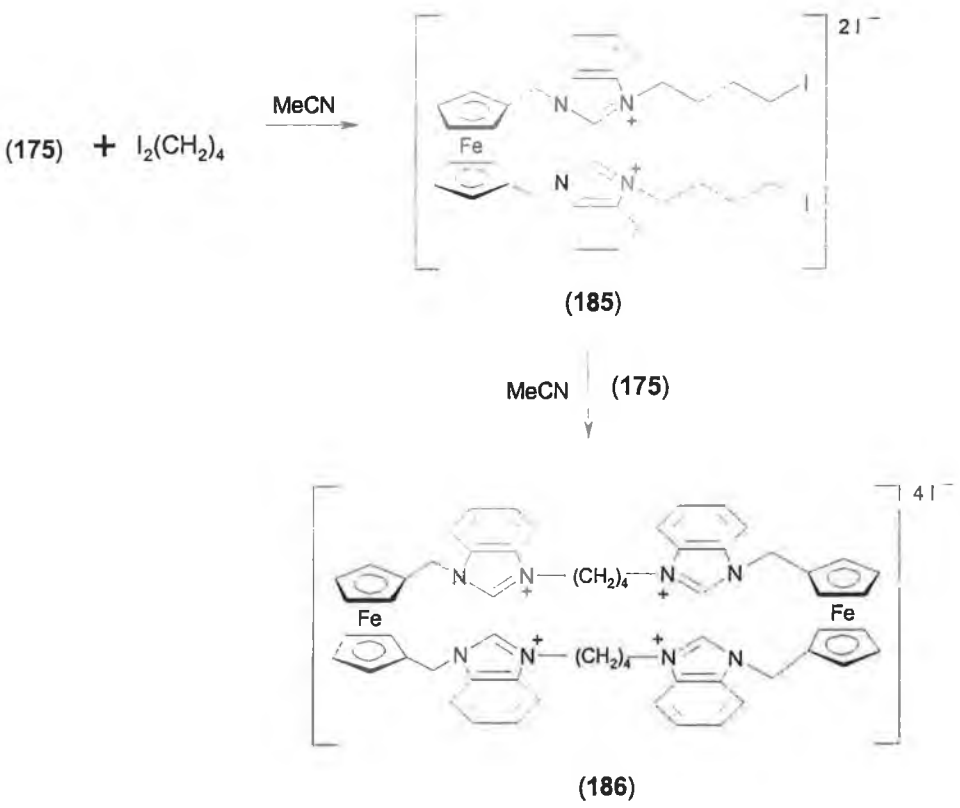

Scheme 2.22. *Preparation of bis{1-[(1,1′-ferrocenylmethyl-3-butyl)benzimidazolium] -3-ferrocenylmethyl}benzimidazolium tetraiodide (**186**).*

Both compounds were obtained by heating to reflux in acetonitrile for 2 h, then stirring at room temperature for a day. A precipitate was formed, collected by filtration and washed with diethyl ether. Both the intermediate (**185**) and the product (**186**) are insoluble in most solvents, being only soluble in DMSO and DMF, so further purification by column chromatography or crystallisation was not possible. Fortunately, while it was shown that some impurities were present, possibly polymeric products or salt impurities, **186** was approximately 90% pure. The yields obtained were 22% for **185** and 33% for **186**, with an overall yield from **175** of 7%.

The ^{1}H NMR spectrum of **186** is given in Figure 2.14. The 2-bzim H peak is seen at 9.84 ppm, the methylene linker is at 5.77 ppm and the butyl chain peaks are at 4.44 and 2.01 for $-CH_2CH_2CH_2CH_2-$ and $-CH_2CH_2CH_2CH_2-$, respectively. These shifts compare well with the shifts for compounds **164** and **166**.

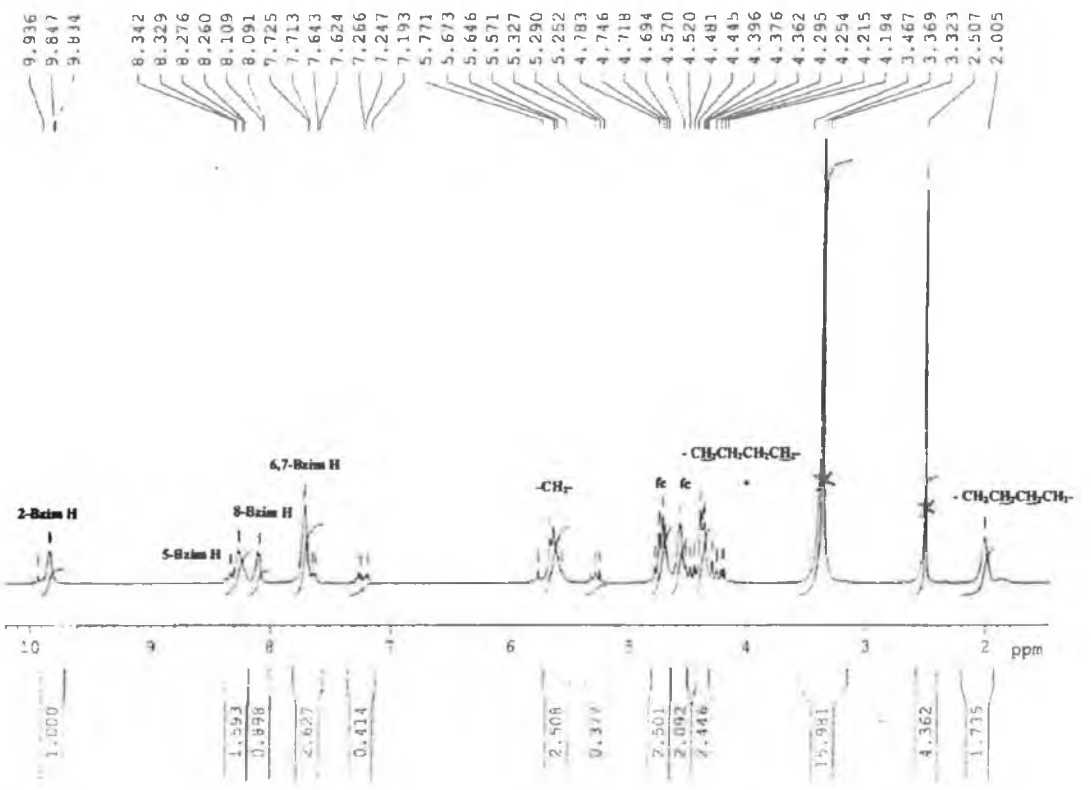

Figure 2.14. *The ^{1}H NMR spectra of* ***186*** *(DMSO-d_6).*

Computer modelling experiments, conducted by Dr Dermot Brougham of Dublin City University, showed that **186** may exist as different rotameric isomers. There are several possible rotamers of this compound where the contortion of the benzimidazolium moieties and the butyl spacer groups leads to different cavity shapes. In Figures 2.15 and 2.16, four different projected geometries are given using MM+ and PM3 optimisation. Figure 2.17, four possible rotamers are given in a space filling computer modelling projections. The existence of **186** as different rotational isomers could explain the poor resolution of the signals in the ^{1}H NMR.

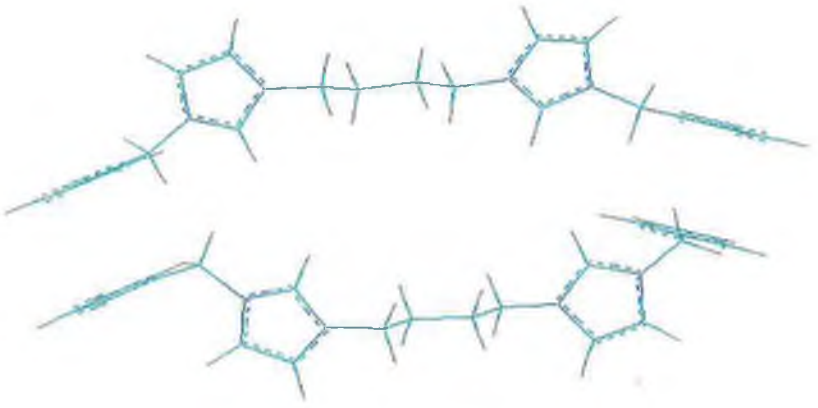

Figure 2.15. *MM+ optimisation of a model of the structure. The Fe atoms are removed, showing the Cp rings to be constrained to be 3.32Å apart. The cavity is asymmetric; c. 5.5×8.5Å (aspect ratio 1:1.55).*

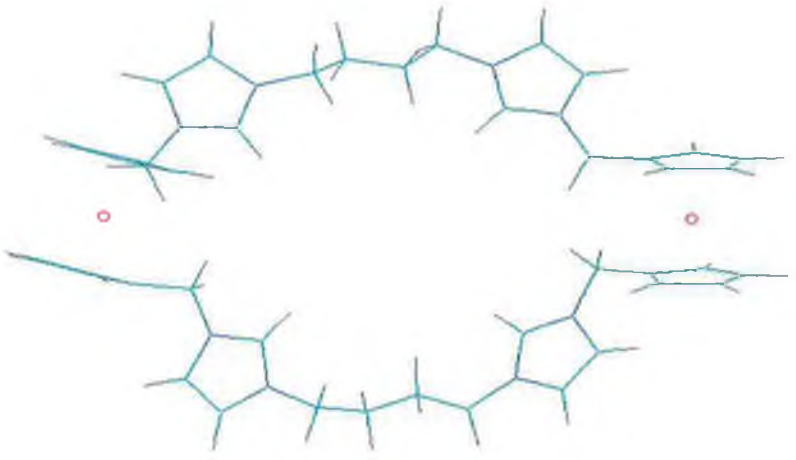

Figure 2.16. *PM3 optimisation of* ***186*** *(starting at MM+ opt geometry; using no constraints), showing an asymmetric cavity; c.8.5×10.5 Å (aspect ratio 1:1.24).*

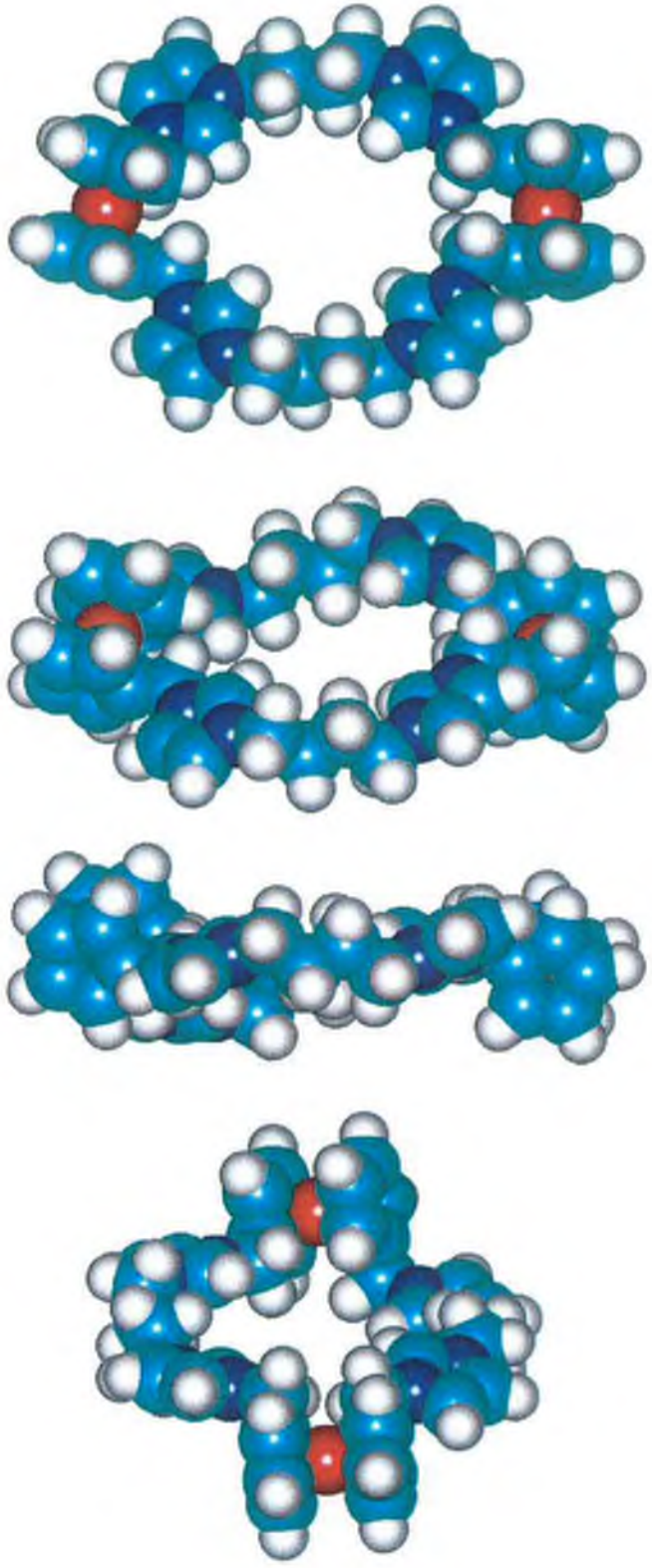

Figure 2.17. *Computer modelling projections of four possible rotamers of* ***186****, using PM3 optimisation.*

2.3 Conclusion

A range of monosubstituted 1-methylferrocenylazolium salts was prepared along with the 1,1′-bis(1-methylazolium)ferrocenyl iodide analogues. The monosubstituted 1-methylferrocenylazolium salts were prepared either from 1-methylferrocenylazole or from (ferrocenylmethyl)trimethylammonium iodide (150). The syntheses were simple and high-yielding (Scheme 2.23).

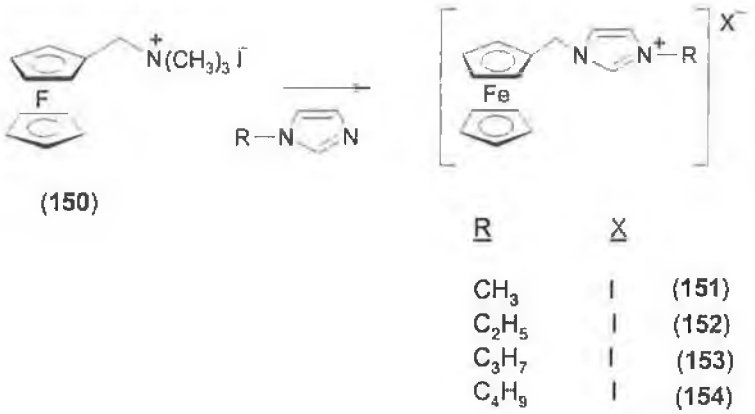

R	X	
CH_3	I	(151)
C_2H_5	I	(152)
C_3H_7	I	(153)
C_4H_9	I	(154)

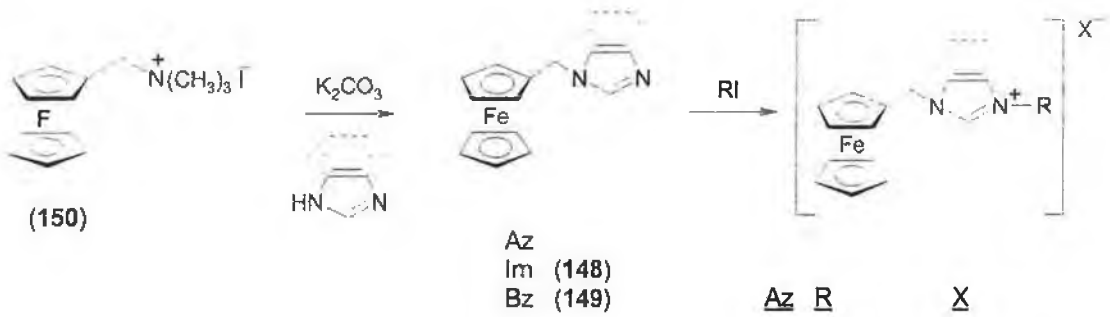

Az	R	X	
Im	$CH_2C_6H_5$	Cl	(155)
Bzim	CH_3	I	(156)
Bzim	C_2H_5	I	(157)
Bzim	C_3H_7	I	(158)
Bzim	C_4H_9	I	(159)
Bzim	$CH_2C_6H_5$	Cl	(160)

Scheme 2.23. *The preparation of the 1-methylferrocenyl-3-alkylazolium halides (151)–(160).*

While the 1-methylferrocenylazolium halides were prepared in a simple route from (ferrocenylmethyl)trimethylammonium iodide (**150**), a novel synthetic route was needed to obtain the 1,1′-bis(azolium)ferrocenyl salts. A few different procedures were employed to obtain the precursor 1,1′-bis(1-methylazole)ferrocene compound. Two efficient routes were found: the treatment of 1,1′-ferrocenyldimethanol (**168**) with CDI to yield 1,1′-bis(1-methylimidazole)ferrocene (**170**) and the treatment of ferrocene-1′-diylbis-(methyltrimethylammonium iodide) (**174**) with benzimidazole and potassium carbonate to yield **175**. These intermediates were then treated with the appropriate alkyl halide to obtain the azolium salt (Scheme 2.24).

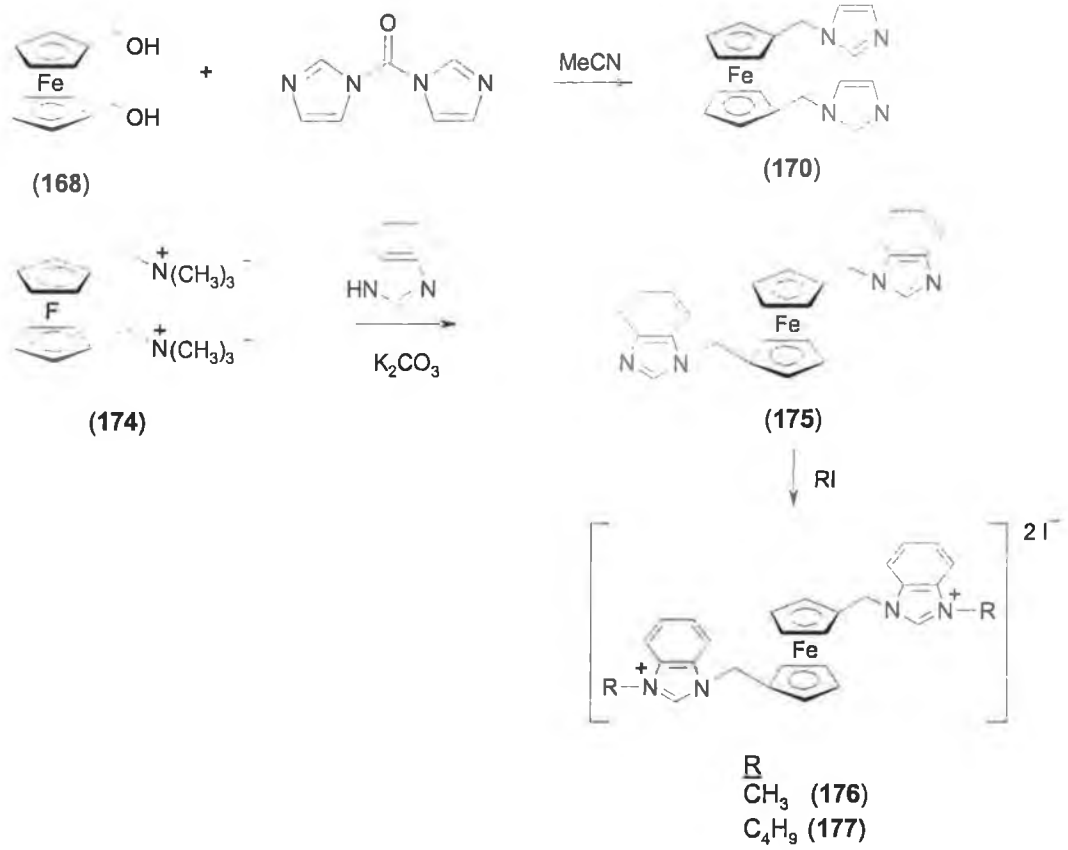

Scheme 2.24. *The preparation of 1,1′-bis(1-methylazolium)ferrocenyl iodides (**176** and **177**).*

The coupling of two 1-methylferrocenylazole compounds to prepare linear bisazolium–ferrocenyl compounds (**164**) and (**166**) was carried out. The 1-methylferrocenylazoles were used as the starting materials and an *n*-butyl group was the spacer (Scheme 2.25).

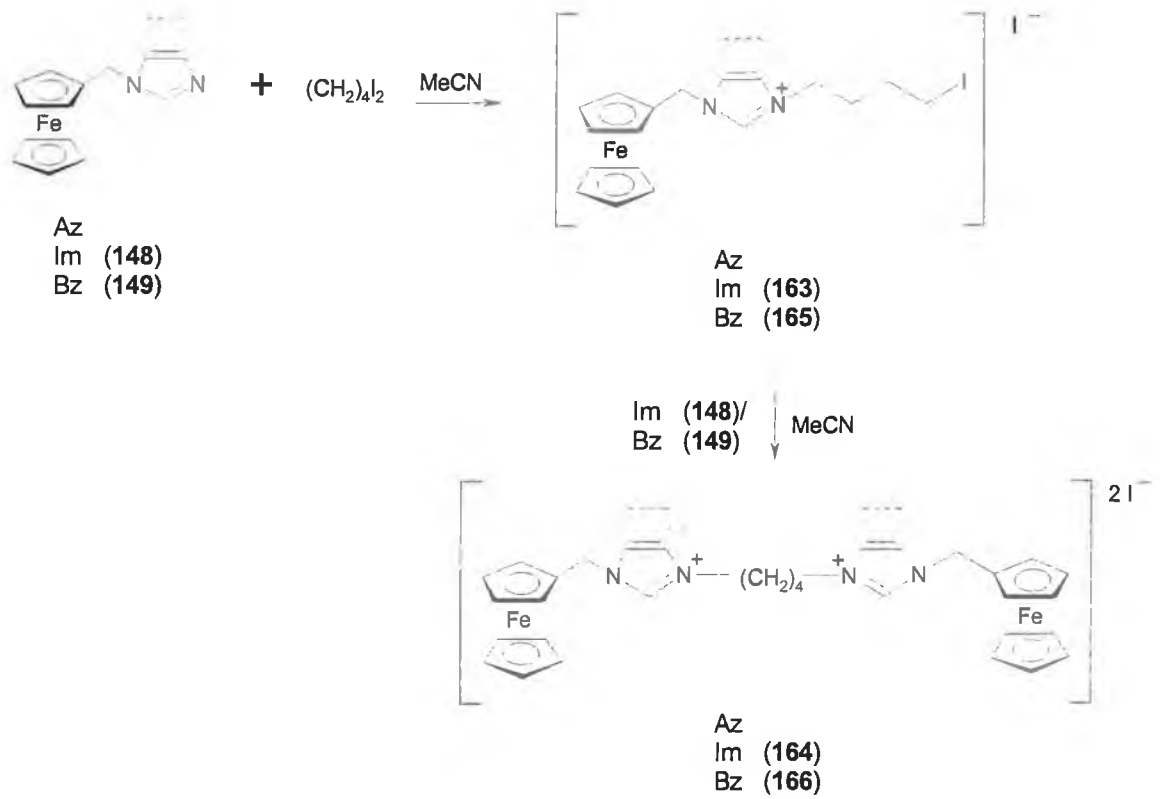

Scheme 2.25. *The preparation of the 1-[(1-ferrocenylmethyl-3-butyl)azolium]-3-ferrocenylmethylazolium diiodides (**164**) and (**166**).*

This system was extended to the preparation of the benzimidazolium cyclophane (**186**) (Figure 2.18, see Scheme 2.22). This is a novel tetracationic, macrocycle that has a flexible cavity, thus, it is a very interesting compound structurally and has a lot of potential for application in systems requiring selective associations.

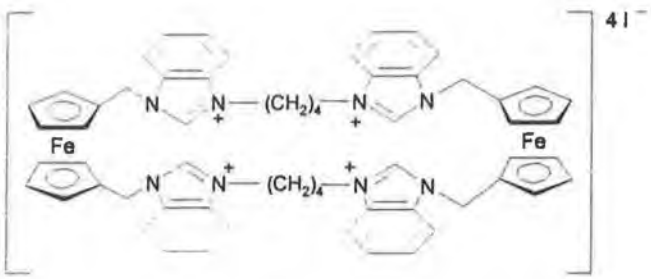

(186)

Figure 2.18. Benzimidazolium cyclophane (186).

Thus, a series of ferrocenyl–azolium systems had been prepared for application in transition metal-mediated catalysis, chemorecognition and antimicrobial activity. The compounds ranged from simple monosubstituted ferrocenyl–azolium salts and bisazolium–ferrocenyl systems, linked by an alkyl spacer or the ferrocene unit, to a macrocyclic tetrabenzimidazolium–ferrocenyl cyclophane.

Chapter 3

Application of Azolium Systems to Transition Metal Catalysed Cross-Coupling Reactions: the Heck Reaction

3.1 Results and discussion

3.1.1 Azolium salts as auxiliary ligands in the Heck reaction

In order to investigate the catalytic properties of the monosubstituted ferrocenyl–azolium salts and the chelate bisazolium–ferrocenyl salts, a very simple Heck reaction system was chosen. Ethyl acrylate and a substituted bromobenzene together with sodium acetate as the base, DMF as the solvent and $Pd(OAc)_2$ as the catalyst precursor were employed (Scheme 3.1). The DMF/sodium acetate/$Pd(OAc)_2$ system had previously been shown to be a highly effective system [186] using triphenylphosphine as the auxiliary ligand. Therefore, in order to base a comparison, two additional reaction runs were carried out: one with triphenylphosphine as a co-

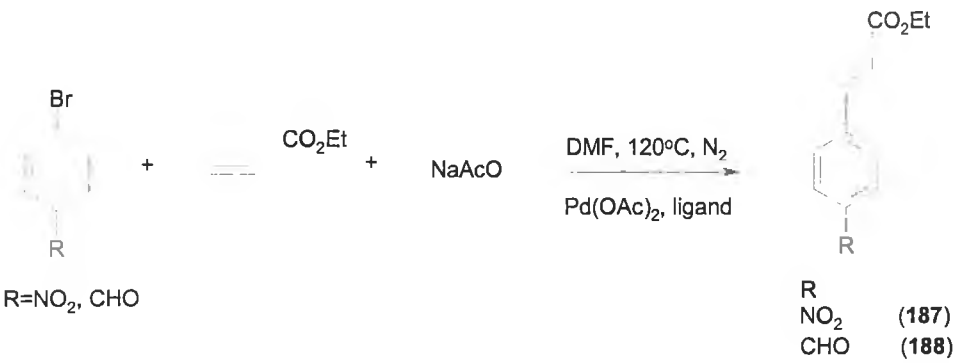

ligand and one without any ligand.

Scheme 3.1. *The Heck reaction system employed.*

The ferrocenyl–azole compounds used were varied. In each case, the following imidazolium and benzimidazolium analogues were employed: the methyl and butyl salts of the monosubstituted ferrocenyl–azolium salts (**151**), (**154**), (**156**) and (**159**); 1,3-di(ferrocenylmethyl)azolium iodides (**161**) and (**162**); the bridged structures (**164**) and (**166**) and the 1,1'-di(1-methyl-3-benzimidazolium)ferrocenyl salts (**176**). The reaction conditions employed were as follows: DMF as solvent, 1.25 equivalents of

sodium acetate, $Pd(OAc)_2$ at 1 mol%, the ligand at 1 mol% for bidentate ligands or at 2 mol% for monodentate ligands, under nitrogen, for 24 h and at 120°C.

The first reaction to be carried out was the coupling of bromobenzaldehyde and ethyl acrylate. The relative yields are shown in Table 3.1. It was observed that the imidazolium ligands outperformed the benzimidazolium ligands. Salt **151** produced a product yield of 95%; however, the benzimidazolium analogue **156** only produced a yield of 42%. It was also found that the monodentate ligands performed better than the bidentate ligands. The yield with compound **164** was 85%, which was less than that of **151**. It should noted that compound **151** performed on a comparable level with triphenylphosphine.

Compound	Yield (%)
151	95
156	42
164	85
176	41
PPh_3	100
No auxiliary ligand	3

Table 3.1. *A comparison of the yields for the cross-coupling reaction between 4-bromobenzaldehyde and methyl acrylate using ferrocenyl–azolium salts as auxiliary ligands.*

The second set of reactions was the coupling of 4-bromonitrobenzene with ethyl acrylate. However, with this set of reactions, while overall all the ferrocenyl–azoles

performed very well in relation to triphenylphosphine, a couple of patterns emerge which show that the benzimidazolium salts performed slightly better than the imidazolium salts. Compound **156** produced a higher yield than **151** (89 vs. 74%). Also while there proved to be no significant difference between the monodentate and bidentate ligands (Table 3.2), the bidentate ligands did produce slightly higher yields.

Compound	Yield (%)
151	74
156	89
154	78
162	91
164	94
166	85
177	91
PPh_3	100
No auxiliary ligand	20

Table 3.2. *A comparison of the yields for the cross-coupling reaction between 4-bromonitrobenzene and ethyl acrylate using ferrocenyl–azolium salts as auxiliary ligands.*

In the Heck reaction the role of the ligand in the catalytic cycle is essential to the efficiency of the reaction. So far the exact mechanism by which the ligand stabilises the palladium centre is unknown; however, from experimental studies it has been concluded that electron donating and/or sterically demanding ligands are able to promote the reaction as outlined in Chapter 1 [59–61].

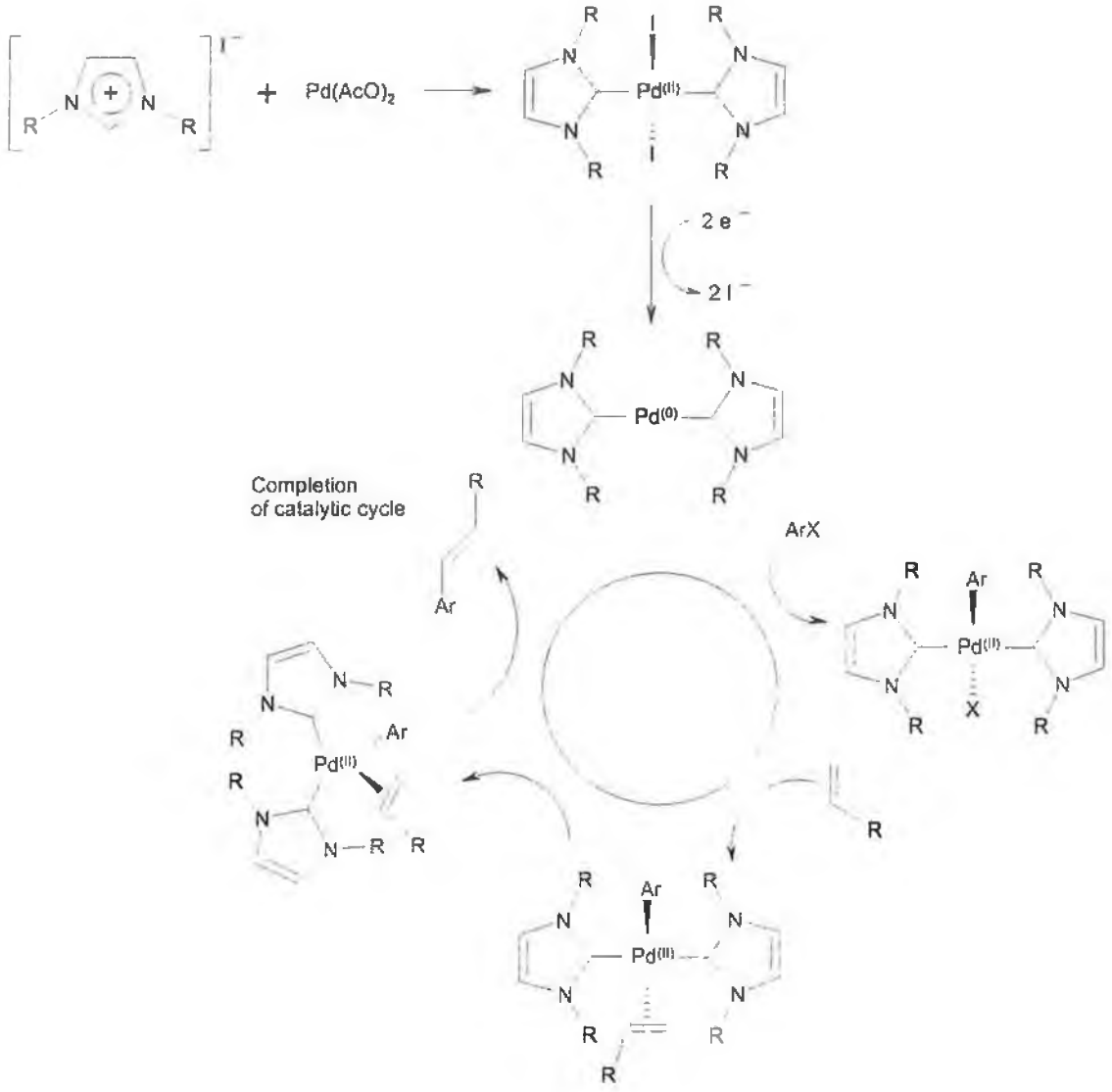

Scheme 3.2 *The mechanism of the Heck reaction with N-heterocyclic carbene ligands as the auxiliary ligands.*

The precursor Pd(II) complex $[Pd(HCN)_2I_2]$ (HCN=*N*-heterocyclic carbene) is generated in situ (Scheme 3.2) by the reaction of an imidazolium salt with $Pd(OAc)_2$. Reduction of this complex forms the co-ordinatively unsaturated 14-electron complex $[Pd(HCN)_2]$, which is the catalytically active species. This complex then undergoes a nucleophilic attack on the aryl halide to give the oxidative addition product. It is this step which is recognised as being the rate determining step. Then, via migratory

insertion and reductive elimination the aryl and alkene species are coupled and the catalyst is regenerated.

The effect of the imidazolium and benzimidazolium salt compounds on the Heck reaction efficiencies are best examined with the results from the reaction between 4-bromobenzaldehyde and ethyl acrylate. 4-Nitrobromobenzene is a highly activated system towards cross-coupling reactions and so distinctive patterns in the catalytic efficiencies of different ligands are harder to discern. However, the aldehyde group is not as activating towards this reaction, so the relative efficiencies of the different compounds as auxiliary ligands are easier to evaluate.

It was seen that the imidazolium salts (**151** and **164**) increased the product yield much more effectively than the benzimidazolium salts (**156** and **176**). This indicates that there are clear differences between the stability of the imidazolium and benzimidazolium palladium complexes that are formed during the catalytic cycle. So far there have not been any reported comparative studies in the literature on the stability of imidazolylidene and benzimidazolylidene palladium complexes.

As the rate determining step is the oxidative addition of the aryl halide to the metal centre [59], it is the availability of the Pd(0) species and its 'nucleophilicity' that will determine the reaction rate. As both azolium salts are known to readily form carbene complexes perhaps it is the relative nucleophilicity of the resulting azolylidene Pd(0) complexes that determines which one will be the more effective auxiliary ligand in the catalytic cycle. As the benzimidazolium 2-H is known to be more acidic than the imidazolium 2-H, it would seem that the imidazole ring would be able to act as a

better electron donor and, thus, increase the nucleophilicity of the resulting Pd(0) complex. In this study the imidazolium salts have been shown to be more effective in the reaction between ethyl acrylate and 4-bromobenzaldehyde and so it can be concluded that the imidazolylidene complexes are more electron rich and thus more nucleophilic.

However, in the case of the 4-nitrobromobenzene and ethyl acrylate, the benzimidazolium salts perform considerably better than in the first reaction, almost doubling their efficiencies. As the 4-nitrobromobenzene is such a highly activated system, perhaps the electronic factors that may have been responsible for the imidazolium salts performing well in the first reaction are not as important in this reaction. The efficiency of triphenylphosphine as an auxiliary ligand has been attributed to its bulkiness as well its electron donating abilities, therefore in this reaction perhaps the extra bulk of the benzimidazolium moiety adds to its efficiency, thus making it a more effective auxiliary ligand relative to the imidazolium ligand.

On examination of both reactions, there appears to be little appreciable difference between the monosubstituted and disubstituted azolium salts. In the literature some groups have found chelating azolium ligands can promote organometallic cross-coupling reactions more effectively [64], while others have seen monosubstituted azolium ligands to be more effective [42]. In the first reaction with bromobenzaldehyde, it is seen that the 1-methylferrocenyl-3-methylimidazolium iodide (**151**) is more efficient than the bridged bisimidazolium iodide (**164**), while the 1-methylferrocenyl-3-methylbenzimidazolium iodide (**156**) and 1,1′-bis(1-methyl-3-methylbenzimidazolium)ferrocenyl iodide (**176**) salts show the same reactivity. In the

second reaction, the reaction yields are all fairly similar so it is more difficult to identify relationships.

In conclusion, it has been shown that the ferrocenyl–azolium salts are effective auxiliary ligands in the catalysis of the Heck reaction. It has been shown that the effectiveness of these salts as ligands, however, depends on the system employed. It can be argued that for a less activated system, such as the olefination of 4-bromobenzaldehyde, electronic factors are more important and, therefore, the imidazolium salts and monosubstituted ligands are more effective. If a more activated system is considered, such as the 4-bromonitrobenzene, it is seen that steric factors have a greater priority. Therefore the benzimidazolium salts become more effective than the imdazolium salts. This interplay of steric and electronic factors should be considered when applying a salt as a potential auxiliary ligand in organometallic cross-coupling reactions.

3.1.2 Azolium salts as solvents for the Heck reaction

Ionic liquids are ideal candidates for use in biphasic catalysis. As such, a system can be designed where the appropriate ionic liquid is coupled together with an organic solvent that it is immiscible with. The organic reactants, and the products, will be contained in the organic phase, while the ionic liquid will then be able to provide a weakly co-ordinating medium to dissolve the catalyst (very often transition metal complexes) and be able to recycle it. Or ionic liquids may be found to be superior solvents for the reaction and replace the organic solvent completely, with the products being collected by distillation. Thus, the ionic liquids may enable recycling of the catalyst.

The use of a 1,3-dialkylimidazolium salt as a solvent in homogenous catalysis was examined. It was decided that the Heck reaction would provide a good model system. Presently, due to their favourable characteristics, it is the 1-methylimidazolium-based ionic liquids that are the most commonly used and investigated systems. One of the most popular of these in use currently is [BMIM]PF_6 (**189**). It is a neutral (non-acidic) stoichiometric compound, has a viscosity of 3.12 g cm^{-3} s at 30°C, is air and moisture insensitive and is inexpensive to prepare. It was this salt that we decided to employ as the solvent for the Heck reaction. We hoped to prove that the Heck reaction can be carried out in **189** and that the catalyst and ionic liquid could be recycled.

The Heck reaction has so far been carried out in the tetraalkylammonium and tetraalkylphosphonium salts. Kaufmann et al. first used tetraalkylammonium and tetraalkylphosphonium bromides in which to immobilise the Pd(0) catalyst precursor [61]. The vinylation of bromobenzene by *n*-butyl acryate to butyl *trans*-cinnamate

was successfully carried out in these melts at 100°C and the product was collected by distillation.

Hermann and Böhm used tetraalkylammonium melts also, and showed that they were superior to the commonly used aprotic organic solvents used, such as DMF [44]. In one example, a molten $[NBu_4]Br$ (m.p.=103°C) system with bromobenzene and styrene and a diiodobis(1,3-dimethylimidazolin-2-ylidene)palladium(II) catalyst produced stilbene in a 99% yield compared to the 20% yield when DMF was the reaction medium used. Furthermore, they demonstrated easy product isolation using distillation and were able to recycle the catalyst.

For our investigation we selected a simple model system, using a number of bromobenzene derivatives with methyl acrylate and $Pd(OAc)_2/PPh_3$ as the catalytic system and sodium acetate as the base (see Scheme 3.3). A comparative study was then performed, between DMF and $[BMIM]PF_6$, to determine the efficiency of $[BMIM]PF_6$ for the Heck reaction.

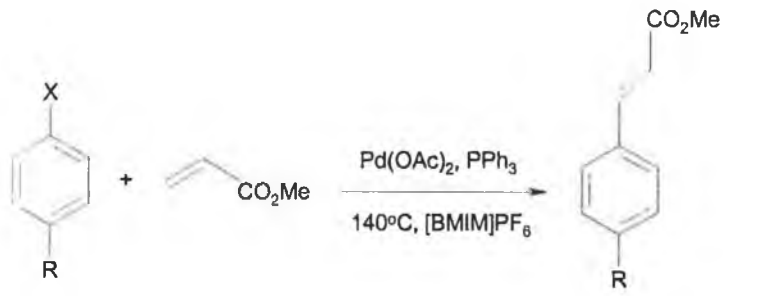

R	
OCH_3	**(190)**
NO_2	**(191)**
CHO	**(192)**
Cl	**(193)**
H	**(194)**

Scheme 3.3. *The model Heck reaction system used.*

The reaction conditions used were as follows: the catalytic system of $Pd(OAc)_2/PPh_3$ was added to the ionic liquid and after slight heating and stirring was fully dissolved, then the base (sodium carbonate), bromobenzene derivative and methyl acrylate were added. The reaction mixture was heated to 140°C with stirring for 17 h. After completion of the reaction, two work-up procedures were attempted. The first of these involved the addition of water to the reaction mixture with thorough stirring and separation to remove the halide salt by-products. After removal of the water and subsequent filtering, the ionic liquid was extracted with diethyl ether and the products were dried over $MgSO_4$, filtered and evaporated to dryness, then finally purified on silica gel using dichloromethane. The products were identified by ^1H NMR spectroscopy, and all the spectral data for the compounds were found to be in agreement with those given in the literature [186–190].

The alternative work-up procedure involved the addition of water to the reaction mixture followed by its removal and filtration. The reaction was then heated under vacuum and the product collected by distillation. Using both of these methods the product was efficiently collected and the ionic liquid/palladium catalyst was reused and the reaction repeated with similar yields being obtained, thus showing that the palladium catalytic system had remained in the ionic liquid and was still active. The results are given in Table 3.3.

Product	Solvent	Yield (%)
190	DMF	35
	$[BMIM]PF_6$	29
191	DMF	95
	$[BMIM]PF_6$	83
192	DMF	70
	$[BMIM]PF_6$	62
193	DMF	70
	$[BMIM]PF_6$	69
194	DMF	76
	$[BMIM]PF_6$	61

Table 3.3. *The yields of the products from the model Heck reactions (using the separation technique of work-up).*

It was found that the yields of the reactions carried out in DMF and $[BMIM]PF_6$ were comparable. Although the yields of the products from the DMF system were slightly higher, this could be due to the reaction conditions not being fully optimized as these were a preliminary qualitative set of experiments. Also, for a set volume of ionic liquid used, a substantially greater amount of product can be produced due to the recyclability of the catalyst.

It appears that there was negligible leaching of the catalyst, since when the ionic liquid was used the catalyst could be recycled for a repeat reaction. Each yield was similar, any slight decrease could be due to the slight loss of solvent in the work up procedure, and hence loss of the catalyst. Also, a solution of ionic liquid with

$Pd(OAc)_2/PPh_3$ contained in it was extracted with water six times, then diethyl ether six times. Upon removal of the water and diethyl ether, respectively, catalyst was recovered, indicating that the extraction techniques used in the work-up procedures do not remove the catalyst from the ionic liquid.

Therefore, it can be concluded that $[BMIM]PF_6$ can be used as a viable, efficient solvent for the Heck reaction, having comparable efficiency to the most commonly used solvent, DMF. Furthermore, it provides the advantage of being able to anchor the catalyst in solution enabling it to be reused for further reactions to be carried out. Hence, after product isolation the palladium moiety is not lost, unlike in the DMF system. Thus, the ionic liquids clearly show that they would offer obvious environmental and economical advantages over the presently used organic solvents.

3.2 Conclusion

Thus, it has been shown that azolium salts can aid transition metal-mediated cross-coupling reactions in two ways: First they can act as auxiliary ligands for palladium in the Heck reaction, as has already been reported; however, we have shown that the ferrocenyl–azolium salts were able to aid the catalysis of the Heck reaction and that benzimidazolium salts could be as effective as the imidazolium ligands in certain systems.

Second, while the use of air and moisture stable azolium salts that are liquid at room temperature in transition metal catalysis has been the subject of many investigations, it has now been shown that they are able to act as efficient solvents in the Heck reaction and are capable of retaining the catalyst for repeated use.

Chapter 4

Biological and Chemoreceptor Studies on Ferrocenyl–Azolium Compounds

4.1 Introduction

As demonstrated in Chapter 1, the azole/azolium class of compounds is remarkably versatile in its functions. Having employed azolium salts in the catalysis of cross-coupling reactions and as solvents in the Heck reaction, their application to anion recognition and biological objectives was examined.

One area of biological relevance (and environmental applications) where there is a lively field of research is anion recognition. Anions play a role in numerous biological and chemical processes and have great impact in both medicine and the environment. For example, many metabolic systems and pathological pathways are dependent on anions, e.g., the misregulation of chloride channels will result in cystic fibrosis and Alzheimer's has been linked to anion-binding enzymes.

Azolium salts are now beginning to be applied as ionophores. They make very attractive centres for anion co-ordination as they have the ability to form hydrogen bonds with anions through the acidic 2-H and electrostatic interactions between the positively charged azolium ring and the negatively charged ion. If they are then introduced into a system that allows only selective co-ordination then a very efficient system could be developed.

One of the rationales behind the design of these compounds was that their selectivity as anion chemoreceptors could be examined. It has been reported that simple monosubstituted ferrocenyl–imidazolium and ferrocenyl–benzimidazolium systems were capable of anion co-ordination [125,126]. However, these systems did not show any selectivity, an essential feature in a chemoreceptor for practical application. The

macrocyclic salt and the bisazolium–ferrocenyl salts prepared (Chapter 2) were proposed to be an extension to the early prototype monosubstituted ferrocenyl–azolium salts (Chapter 1, Figure 1.25, [125,126]). It was thought that these bisazolium–ferrocenyl salts could 'wrap' around the anion, thus, having a three-dimensional structure induced in them by an anion of a particular geometry or the cavity in the macrocycle, could 'hold' an anion (Figure 4.1). Perhaps through one of these modes of binding a greater degree of selectivity for anion binding might be observed.

Of the compounds prepared, the bridged 1-[(1-ferrocenylmethyl-3-butyl)imidazolium]-3-ferrocenylmethylimidazolium diiodide (**164**), the 1,1′-bisazolium ferrocenyl – 1,1′-bis(1-methyl-3-*n*-butylbenzimidazolium)ferrocenyl iodide (**177**) and the macrocyclic salt – bis{1-[(1,1′-ferrocenylmethyl-3-butyl)benzimidazolium]-3-ferrocenylmethyl}benzimidazolium tetraiodide (**186**) ligands were chosen for anion recognition studies. These compounds and their possible co-ordination modes with anions are shown in Figure 4.1 (**195–197**).

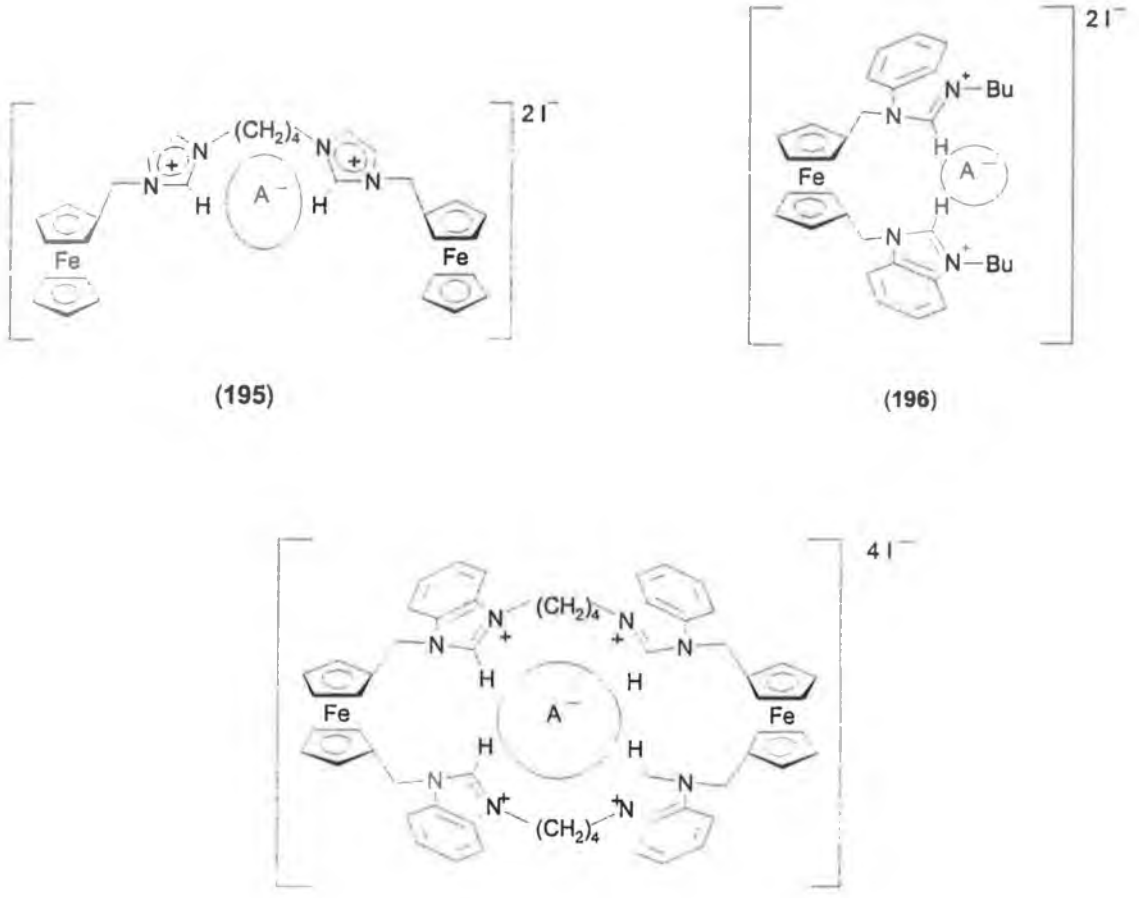

Figure 4.1. *The application of compounds* ***164, 177 and 186*** *as anion receptors, forming complexes* ***195–197.***

4.2 Results and discussion

4.2.1 ^{1}H NMR titration studies

Anion co-ordination studies were attempted on compounds **164**, **177** and **186** to see if these ligands would selectivity bind to anions, thus conferring a greater degree of specificity than the ferrocenyl–azolium salts (**83–87**) already investigated [125,126]. In compounds where hydrogen bonding is thought to be one of the main modes of anion co-ordination, ^{1}H NMR spectroscopy titration experiments were used to evaluate the degree of anion binding. The reports of 1,3-dialkylazolium salts as anion

chemoreceptors have shown that the signal corresponding to the 2-H proton shifts significantly downfield on addition of anion guests [105,107–111,125,126]. Thus, ^{1}H NMR spectroscopy is a valuable tool for the monitoring of host–guest interactions. Compounds **164** and **177** were chosen as they represented a comparison of the spacer group and a comparison of the azolium functionalities. Furthermore, they were soluble in acetonitrile-d_3, the solvent that had been used in the previous anion binding studies.

Stoichiometric amounts of various anions as their tetrabutylammonium salts, $[NBu_4]X$ (X=Cl, Br, I, NO_3, HSO_4) were added to solutions of the ferrocenyl–azolium salts in acetonitrile-d_3. In our ^{1}H NMR titration experiments, we were aiming to observe the interaction of a ligand with a specific anion only.

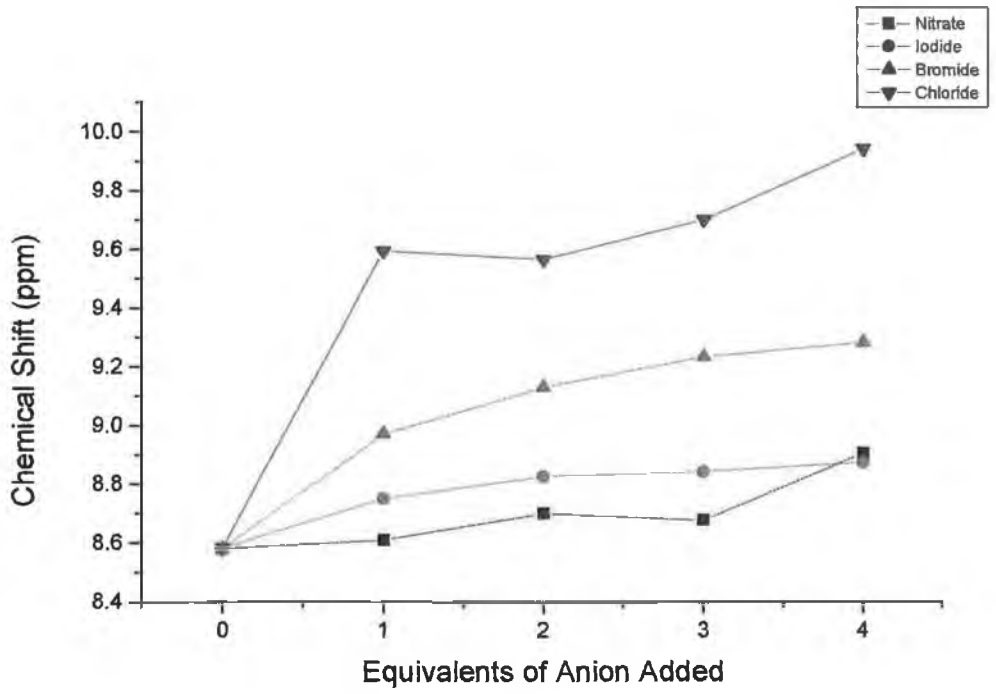

Figure 4.2 *Plot of chemical shift of C-2 proton of* ***164*** *versus equivalent of anion added in acetonitrile-d_3.*

It would appear from Figure 4.2 that **164** is interacting with all of the halides. The titration results indicate that **164** binds with bromide in a 1:4 stoichiometric ratio, alternatively it would seem that **164** binds with iodide in a 1:2 ratio. For bromide, we believe that both anion exchange and H-bonding with **164** is occurring, in the case of iodide we observe solely H-bonding since **164** is an iodide salt. Chloride is interesting in that it would appear that a 1:1 complex with **164** has occurred. Chloride may bind with **164** in a chelate fashion as outlined by structure **195**. The oxyanion, nitrate, interacts with **164** in a non-stoichiometric fashion, thus, binding ratios and mode of binding cannot be determined.

Titration data for **177** is outlined in Figure 4.3.

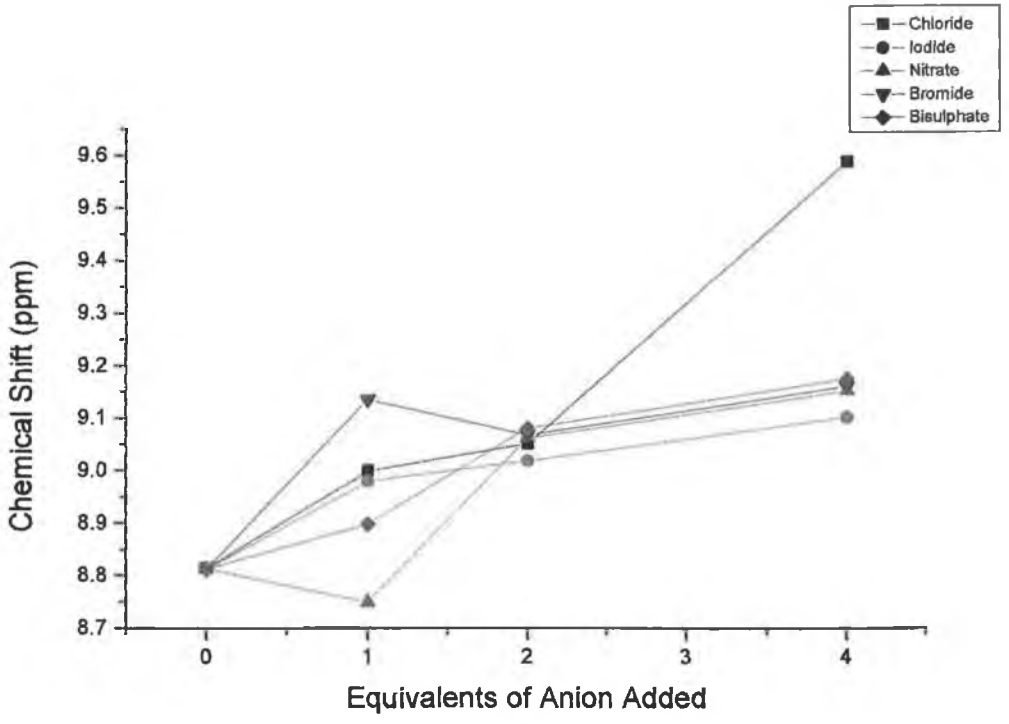

Figure 4.3. *Plot of chemical shift of the C-2 proton of* ***177*** *versus equivalent of anion added in acetonitrile-d_3.*

The titration data for **177** again show interaction between the ligand and all anions. Determination of stoichiometric binding from this data is not possible, it would appear that the proposed mode of binding for **177**, as outlined in Figure 4.1 (**196**), is not occurring. Perhaps the cleft outlined in **196** is either too small to fit the halides tested or there is too much steric hindrance between the benzimidazole groups on the ferrocene to form the proposed binding cleft in the first place.

The benzimidazolium cyclophane (**186**), however, proved to be too insoluble for ^{1}H NMR titration experiments to be conducted, as it was only soluble in DSMO-d_6. A control titration experiment was carried out with **162** (previously carried out in acetonitrile [126]) in DMSO-d_6. Results of this experiment showed no shift in the C-2 proton chemical shift upon addition of anion. This result is contrary to what was found in acetonitrile and can be best explained by the strong solvating effect of DMSO-d_6. Thus DMSO-d_6 is not a suitable solvent for these imidazole/benzimidazole systems. We will be testing **186** using potentiometric techniques, particularly ion selective electrode analysis. Results of this testing are not available at this time.

4.2.2 Antimicrobial activities of ferrocenyl–azoles and ferrocenyl–azolium compounds

It was decided to screen the antimicrobial activities of the ferrocenyl–azole/azolium compounds against a yeast, *Candida albicans*, and a Gram-negative bacterium, *Pseudomonas aeruginosa.* Both of these microbes form biofilms that are resistant to antimicrobial agents [191] and have been recognised as opportunistic pathogens that infect immunocompromised human hosts [192,193]. *The Candida* species are the principal etiological agents of nosocomical fungal infections, of which *C. albicans* is

the most abundant and significant [194]. *C. albicans* forms biofilms in vitro on various inert surfaces and under different nutrient conditions, and hence can cause infections associated with biomedial implants [195–198]. *P. aeruginosa* is one of the most nosocomical acquired pathogens and has a great ability to adapt to varied environments. Thus, it is found ubiquitously in hospitals, and is nearly impossible to eliminate from hospital environments, has a wide range of pathogencity and, therefore, poses a great threat to seriously immunocomprised individuals in care [199].

A representative selection of the ferrocenyl–azole/azolium salts prepared was screened for their antibiotic capabilities against *P. aeruginosa* and *C. albicans*. These antimicrobial screenings were carried out by Dr Alan Farrell and Dr Brid Quilty from the School of Biotechnology, Dublin City University. The compounds tested were the neutral 1-methylferrocenylazoles (**148** and **149**), 1-methylferrocenyl-3-methylazolium iodides (**151** and **156**), 1,3-di(1-methylferrocenyl)azolium iodides (**161** and **162**) and the 1-[(1-ferrocenylmethyl-3-butyl)benzimidazolium]-3-ferrocenylmethylazolium diiodides (**164** and **166**). The results are given in Tables 4.1 and 4.2 for *P. aeruginosa* and *C. albicans*, respectively.

The antibiotic activities were calculated as reductions in cell growth calculated using the following formula:

$$\text{reduction in growth} = \{[(C-B)-(T-B)]/C-B)\} \times 100,$$

where C is the average absorbance per well for control wells (organism with no compound), B is the average absorbance per well for blank wells (no organism with

no broth) and *T* is the average absorbance per well for treated wells (organism and compound).

Compound	Percentage reduction in growth (%)					
	Compound concentration (μg ml^{-1})					
	25	50	75	100	250	500
*1-Ferrocenylmethylazoles (**148** and **149**)*						
148	0.00	10.27	0.00	9.08	6.38	0.00
149	0.00	30.80	29.40	210.29	0.00	0.00
*1-Ferrocenylmethyl-3-methylazole iodides (**151** and **156**)*						
151	2.16	0.00	0.00	0.00	0.00	0.00
156	0.00	0.00	6.59	17.19	21.18	28.43
*1,3-Di(1-methylferrocenyl)azolium iodides (**161** and **162**)*						
161	0.00	5.30	0.00	7.67	0.00	0.00
162	0.00	0.00	0.00	0.00	2.81	0.00
*1-[(1-Ferrocenylmethyl-3-butyl)benzimidazolium]-3-ferrocenylmethylazolium diiodides (**164** and **166**)*						
164	0.00	13.29	0.00	1.84	8.75	18.37
166	0.16	31.02	11.02	15.02	0.00	0.00

Table 4.1. *The antimicrobial activities of ferrocenyl–azole compounds against P. aeruginosa.*

Compound	Percentage reduction in growth (%)					
	Compound concentration (μg ml^{-1})					
	25	50	75	100	250	500
*1-Ferrocenylmethylazoles (**148** and **149**)*						
148	0.00	0.00	0.53	0.16	0.00	0.00
149	3.72	6.10	6.35	5.23	9.11	11.23
*1-Ferrocenylmethyl-3-methylazole iodides (**151** and **156**)*						
151	0.00	0.41	0.78	0.00	1.35	33.89
156	0.00	0.00	0.00	0.00	2.22	0.47
*1,3-Di(1-methylferrocenyl)azolium iodides (**161** and **162**)*						
161	3.72	18.18	21.69	11.30	71.95	88.16
162	2.10	2.85	1.85	0.00	0.00	0.00
*1-[(1-Ferrocenylmethyl-3-butyl)benzimidazolium]-3-ferrocenylmethylazolium diiodides (**164** and **166**)*						
164	0.00	1.47	2.79	1.97	4.73	7.54
166	3.10	12.74	30.14	89.60	91.16	90.60

Table 4.2. *The antimicrobial activities of ferrocenyl–azole compounds against C. albicans.*

From the data summarised in Tables 4.1 and 4.2, it can be seen that some of the ferrocenyl–azolium compounds are showing antifungal activity. All compounds tested gave very poor responses as antibacterial agents.

It would appear that compounds **161** and **166** have excellent potential as antifungal agents with calculated LD_{50} values of 175 and 84 μg ml^{-1}, respectively. It is

interesting to note that both **161** and **166** are bisferrocenyl–azolium derivatives. It would appear that both the neutral and charged monoazole–ferrocenyl compounds show little bioactivity. The presence of two ferrocenes seems to be essential for bioactivity. Perhaps the ferrocene groups are playing an electrochemical role, as has been seen with ferrocenyl antimalarials [126]. To better understand the bioactivity of both **161** and **166** a series of structural modifications on these compounds will have to performed in the future and from these studies a new pharmacophore can be generated.

4.3 Conclusion

In the employment of ferrocenyl–azole/azolium salts to biological applications, it has been shown that the ferrocenyl–azolium salts have potential as pharmocophores but would need great optimisation of the current compounds for use as ionophores.

The ^{1}H NMR titration experiments showed that selected bisazolium–ferrocenyl compounds were capable of interaction with anions. Compound **164** showed prefential binding with chloride, binding in a 1:1 stoichiometry; however, salt **177** did not show any such specificity and did not show the same degree of anion co-ordination as **164**. Perhaps **164** was able to wrap around the chloride anion in the way predicted, while **177** is a too sterically constrained system for this mode of anion co-ordination. Thus, the *n*-butyl spacer group appears to allow the conformational change necessary in anion co-ordination as opposed to the ferrocene unit which appears not to. It was hypothesised that of the ferrocenyl–azolium systems developed macrocycle **186** would be able to co-ordinate most selectively to anions due to its cavity.

However, **186** proved to be only soluble in DMSO-d_6, which unfortunately proved to be a poor solvent for the observation of anion binding.

Two bisferrocenyl–azolium compounds (**161** and **166**) were able to act as very effective antifungal agents against *C. albicans* with impressive LD_{50} values being observed in antimicrobial testing. However, they did not show any significant antibacterial activity against *P. aeruginosa*.

Chapter 5

Design and Synthesis of

Ferrocenyl–Azole–Phosphine Systems

5.1 Introduction

As the application of the ferrocenyl–azolium salts to catalysis, complexation and anion recognition had proved successful, we decided to introduce another co-ordinating functionality into the ferrocenyl–azolium salts. The purpose of this was so that it could act as a second co-ordination point in addition to the carbene moiety that could be generated in the case of complex formation. Ideally, it was thought that it should be a different functionality and so have different ligating properties, thereby creating a hemilabile ligand.

A hemilabile ligand can often increase the reactivity of a catalyst compared to an inert diphosphine system. In some instances, a very weak chelate is needed to activate a transition metal to act in a catalytic system. But on the other hand, a strong chelate ligands can perform very well in asymmetric catalysis by not allowing unselective monodentate ligands to compete and reduce the enantioselectivity of the calalyst. Therefore, in addition to the carbene co-ordination point, a phosphine functionality seemed a good choice for the second group to create a bidentate ligand, as the efficiency of the phenylphosphines as ligands is well known.

The target compounds are shown in (Figure 5.1). The first compound was based on the introduction of a diphenylphosphine on the second Cp ring of the ferrocene–azolium salt, giving a 1-diphenylphopsphine-1′-(1-alkyl-3-methyl)imdazolium ferrocenyl salt (**198**) – a 1,1′-disubstituted ferrocene. The second compound has a diphenylphosphine functionality introduced onto the same Cp ring as the azolium ring on the ferrocene, thereby creating a chiral 1-diphenylphopsphine-2-(1-alkyl-3-methylimidazolium)ferrocenyl salt (**199**) – a 1,2-disubstituted ferrocene.

(198) **(199)**

Figure 5.1. *The proposed ferrocenyl–azolium systems with the introduction of a phosphine functionality.*

5.2 Results and discussion

5.2.1 Synthesis of a 1-diphenylphopsphine-1′-(1-alkyl-3-methyl)imdazolium ferrocenyl salt

A very convenient starting point for the preparation of (**198**) was the ferrocenophane – (1,1′-ferrocenediyl)phenylphosphine (**200**) – which could be nucleophilically opened using phenyl lithium. This allows the desired diphenylphosphine group to be generated on one Cp ring, while the other is open to reaction with an electrophile. This was seen as perhaps the best way to introduce the imidazole or other precusor functional groups.

It was decided to employ DMF as the electrophile, resulting in the formation of an aldehyde group. From here simple reduction to an alcohol was envisaged. The next step was the linking of the imidazole species via the alcohol and finally conversion to the imidazolium salt.

While these were the major steps, a further stage was required: the protection of the phosphine group so that it would not be converted to a phosphonium ion during

alkylation of the imidazole. The final step would then be the deprotection of the phosphorus yielding the desired product **198**. (See Scheme 5.1 for the outline of the synthetic route to **198**).

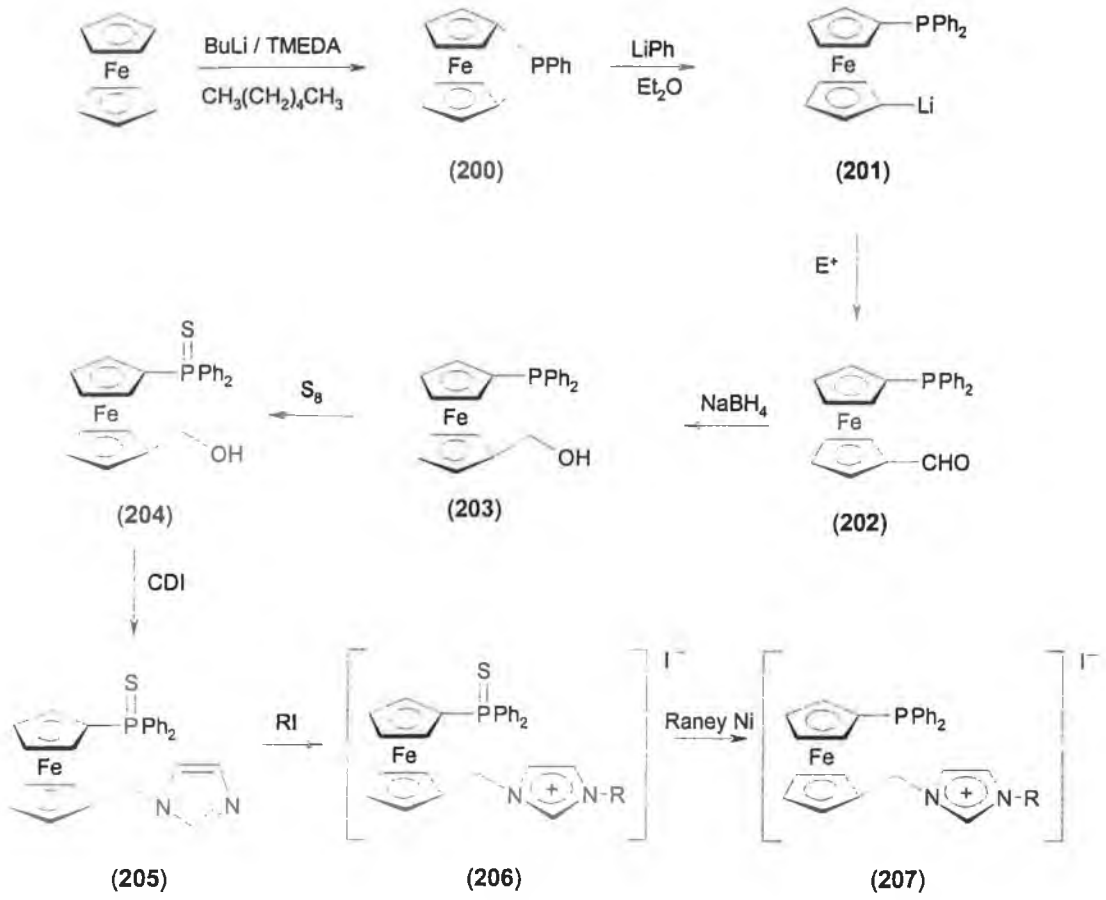

Scheme 5.1. *Synthetic outline of the preparation of **198**.*

5.2.1.1 Synthesis of [1′-(diphenylphosphinosulphide) ferrocenyl]methanol (204)

The starting point of the synthesis was the preparation of the ferrocenophane (**200**) [200], which was then nucleophilically opened using phenyl lithium (Scheme 5.2). Reaction of the 1'-(diphenylphosphino)lithioferrocene intermediate (**201**) with DMF and subsequent crystallisation gave 1′-(diphenylphosphino)ferrocenecarboxaldehyde [Fe(η^5-$C_5H_4PPh_2$)(η^5-C_5H_4CHO)] (**202**) in 69% yield. Reduction of **202** to the

methylhydroxy functionality using sodium borohydride then afforded [1′-(diphenylphosphino)ferrocenyl]methanol [Fe(η^5-$C_5H_4PPh_2$)(η^5-$C_5H_4CH_2OH$)] (**203**).

The diphenylphosphine group was protected by conversion into a phosphine sulphide (P=S) group. This was achieved by reaction of **203** with sulphur in dry benzene, giving [1′-(diphenylphosphinosulphide)ferrocenyl]methanol {Fe[η^5-$C_5H_4P(S)Ph_2$](η^5-$C_5H_4CH_2OH$)} (**204**) in a yield of 65% after purification by column chromatography.

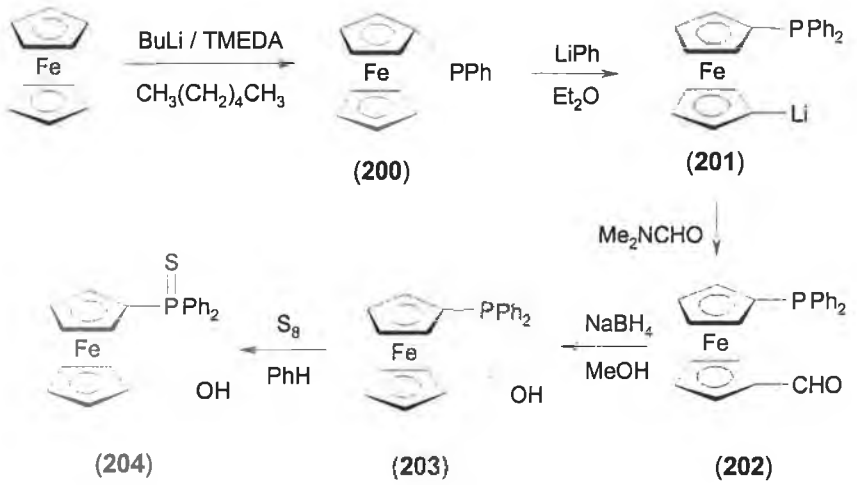

Scheme 5.2. *Synthesis of {1'-(diphenylphosphinosulphide)ferrocenyl}methanol (**204**).*

The structures of **202–204** were confirmed by NMR and IR spectroscopy and microanalysis. The standard techniques of ^1H, ^{13}C and ^{31}P NMR spectroscopy allowed the structures to be determined, with the shifts being consistent with previously reported compounds. The methylene shift at 4.28 and 60.42 ppm in the ^1H and ^{13}C NMR spectra, respectively, for **204** is noteworthy as this becomes an important barometer of change in the adjoining functional group. The phosphorus NMR

spectrum of **203** has a chemical shift of −16.3 ppm. This is shifted to a value of 42.6 ppm with the introduction of sulphur.

5.2.1.2 Introduction of the imidazole (205)

Once, the alcohol was obtained and the phosphorus protected, then the imidazole moiety was introduced to give compound **205**, which could then be converted to the imidazolium salt (**206**). This was attempted in two ways: conversion of the hydroxy group to a tosylate derivative for the nucleophilic substitution of imidazole or the use of CDI with the alcohol.

5.2.1.2.1 Tosylation

Using a procedure reported in the literature [201], the preparation of a tosylate followed by displacement by an imidazole in situ was attempted (Scheme 5.3). Here **204**, *p*-tosyl chloride, sodium hydride and imidazole were stirred overnight in dimethoxyethane (DME) under nitrogen. However, this was unsuccessful. So the intermediate tosylate (**208**) was prepared by reaction of **204** with *p*-tosyl chloride and pyridine in chloroform at room temperature for 4 h. Purification was attempted by column chromatography. This proved very difficult and a yield of over 100% was observed, showing that impurities were still present. However, ^{1}H NMR spectroscopy showed the introduction of a $-CH_3$ group, the shift of the $-C\underline{H}_2O-$ protons from 4.28 to 5.82 ppm and a large multiplet of aromatic protons with an integration of approximately 14, indicating that **208** had been prepared. No further characterisation was carried out, due to the difficulties in purification.

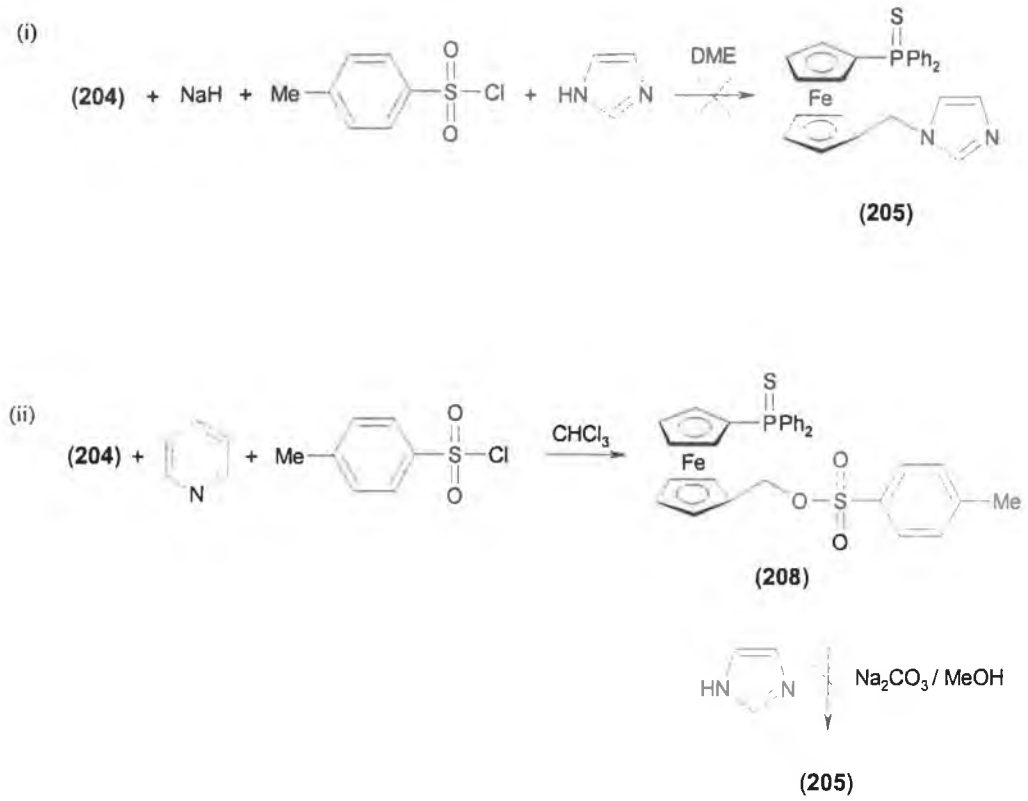

Scheme 5.3. *Attempted synthesis of* ***205*** *via a tosylate intermediate (****208****) (i) without isolation of* ***208*** *and (ii) with isolation of* ***208****.*

It was felt that **208** could be reacted further and the final purification carried out after the substitution of the imidazole. Compound **208** was treated with sodium imidazolium to see if it could nucleophilically displace the tosylate and yield 1-diphenylphosphinosulphide-1′-(1-methylimidazole) ferrocene (**205**). However, this was unsuccessful, as was the case with the 1,1′-bis(1-methylimidazole)ferrocene (**170**). It appears that nucleophilic substitution of a tosylate with an imidazole moiety does not work for these ferrocene systems, possibly due to steric factors. The approach of the imidazole to the electrophilic carbon may be hindered by the ferrocene, tosylate and bulky diphenylphosphine groups. It could be argued that the ferrocene system is too constrained to allow nucleophilic displacement of such a large leaving group as the tosylate.

5.2.1.2.2 Using CDI

An alternative method using CDI was attempted. Treatment of **204** with CDI in acetonitrile produced **205** in a yield of 61% after purification by column chromatography (Scheme 5.4).

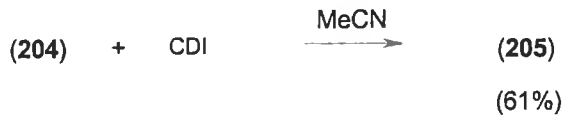

Scheme 5.4. *The introduction of imidazole to obtain **205**.*

The ^{1}H and ^{13}C NMR spectra confirmed the replacement of the –OH functionality with the imidazole unit. The –OH peak at 2.04 ppm was lost and the characteristic imidazole peaks at 6.79, 6.95 and 7.20 ppm (5-H, 4-H and 2-H Im) were seen, as was confirmed with the ^{13}C NMR spectrum with three additional peaks at 84.86, 134.20 and 135.22 ppm (2-H, 4-H and 5-H Im, respectively). Also a change in the chemical shift for the methylene linkage was seen in both the ^{1}H and ^{13}C NMR spectra, from 4.28 to 4.65 ppm and 60.42 to 46.28 ppm, respectively. Furthermore, in the IR spectra the broad O–H band at 3467 cm^{-1} disappeared indicating the loss of the –OH group.

5.2.1.3 Quarternisation of the imidazole moiety

Using the established procedure of treating an imidazole species with an alkyl iodide to obtain an imidazolium salt, **205** was refluxed in iodoethane, whereupon adding diethyl ether, a yellow precipitate was formed and collected (see Scheme 5.5) in a yield of 94%, giving 1-diphenylphosphinosulphide-1′-(1-ethyl-3-methyl)imdazolium ferrocenyl iodide $\{Fe[\eta^5\text{-}C_5H_4P(S)Ph_2](\eta^5\text{-}C_5H_4CH_2C_3H_3N_2CH_2CH_3)\}$ I (**209**).

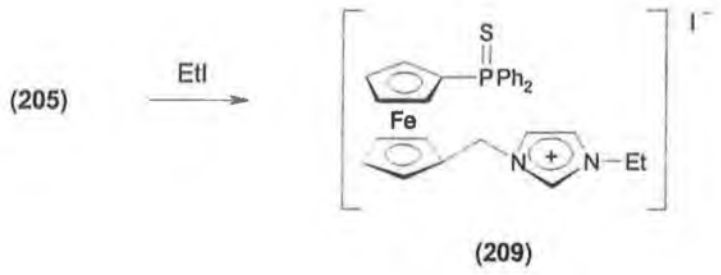

(209)

Scheme 5.5. Preparation of 1-diphenylphosphinosulphide-1'-(1-ethyl-3-methyl)imdazolium ferrocenyl iodide (209).

There was clear confirmation by ^{1}H and ^{13}C NMR spectroscopy of the formation of the imidazolium salt as the proton and carbon at the 2-position of the imidazole/imidazolium shifted from 7.20 ppm in (**205**) to 10.04 ppm in (**209**) and from 84.86 to 207.48 ppm, due to the increased acidity of the proton. The ^{1}H NMR spectra for **205** and **209** are given in Figure 5.2.

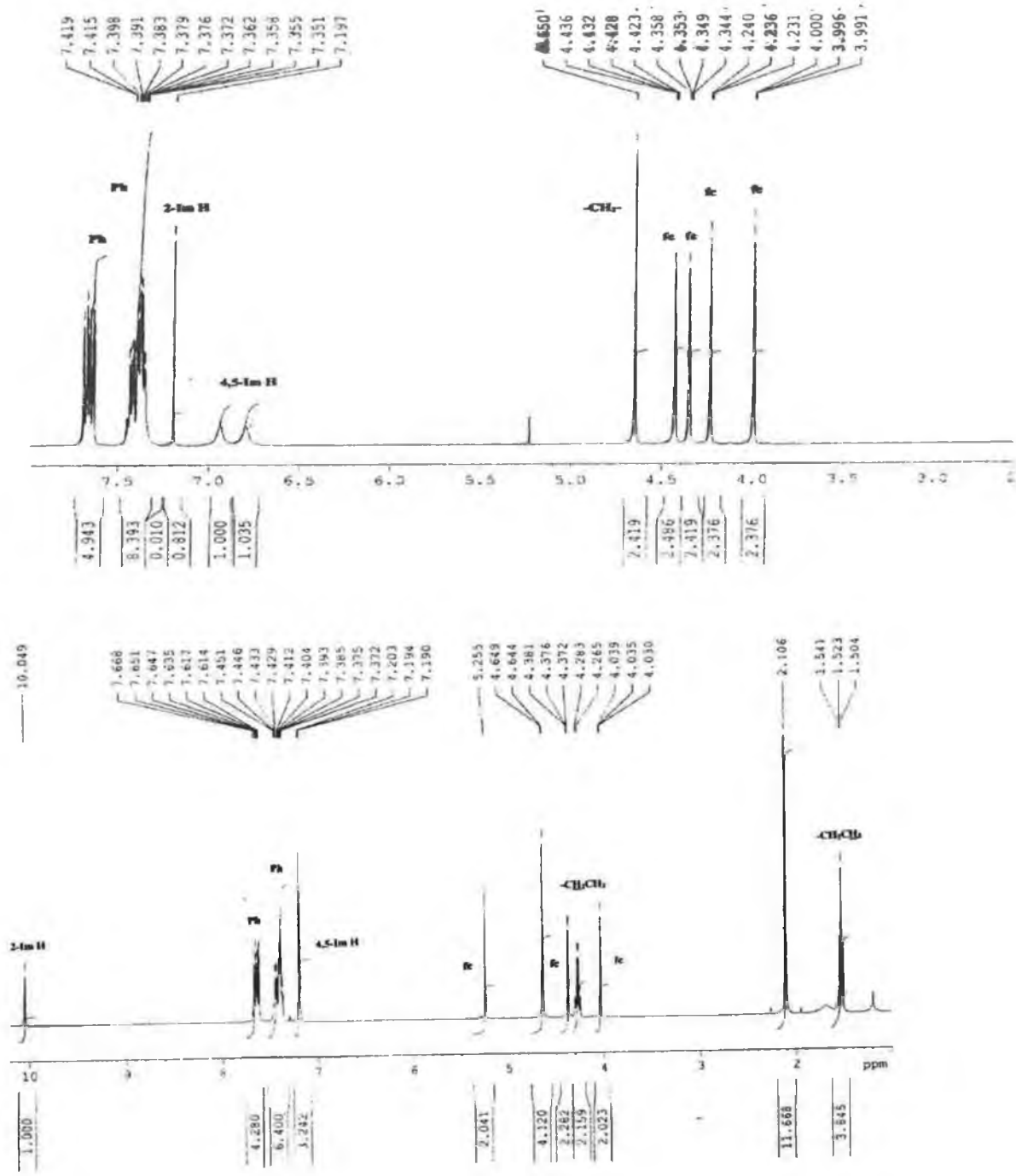

Figure 5.2. *^{1}H NMR spectra for* ***205*** *and* ***209*** *($CDCl_3$).*

The deprotection of the phosphine group was the next stage in the total synthesis of the 1-diphenylphopsphine-1′-(1-alkyl-3-methyl)imdazolium ferrocenyl salt (**198**). Due to having trace amounts of **209**, the deprotection was attempted using a model compound (**210**) (Scheme 5.6). Raney nickel was used as the deprotecting agent [202], however, in monitoring the reaction by t.l.c., none of the deprotected compound (**211**) was observed

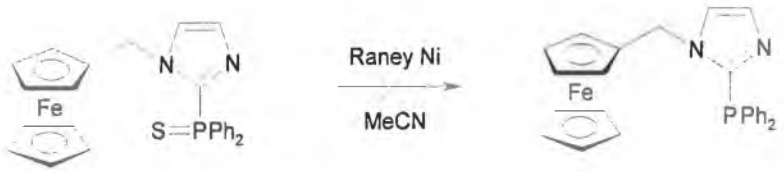

(**210**) (**211**)

Scheme 5.6. *The attempted deprotection of a diphenyl phosphinosulphide using a Raney nickel on a model system.*

Thus, it was concluded that either this reaction did not work in these conditions or only a very poor yield would be obtained. So it was decided that the sulphide could potentially be used as a co-ordination point instead of the phosphorus. This could demonstrate a novel bidentate ligand, as no mixed sulphide–nitrogen or sulphide–carbene ligands have been reported in the literature.

5.2.2 Attempted synthesis of a 1-diphenylphopsphine-2-(1-alkyl-3-methylimidazolium)ferrocenyl salt (199)

The synthesis of a 1,2-ferrocenyl–azole–phosphine system – 1-diphenylphopsphine-2-(1-alkyl-3-methylimidazolium)ferrocenyl salt (**199**) – leading to a chiral system had no obvious starting point as with (**198**). Although the preparation of a ferrocene structure with planar chirality was envisaged, we realised that a resolution step would be required.

Three possible methods were employed to prepare **199**: the first involved the introduction of a diphenylphosphine substituent onto the Cp ring of ferrocene followed by the introduction of imidazole; the second involved the introduction of diphenylphosphine into the ferrocene–imidazole system; the third involved the introduction of the diphenylphosphine into a ferrocenyl–imidazolium salt.

5.2.2.1 Route 1: via the synthesis of 1-diphenylphosphino-1′-acetoferrocene (213)

(*R*,*S*)-1-Diphenylphosphino-2-(dimethylaminomethyl)ferrocene (**212**) [203] was seen as a potential starting material as the diphenylphosphine group was already present and with an amino substituent in a 1,2-relationship with it. By manipulation of this group, it was envisaged that the imidazole could be substituted into this position. It was thought that changing the amino group to an acetate group would provide a better leaving group. Therefore, using the route of Hayashi *et al.* [204], the amino substituent was replaced with an acetate functionality by heating **212** to reflux in acetic anhydride producing 1,2-bis(diphenylphosphino)ferrocene methyl acetate (**213**) as orange crystals in a yield of 45% (Scheme 5.7).

The next step involved the displacement of the acetate group with the imidazole unit. This was attempted using imidazole and sodium carbonate to produce the imidazolide anion in situ by refluxing in methanol. Both imidazole and 1-methylimidazole were employed as potential nucleophiles with the target compounds being 1-diphenylphosphino-2-(1-methylimdiazole)ferrocene (**214**) and 1-diphenylphosphino-2-(1-methyl-3-methylimidazolium)ferrocenyl acetate (**215**) (Scheme 5.7). However, neither of these methods were successful in producing either of the targets.

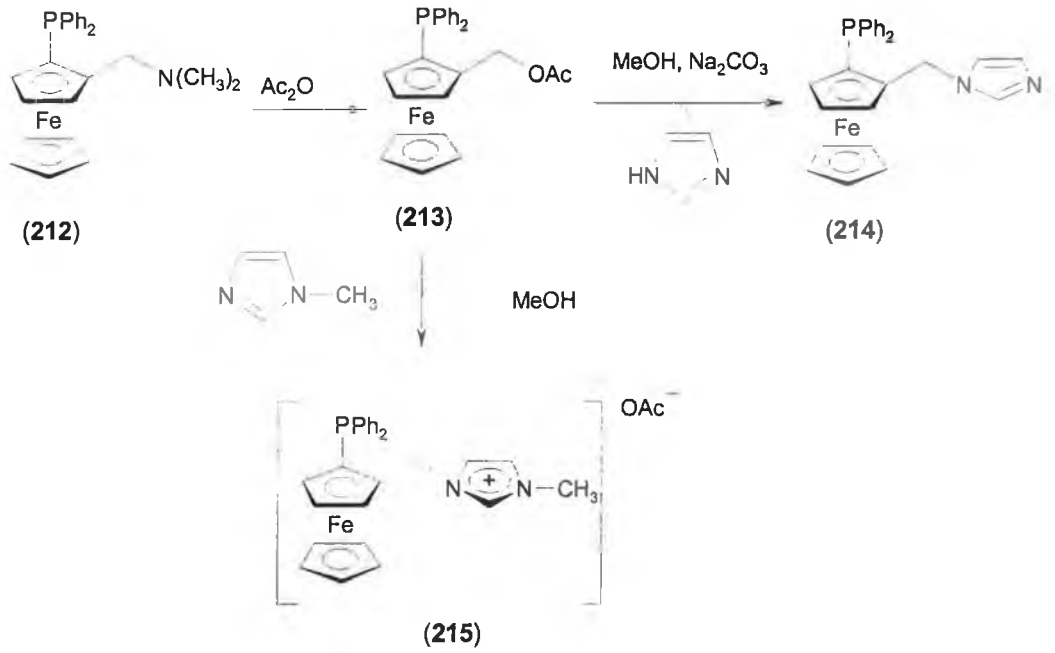

Scheme 5.7. *Attempted synthesis of* ***214*** *and* ***215*** *via* ***213****.*

5.2.2.2 Route 2: via phosphorylation of 1-methylferrocenyl imidazole

This route was based on introducing the diphenylphosphine after the imidazole unit as outlined in Scheme 5.8. Using 1-methylferrocenylimidazole (**148**) as the starting material, the aim was to substitute the phosphine entity into the Cp ring, protect the phosphorus, convert the system into an imidazolium salt and deprotect the phosphorus.

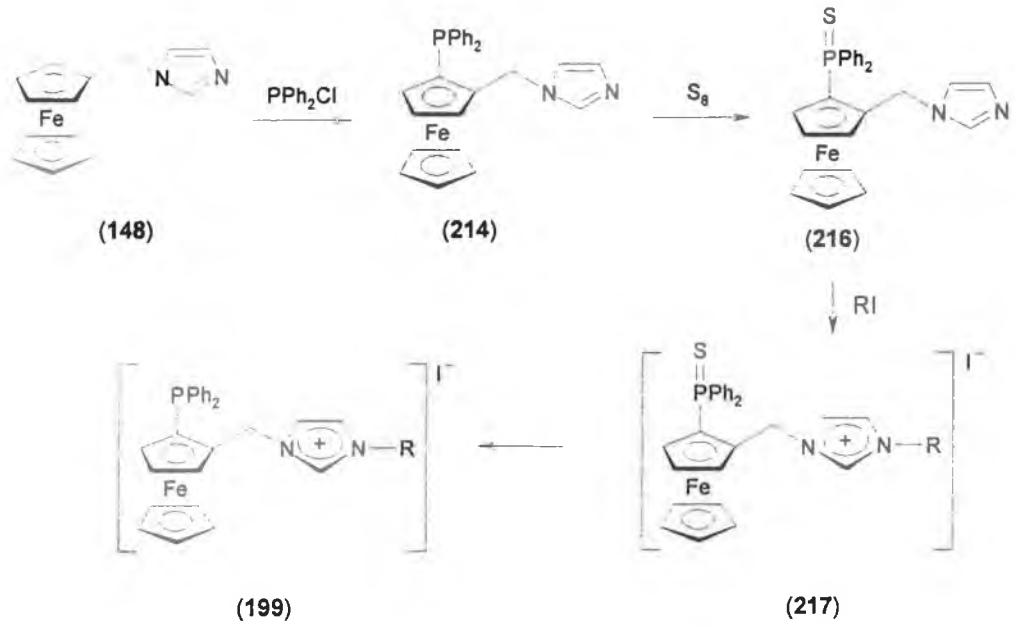

Scheme 5.8. *Synthetic outline of the preparation of a 1-diphenylphopsphine-2-(1-alkyl-3-methylimidazolium)ferrocenyl salt (**199**) from **148**.*

So it was devised that 1-(methylferrocenyl) imidazole (**148**) would be used as the starting material and the experimental method employed was the same as found in the literature for the addition of a diphenylphosphine group to the Cp ring of a ferrocene [204]. It was thought that the α-H of ferrocene would be abstracted with *n*-butyllithium, and using chorodiphenylphosphine, the diphenylphosphine functionality would be nucleophilically substituted into the Cp ring *ortho* to the *N*-methylimidazole moiety.

However, it was found that under the reaction conditions employed [143], with diethyl ether as the solvent, at –78°C, under nitrogen with stirring, that this reaction did not proceed and two different products were yielded. 1-(Methylferrocenyl)-2-(diphenylphosphine)imidazole (**211**) and 1-(methylferrocenyl)-2-

(diphenylphosphineoxide)imidazole (**218**) were produced in yields of 31 and 22%, respectively, and none of the desired product (**214**) (Scheme 5.9).

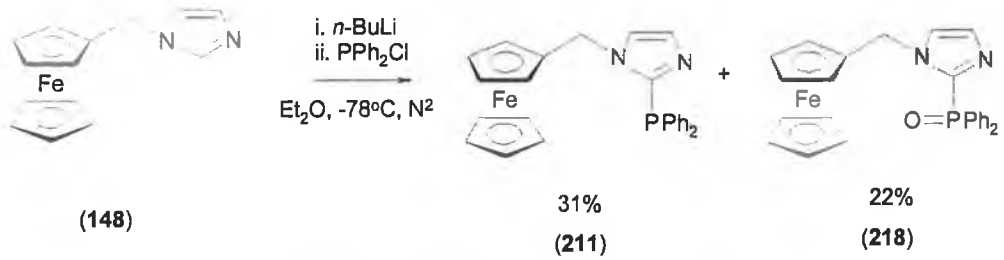

(**148**) 31% (**211**) 22% (**218**)

Scheme 5.9. *Products of the phosphorylation of* ***148****.*

This shows that of the two available acidic hydrogens, the ferrocene α-H and imidazole 2-H, it was the 2-H on the imidazole that was abstracted by the *n*-butyl lithium and not the ferrocene α-H as was wanted. The pK_a values for both the unsubstituted ferroceneα-H and the imidazole 2-H are very similar at 15.00 and 14.52, respectively, with the imidazole 2-H being only slightly more acidic. So it could have been predicted that maybe a mixture of both the isomers would be produced – **211** and **214**. As this was not the case, it could be suggested that in **148** the imidazole hydrogen is significantly more acidic, so will be abstracted first, or alternatively steric factors could be responsible. Perhaps access of the butyl anion to the ferrocene α-H

is hindered by the imidazole group, so the imidazole 2-H will be abstracted preferentially.

The ^{1}H and ^{13}C NMR data for **211** and **218** are very similar to that of. the parent compound **148** (Figure 5.3). The key signals of the methylene linker, 4-im H and 5-im H are shifted downfield, with the diphenylphosphine oxide product showing the greatest shift in signals due to the introduction of the electronegative oxygen atom.

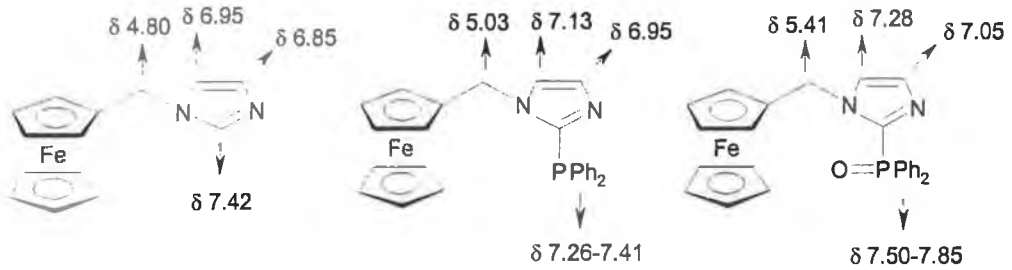

(148) **(211)** **(218)**

Figure 5.3. *The ^{1}H NMR shifts for compounds **148**, **211** and **218**.*

The most significant change is seen in the ^{31}P NMR shifts. In **211**, the phosphorus resonates at −31.53 ppm, while in **218** it resonates at 20.93 ppm. Despite this the structures of these compounds could not be fully determined by NMR spectroscopy, so X-ray crystallographic determinations were carried out to fully elucidate their structures (Chapter 6).

As the diphenylphosphine oxide (**218**) chalogenide had been prepared, it was thought that the sulphide analogue would be an interesting future ligand also. So **211** was heated to reflux with sulphur in benzene, which after purification by column chromatography, gave 1-(methylferrocenyl)-2-(diphenylphosphineoxide)imidazole (**210**) in a yield of 84% (Scheme 5.10).

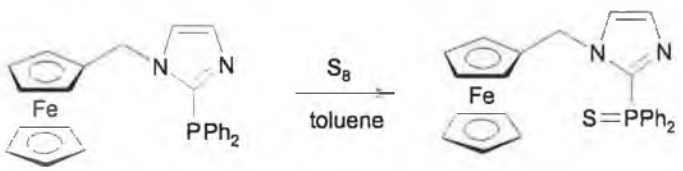

(211) **(210)**

Scheme 5.10. *Preparation of gave 1-(methylferrocenyl)-2-(diphenylphosphineoxide) imidazole (**210**).*

The phosphorus ^{31}P NMR shift was found to be 30.73 ppm. This compares with –31.53 ppm for **211** and +20.93 for **218** ppm. This compound was completely characterised by NMR, IR and microanalysis.

The phosphorylation reaction was carried out using (1-methylferrocenyl)benzimidazole (**149**) under the same reaction conditions (Scheme 5.11). Again none of the desired [1-diphenylphosphine-2-(1-methylbenzimidazole)]ferrocene was prepared, but 1-(methylferrocenyl)-2-(diphenylphosphine)benzimidazole (**219**) was isolated in the absence of any oxide. The pK_a of the 2-H of benzimidazole is more acidic that than of imidazole – (PK_a=13.2) and the benzimidazole even bulkier, so it is unsurprising that none of the 1,2-disubstituted ferrocene product was produced.

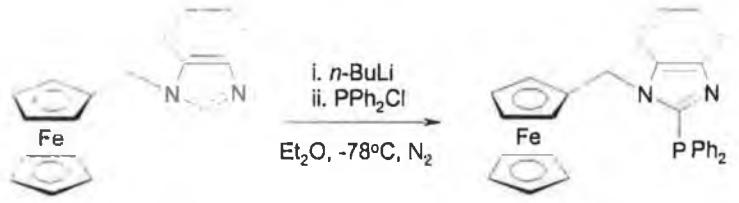

(149) **(219)**

Scheme 5.11. *Phosphorylation of **149**.*

In comparison with **149**, the shifts in the ^1H NMR spectrum are very similar. The Fc Cp protons resonate at 4.19–4.23, $-CH_2-$ at 5.42, 6,7-Bzim H at 7.26, 8-Bzim H at 7.45 and 5-Bzim H at 7.84 ppm. The only marked difference is the downfield shift of

the methylene group and the disappearance of the 2-bzim proton, as to be expected. The phosphorus resonates at –27.48 ppm, which is very close to that of **211**. This along with microanalysis confirmed that the phosphorus had not been oxidised during the reaction.

5.2.2.3 Route 3: via phosphorylation of 1-(methylferrocenyl)-3-alkylimidazolium iodide

A third route was then attempted where the diphenylphosphine functionality would be introduced into a ferrocenyl–imidazolium salt by phosphorylation of a 1,3-dialkylimidazolium salt following the procedure of Brauer et al. [148]. Both 1-(methylferrocenyl)-3-ethylimidazolium iodide (**81**) and1-(methylferrocenyl)-3-butylimidazolium iodide (**83**) were employed (Scheme 5.12). This reaction failed, with no identifiable product being obtained and mostly starting material being recovered. Although in the reactions of Brauer, phosphorylation at the 2-position on the imidazolium ring was achieved, in our case neither phosphorylation of the ferrocene Cp nor the imidazolium ring occurred.

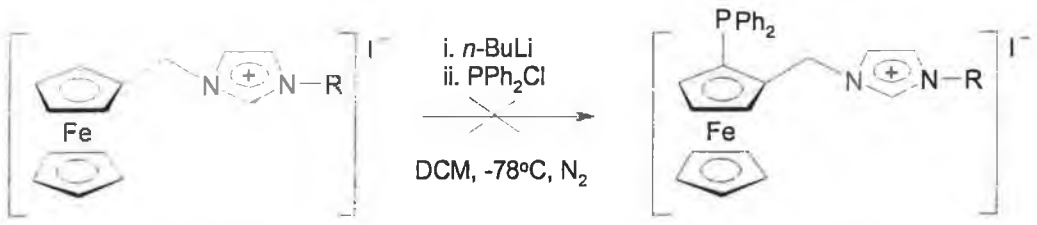

R = Et (**81**), Bt (**83**)

R = Et, Bt

(**198**)

Scheme 5.12. *Attempted phosphorylation of 1-(methylferrocenyl)-3-alkylimidazolium iodide salts.*

5.3 Conclusion

The aim of this work was to introduce a second functionality into the ferrocenyl–azolium framework that had already been developed (Chapter 2). The chosen functionality was diphenylphosphine ($-PPh_2$) due to its co-ordination properties. Thus, an alternative class of chelate ligand to biazolium–ferrocenyl salt compounds could be realised. The target compounds were based on **198** and **199**, so that a 1,1′-disubstituted ferrocene and a 1,2-disubstituted ferrocene could be prepared and investigated. Although neither of these target compounds were prepared, some novel compounds were obtained during our investigations.

Regarding, the first class of target compounds – 1,1′-disubstituted ferrocenes, 1-diphenylphosphinosulphide-1′-(1-methylimidazole) ferrocene (**205**) and 1-diphenylphosphinosulphide-1′-(1-ethyl-3-methyl)imdazolium ferrocenyl iodide (**207**) were prepared. Unfortunately the last reaction, which was the removal of the sulphide protection group, in this multi-step synthesis proved problematic, and as only trace amounts of product **207** were available, the total preparation could not be finished. However, compounds **205** and **207** are very interesting. Sulphur is a good co-ordinating group as well, so the sulphur in these compounds has replaced the phosphorus as the planned second co-ordinating functionality. Therefore, perhaps these ferrocenyl–sulphide–azolium systems could act as novel mixed sulphide/nitrogen or sulphide/carbene ligands.

In the preparation of the second class of ferrocene–phosphine–azolium systems, the 1,2-disubstituted ferrocenes, the synthesis of 1-diphenylphopsphine-2-(1-alkyl-3-methylazolium)ferrocenyl salts (**199**) did not yield any success. However, several novel compounds had been produced during the attempts to prepare **199** (**210**, **211**, **218** and **219**). While phosphine functionalised imidazoles are known in the literature [140–152], they have not been investigated fully, and diphenylphosphine functionalised benzimidazoles have not really been prepared or studied at all apart from a couple of rare instances [205]. These compounds have a lot of potential as mixed P,N donor ligands. Additionally, also the sulphide analogues were prepared as comparative compounds to the oxide (**218**) – 1-(methylferrocenyl)-2-(diphenylphosphinosulphide)imidazole (**210**) – so that a full investigation of the co-ordination properties of these ligands could be carried out in future work.

Chapter 6

Crystallographic Studies of Ferrocenyl–Imidazole–Diphenylphosphine Compounds

As full characterisation of the two products of the phosphorylation reaction of **148** – **211** and **218** – was not possible by NMR and IR spectroscopy and microanalysis, crystals were grown for X-ray structural characterisation. From a DCM/hexane solution, needle-like crystals that were suitable for crystallographic studies were grown. These X-ray crystallographic studies were performed by Dr John Gallagher of the School of Chemical Sciences, Dublin City University. Figure 6.1 shows a perspective view of **211** and **218** with the atomic numbering scheme assigned. All the pertinent crystallographic information is summarised in Table 6.1 for **211** and **218**. Selected bond distances and angles of the non-hydrogen atoms are given in Table 6.2, with the full crystallographic analysis given in Appendix 1.

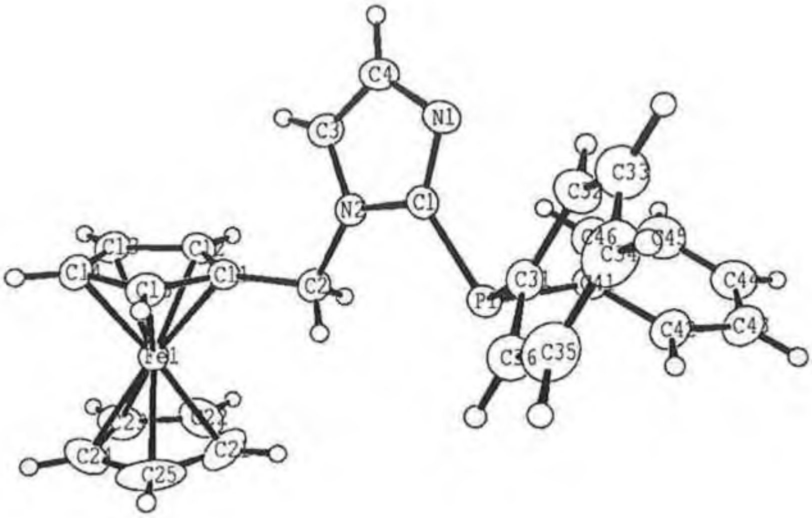
C4
N1
C3
C33
C32
N2
C1
C46
C45
C34
C44
P1
C31
C41
C42
C43
C36
C35
C11
C12
C25
Fe1

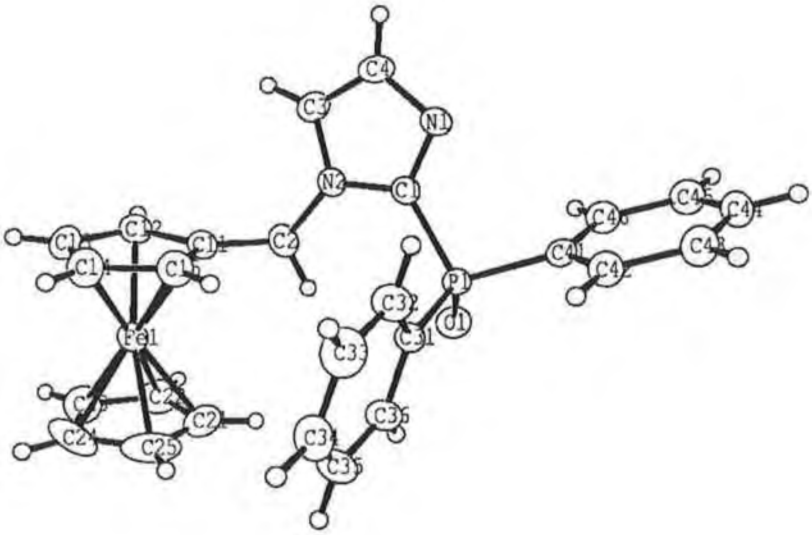
C4
N1
N2
C1
C2
C45
C44
C43
P1
O1
C32
C31
C36
C35
C25
Fe1

Figure 6.1. *ORTEP drawing of the crystal structures of 1-(methylferrocenyl)-2-(diphenylphosphine)imidazole (**211**) and 1-(methylferrocenyl)-2-(diphenylphosphineoxide)imidazole (**218**).*

	211	**218**
Identification code	3-04psi	2-04psi
Empirical formula	$C_{26}H_{23}FeN_2P$	$C_{26}H_{23}FeN_2OP$
Formula weight	450.28	466.28
Temperature (K)	294(2)	293(2)
Wavelength (Å)	0.71073	0.71073
Unit cell dimensions		
a (Å)	15.9066(9)	11.3019(10)
b (Å)	7.9153(8)	7.9563(6)
c (Å)	17.9153(8)	24.449(2)
α (°)	90	90
β (°)	103.089(4)	99.572(6)
γ (°)	90	90
Volume ($Å^3$)	2140.1(3)	2167.9(3)
Z	4	4
Calculated density (Mg m^{-3})	1.398	1.429
Absorption coefficient (mm^{-1})	0.795	0.791
F(000)	936	968
Crystal size (mm)	0.52×0.45×0.35	0.42×0.38×0.25
θ range for data collection (°)	2.40–28.06	1.88–45.45
Index ranges	$-1 \le h \le 21$, $-10 \le k \le 1$, $-23 \le l \le 22$	$-14 \le h \le 1$, $-1 \le k \le 10$, $-32 \le l \le 32$
Reflections collected	6508	6872
Independent reflections	5173 (R_{int}=0.1033)	5253 (R_{int}=0.0261)
Completeness to 2θ=45.45	92.9%	27.4%

Max./min. transmission	0.7683 and 0.6827	0.8268 and 0.7324
Refinement method	Full-matrix least-squares on F^2	Full-matrix least-squares on F^2
Data/restraints/parameters	5173/0/271	5253/0/280
Goodness-of-fit on F^2	1.046	1.049
Final R indices [$I>2\sigma(I)$]	R_1=0.0345, wR_2=0.0870	R_1=0.0458, wR_2=0.1080
R indices (all data)	R_1=0.0451, wR_2=0.0934	R_1=0.0696, wR_2=0.1211
Largest diff. peak and hole (e.Å^{-3})	0.485 and –0.263	0.535 and –0.315

Table 6.1. Crystal data and structure refinement for 211 and 218.

Parameter	Compound	
	211	**218**
C(2)–C(11) (Å)	1.498(2)	1.504(4)
N(2)–C(2) (Å)	1.477(2)	1.478(3)
N(2)–C(2)–C(11) (°)	111.58(14)	111.8(2)
N(1)–C(1) (Å)	1.325(2)	1.330(3)
N(2)–C(1) (Å)	1.370(2)	1.360(3)
N(1)–C(1)–N(2) (°)	110.56(16)	111.4(2)
P(1)–C(1) (Å)	1.8257(18)	1.804(2)
P(1)–C(31) (Å)	1.8302(18)	1.803(2)
P(1)–C(41) (Å)	1.8364(17)	1.808(2)
P(1)–O(1) (Å)	–	1.4825(19)
C(1)–P(1)–C(31) (°)	104.06(8)	104.90(11)
C(1)–P(1)–C(41) (°)	101.22(8)	102.95(11)
C(31)–P(1)–C(41)(°)	101.01(8)	108.82(11)
O(1)–P(1)–C(31) (°)	–	112.20(11)
O(1)–P(1)–C(1) (°)	–	113.90(11)
O(1)–P(1)–C(41) (°)	–	113.34(12)

Table 6.2. *Selected bond distances (Å) and bond angles (°) for* ***211*** *and* ***218****.*

For **211**, the mean distance from the Fe atom to the carbons of the Cp rings is 2.03442 Å, which compares well with other reported ferrocene–azole structures, such as 1-methylferrocenyl-2-ferrocenylbenzimidazole (**88**) [127]. The internal C–C bond lengths in the Cp ring are 1.410–1.429 (mean 1.405 Å) for the substituted ring and

1.386–1.407 (mean 1.3902) for the unsubstituted ring. Thus, the bond lengths are slightly longer in the substituted Cp ring than the unsubstituted ring.

The bond lengths and angles for the imidazole nucleus are in agreement with other reported values for imidazole compounds, such as [(1-methyl-2-*para*-phenyl)imidazole]diphenylphosphine (**128**) [150]: N(2)–C(1) is 1.320(2) and C(1)–N(1) is 1.325(2) Å for **211** compared to 1.323(2) and 1.366(2) Å for **128**, respectively, and the N(2)–C(1)–N(1) bond angle is 110.56(16)° for **211** compared to 110.6(2)° for **128**.

For the methylene spacer the C(11)–C(2) bond length is slightly longer at 1.498 Å and the N(2)–C(2) bond length is 1.477 Å. While the angle of the bond angle of N(2)–C(2)–C(11) is 111.58(14)°, which is similar to reported values for **88** and 1-methylferrocenyl-2-(4-methoxyphenyl)benzimidazole **85** [126] of 112.4(4)° and 112.15(16)°, respectively.

The diphenylphosphine substituent has C–P bond lengths typical of other trisubstituted phosphine compounds. P(1)–C(1) measures 1.8257(18), P(1)–C(31) is 1.8302(18) and P(1)–C(41) is 1.8364(17) Å, which compares well to normal P–C(phenyl) bond lengths of 1.835 Å [206]. The C–P–C bond angles of C(1)–P(1)–C(31)=104.06(8), C(1)–P(1)–C(41)=101.22(8) and C(31)–P(1)–C(41)=101.01(8)° also compare well to the expected value for C(alkyl)–P–C(phenyl) bond angles of ~101° [206].

In compound **218**, the mean Fe–C distance is 2.0323 Å, which compares well with other ferrocene–azole structures and is very close to the value for **211** of 2.03442 Å. Again, the substituted Cp ring has slightly longer internal C–C bond lengths of 1.418–1.429 Å (mean 1.4196 Å) compared to 1.384–1.422 Å (mean 1.3974 Å) for the unsubstituted ring.

The imidazole bond distances are very similar to those in **211**, being 1.360(3) and 1.330(3) Å for N(2)–C(1) and C(1)–N(1) Å. The N(2)–C(1)–N(1) bond angle is slightly wider at 114.4° compared to 110.56°. For the methylene spacer, the C(11)–C(2) bond length is 1.504(4) Å, making it slightly longer than in **211**, while the N(2)–C(2) bond length at is very nearly the same at 1.478(3) Å compared to **211**. The bond angle of N(2)–C(2)–C(11) is 111.8(2) is again very close to the expected value.

In **218**, the diphenylphosphine substituent has been oxidised. The C–P bond lengths are shorter than those of **211** and other aryl phosphine compounds, with the mean P(1)–C bond distance measuring 1.805 Å, compared to a mean distance of 1.8307 Å for **211**. The P(1)–O(1) bond distance is 1.4825(19) Å which compares well to other P=O bond distances of approximately 1.489 Å [207]. The C–P–C bond angles are close to that of **211**, for the C(1)–P(1)–C(31) and C(1)–P(1)–C(41) angles the values are very close [104.90(11) and 102.95(11)° for **218** vs. 104.06(8) and 101.22(8) for **211**]. However, for C(31)–P(1)–C(41) there is a larger change in the angle from 101.01(8) in **211** to 108.82(11)° in **218**. The mean C–P(1)–O(1) bond angle is 113.14°, which is slightly smaller than other reported values of 118.6(1)° for diphenyl(*tert.*-butylamino) phosphine oxide [207].

Chapter 7

Conclusion

Azole and azolium salt moieties are currently being employed in a great many applications. Having previously prepared a series of monosubstituted ferrocenyl–azolium salt compounds [125,126], it was decided to extend this range so that bisazolium–ferrocenyl and macrocyclic salts could be realised and together with their application in some of these research areas.

In this work we prepared 1-ferrocenylmethy-3-alkylimidazolium halides, 1-ferrocenylmethy-3-alkylbenzimidazolium halides, thus, completing the series of 1-ferrocenylmethyl-3-alkylazolium halide salts. These were prepared from 1-ferrocenylmethylazole precursor molecules (**148** and **149**) or (ferrocenylmethyl)trimethylammonium iodide (**150**).

In order to incorporate two azolium functionalities into the ferrocenyl–azolium system, two routes were chosen. The first involved coupling two monosubstituted ferrocene–azole salts using the 1-ferrocenylmethylazole (**148**/**149**) and 1,4-diiodobutane as the starting materials. In this way 1-[(1-ferrocenylmethyl-3-butyl)imidazolium]-3-ferrocenylmethylimidazolium diiodide (**164**) and 1-[(1-ferrocenylmethyl-3-butyl)imidazolium]-3-ferrocenylmethylbenzimidazolium diiodide (**166**) were prepared. The second route involved introducing two azolium moieties onto each Cp ring of the ferrocene functionality, preparing 1,1′-bisazolium–ferrocenyl salts. The salts 1,1′-bis(1-methyl-3-methylbenzimidazolium)ferrocenyl iodide (**176**) and 1,1′-bis(1-*n*-butyl-3-methylbenzimidazolium)ferrocenyl (**177**) were obtained. Ferrocene-1′-diylbis-(methyltrimethylammonium iodide) (**174**) was converted into 1,1′-bis-(1-methylbenzimidazole)ferrocene (**175**), which was alkylated to yield the

corresponding benzimidazolium salt. Finally, a novel macrocyclic ferrocenyl–azolium salt system was prepared. From **175,** using the same procedure as that used to generate the acyclic analogues **164** and **166,** bis{1-[(1,1′-ferrocenylmethyl-3-butyl)benzimidazolium]-3-ferrocenylmethyl}benzimidazolium tetraiodide (**186**) was prepared. Thus, a series of compounds comprising of monosubstituted ferrocenyl–imidazolium, monosubstituted ferrocenyl–benzimidazolium, bisimidazolium–bisferrocenyl, bisbenzimidazolium–bisferrocenyl, 1,1′-bisbenzimidazolium–ferrocenyl and macrocyclic tetrabenzimidazolium–bisferrocenyl cyclophane halide salts had been prepared. This diversity of azolium–ferrocenyl salts allowed the catalytic, chemoreceptor and biological properties of these azolium salts to be investigated.

Imidazolium salts are becoming increasingly recognised as stable alternatives to triarylphosphines as auxiliary ligands in transition metal-mediated catalysis. So far though, while benzimidazolium salts have been employed as *N*-heterocyclic carbene precursors their application to transition metal catalysis has not been employed. It was shown that the ferrocenyl–azolium salts were able to act as effective catalysts in the Heck reaction and that benzimidazolium salts are also able to act as auxiliary ligands in these reactions. It was concluded that imidazolium and benzimidazolium salts possibly aid the catalysis of the Heck reaction in different ways, with the imidazolium systems being more suited to less activated systems, while the benzimidazolium salts proved to be more effective at catalysing more activated systems. However, no significant difference in the effects of the chelates and the monosubstituted ferrocenyl–azolium salts was seen. As the monosubstituted salts are prepared in higher yields, it must be concluded that these would be preferred ligands for use in

organometallic coupling reactions. For complete analysis of the comparative efficiencies of the benzimidazolium and imidazolium salts on the Heck reaction, another set of reactions should be carried out in future work using a considerably less activated substrate, such as 4-bromoanisole.

Also it was shown that at ambient temperature the ionic liquid 1,3-dialkylimidazolium salt – ([BMIM]PF_6) – was able to act as a highly efficient solvent for the Heck reaction. It was demonstrated to be recyclable, as the palladium catalyst remained in the ionic liquid after the work-up procedure. Furthermore, the product could be obtained by distillation, allowing easy isolation of the product and repeated use of the solvent. Employment of ionic liquids as solvents for organometallic processes has been an important development for environmental chemistry, as they could substantially reduce the amount of VOCs currently employed in industrial processes.

Selected salts were then applied to chemoreceptor studies (**164** and **177**). As the previously prepared monosubstituted ferrocenyl–azolium salts had shown anion co-ordination properties, it was thought that perhaps the acyclic bisazolium–ferrocenyl or macrocyclic tetraazolium–ferrocenyl systems may be able to confer a greater degree of selective anion binding by chelate anion co-ordination. Compound **164** was observed to form a 1:1 complex with chloride, and thus it appears to bind by wrapping around the anion. However, compound **177** did not show any selective binding. This is a more sterically demanding system with the bulky benzimidazolium rings being in such close proximity, so perhaps the system is too constrained for anion co-ordination in the manner proposed. Thus, it can be concluded that the bisazolium–ferrocenyl

systems do not appear to offer an increase in selectivity compared to the monosubstituted ferrocenyl–azolium salts.

Macrocycle **186** proved to be to be only soluble in DMSO-d_6, which was determined not to be a suitable solvent for anion binding studies when tested with other compounds. Therefore, potentiometric techniques, such as ion selective electrode analysis, are needed to evaluate the anion co-ordination abilities of this salt, which will be carried out in future work.

Antimicrobial studies were carried out on key ferrocenyl–azole/azolium compounds, where a selection of compounds was screened against *P. aeruginosa* and *C. albicans*. It was observed that compounds **161** and **166** had good antifungal properties against *C. albicans*, having LD_{50} values of 175 and 84 $\mu g\ ml^{-1}$, although no significant activity against *P. aeruginosa* was seen by any compounds. No significant differences between the charged azolium salts or the azole compounds were found. It was observed that azolium compounds with two ferrocene units in their structure had good antifungal properties, from which it has been suggested that the redox behaviour of the ferrocenes may be involved in this activity. Future work here would require the structural modifications of the bisferrocenyl–bisazolium compounds for a lead compound to be established.

As the imidazolium salts are well known to be excellent precursors to *N*-heterocyclic carbene co-ordination complexes, it was thought to be a novel idea to introduce a second co-ordination functionality into the ferrocenyl–azolium system. Thus, the preparation of a 1,1′-disubstituted ferrocenyl salt system with an imidazolium nucleus

on one Cp ring and a diphenyl(sulphido)phosphine entity on the second Cp ring and a range of 1-ferrocenylmethylazole–diphenylphosphine functionalised compounds was carried out. 1-Diphenylphosphinosulphide-1′-(1-methylimidazole) ferrocene (**205**) and 1-diphenylphosphinosulphide-1′-(1-ethyl-3-methyl)imdazolium ferrocenyl iodide (**209**) and 1-(methylferrocenyl)-2-(diphenylphosphineoxide)imidazole (**210**), 1-(methylferrocenyl)-2-(diphenylphosphine)imidazole (**211**), 1-(methylferrocenyl)-2-(diphenylphosphineoxide)imidazole (**218**) and 1-(methylferrocenyl)-2-(diphenylphosphine)benzimidazole (**219**) were prepared as compounds that show great potential as ligands. The structure of compounds **211** and **218** were fully elucidated by X-ray crystallography. The application of these compounds as ligands in co-ordination compounds is an area of promising future work.

Chapter 8

Experimental

^{1}H and ^{13}C NMR spectra were recorded using a Bruker Avance 400 MHz spectrometer. IR spectra were recorded on a Perkin Elmer Spectrum GX FT-IR System. Microanalysis was performed at University College Dublin. The reagents and chemicals were obtained from the Aldrich Chemical Company (UK) and were used as received unless otherwise stated. Diethyl ether and THF were dried over sodium, acetonitrile was dried over 4 Å molecular sieves, chloroform washed with water then dried over calcium chloride and pyridine, dichloromethane was stored over potassium carbonate and TMEDA was dried over sodium hydroxide pellets. All reactions were performed under a nitrogen atmosphere unless otherwise stated.

Synthesis:

1-Ferrocenylmethylimidazole (148)

A solution of (ferrocenylmethyl)trimethylammonium iodide (**150**) (3.05 g, 7.79 mmol), sodium imidazolium salt (0.77 g, 18.57 mmol) in dry acetonitrile (75 ml) was refluxed for 24 h. The cooled solution was poured into water (100 ml) and extracted with chloroform (3×75 ml). The extracts were washed with water (2×50 ml), dried over $MgSO_4$, filtered and evaporated in vaccu to give an orange oil, which was purified by column chromatography on silica gel using DCM–methanol (95:5) as the eluant (1.43 g, 72% yield). m.p. 78–81°C.

^{1}H NMR ($CDCl_3$): ppm 4.09 (s, 7 H, Cp H), 4.13 (s, 2 H, Cp H), 4.80 (s, 2 H, Fc–CH_2–), 6.85 (s, 1 H, 5-im H), 6.95 (s, 1 H, 4-im H), 7.42 (s, 1 H, 2-im H). ^{13}C NMR ($CDCl_3$): ppm 44.72 (Fc–CH_2–), 68.77 (Cp C–H), 82.5 (Cp C_{ipso}), 120.29 (5-im C), 122.03 (4-im C), 122.79 (2- Im C). IR (KBr) ν (cm^{-1}) 3051, 2971, 1506, 1219, 1110, 1076, 1036, 1007, 990, 818, 731. $C_{14}H_{14}N_2Fe$ (266.13): calculated C 63.18, H5.3, N 20.99; found: C 62.88, H 5.39, N 20.81%.

1-Ferrocenylmethylbenzimidazole (149)

A solution of **150** (10.03 g, 26.05 mmol), benzimidazole (3.23 g, 27.35 mmol) and potassium carbonate (3.96 g, 28.66 mmol) in dry acetonitrile (100 ml) was heated to reflux for 12 h. The cooled solution was poured into water (100 ml) and extracted with chloroform (3×75 ml). The extracts were washed with water (3×75 ml), dried over $MgSO_4$, filtered and evaporated in vaccu to give a brown oil, which was purified by column chromatography on silica gel using DCM–methanol (95:5) as the eluant (6.50 g, 81% yield). m.p. 115–119°C.

^{1}H NMR ($CDCl_3$): ppm 4.17 (s, 7 H, Cp H), 4.25 (s, 2 H, Cp H), 5.05 (s, 2 H, Fc–CH_2–), 7.27 (m, 2 H, *J*=6 Hz, 6,7-bzim H), 7.43 (d, 1 H, *J*=7.2 Hz, 5-bzim H), 7.78 (d, 1 H, *J*=7.2 Hz, 8-bzim H), 7.86 (s, 1 H, 2-bzim H). ^{13}C NMR ($CDCl_3$): ppm 44.67 (Fc–CH_2–), 68.75 (Cp C–H), 83.98 (Cp C_{ipso}), 109.68 (6-bzim C), 120.27 (5-bzim C), 122.10 (7-bzim C), 122.80 (8-bzim C), 133.71 (4-bzim C), 142.47 (9-bzim C), 143.70 (2-bzim C). IR (KBr) ν (cm^{-1}) 3077, 2927, 1489, 1456, 1443, 1348, 1283, 1263, 1157, 1101, 1038, 1026, 1003, 739, 509, 488. $C_{18}H_{16}N_2Fe$ (316.19): calculated C 68.38, H 5.10, N 8.86; found C 67.81, H 5.04, N 8.83%.

General procedure for the synthesis of the 1-ferrocenylmethylimidazolium iodide salts (151)–(155)

Method (a):

1-Ferrocenylmethylimidazole (**148**) (1.67 g, 6.28 mmol) and *n*-butyl iodide (0.79 ml, 6.91 mmol) were dissolved in acetonitrile (20 ml) and heated to reflux for 2 h. The reaction mixture was cooled, poured into water (30 ml) and extracted with chloroform (3×20 ml). The organic extracts were dried over Mg_2SO_4, filtered and evaporated to

afford a brown oil. The product was purified by column chromatograhy on silica gel using DCM/methanol (95:5) as the eluant, affording an orange oil (2.91 g, 98% yield).

Method (b):

To 1-ferrocenylmethylimidazole (**148**) (0.77g, 2.9 mmol) dissolved in dry acetonitrile (10 ml), benzyl chloride (0.4 ml, 3.5 mmol) was added and the reaction mixture left to stand at room temperature for 18 h. A large volume of diethyl ether was added very slowly to form a separate layer. After 48 h, crystals were collected by filtration. The filtrate was poured in water (10 ml) and extracted with DCM (3×10 ml). The organic extracts were washed with water (3×20 ml), dried over $MgSO_4$ and evaporated to afford a brown powder (0.937 g, 82% yield).

Method (c):

A solution of (ferrocenylmethyl)imidazolium iodide (**150**) (7.00 g, 18.2 mmol) and the appropriate 1-methylimidazole derivative (2.2 ml, 27.3 mmol) in dry acetonitrile (100 ml) was refluxed for 18 h. The cooled solution was poured into water (75 ml) and extracted with chloroform (3×50 ml). The extracts were washed with water (2×50 ml), dried over $MgSO_4$ and evaporated to give an orange oil. The product was purified by column chromatograhy on silica gel using DCM/methanol (95:5) as the eluant, affording a yellow powder (5.27 g, 71% yield).

1-Ferrocenylmethyl-3-methylimidazolium iodide (151)

Method (a) 74%, method (b) 80%, method (c) 71%; yellow powder; m.p. 146–148°C. ^{1}H NMR ($CDCl_3$): ppm 4.02 (s, 3H, CH_3), 4.23 (m, 7H, Cp H), 4.49 (m, 2H, Cp H), 5.36 (s, 2H, Fc–CH_2–), 7.41 (s, 1H, 5-im H), 7.47 (s, 1H, 4-im H), 9.72 (s, 1H, 2-im

H). ^{13}C NMR ($CDCl_3$): ppm 36.57 (NCH_3), 49.34 (Fc–CH_2–), 69.09–69.28 (Cp C), 121.27 (4-im C), 123.0 (5-im C), 135.11 (2- Im C). IR (KBr) ν (cm^{-1}) 2123, 2975, 1560, 1319, 1097, 831, 756, 503, 497.

1-Ferrocenylmethyl-3-ethylimidazolium iodide (152)

Method (a) 86%, method (c) 67%; yellow powder; m.p. 60–62°C.

^{1}H NMR ($CDCl_3$): ppm 1.41 (t, *J*=7.4 Hz, 3 H, $CH_2C\underline{H}_3$), 4.25 (s, 7 H, Cp H), 4.34 (q, *J*=7.4 Hz, 2 H, $C\underline{H}_2CH_3$), 4.48 (t, 2 H, *J*=1.5 Hz, Cp H), 5.38 (s, 2 H, Fc–CH_2–), 7.28 (s, 1 H, 5-im H), 7.34 (s, 1 H, 4-im H), 9.94 (s, 1 H, 2-im H). ^{13}C NMR ($CDCl_3$): ppm 15.18 ($NCH_2C\underline{H}_3$), 44.85 ($NC\underline{H}_2CH_3$), 49.92 (Fc–CH_2–), 68.68–71.81 (Cp C–H), 121.31 (4-im C), 121.35 (5-im C), 134.44 (2- Im C). IR (KBr) ν (cm^{-1}) 3043, 1553, 1441, 1237, 1156, 1106, 505, 480.

1-Ferrocenylmethyl-3-propylimidazolium iodide (153)

Method (c) 68%, yellow powder; m.p. 102–104°C.

^{1}H NMR ($CDCl_3$): ppm 0.98 (t, *J*=7.4 Hz, 3 H, $CH_2CH_2C\underline{H}_3$), 1.95 (m, *J*=7.4 Hz, 2 H, $CH_2C\underline{H}_2CH_3$), 4.24–4.27 (m, 9 H, Cp H and $C\underline{H}_2CH_2CH_3$), 4.49 (q, 2 H, *J*=1.5 Hz, Cp H), 5.41 (s, 2 H, Fc–CH_2–), 7.28–7.29 (m, 2 H, 4- and 5-im H), 10.08 (s, 1 H, 2-im H). ^{13}C NMR ($CDCl_3$): ppm 10.29 ($NCH_2CH_2C\underline{H}_3$), 23.06 ($NCH_2C\underline{H}_2CH_3$), 49.93 ($NC\underline{H}_2CH_2CH_3$), 51.15 (Fc–$CH_2$–), 68.66–71.80 (Cp C), 121.32 (4-im C), 121.71 (5-im C), 134.59 (2-im C). IR (KBr) ν (cm^{-1}) 3079, 1558, 1444, 1237, 1150, 500, 479.

1-Ferrocenylmethyl-3-n-butylimidazolium iodide (154)

Method (a) 98%, method (c) 82%, an orange oil.

^{1}H NMR ($CDCl_3$): ppm 0.88 (t, *J*=7.4 Hz, 3 H, $CH_2CH_2CH_2C\underline{H}_3$), 1.27 (m, 2 H, *J*=4.4 Hz, $CH_2CH_2C\underline{H}_2CH_3$), 1.80 (m, 2 H, *J*=7.2 Hz, $CH_2C\underline{H}_2CH_2CH_3$), 4.18–4.22 (m, 9 H, *J*=7.2 Hz, Cp H and $C\underline{H}_2CH_2CH_2CH_3$), 4.45 (t, 2 H, *J*=1.2 Hz, Cp H), 5.33 (s, 2 H, Fc–CH_2–), 7.35 (d, 2 H, *J*=10.4 Hz, 4- and 5-im H), 9.86 (s, 1 H, 2-im H). ^{13}C NMR ($CDCl_3$): ppm 12.97 ($NCH_2CH_2CH_2C\underline{H}_3$), 18.81 ($NCH_2CH_2C\underline{H}_2CH_3$), 31.48 ($NCH_2C\underline{H}_2CH_2CH_3$), 46.59 ($NC\underline{H}_2CH_2CH_2CH_3$), 49.03 (Fc–$CH_2$–), 68.62–71.77 (Cp C), 121.34 (4-im C), 121.64 (5-im C), 134.51 (2-im C). IR (KBr) ν (cm^{-1}) 3072, 1558, 1463, 1237, 1151, 1105, 512, 499.

1-Ferrocenylmethyl-3-benzylimidazolium iodide (155)

Method (a) 82%; yellow powder; m.p. .

^{1}H NMR ($CDCl_3$): ppm 4.37 (s, 7 H, Cp H), 4.57 (s, 2 H, Cp α-H), 5.09 (s, 2 H, Fc–$C\underline{H}_2$–) 5.26 (s, 2 H, $C\underline{H}_2$–Ph), 6.90 (s, 2 H, 4,5-im H), 7.16 (s, 3 H, *m,p*-Ph H), 7.42 (s, 2 H, *o*-Ph H), 10.75 (s, 1 H, 2-im H). ^{13}C NMR ($CDCl_3$): ppm 50.28 (Fc–$\underline{C}H_2$–), 53.73 ($C\underline{H}_2$–Ph), 69.54–70.12 (Cp C), 79.50 (Cp C_{ipso}), 121.66 (4-im C), 121.80 (5-im C), 129.76–129.48 (*o,m,p*-Ph C), 133.56 (2-im C), 137.36 (Ph C_{ipso}). IR (KBr) ν (cm^{-1}) 3161, 3038, 2668, 1560, 1445, 1155, 813, 711. $C_{21}H_{21}N_2FeCl$ (392.70): calculated C 64.23, H 5.39, N 7.13; found: C 63.53, H 5.78, N 6.91%.

General procedure for the synthesis of the 1-ferrocenylmethylbenzimidazolium iodide salts (156)–(160)

1-Ferrocenylmethyl-3-methylbenzimidazolium iodide (156)

1-Ferrocenylmethylbenzimidazole (**33**) (0.224 g, 0.70 mmol) and methyl iodide (1.2 ml, 19.5 ml) were dissolved in acetonitrile (20 ml) and heated to reflux for 2 h until a yellow precipitate was formed. The reaction mixture was cooled, poured into water (30 ml) and extracted with chloroform (3×20 ml). The organic extracts were dried over Mg_2SO_4, filtered and evaporated to afford a fine yellow powder (0.306 g, 95% yield).

^{1}H NMR ($CDCl_3$): ppm 4.21 (s, 3 H, –C<u>H</u>$_3$), 4.33 (s, 7 H, Cp H), 4.63 (t, 2 H, *J*=1.6 Hz, Cp H), 5.64 (s, 2 H, Fc–C<u>H</u>$_2$–), 7.63–7.69 (m, 3 H, *J*=3.2 Hz, Bzim H), 7.79–7.82 (m, 1 H, *J*=2.8 Hz, 8-bzim H), 10.95 (s, 1 H, 2-bzim H). ^{13} C NMR ($CDCl_3$): ppm 31.35 (–<u>C</u>H$_3$), 69.71–70.25 (Cp C), 48.08 (Fc–<u>C</u>H$_2$–), 79.10 (Cp C_{ipso}) 113.14 (6-bzim C), 113.72 (5-bzim C), 127.67 (7-bzim C), 131.18 (8-bzim C), 132.37 (4-bzim C), 142.08 (9-bzim C), 207.48 (2-bzim C). IR (KBr) ν(cm^{-1}) 3489, 3436, 3135, 3082, 3045, 2992, 1561, 1104, 763. $C_{19}H_{19}N_2FeI$ (458.13): calculated C 49.81, H 4.18, N 6.11; found: C 47.41, H 4.19, 5.60%.

1-Ferrocenylmethyl-3-ethylbenzimidazolium iodide (157)

Yellow powder (0.48 g, 42% yield); m.p.,

^{1}H NMR ($CDCl_3$): ppm 1.66 (t, 3 H, *J*=7.2 Hz, –CH$_2$C<u>H</u>$_3$), 4.21 (s, 7 H, Cp H), 4.50 (m, 2 H, *J*=4.4 Hz, –C<u>H</u>$_2$CH$_3$), 4.56 (s, 2 H, *J*=2 Hz, Cp H), 5.63 (s, 2 H, Fc–C<u>H</u>$_2$–), 7.56 (m, 4 H, *J*=2.8 Hz, Bzim H), 10.85 (s, 1 H, 2-bzim H). ^{13}C NMR ($CDCl_3$): ppm 12.80 (–CH$_2$<u>C</u>H$_3$), 41.00 (–<u>C</u>H$_2$CH$_3$), 45.64 (Fc–CH$_2$), 67.33 (Cp C–H), 77.01 (Cp C_{ipso}), 110.97 (5-bzim C), 111.42 (5-bzim C), 111.60 (7-bzim C), 114.52 (8-bzim C),

125.05 (4-bzim C), 128.96 (9-bzim C), 138.58 (2-bzim C). IR (KBr) ν (cm^{-1}) 3076, 1497, 1266, 1232, 1160, 747.

1-Ferrocenylmethyl-3-propylbenzimidazolium iodide (158)

Yellow powder (51%); m.p. °C,

^{1}H NMR ($CDCl_3$): ppm 0.98 (t, 3 H, *J*=7.2 Hz, $-CH_2CH_2C\underline{H}_3$), 2.03 (m, 2 H, *J*=7.6 Hz, $-CH_2C\underline{H}_2CH_3$), 4.15 (s, 2 H, Cp H), 4.26 (5 H, Cp H), 4.42 (t, 2 H, *J*=7.6 Hz, $-C\underline{H}_2CH_2CH_3$), 5.64 (s, 2 H, Fc–$CH_2$–), 7.55 (m, 2 H, *J*=12 Hz, 6,7-bzim H), 7.60 (m, 1 H, *J*=3.2 Hz, 8-bzim H), 7.40 (m, 1 H, *J*=2.8 Hz, 5-bzim H), 10.96 (s, 1 H, 2-bzim H). ^{13}C NMR ($CDCl_3$): 11.53 ($-CH_2CH_2\underline{C}H_3$), 23.18 ($-CH_2\underline{C}H_2CH_3$), 48.03 ($-\underline{C}H_2CH_2CH_3$), 49.49 (Fc–$CH_2$–), 69.96 (Cp C–H), 79.45 (Cp C_{ipso}), 113.35 (6-bzim C), 113.96 (5-bzim C), 127.53 (7-bzim C), 127.5 (8-bzim C), 131.41 (4-bzim C), 131.67 (9-bzim C), 141.58 (2-bzim C). IR (KBr) ν (cm^{-1}) 3118, 2965, 1559, 1406, 761. $C_{21}H_{23}N_2FeI$ (486.18): calculated C 51.88, H 4.77, N 5.76; found: C 51.84, H 4.68, N 5.76%.

1-Ferrocenylmethyl-3-butylbenzimidazolium iodide (159)

Yellow powder (42% yield); m.p. °C.

^{1}H NMR ($CDCl_3$): 0.98 (t, 3 H, *J*=7.2 Hz, $-CH_2CH_2CH_2C\underline{H}_3$), 1.47 (m, 2 H, *J*=4.4 Hz, $-CH_2CH_2C\underline{H}_2CH_3$), 2.06 (m, 2 H, 7.2 Hz, $-CH_2C\underline{H}_2CH_2CH_3$), 4.22 (s, 2 H, Cp H), 4.33 (s, 5 H, Cp H), 4.54 (t, 2 H, *J*=7.6 Hz, $-C\underline{H}_2CH_2CH_2CH_3$), 4.65 (s, 2 H, Cp H), 5.72 (s, 2 H, Fc–$C\underline{H}_2$–), 7.63 (m, 1 H, *J*=2.8 Hz, 6,7-bzim H), 7.68 (m, 1 H, *J*=6 Hz, 8-bzim H), 7.82 (m, 1 H, 5-bzim H), 11.08 (s, 1 H, 2-bzim H). ^{13}C NMR ($CDCl_3$): 13.93 ($-CH_2CH_2CH_2\underline{C}H_3$), 20.26 ($-CH_2CH_2\underline{C}H_2CH_3$), 31.62 ($-CH_2\underline{C}H_2CH_2CH_3$),

47.91 (–$\underline{C}H_2CH_2CH_2CH_3$), 48.04 (Fc–$CH_2$–), 69.96 (Cp C–H), 79.44 (Cp C_{ipso}), 113.35 (6-bzim C), 113.78 (5-bzim C), 113.99 (7-bzim C), 127.42 (8-bzim C), 127.54 (4-bzim C), 131.41 (9-bzim C), 141.56 (2-bzim C). IR (KBr) ν (cm^{-1}) 3117, 3104, 2931, 1555, 1402, 759. $C_{22}H_{25}N_2FeI$ (500.21): calculated C 52.83, H 5.04, N 5.60; found: C 52.60, 4.84, 5.49%.

1-Ferrocenylmethyl-3-benzylbenzimidazolium chloride (160)

Yellow powder (0.173 g, 48%); m.p. °C.

^{1}H NMR (DMSO-d_6): ppm 4.20 (s, 5 H, Cp H), 4.24 (s, 2 H, Cp H), 4.45 (s, 2 H, Cp H), 5.19 (–CH_2–Ph), 5.44 (Fc–CH_2–), 7.40 (m, 7 H, 6,7-bzim H and phenyl H), 7.83 (5,8-bzim H), 9.54 (2-bzim H). IR (KBr) ν (cm^{-1}) 3462, 3098, 3063, 1551, 1382, 1105, 822, 503.

1,3-Di(ferrocenylmethyl)imidazolium iodide (161)

A solution of **150** (5.00 g, 0.01 mol), imidazole (0.45 g, 0.01 mol) and potassium carbonate (1.35 g, 0.01 mol) in acetonitrile (100 ml) was heated to reflux for one week. The cooled solution was poured into water (100 ml) and extracted with chloroform (3×75 ml). The extracts were washed with water (2×50 ml), dried over $MgSO_4$ and evaporated to give an orange oil. The product was purified by column chromatography, using silica gel and methanol/DCM (5:95) as the eluant, yielding a yellow powder (2.6 g, 68% yield). m.p. 170°C (decomp).

^{1}H NMR ($CDCl_3$): ppm 4.22 (s, 14H, Cp H), 4.44 (s, 4H, Cp H), 5.31 (s, 4H, Fc–CH_2–), 7.17 (s, 2 H, 4- and 5-m H), 9.92 (s, 1 H, 2-im H). ^{13}C NMR ($CDCl_3$): ppm 49.85 (Fc–CH_2–), 68.75–69.66 (Cp C–H and C–C), 120.82 (4- and 5-im C), 134.66 (2-im C). IR (KBr) ν (cm^{-1}): 3066, 2938, 1550, 1142, 1100, 826, 514, 498.

$C_{25}H_{25}N_2Fe_2I_2$ (718.99): calculated C 50.71, H, 4.25, 4.73; found: C 50.14, H 4.24, N 4.95%.

1,3-Di(ferrocenylmethyl)benzimidazolium iodide (162) [126]

A solution of **150** (6.17 g, 16 mmol) and **149** (5.0 g, 16 mmol) were heated to reflux in acetonitrile (150 ml) for 24 h. The reaction was cooled to room temperature, water was added and the suspension was extracted into chloroform. The organic layer was washed with water, dried over $MgSO_4$ and evaporated to leave an orange residue. This was treated with diethyl ether precipitating out an orange powder, which was collected by filtration (5.8 g, 57% yield). m.p. 121°C (decomp).

^{1}H NMR ($CDCl_3$): ppm 4.20 (s, 4 H, Cp β-H), 4.25 (s, 10 H, Cp H), 4.45 (s, 4 H, Cp α-H), 5.41 (s, 4 H, Fc–C$\underline{H}_2$–), 7.55–7.57 (q, 2 H, J=3.6 Hz, 6,7-bzim H), 7.69–7.71 (m, 2 H, J=3.2 Hz, 5,8-bzim H), 9.47 (s, 1 H, 2-bzim H). ^{13}C (DMSO-d_6): ppm 46.36 (Fc–$\underline{C}H_2$), 68.98 (Cp C–H), 69.51 (Fc Cp C–H), 80.23 (Cp C_{ipso}), 114.02 (5,8-bzim C), 126.82 (6,7-bzim C), 130.71 (4,9-bzim H), 140.90 (2-bzim C). IR (KBr) ν (cm^{-1}): 3064, 1615, 1559, 1495, 1265, 1171, 1106, 820, 750. $C_{29}H_{27}N_2FeI$ (642.15): calculated C 52.24, H 4.24, N 4.36; found C 52.15, H 4.00, N 4.07%.

1-(1-Ferrocenylmethyl)-3-(4-iodobutyl)imidazolium iodide (163)

1-Ferrocenylmethylimidazole (**148**) (1.24 g, 4.65 mmol) and 1,4diiodobutane (1.23 ml, 9.30 mmol) were dissolved in dry acetonitrile (10 ml) and left to stand overnight. An orange separated out. The solvent was removed in vaccu and the product collected by column chromatography on silica gel using DCM–methanol (95:5) as the eluant, yielding a yellow solid (0.20 g, 74%).

^{1}H NMR ($CDCl_3$): ppm 1.86 (m, 2 H, *J*=7.6 Hz, $-CH_2CH_2C\underline{H}_2CH_2I$), 2.51 (m, 2 H, *J*=7.6 Hz, $-CH_2C\underline{H}_2CH_2CH_2I$), 4.24 (m, 9 H, *J*=2.8 Hz, Cp H), 4.45 (t, 2 H, *J*=1.6 Hz, $-CH_2CH_2CH_2C\underline{H}_2I$), 5.19 (s, 2 H, $-CH_2CH_2CH_2C\underline{H}_2I$), 5.75 (s, 2 H, $-C\underline{H}_2CH_2CH_2CH_2I$), 7.77 (s, 1 H, 4-im H), 7.80 (s, 1 H, 5-im H), 9.21 (s, 1 H, 2-im H). ^{13}C NMR $CDCl_3$): ppm 30.18 ($-CH_2CH_2\underline{C}H_2CH_2I$), 30.45 ($-CH_2\underline{C}H_2CH_2CH_2I$), 46.98 ($-\underline{C}H_2CH_2CH_2CH_2I$), 48.25 (Fc–$\underline{C}H_2$–), 69.8–70.24 (Cp C), 79.70 (Cp C_{ipso}), 127.68 (4-im C), 131.35 (5-im C), 141.42 (2-im C).

1-[(1-Ferrocenylmethyl-3-butyl)imidazolium]-3-ferrocenylmethylimidazolium diiodide (164)

1-Ferrocenylmethylimidazole (0.75 g, 1.88 mmol) and (**163**) were suspended in acetonitrile (30 ml) and heated to reflux overnight, with stirring and under nitrogen. A yellow precipitate was formed that was collected by filtration and washed with diethyl ether. The filtrate was poured into water (50 ml) and extracted with chloroform (3×40 ml), the organic extracts were combined, dried over Mg_4SO_4 and evaporated to afford a yellow powder (0.79 g, 50% yield).

^{1}H NMR ($CDCl_3$): ppm 2.13 (s, 4 H, $-CH_2C\underline{H}_2C\underline{H}_2CH_2$–), 4.202 (s, 14 H, Cp H and 4 H, $-C\underline{H}_2CH_2CH_2C\underline{H}_2$–), 4.38 (s, 4 H, Cp H), 5.20 (s, 2 H, *J*=1.6 Hz, Fc–CH_2–), 7.02 (s, 1 H, 5-im H), 7.64 (s, 1 H, 5-im H), 9.74 (s, 1 H, 2-im H). ^{13}C NMR ($CDCl_3$): 27.02 ($-CH_2\underline{C}H_2\underline{C}H_2CH_2$–), 49.51 ($-\underline{C}H_2CH_2CH_2\underline{C}H_2$–), 50.68 (Fc–$CH_2$–), 70.08 (Cp C–H), 78.59 (Cp C_{ipso}), 121.40 (4-im H), 123.41 (5-im C), 135.80 (2-im C). IR (KBr) ν (cm^{-1}): 3129, 3068, 1561, 1400, 1155, 1104, 924, 731. $C_{32}H_{36}N_4Fe_2I_2$ (842.17): calculated C 45.64, H 4.31, N 6.65; found: C 44.66, H 4.16, N 6.30%.

1-(1-Ferrocenylmethyl)-3-(4-iodobutyl)benzimidazolium iodide (165)

1-Ferrocenylmethylbenzimidazole (3.0128 g, 9.53 mmol) and 1,4-diiodobutane were suspended in acetonitrile (100 ml) and heated to reflux with stirring under nitrogen until all the solid had dissolved. The reaction mixture was left to cool and a yellow solid precipitated. The solid was collected, and the filtrate was poured into water (100 ml) and extracted with chloroform (3×50 ml). The organic layers were combined, washed with water, dried over Mg_4SO_4, filtered and evaporated to afford a yellow solid, which proved to be the same as the collected solid. Both solids were combined and washed with diethyl ether (4.7 g, 79%).

^{1}H NMR (DMSO-d_6): ppm 1.95 (m, 2 H, J=7.2 Hz, $-CH_2CH_2\underline{C}H_2CH_2I$), 2.24 (m, 2 H, J=7.2 Hz, $-CH_2\underline{C}H_2CH_2CH_2I$), 4.22 (d, 2 H, J=8.4 Hz, $-CH_2CH_2CH_2\underline{C}H_2I$), 4.24–4.31 (m, 7 H, J=2.0 Hz, Fc Cp H), 4.64 (m, 2 H, J=2.0 Hz, $-\underline{C}H_2CH_2CH_2CH_2I$), 4.62–4.66 (m, 2 H, $-\underline{C}H_2CH_2CH_2CH_2I$ and 2 H Fc Cp), 7.63–7.66 (m, 2 H, J=2.4 Hz, 6,7-bzim H), 7.76–7.83 (m, 1 H, J=3.6 Hz, 5-bzim H), 7.84 (m, 1 H, J=2.0 Hz, 8-bzim H), 11.01 (s, 1 H, 2-bzim H). ^{13}C NMR (DMSO-d_6): ppm 29.78 ($-CH_2CH_2\underline{C}H_2CH_2I$), 29.76 ($-CH_2\underline{C}H_2CH_2CH_2I$), 30.85 ($-CH_2\underline{C}H_2CH_2CH_2I$), 45.82 ($-\underline{C}H_2CH_2CH_2CH_2I$), 46.56 (Fc–$\underline{C}H_2$–), 68.98–69.54 (Cp C), 113.82–114.10 (5,8-bzim C), 126.80 (6,7-bzim C), 130.98 (4-bzim C), 141.57 (9-bzim C), 207.01 (2-bzim C). IR (KBr) ν (cm^{-1}): 3103, 3010, 1555, 1426, 1238, 1002, 753, 499. $C_{22}H_{24}N_2FeI_2$ (626.11): calculated C 42.20, H 3.86; found: C 41.71, H 3.69%.

1-[(1-Ferrocenylmethyl-3-butyl)benzimidazolium]-3-ferrocenylmethyl benzimidazolium diiodide (166)

1-Ferrocenylmethylbenzimidazole (0.59 g, 1.88) and (**165**) were suspended in acetonitrile (30 ml) and heated to reflux overnight, with stirring and under nitrogen. A yellow precipitate was formed that was collected by filtration and washed with diethyl ether. The filtrate was poured into water (50 ml) and extracted with chloroform (3×40 ml), the organic extracts were combined, dried over Mg_4SO_4 and evaporated to afford a yellow powder (0.9761 g, 55% yield).

^{1}H NMR (DMSO-d_6): ppm 2.00 (d, 4 H, J=19.6 Hz, –$CH_2C\underline{H}_2C\underline{H}_2CH_2$–), 4.24 (s, 10 H, Cp H), 4.29 (s, 4 H, Cp H), 4.53 (m, 4 H, J=2.8 Hz, Cp α-H), 4.56 (m, 4 H, J=2.0 Hz, –$\underline{C}H_2CH_2CH_2\underline{C}H_2$–), 5.51 (t, 2 H, J=7.6 Hz, Fc–$C\underline{H}_2$), 7.68 (m, 4 H, J=2.0 Hz, 6,7-bzim H), 8.05 (m, 2 H, 4.8 Hz, 8-bzim H), 8.19 (m, 2 H, J=1.6 Hz, 5-bzim H), 9.72 (s, 2 H, 2-bzim H). ^{13}C NMR (DMSO-d_6): ppm 31.5 (–$CH_2\underline{C}H_2\underline{C}H_2CH_2$–), 46.68 (–$\underline{C}H_2CH_2CH_2\underline{C}H_2$–), 46.80 (Fc–$\underline{C}H_2$–), 69.24 (Cp C–H), 69.89 (Cp C–H), 80.46 (Cp C_{ipso}), 114.06 (8-bzim C), 114.33 (5-bzim C), 127.01 (6,7-bzim H), 130.98 (4-bzim H) 141.75 (9-bzim H), 207.18 (2-bzim H). IR (KBr) ν (cm^{-1}): 3025, 2956, 1556, 1379, 1238, 1171, 1104, 757, 484. $C_{40}H_{40}N_4Fe_2I_2$ (942.29): calculated C 50.99, H 4.28, N 5.95; found: C 49.74, H 4.22, N 5.86%.

1,1'-Bis-(1-methylimidazole)ferrocene (170) – Route (1):

1,1'-Ferrocenyldicarboxaldehyde (167)

To a stirred solution of TMEDA (20.00 ml, 13.5 mmols) and *n*-butyl lithium (2.5 M in hexanes; 54 ml, 13.5 mmols) in dry diethyl ether (200 ml), under an argon atmosphere ferrocene (10 g, 5.3 mmols) was added portionwise. After stirring overnight, the resulting red suspension was cooled to –78°C using a liquid

nitrogen–methanol bath, anhydrous DMF (21 ml, 27 mmols) was added dropwise. The reaction mixture was stirred at −78°C for 3 h then left to return to room temperature. Water (200 ml) was added, the organic layer was separated and the aqueous layer extracted with DCM (3×100 ml). The combined organic portions were then washed with water (100 ml), dried over $MgSO_4$, filtered and evaporated in vaccu to dryness and the crude purple product was purified by column chromatography using diethyl ether as the eluant to yield red crystals (5.7 g, 45% yield).

^{1}H NMR ($CDCl_3$): ppm 4.67 (d, 4H, Cp H), 4.82 (d, 4H, Cp H), 9.94 (s, 2H, CHO).

1,1′-Ferrocenyldimethanol (168)

To solution of **167** (2.39 g, 9.7 mmols) in methanol (100 ml), sodium borohydride (1.1 g, 29 mmols) was added portionwise and left at room temperature for 1 h. The brown reaction mixture was then poured into water (50 ml) and diethyl ether added (50 ml). The organic layer was separated and the aqueous layer was extracted with diethyl ether (3×50 ml). The combined organic layers were dried over $MgSO_4$, filtered and evaporated to dryness giving a yellow powder. The crude product was purified by column chromatography using 80:20 ethyl acetate:hexane as the eluant (or could be used crude for the next reaction) (2.87 g, 85%).

^{1}H NMR ($CDCl_3$): ppm 4.18 (d, 4H, Cp H), 4.22 (d, 4H, Cp H), 4.39 (s, 2H, CH_2).

1,1′-Bis-(1-methylimidazole)ferrocene (170) via (1,1′-ferrocenylmethyl)chloride (169)

1,1′-Ferrocenyldimethanol (1.10 g, 4.47 mmols) was dissolved in dry THF (50 ml) and at −5°C, and pyridine (0.72 ml, 8.98 mmols) in dry THF (3 ml) was added dropwise with stirring. Phosphorus trichloride (0.8 ml, 8.98 mmols) in dry THF (5 ml)

was then added dropwise. An orange precipitate fell out of solution immediately. The reaction mixture was filtered under nitrogen and to the filtrate imidazole (0.61 g, 8.94 mmols) and sodium carbonate (1.42 g, 13.41 mmols) were added. The reaction mixture was then evaporated to give an orange residue. Dry acetonitrile was replaced as the solvent and the suspension was heated to reflux overnight under a nitrogen atmosphere. After cooling, water was added and the product extracted with chloroform (3×50 ml), dried over $MgSO_4$, filtered and evaporated in vaccu to yield an orange oil. After purification on silica gel, using diethyl ether/methanol (50:50) as the solvent, a yellow powder was recovered (0.05g, 3% yield).

^{1}H NMR ($CDCl_3$): ppm 4.10 (s, 8 H, Cp H), 4.73 (d, 4 H, *J*=8 Hz, fc–CH_2), 6.84 (d, 2 H, *J*=8 Hz, 5-im H), 6.97 (s, 2 H, 4-im H), 7.42 (s, 2 H, 2-im H). ^{13}C NMR ($CDCl_3$): ppm 46.68 (Fc–CH_2), 69.61 (Cp C), 70.04 (Cp C), 84.05 (Cp C_{ipso}), 119.24 (4-im H), 129.77 (5-im H), 137.07 (2-im H). $C_{18}H_{12}N_4Fe$ (344.2) C 62.81, H 4.69, N; found: C 62.02, H 5.21%.

(1,1′-Ferrocenylmethyl)-p-toluenesulphonate (171)

1,1′-Ferrocenedimethanol (0.10 g, 0.4 mmols), pyridine (0.13 ml, 1.6 mmols) and *p*-toluenesuphonyl chloride (0.23 g, 1.2 mmols) in purified ethanol (40 ml) (washed with water and dried over $MgSO_4$, filtered and distilled from calcium chloride) were stirred together for 2 h. Water (10 ml) was poured into the reaction mixture and the organic layer separated. The aqueous layers were extracted with chloroform (3×10 ml) and the organic extracts combined, dried over $MgSO_4$, filtered and evaporated in vaccu to yield a brown gum. After column chromatography using methanol as the eluant, a brown powder was obtained (0.18 g, 81% yield).

^{1}H NMR (DMSO-d_6): ppm 2.49 (s, 6H, Ar-CH_3), 4.36 (d, 4H, Cp-H), 4.67 (d, 4H, Cp-H), 5.74 (s, 4H, Cp–CH_2–OTs), 7.10 (d, 4H, 2- and 6-Ar), 7.66 (d, 4H, 3- and 5-Ar).

N,N-Dimethyl(methylene)ammonium chloride (172)

To a stirred solution of *N,N,N',N'*-tetramethyldiaminomethane (5.4 ml, 39.1 mmol) in DCM (50 ml), cooled to 0°C, under a nitrogen atmosphere and with vigorous stirring, acetyl chloride (5.6 ml, 78.5 mmol) was added dropwise to keep the temperature below 5°C. A white precipitate was formed that was collected by filtration under nitrogen and was washed with dry DCM (50 ml) and dry THF (50 ml). The product is highly hydroscopic and so was placed in a dessicator under vaccum overnight before use. (3.57 g, 97% yield).

^{1}H NMR (DMSO-d_6): ppm 3.76 (6 H, $N^+(C\underline{H}_3)_2$), 8.32 (2 H, $C\underline{H}_2$=).

1,1'-Bis-(N,N-dimethylaminomethyl)ferrocene (173)

To a stirred solution of ferrocene (2.5 g, 13.4 mmol) and TMEDA (4.9 ml, 32.2 mmol) in hexane (80 ml), *n*-butyl lithium (13 ml, 2.5 M, 32.9 mmol) was added dropwise under an argon atmosphere and left to stir overnight. Diethyl ether (80 ml) was added and *N,N*-dimethylmethyleneammonium chloride (2.59 g, 27.7 mmol) was added in one portion. The reaction mixture was stirred for a further 18 h, heated to reflux for 10 min and cooled. Water (30 ml) was added dropwise and stirring was continued for 15 min. Then more water was added (60 ml). The organic layer was separated and the aqueous layer extracted with 3×50 ml of diethyl ether. The combined organic layers were combined, dried over Mg_2SO_4, filtered and evaporated to afford a red liquid as the crude product. The desired product was isolated using

column chromatography on alumina. Pet. ether (40–60%) was used to elute unreacted ferrocene, 30% diethyl ether/pet. ether (40–60%) eluted the mono-dimethylaminomethyl derivative and 3% methanol/diethyl ether eluted the product as a orange/brown liquid (2.38 g, 65% yield).

^{1}H NMR ($CDCl_3$): ppm 2.17 (s, 12 H, –NC$\underline{H}_3$), 3.26 (s, 4 H, –C$\underline{H}_2$–), 4.07 (m, 4 H, Fc Cp $\underline{H}$), 4.11 (m, 4 H, Fc Cp $\underline{H}$).

Ferrocene-1′-diylbis-(methyltrimethylammonium iodide) (174)

To **173** (0.26 g, 0.86 mmol) in methanol (2.5 ml), methyl iodide was added dropwise with stirring. The reaction mixture was heated to reflux for 15 min, and after cooling to room temperature, diethyl ether was added and the product precipitated out with some scratching of the glass. A pale yellow powder was collected by filtration and washed with diethyl ether (0.27 g, 53%).

^{1}H NMR ($CDCl_3$): ppm 3.09 (s, 18 H, $(-CH_3)_3$), 4.53 (s, 4 H, Cp H), 4.67 (s, 4 H, Cp H), 4.80 (s, 4 H, Fc–C$\underline{H}_2$–). ^{13}C NMR ($CDCl_3$): ppm 53.00 ($(-CH_3)_3$), 67.2 (–$\underline{C}H_2$–), 72.9 (Cp C), 74.8 (Cp C), 75.6 (Cp C_{ipso}).

1,1′-Bis(1-methylimidazole)ferrocene (170) via 174

Ferrocene-1′-diylbis-(methyltrimethylammonium iodide) (**174**) (1.00 g, 1.7 mmol), imidazole (0.24 g, 3.5 mmol) and potassium carbonate (0.49 g, 3.57 mmol) were heated to reflux for 5 days in acetonitrile, with stirring, under nitrogen. The reaction mixture was cooled and poured into water (30 ml) and chloroform (30 ml). The organic layer was separated and the aqueous layer extracted with chloroform (3×20 ml). The combined organic layers were combined, dried over Mg_2SO_4, filtered and evaporated in vaccu to yield a brown oil. The crude product was purified by column

chromatography using 50% methanol/diethyl ether, yielding a yellow powder (0.074 g, 12% yield). Characterisation data as before.

1,1'-Bis(1-methylimidazole)ferrocene (170) via 168

1,1'-Ferrocenyldimethanol (**168**) (0.110 g, 0.45 mmol) and CDI (0.100 g, 0.59 mmol) were heated to reflux in dry acetonitrile (15 ml) for 5 h with sitrring. The solvent was removed in vaccu and the crude product purified by column chromatography on silica get using MeOH/DCM (50:50) to collect the product as a yellow solid (0.110 g, 71% yield). Characterisation data as before.

1,1'-Bis(1-methylbenzimidazole)ferrocene (175)

Compound **174** (6.5 g, 11.10 mmol), benzimidazole (2.96 g, 25.03 mmol) and potassium carbonate (3.83 g, 27.75 mmol) were heated to reflux for 6 days in acetonitrile (150 ml), with stirring, under nitrogen. The reaction mixture was cooled and poured into water (100 ml) and DCM (100 ml). The organic layer was separated and the the aqueous layer extracted with DCM (3×50 ml). The combined organic layers were combined, dried over Mg_2SO_4, filtered and evaporated to yield a brown oil. The crude product was purified by column chromatography using ethyl acetate as the eluant, yielding a yellow powder (1.72 g, 20%).

^{1}H NMR ($CDCl_3$): ppm 4.13 (s, 4 H, Cp H), 4.18 (t, 4 H, *J*=1.6 Hz, Cp H), 4.92 (d, 4 H, *J*=1.6 Hz, fc–C<u>H</u>$_2$–), 7.25 (q, *J*=3.4 Hz, 4 H, 6,7-bzim H), 7.35 (d, *J*=4.2 Hz, 2 H, 5-bzim H), 7.73 (d, *J*=6.8 Hz, 2 H, 8-bzim H), 7.80 (s, 2 H, 2-bzim H). ^{13}C NMR ($CDCl_3$): ppm 66.65 (fc–<u>C</u>H$_2$–), 69.90 (Cp C), 70.03 (Cp C), 83.79 (Cp C_{ipso}), 110.08 (5,8-bzim H), 120.89 (9-bzim H), 122.68 (6,7-bzim H), 123.41 (4-bzim H), 142.85 (2-bzim H). IR (KBr) ν(cm^{-1}): 3090, 2932, 1497, 1264, 1238, 746, 434.

1,1'-Bis(1-methyl-3-methylbenzimidazolium)ferrocenyl iodide (176)

Compound **175** (0.11 g, 0.25 mmol) was suspended in acetronitrile (15 ml) and heated to reflux with methyl iodide (2 ml) for 2 h with stirring, under nitrogen. A yellow precipitate formed and was collected by filtration, washed with diethyl ether. The filtration was poured into water (10 ml) and the product extracted with chloroform (3×20 ml). The organic extracts were dried over $MgSO_4$, filtered, evaporated and purified by column chromatography on silica gel using DCM/methanol (95:5) as the eluant (0.11 g, 60% yield).

^{1}H NMR ($CDCl_3$): ppm 3.87 (s, 3 H, $-CH_3$), 4.18 (t, 4 H, *J*=1.6 Hz, Cp), 4.47 (s, 4 H, Cp), 5.40 (s, 4 H, fc$-CH_2-$), 7.51 (m, *J*=3.6 Hz, 4 H, 6,7-bzim H), 7.82 (m, *J*=2.8 Hz, 2 H, 5-bzim H), 8.05 (q, *J*=2.4 Hz, 2 H, 8-bzim H), 9.64 (s, 2 H, 2-bzim H). ^{13}C NMR ($CDCl_3$): ppm ^{13} C NMR ($CDCl_3$): ppm 31.89 ($-CH_3$), 68.99–70.02 (Cp C), 47.96 (Fc$-\underline{C}H_2-$), 81.05 (Cp C_{ipso}) 113.84 (6-bzim C), 114.12 (5-bzim C), 128.17 (7-bzim C), 131.38 (8-bzim C), 133.01 (4-bzim C), 143.16 (9-bzim C), 208.16 (2-bzim C).

IR (KBr) ν (cm^{-1}): 3511, 3445, 3125, 3063, 1561, 1400, 761, 498. $C_{28}H_{28}N_4I_2Fe$ (730.22): calculated C 46.06, H 3.87, N 7.67; found: C 46.30, H 3.53, N 7.05%.

1,1'-Bis(1-methyl-3-n-butylbenzimidazolium)ferrocenyl iodide (177)

The procedure was for as above (75% yield).

^{1}H NMR ($CDCl_3$): 0.91 (t, 3 H, *J*=7.6 Hz, $-CH_2CH_2CH_2\underline{C}H_3$), 1.40 (m, 2 H, *J*=7.6 Hz, $-CH_2CH_2\underline{C}H_2CH_3$), 1.96 (m, 2 H, *J*=7.6 Hz, $-CH_2\underline{C}H_2CH_2CH_3$), 4.16 (t, 2 H, *J*=2.0 Hz, Cp H), 4.26 (d, 4 H, *J*=3.6 Hz, Cp H), 4.46 (t, 2 H, *J*=7.6 Hz, $-\underline{C}H_2CH_2CH_2CH_3$), 5.63 (fc$-CH_2$), 7.57 (m, 3 H, *J*=4.0 Hz, 6,7,8-bzim H), 7.72 (t, 1 H, *J*=4.4 Hz, 5-bzim H), 11.03 (s, 1 H, 2-bzim H). ^{13}C NMR ($CDCl_3$): 19.82 ($-CH_2CH_2CH_2\underline{C}H_3$), 30.91 ($-CH_2CH_2\underline{C}H_2CH_3$), 31.18 ($-CH_2\underline{C}H_2CH_2CH_3$), 47.44

(–$\underline{C}H_2CH_2CH_2CH_3$), 47.56 (Fc–$CH_2$–), 69.51 (Cp C–H), 78.98 (Cp C_{ipso}), 112.88 (6-bzim H), 113.49 (5-bzim H), 127.07 (7-bzim H), 127.09 (8-bzim H), 130.97 (4-bzim H), 131.22 (9-bzim H), 141.16 (2-bzim H). IR (KBr) ν (cm^{-1}): 3118, 3015, 1560, 1400, 1323, 760. $C_{34}H_{40}N_4FeI_2$ (814.38): calculated C 50.15, H 4.95, H 6.88; found: C 51.99, H 4.46, N 4.11%.

Bis[1-(1,1'-ferrocenylmethyl)-3-(4-iodobutyl)]benzimidazolium iodide (185)

Compound **175** (0.257 g, 0.58 mmol) and 1,4-diiodobutane (1 ml, 7.58 mmol) were suspended in acetonitrile (10 ml), heated to reflux for 4 h and let stand for 2 days at room temperature. A yellow precipitate was formed which was collected by filtration (0.141 g, 22% yield).

^{1}H NMR (DMSO-d_6): 1.86 (d, 4 H, J=6.4 Hz, –$CH_2C\underline{H}_2CH_2CH_2I$), 1.97 (d, 4 H, J=8.0 Hz, –$CH_2CH_2CH_2CH_2I$), 3.34 (m, 4 H, J=5.6 Hz, –$CH_2CH_2CH_2C\underline{H}_2I$), 4.36 (t, 4 H, J=6.8 Hz, Cp H), 4.54 (t, 4 H, J=8.4 Hz, Cp H), 4.69 36 (m, 4 H, J=6.6 Hz, –$CH_2CH_2CH_2C\underline{H}_2I$), 7.73 (d, 4 H, J=6.0 Hz, 6,7-bzim H), 8.11 (t, 2 H, J=4.0 Hz, 8-bzim H), 8.25 (t, 2 H, J=6.4 Hz, 5-bzim H), 9.82 (t, 2 H, J=4.2 Hz, 2-bzim H). ^{13}C NMR (DMSO-d_6): ppm 24.40 (–$CH_2CH_2\underline{C}H_2CH_2I$), 28.55 (–$CH_2\underline{C}H_2CH_2CH_2I$), 29.52 (–$CH_2\underline{C}H_2CH_2CH_2I$), 44.53 (–$\underline{C}H_2CH_2CH_2CH_2I$), 45.02 (Fc–$\underline{C}H_2$–), 68.95–69.59 (Cp C), 79.52 (Cp C_{ipso}), 112.61 (5-bzim C), 112.87 (8-bzim H), 125.43 (6-bzim C), 129.44 (7-bzim H), 129.85 (4-bzim C), 140.28 (9-bzim C), 205.39 (2-bzim C). IR (KBr) ν (cm^{-1}): 3134, 3015, 2949, 1559, 1236, 1171, 753, 489.

Bis{1-[(1,1'-ferrocenylmethyl-3-butyl)benzimidazolium]

-3-ferrocenylmethyl}benzimidazolium tetraiodide (186)

Compounds **185** and **175** were suspended in acetonitrile, heated to reflux for 4 h and let stand for 2 days at room temperature. A yellow precipitate formed, which was collected by filtration (0.055 g, 33% yield).

^{1}H NMR (DMSO-d_6): 2.01 (s, 8 H, $-CH_2\underline{C}H_2\underline{C}H_2CH_2-$), 4.28 (d, 8 H, J=20 Hz, $-\underline{C}H_2CH_2CH_2\underline{C}H_2-$), 4.57 (s, 8 H, Cp H), 4.75 (d, 8 H, J=14.8 Hz, Cp H), 5.77 (d, 8 H, J=10.8 Hz, fc–CH_2–), 7.71 (d, 8 H, J=4.8 Hz, 6,7-bzim H), 8.26 (d, 4 H, J=6.4 Hz, 8-bzim H), 8.33 (d, 4 H, J=5.2 Hz, 5-bzim H), 9.83 (d, 4 H, J=5.2 Hz, 2-bzim H). ^{13}C NMR (DMSO-d_6): ppm 31.05 ($-CH_2\underline{C}H_2\underline{C}H_2CH_2-$), 40.09 ($-\underline{C}H_2CH_2CH_2\underline{C}H_2-$), 46.50 (Fc–$\underline{C}H_2$–), 70.47 (Cp C), 71.09 (Cp C), 85.25 (Cp C_{ipso}), 109.92 (8-bzim C), 110.50 (5-bzim C), 125.65 (6-bzim H), 126.67 (7-bzim H), 127.01 (4-bzim H) 135.78 (9-bzim H), 206.47 (2-bzim H). IR (KBr) ν (cm^{-1}) 3128, 1560, 1400, 1578, 753, 503. $C_{60}H_{60}N_8Fe_2I_4$ (1512.51): calculated C 47.65, H 4.00, N 7.41; found: C 45.71, H 3.89, N 6.85%.

[BMIM] PF_6 (185)

A stirred solution of 1-methylimidazole (11.61 g, 0.14 mols) and bromobutane (19.50 g, 0.14 mols) in a round-bottomed flask fitted with a reflux condenser was heated at 70°C for 48–72 h. The resulting viscous liquid was allowed to cool to room temperature and was then washed with ethyl acetate (3×200 ml). The solution was then placed under vacuum at 70°C overnight to remove the last of the ethyl acetate. To the thus prepared 1-butyl-3-methylimidazolium bromide (12.73 g, 0.058 mols) in water (500 ml), hexafluorophosphoric acid (11.01 g, 0.078 mols) was added with vigorous stirring and the resulting reaction mixture left to stir for a further 12 h. The

upper aqueous layer was decanted d the lower ionic liquid layer was washed with water (10×50 ml) until the washings were no longer acidic. The ionic liquid was then heated under vacuum (60°C) overnight to remove excess water (7.05 g, 43% yield). ^{1}H NMR (acetone-d_6): ppm 0.96 (t, 3 H, $-CH_2CH_2CH_2C\underline{H}_3$), 1.37 (m, 2 H, $-CH_2CH_2C\underline{H}_2CH_3$), 1.96 (m, 2 H, $-CH_2C\underline{H}_2CH_2CH_3$), 4.16 (m, 3 H, $-C\underline{H}_3$), 4.50 (t, 2 H, $-C\underline{H}_2CH_2CH_2CH_3$), 8.01 (s, 1 H, 5-im H), 8.10 (s 1 H 4-im H), (10.17 s, 1 H, 2-im H).

General experimental procedure for the Heck reaction in [BMIM]PF_6: synthesis of (191)–(195)

To a solution of palladium acetate (0.011 g, 0.05 mmol, 0.10%) and triphenylphosphine (0.026 g, 0.10 mmol, 0.20%) dissolved in anhydrous and degrgassed [BMIM] PF_6 (20 ml), 4-bromodanisole (0.990 g, 5 mmol), methyl acrylate (0.431 g, 5 mmol) and sodium acetate (0.450 g, 6.25 mmol) were added with stirring under argon. The reaction mixture was heated to 140°C for 17 h to ensure that the reaction had gone to completion. The mixture was extracted with diethyl ether (3×70 ml), the extracts were dried over $MgSO_4$, filtered and the solvent removed in vacuo to yield the crude product. After column chromatography on silica gel with DCM, the produce was obtained. Alternatively, after completion of the reaction, the ionic liquid was heated under vacuum and the product collected by distillation at 0.05 mmHg, 70–72°C.

General experimental procedure for the Heck reaction in DMF)

As above, except that anhydrous DMF (20 ml) was employed as the solvent.

1′-(Diphenylphosphino)ferrocenecarboxaldehyde [Fe(η^5-$C_5H_4PPh_2$)(η^5-C_5H_4CHO)] (201)

To a solution of ferrocenophane (4.17 g, 14.3 mmol) in diethyl ether (250 ml), a solution of phenyl lithium (14.5 ml. 1.8 M, 27.7 mmol) was added slowly at –78°C. The reaction mixture was stirred for 30 min at –78°C and for a further 30 min with the cooling bath removed. After cooling again to –78°C, DMF (2.8 ml, 16 mmol) was added dropwise and stirred for 15 min at –78°C, allowed to warm to room temperature and stirred for 24 h. Water (100 ml) was added, the organic phase separated, washed with water (3×100 ml), dried over magnesium sulphate and the solvent removed under vacuum. The residue was dissolved in small volume of ethyl acetate and the solution filtered through a plug of silica gel. On crystallization of the crude product from ethyl acetate/hexane, orange crystals were yielded (3.92 g, 69%, m.p. 148–150°C).

^{1}H NMR ($CDCl_3$): ppm 4.21 (q, 2 H, Cp^P α-CH), 4.49 (t, 2 H, Cp^P β-CH), 4.49 (t, 2 H, Cp^C β-CH), 4.69 (t, 2 H, Cp^C α-CH), 7.31–7.39 (m, 10 H, PPh_2), 9.67 (s, 1 H, CHO). ^{13}C NMR ($CDCl_3$): ppm 70.52 (Cp^C β-CH), 72.36 (d, Cp^P β-CH), 74.16 (d, Cp^P α-CH), 78.66 (d, Cp^P C_{ipso}), 79.69 (Cp^C C_{ipso}), 128.32 (d, PPh_2 C_{ipso}), 128.85 (PPh_2 *p*-CH), 134.45 (d, PPh_2 *o*-CH, 138.20 (d, PPh_2 C_{ipso}), 193.44 (–HO). ^{31}P NMR ($CDCl_3$): ppm –17.3 (s). IR (Nujol) ν(cm^{-1}) 1677 s, 1662 s; 1244 s, 1191 m, 1161 m, 1092 w, 1068 w, 1036 m, 1027 m, 998 w, 849 w, 827 m, 754 s, 747 s, 699 s, 534 w, 515 w, 507–493 m, 462 m, 458 m, 426 w. $C_{23}H_{19}FeOP$ (398.2): calculated C 69.37, H 4.82; found: C 69.44, H 5.13%.

[1′-(Diphenylphosphino)ferrocenyl]methanol [Fe(η^5-$C_5H_4PPh_2$)(η^5-$C_5H_4CH_2OH$)]

(202)

To a suspension of (**5**) (1.99 g, 5.0 mmol) in dry methanol, sodium borohydride (1.13 g, 30.0 mmol) was added portionwise over 90 min. The reaction mixture was then left to stir overnight at room temperature. Aqueous NaOH (100 ml, 1 M) was added and a yellow precipitate formed that was extracted into chloroform (2×100 ml). The organic extracts were then dried over magnesium sulphate and the solvent removed under pressure, yielding a brown oil (2.42 g).

Crystallisation could be induced by standing in cold temperatures for long periods, but it was found: that the oil produced was of sufficient purity to be used without the need for recrystallization.

^{1}H NMR ($CDCl_3$): ppm 1.86 (q, 1 H, *J*=6.0 Hz, CH_2OH), 4.06 (d, 2 H, Cp^C α-CH), 4.10 (t, 2 H, Cp^P α-CH), 4.16 (t, 2 H, Cp^C β-CH), 4.20 (s, 2H, *J*=6.0 Hz, CH_2OH), 4.37 (t, 2 H, Cp^P β-CH), 7.31–7.37 (m, 10 H, PPh_2). ^{13}C NMR ($CDCl_3$): ppm 60.42 (CH_2OH), 68.72 (Cp^C β-CH), 69.31 (Cp^C α-CH), 71.00 (Cp^P β-CH), 73.09 (Cp^P α-CH), 76.26 (Cp^P C_{ipso}), 89.06 (Cp^C C_{ipso}), 128.18 (PPh_2 *m*-CH), 128.62 (PPh_2 *p*-CH), 134.45 (PPh_2 *o*-CH), 138.63 (PPh_2 C_{ipso}). ^{31}P NMR ($CDCl_3$): ppm –16.3 (s). IR (Nujol) ν (cm^{-1}): 3328 br s; 1667 w; 1310 m, 1235 m, 1160 m, 1028 m, 997 s, 987 s, 926 m, 845 m, 807 m, 752 s, 743 s, 701 s, 698 s, 629 m, 503 s, 492 m, 458 m, 444 m. $C_{23}H_{21}FeOP$ (400.2): calculated C 69.02, H 5.29; found: C69.33, H 5.40%.

[1′-(Diphenylphosphinosulphide)ferrocenyl]methanol {Fe[η^5-$C_5H_4P(S)Ph_2$](η^5-$C_5H_4CH_2OH$)} (203)

A solution of the alcohol derivative (**6**) (3.65 g, 9.14 mmol) and sulphur (0.32 g, 10.06 mmol) in dry benzene (70 ml) were heated to reflux for 6 h. After cooling, the solvent was evaporated and a yellow/brown slurry obtained. The crude product was purified by column chromatography on alumina, using 1:1 ethyl acetate/hexane as the eluant, yielding a yellow powder (5.96 g, 65%).

^{1}H NMR ($CDCl_3$): ppm 2.04 (s, 1 H, CH_2OH), 3.98 (t, 2 H, *J*=1.6 Hz, Cp^C α-CH), 4.28 (t, 2 H, *J*=2.0 Hz, Cp^P α-CH), 4.28 (q, 2 H, *J*=2.0 Hz, fc–CH_2), 4.46 (q, 2 H, *J*=1.6 Hz, Cp^C β-CH), 4.53 (q, 2 H, *J*=2.0 Hz, Cp^P β-CH), 7.34–7.52 (m, 6 H, *o*- and *p*-H PPh_2), 7.69–7.74 (m, 4H, *m*-H PPh_2). ^{13}C NMR ($CDCl_3$): ppm 60.42 (CH_2OH), 69.67 (Cp^C β-CH), 72.53 (Cp^C α-CH), 73.80 (Cp^P β-CH), 77.15 (Cp^P α-CH), 77.47 (Cp^P C_{ipso}), 77.79 (Cp^C C_{ipso}), 128.93 (PPh_2 *m*-CH), 129.05 (PPh_2 *p*-CH), 132.12 (PPh_2 *o*-CH), 132.29 (PPh_2 C_{ipso}). ^{31}P NMR ($CDCl_3$): ppm +42.52 (s). IR (KBr) ν (cm^{-1}): 3467 br s; 2364 s; 1477 w; 1434 m; 1170 m; 1103 s; 1025 m; 1000 m; 837 m; 821 m; 754 m; 716 s; 696 s; 653 s; 543 m; 502 m; 492 s; 448 m.

1-Diphenylphopsphine-1′-(1-methyltosyl) ferrocene (207)

Chloroform before use was washed with 2 aliquots of water, dried over $MgSO_4$ and distilled from $CaCl_2$. The alcohol **203** (0.1691 g, 0.39 mmol), pyridine (0.062 g, 0.78 mmol) and tosyl chloride (0.112 g, 0.58 mmol) were dissolved in chloroform (7 ml) and stirred at room temperature in a closed flask. The reaction mixture was poured into water (10 ml), the organic layer separated and the aqueous layer extracted with chloroform (2×10 ml). The combined organic layers were washed with water (2×10 ml), dried over $MgSO_4$, filtered and the solvent removed to afford a brown oil. The

crude product was purified by column chromatography on alumina using 100% methanol as the eulant (brown oil, yield 0.2200 g, 130%).

^{1}H NMR: ppm 2.34 (s, 3 H, $-CH_3$), 4.11 (s, 2 H, Cp^C, α-CH), 4.44 (s, 2 H, Cp^P, α-CH), 4.72 (s, 4 H, β-Cp^C and β-Cp^P), 5.82 (s, 2 H Cp–CH_2–OTs), 7.17–7.95 (m, 14 H, Ph).

1-Diphenylphopsphine-1′-(1-methylimidazole) ferrocene {Fe[η^5-$C_5H_4P(S)Ph_2$](η^5-$C_5H_4CH_2C_3H_3N_2$)} (208)

A solution of compound **203** (0.108 g, 0.25 mmol) and CDI (0.053 g, 0.33 mmol) were heated to reflux for 4 h in dry acetonitrile (20 ml), under nitrogen with stirring. The reaction mixture was cooled and diluted with water (20 ml) and chloroform (20 ml). The organic layer was separated and the aqueous layer extracted with chloroform (2×10 ml). The combined organic layers were washed with water (4×10 ml), dried over magnesium sulphate and evaporated to afford a brown/black solid. The crude product was then purified by column chromatography using 10% methanol/diethyl ether (0.074 g, 61% yield).

^{1}H NMR ($CDCl_3$): ppm 4.00 (t, 2 H, J=2.0 Hz, Cp^C α-CH), 4.23 (t, 2 H, J=1.6 Hz, Cp^P α-CH), 4.35 (q, 2 H, J=1.6 Hz, Cp^C β-CH), 4.43 (q, 2 H, J=1.6 Hz, Cp^P β-CH), 4.65 (s, 2 H, fc–CH_2–), 6.79 (s, 1 H, 5-im H), 6.94 (s, 1 H, 4-im H), 7.20 (s, 1 H, 2-im H) 7.35–7.43 (qd, 6 H, J=2.0 Hz and J=6.8 Hz, o- and p-H PPh_2), 7.63–7.68 (qd, 4 H, J=1.6 Hz and J=4.0 Hz, o- and m-H PPh_2). ^{13}C NMR ($CDCl_3$): ppm 46.28 (CH_2Im), 70.64 (Cp^C β-CH), 72.71 (Cp^C α-CH), 72.75 (Cp^P β-CH), 74.18 (Cp^P α-CH), 73.50 (Cp^P C_{ipso}), 84.86 (Cp^C C_{ipso}), 128.73 (PPh_2 m-CH), 131.82 (PPh_2 p-CH), 131.84 (PPh_2 o-CH), 131.97 (PPh_2 C_{ipso}), 132.07 (4-im C), 134.20 (5-im C), 134.20 (2-im H). ^{31}P NMR ($CDCl_3$): ppm +42.41 (s). IR (KBr) ν (cm^{-1}): 3097 m; 3050 m; 1501 m;

1434 s; 1171 m; 1103 s; 1021 m; 903 w; 843 w; 816 m; 715 s; 700 m; 692 m; 656 s; 540 m; 492; 484 s; 466 m. $C_{26}H_{23}N_2PSFe$ (482.37): calculated C 64.74, H 4.81, N 5.81; found: 63.99, H 4.65, N 5.88%.

1-Diphenylphopsphine-1′-(1-ethyl-3-methyl)imdazolium ferrocenyl iodide {Fe[η^5-$C_5H_4P(S)Ph_2$](η^5-$C_5H_4CH_2C_3H_3N_2CH_2CH_3$)}$^+$ I (209)

Compound (9) (0.0823 g, 0.17 mmol) was suspended in excess iodoethane (2 ml) and heated to reflux for 2 h, whereupon a yellow precipitate was formed. The reaction mixture was left to stir overnight and then the precipitate was collected and washed with diethyl ether (0.1020 g, 94% yield).

^{1}H NMR ($CDCl_3$): ppm 1.52 (t, 3 H, *J*=7.2 Hz, $-CH_2\underline{CH_3}$), 4.03 (t, 2 H, *J*=2.0 Hz, Cp^C *α*-C<u>H</u>), 4.27 (q, 2 H, *J*=7.2 Hz, $-\underline{CH_2}CH_3$), 4.37 (t, 2 H, *J*=2.0 Hz, Cp^P *α*-CH), 4.64 (d, 4 H, *J*=2.0 Hz, Cp^C and Cp^P *β*-CH), 5.26 (s, 2 H, fc–CH_2–im), 7.19 (s, 1 H, 5-im H), 7.20 (s, 1 H, 4-im H), 7.37–7.47 (m, 6 H, *o*- and *p*-H PPh_2), 7.61–7.68 (m, 4 H, *m*-H PPh_2), 10.05 (s, 1 H, 2-im H). ^{13}C NMR ($CDCl_3$): ppm 15.85 ($-CH_2\underline{C}H_3$), 45.89 ($-\underline{C}H_2CH_3$), 49.50 (fc–CH_2–im), 71.54 (Cp^C *β*-CH), 72.49 (Cp^C *α*-CH), 72.75 (Cp^P *β*-CH), 73.64 (Cp^P *α*-CH), 74.50 (Cp^P C_{ipso}), 76.01 (Cp^P C_{ipso}), 80.80 (Cp^C C_{ipso}), 121.90 (PPh_2 *m*-CH), 128.80 (PPh_2 *p*-CH), 131.99 (PPh_2 *o*-CH), 133.83 (PPh_2 C_{ipso}), 134.69 (4-im C), 136.08 (5-im c), 207.48 (2-im C). ^{31}P NMR ($CDCl_3$): ppm +42.66 (s). IR (KBr): ν/cm^{-1} 3006 s; 2363m; 1558 m; 1434 m; 1169 m; 1153 m; 1102 s; 1027 m; 762 m; 752 m; 718 s; 702 s; 657 s; 542 m; 500 m; 487 m; 463 w. $C_{28}H_{28}N_2PSFeI$ (638.34): calculated C 52.69, H 4.42, N 4.39; found: C 52.15, H 4.25, N 4.41%.

1,2-Bis(diphenylphosphino)ferrocene methyl acetate (213)

Compound **212** (0.20 g, 0.47 mmol) was suspended in distilled acetic anhydride (2.5 ml) in a sealed glass container and heated at 90–110°C for 1 h. On cooling to room temperature organe crystals formed, which were collected by filtration (0.094 g, 45%).

^{1}H NMR ($CDCl_3$): ppm 1.60 (s, 3 H, $-CH_3$), 3.77 (t, 1 H, *J*=0.4 Hz, Cp H,), 4.08 (s, 5 H, Cp H), 4.32 (t, 1 H, *J*=0.8 Hz, Cp H), 4.53 (q, 1 H, *J*=0.4 Hz, Cp H), 5.14 (d, 2 H, *J*=1.2 Hz, Fc–CH_2–), 7.21–77.55 (m, 10 H, PPh_2 H). ^{13}C NMR ($CDCl_3$): ppm 20.34 ($-CH_3$), 61.20 (Fc–CH_2–), 70.03 (Cp C–H), 86.89 (Cp C_{ipso}), 128.61 (PPh_2 *m*-CH), 128.80 (PPh_2 *p*-CH), 133.34 (PPh_2 *o*-CH), 135.81 (PPh_2 C_{ipso}). ^{1}P NMR ($CDCl_3$): ppm –22.72 (s).

1-(Methylferrocenyl)-2-(diphenylphosphinesulphido) imidazole (210)

Sulphur (0.035 g, 1.09 mmol) was added to a solution of compound **211** (0.432 g, 0.99 mmol) in toluene (15 ml). The reaction mixture was heated to reflux overnight, cooled to room temperature and then the solvent removed to afford a yellow powder (0.391 g, 84% yield).

^{1}H NMR ($CDCl_3$): ppm 3.94 (d, 2 H, *J*=1.6 Hz, Cp H), 4.00 (m, 7 H, *J*=1.6 Hz, Cp H), 5.23 (d, 2 H, Fc–CH_2–), 6.93 (m, 1 H, 5-im H), 7.04 (d, 1 H, Hz, 4-im H), 7.19 (s, 1 H, 2-im H), 7.42 (m, 4 H, *o*-H PPh_2), 7.45 (m, 2 H, *p*-H PPh_2), 7.65 (m, 4 H, m-H PPh_2). ^{13}C NMR ($CDCl_3$): ppm 47.92 (CH_2), 69.09 (Cp^C β-CH), 69.21 (Cp^C α-CH), 69.79 (Cp), 81.70 (Cp^C C_{ipso}), 124.33 (4-im C), 128.88 (PPh_2 *m*-CH), 129.01 (PPh_2 *p*-CH), 130.28 (PPh_2 *o*-CH), 134.44 (PPh_2 C_{ipso}) 131.98 (5-im C), 132.36 (2-im C). ^{31}P NMR ($CDCl_3$): ppm +30.72 (s). IR (KBr) ν(cm^{-1}): 3107, 3048, 2365, 1437, 1261,

1096, 771, 653. $C_{26}H_{23}N_2PFeS$ (482.37): calculated C 64.74, H 4.81, N 5.81; found C 63.31, H 4.67, N 5.51%.

1-(Methylferrocenyl)-2-(diphenylphosphine)imidazole [Fe{η^5-$C_5H_4[C_3H_2N_2(PPh_2)]$}(η^5-C_5H_5)] (211) and 1-(methylferrocenyl)-2-(diphenylphosphineoxide)imidazole [Fe{η^5-$C_5H_4(C_3H_2N_2(P(O)Ph_2))$}($\eta^5$-$C_5H_5$)] (218)

To a solution of (1-methylferrocenyl)imidazole (4.06 g, 19.3 mmol) in diethyl ether (125 ml), at –78°C, *n*-butyl lithium (8.1 ml, 2.5 M in hexane, 20.3 mmol) was added dropwise under nitrogen, with stirring. The reaction mixture was stirred for 45 min at –78°C, then chlorodiphenylphosphine (3.6 ml, 20.3 mmol) was added dropwise. Stirring was continued for a further hour at –78°C, allowed to warm to room temperature and stirred overnight. Saturated potassium hydrogencarbonate solution was added and the reaction mixture was stirred for 2 h at room temperature. DCM (50 ml) was added, the organic layer separated and the aqueous layer extracted with (2×30 ml) of DCM. The combined organic layers washed with (2×30 ml) of water, dried over magnesium sulphate, filtered and the solvent removed under vacuum, affording an orange oil. The crude product was purified by column chromatography.

Compound **211** was collected using 1:1 petroleum ether/diethyl ether as the eluant, yielding an orange powder, 2.71 g, 31%.

^{1}H NMR ($CDCl_3$): ppm 4.01 (t, 2 H, *J*=2.0 Hz, Cp^C α-CH), 4.02 (d, 2 H, Cp^C β-CH), 4.06 (, 5 H, Cp CH), 5.03 (d, 2 H, *J*=0.8 Hz, CH_2), 6.95 (s, 1 H, *J*=1.2 Hz, 5-im H), 7.13 (s, 1 H, 4-im H), 7.26–7.28 (m, 6 H, *o*- and *p*-H PPh_2), 7.36–7.41 (m, 4 H, *m*-H PPh_2). ^{13}C NMR ($CDCl_3$): ppm 47.05 (CH_2), 66.27 (Cp^C β-CH), 68.96 (Cp^C α-CH),

69.15 (Cp), 83.28 (Cp^C C_{ipso}), 122.06 (4-C Im), 128.94 (PPh_2 *m*-CH), 128.95 (PPh_2 *p*-CH), 131.61 (PPh_2 *o*-CH), 134.20 (PPh_2 C_{ipso}) 135.62 (5-C Im), 145.20 (4-C Im). ^{31}P NMR ($CDCl_3$): ppm –31.53 (s). IR (KBr): ν(cm^{-1}): 3448 br; 3053; 2365; 1477; 1432; 1252; 1102; 1026; 809; 746; 740; 692; 515; 498; 466; 423. $C_{26}H_{23}N_2PFe$ (450.31): calculated C 69.3, H 5.15, N 6.22; found: C 69.24, C 5.18, N 6.98%.

Compound **218** was collected using 100% diethyl ether as the eluant, yielding an orange powder, 2.00 g, 22%.

^1H NMR ($CDCl_3$): ppm 4.08 (s, 2 H, Cp^C α-CH), 4.13 (s, 8 H, Cp^C β-CH), 5.41 (s, 2 H, CH_2), 7.05 (s, 1 H, 5-im H), 7.28 (s, 1 H, 4-im H), 7.50–7.57 (m, 6 H, *o*- and *p*-H PPh_2), 7.80–7.85 (m, 4 H, *m*-H PPh_2). ^{13}C NMR ($CDCl_3$): ppm 47.42 (CH_2), 69.05 (Cp^C β-CH), 69.20 (Cp^C α-CH), 69.61 (Cp CH), 82.73 (Cp^C C_{ipso}), 123.75 (4-C Im), 128.92 (PPh_2 *m*-CH), 130.97 (PPh_2 *p*-CH), 131.14 (PPh_2 *o*-CH), 134.20 (PPh_2 C_{ipso}) 135.62 (5-C Im), 145.20 (2-C Im). ^{31}P NMR ($CDCl_3$): ppm +20.93 (s). IR (KBr): ν/cm^{-1} 3448 br; 3096; 1435; 1195; 1185; 1122; 1105; 823; 817; 794; 748; 730; 700; 692; 565; 535. 499; 481; 457; 420. $C_{26}H_{23}N_2PFeO$ (466.31): calculated C 66.97, H 4.97, N 6.00; C 66.80, H 4.98, N 6.25%.

1-(Methylferrocenyl)-2-(diphenylphosphine)benzimidazole

[Fe{η^5-C_5H_4[$C_3H_2N_2$(PPh_2)]}(η^5-C_5H_5)] (219)

To a solution of (1-methylferrocenyl)benzimidazole (0.25 g, 0.79 mmol) in diethyl ether (125 ml), at –78°C, *n*-butyl lithium (0.33 ml, 2.5 M in hexanes, 0.825 mmol) was added dropwise under nitrogen, with stirring. The reaction mixture was stirred for 45 min at –78°C, then chlorodiphenylphosphine (0.15 ml, 0.825 mmol) was added dropwise. Stirring was continued for a further hour at –78°C, allowed to warm to

room temperature and stirred overnight. Saturated potassium hydrogencarbonate solution was added and the reaction mixture was stirred for 2 h at room temperature. DCM (50 ml) was added, the organic layer separated and the aqueous layer extracted with (2×30 ml) of DCM. The combined organic layers washed with (2×30 ml) of water, dried over magnesium sulphate, filtered and the solvent removed under vacuum, affording an orange oil. The crude product was purified by column chromatography using diethyl ether/hexane (1:1) as the eluant obtaining orange/brown crystals (0.135 g, 36% yield).

^{1}H NMR ($CDCl_3$): ppm 4.04 (d, 2 H, *J*=1.6 Hz, Cp^C α-C<u>H</u>), 4.19 (d, 5 H, *J*=1.6 Hz, Cp C<u>H</u>), 4.23 (t, 2 H, *J*=1.6 Hz, Cp^C β-), 5.42 (d, 2 H, *J*=2.4 Hz, fc–C<u>H</u>$_2$–), 7.26 (m, 2 H, *J*=1.6 Hz, 6,7-im H), 7.39–7.41 (m, 7 H, *o*- and *p*-<u>H</u> PPh_2 and 8-bzim H), 7.56 (m, 4 H, *m*-<u>H</u> PPh_2), 7.85 (d, 4 H, *J*=1.6 Hz, 5-bzim H). ^{13}C NMR ($CDCl_3$): ppm 45.05 (CH_2), 68.68 (Cp^C β-CH), 69.19 (Cp^C α-CH), 69.71 (Cp CH), 83.22 (Cp^C C_{ipso}), 110.73 (6-bzim C), 121.00 (5-bzim C), 122.45 (7-bzim C), 123.37 (8-bzim C), 129.06 (PPh_2 *m*-<u>C</u>H), 129.83 (PPh_2 *p*-<u>C</u>H), 134.59 (PPh_2 *o*-<u>C</u>H), 136.14 (PPh_2 C_{ipso}), 144.86 (4-bzim C), 144.89 (9-bzim C), 153.68 (2-bzim C). ^{31}P NMR ($CDCl_3$): ppm –27.38 (s). IR (KBr) (ν cm^{-1}) 3448, 2363, 2343, 1478, 1436, 1322, 1156, 1103, 824, 806, 743, 697, 504. $C_{26}H_{26}N_2PFe$ (502.38): calculated C 71.72, H 5.42, N 5.58; found C 71.79, H 5.05, N 5.75%.

Chapter 9

Bibliography

[1] P.G. Sammes (Ed.), Comprehensive Organic Chemistry, Vol. 4, Heterocyclic compounds, Pergamon Press, Exeter, 1979, pp. 357–407.

[2] G.C. Fu, S.T. Nguyen, R.H. Grubbs, *J. Am. Chem. Soc.*, 115 (1993) 9856.

[3] S.T. Nguyen, R.H. Grubbs, *J. Am. Chem. Soc.*, 115 (1993) 9858.

[4] C.A. Tolman, *Chem. Res.*, 77 (1977) 313.

[5] H.-W. Wanzlick, E. Schikora, *Angew. Chem.*, 72 (1960) 494.

[6] H.-W. Wanzlick, *Angew. Chem.*, 74 (1962) 129.

[7] H.-W. Wanzlick, *Angew. Chem. Int. Ed. Engl.*, 1 (1962) 75.

[8] H.-W. Wanzlick, H.-I. Schönherr, *Liebigs Ann. Chem.*, 731 (1970) 176.

[9] H.-W. Wanzlick, H.-I. Schönherr, *Angew. Chem.*, 80 (1968) 154.

[10] H.-W. Wanzlick, H.-I. Schönherr, *Angew. Chem. Int. Ed. Engl.*, 7 (1968) 141.

[11] H.-I. Schönherr, H.-W. Wanzlick, *Chem. Ber.*, 103 (1970) 1037

[12] A.J. Arduengo III, M. Kline, J.C. Calabrese, F. Davidson, *J. Am. Chem. Soc.*, 113 (1991) 9704.

[13] E.A. Carter, W.A. Goddard, *J. Phys. Chem.*, 90 (1986) 998.

[14] S.S. Krishnamurthy, *Curr. Sci. India*, 60 (1991) 619.

[15] W.A. Herrmann, Ch. Köcher, *Angew. Chem. Int. Ed. Engl.*, 36 (1997) 2162.

[16] K. Öfele, W.A. Herrmann, D. Mihalios, M. Elison, E. Herdtweck, Th. Priermeier, P. Kiprof, *J. Organomet. Chem.*, 498 (1995) 1.

[17] N. Kuhn, H. Bohnen, J. Fahl, D. Bläser, R. Boese, *Chem. Ber.*, 129 (1996) 1579.

[18] N. Kuhn, H. Bohnen, G. Henkel, J. Kreutzberg, *Z. Naturforsch.*, B51 (1996) 1267.

[19] N. Kuhn, T. Kratz, D. Bläser, R. Boese, *Inorg. Chim. Acta*, 238 (1995) 179.

[20] N. Kuhn, T. Kratz, R. Boese, D. Bläser, *Chem. Ber.*, 128 (1995) 245.

[21] N. Kuhn, T. Kratz, R. Boese, D. Bläser, *J. Organomet. Chem.*, 470 (1994) C8.

[22] D. Enders, K. Breuer, J. Runsink, J.H. Teles, *Helv. Chim. Acta*, 79 (1996) 1483.

[23] D. Enders, H. Gielen, G. Raabe, J. Runsink, J.H. Teles, *Chem. Ber.*, 129 (1996) 1483.

[24] D. Enders, K. Breuer, G. Raabe, J. Runsink, J.H. Teles, J.-P. Melder, K. Ebel, S. Brode, *Angew. Chem.*, 107 (1995) 1119.

[25] D. Enders, K. Breuer, G. Raabe, J. Runsink, J.H. Teles, J.-P. Melder, K. Ebel, S. Brode, *Angew. Chem. Int. Ed. Engl.*, 34 (1995) 1021.

[26] J.H. Teles, J.-P. Melder, K. Ebel, R. Schneider, E. Gehrer, W. Harder, S. Brode, D. Enders, K. Breuer, G Raabe, *Helv. Chim. Acta*, 79 (1996) 61.

[27] R.W. Alder, P.R. Allen, M. Murray, A.G. Orpen, *Angew. Chem.*, 108 (1996) 1211.

[28] R.W. Alder, P.R. Allen, M. Murray, A.G. Orpen, *Angew. Chem. Int. Ed. Engl.*, 35 (1995) 1121.

[29] U. Kernbach, M. Ramm, P. Luger, W.P, Fehlhammer, *Angew. Chem.*, 108 (1996) 333.

[30] U. Kernbach, M. Ramm, P. Luger, W.P, Fehlhammer, *Angew. Chem. Int. Ed. Engl.*, 35 (1996) 310.

[31] X.-W. Li, J. Su, G.H. Robinson, *Chem. Comun.*, (1996) 2683.

[32] H.V.R. Dias, W.C. Jin, *Tet. Lett.*, 35 (1994) 1365.

[33] N. Fröhlich, U. Pidun, M. Stahl, G. Frenking, *Organometallics*, 16 (1997) 442.

[34] C. Heinemann, T. Müller, Y. Apeloig, H. Schwarz, *J. Am. Chem. Soc.*, 118 (1996) 2023.

[35] C. Boehme, G. Frenking, *J. Am. Chem. Soc.*, 118 (1996) 2039.

[36] D.A. Dixon, A.J. Arduengo III, *J. Phys. Chem.*, 95 (1991) 4180.

[37] W.A. Herrmann, *Angew. Chem. Int. Ed. Engl.*, 41 (2000) 1290.

[38] R.W. Alder, P.R. Allen, S.J. Williams, *Chem. Commun.*, (1995) 1276.

[39] Y.-J. Kim, A. Streitwieser, *J. Am. Chem. Soc.*, 124 (2002) 5757.

[40] M.C. Perry, K. Burgess, *Tet.: Asym.*, 14 (2003) 951.

[41] B. Bildstein, *J. Organomet. Chem.*, 617–618 (2001) 28.

[42] A.C. Hillier, G.A. Grasa, M.S. Viciu, H.M. Lee, C. Yang, S.P. Nolan, *J. Organometal. Chem.*, 653 (2002) 69.

[43] J. Schwarz, V.P.W. Böhm, M.G. Gardiner, M. Grosche, W.A. Hermann, W. Hieringer, G. Radaschl-Sieber, *Chem. Eur. J.*, 6 (2000) 1773.

[44] V.P.W. Böhm, W.A. Herrmann, *Angew. Chem. Int. Ed. Engl.*, 39 (2000) 40.

[45] F. Zaragoza Dörwald, Metal Carbenes in Organic Synthesis, Wiley–VCH, Weinheim, 1998.

[46] W.A. Herrmann, M. Elison, J. Fischer, Ch. Köcher, G.R.J. Artus, *Angew. Chem. Int. Ed. Engl.*, 34 (1995) 2371.

[47] C. Zhang, J. Huang, M.L. Trudell, S.P. Nolan, *J. Org. Chem.*, 64 (1999) 3804.

[48] J. Cheng, M.L. Trudell, *Org. Lett.*, 3 (2001) 1371.

[49] S. Lee, J.F. Hartwig, *J. Org. Chem.*, 66 (2001) 3402.

[50] D. Enders, H. Gielen, G. Raabe, J. Runsink, J.H. Teles, *Chem. Ber.*, 129 (1996) 1483.

[51] M.G. Gardiner, W.A. Herrmann, C.-P. Reisinger, M. Spiegler, *J. Organomet. Chem.*, 572 (1999) 239.

[52] V.P.W. Böhm, T. Weskamp, C.W.K. Gstöttmayr, W.A. Herrmann, *Angew. Chem. Int. Ed. Engl.*, 112 (2000) 1602.

[53] J. Huang, S.P. Nolan, *J. Am. Chem. Soc.*, 121 (1999) 9889.

[54] G.A. Grasa, S.P. Nolan, *Org. Lett.*, 3 (2000) 119.

[55] B. Cetinkaya, R. Özdemir, C. Bruneau, P.H. Dixneuf, *J. Mol. Catal. A*, 118 (1997) L1.

[56] B. Cetinkaya, R. Özdemir, P.H. Dixneuf, *J. Organomet. Chem.*, 534 (1997) 153.

[57] A. Fürstner, H. Krause, *Adv. Synth. Catal.*, 343 (2001) 343.

[58] C. Desmarets, S. Kühl, R. Schneider, Y. Fort, *Organometallics*, 21 (2002) 1554.

[59] R.F. Heck, *J. Am. Chem. Soc.*, 90 (1986) 4546.

[60] T. Mizorki, K. Mori, A. Ozaki, *Bull. Soc. Jpn.*, 44 (1971) 581.

[61] D.E. Kaufmann, M. Nouroozian, H. Henze, *Synlett*, (1996) 1091.

[62] A.C. Hillier, G.A. Grasa, M.S. Viciu, H.M. Lee, C. Y, S.P. Nolan, *J. Organomet. Chem.*, 653 (2002) 69.

[63] C. Yang, S.P. Nolan, *Synlett*, 10 (2001) 1539.

[64] A.M. Magill, D.S. McGuinness, K.J. Cavell, G.J.P. Britovsek, V.C. Gibson, A.J.P. White, D.J. Williams, A.H. White, B.W. Skelton, *J. Organomet. Chem.*, 617 (2001) 560.

[65] D.S. McGuinness, K.J. Cavell, *Organometallics*, 19 (2000) 741.

[66] T. Welton, *Chem. Rev.*, 99 (1999) 2071.

[67] S. Seddon, M.J. Earle, *Pure Appl. Chem.*, 72 (2000) 1391.

[68] P. Bonhôte, A.P. Dias, N. Papageorgiou, K. Kalyanasundaram, M. Grätzel, *Inorg. Chem.*, 35 (1996) 1168.

[69] C.L. Hussey, *Adv. Molten Salt Chem.*, 5 (1983) 185.

[70] P. Walden, *Bull. Acad. Imper. Sci. (St. Petersburg)*, (1914) 1800.

[71] F.H. Furley, T.P. Weir, *J. Electrochem. Soc.*, 98 (1951) 203.

[72] J.S. Wilkes, J.A. Levisky, R.A.Wilson, C.L. Hussey, *Inorg. Chem.*, 21 (1982) 1263.

[73] J.S. Wilkes, M.J. Zworotko, *J. Chem. Soc., Chem. Commun.*, (1992) 965.

[74] J. Fuller, R.T. Carlin, R.A. Osteryoung, *J. Electrochem. Soc.*, 144 (1997) C67.

[75] J. Dupont, P.A.Z. Suarez, R.F. De Souza, R.A. Burrow, J.P. Kinzinger, *Chem. Eur. J.*, 6(13) (2000) 2377.

[76] R.T. Mutch, J.S. Wilkes, *Electrochem. Soc. Proc.*, 98 (1998) 55.

[77] P.H. Shetty, P.J. Youngberg, B.R. Kersten, C.F. Poole, *J. Chromatogr.*, 411 (1987) 61.

[78] K.G. Furton, R. Morales, *Anal. Chem. Acta*, 246 (1991) 171.

[79] A. Stark, B.L. Maclean, R.D. Singer, *J. Chem. Soc., Dalton Trans.*, 1 (1999) 63.

[80] L. Green, I. Hemeon, R.D. Singer, *Tet. Lett.*, 41 (2000) 1343.

[81] D.A. Jaeger, C.E. Tucker, *Tet. Lett.*, 30 (1989) 1785.

[82] T. Fischer, A. Sethi, T. Welton, J. Woolf, *Tet. Lett.*, 40 (1999) 793.

[83] M.J. Earle, P.B. McCormac, K.R. Seddon, *Green Chem.*, 1 (1999) 23.

[84] J. Howarth, K. Hanlon, D. Fayne, P. McCormac, *Tet. Lett.*, 38 (1997) 3097.

[85] Y. Chauvin, B. Gilbert, I. Guilbard, *J. Chem. Soc., Chem. Commun.*, (1990) 1715.

[86] S. Einloft, F.K. Dietrich, R.F. De Souza, J. Dupont, *Polyhedron*, 15 (1996) 3257.

[87] L.C. Simon, J. Dupont, R.F. De Souza, *Appl. Catal. A: Gen.*, 175 (1998) 215.

[88] R. Ellis, P. Wasserscheid, W. Keim, *J. Chem. Soc., Chem. Commun.*, (1999) 337.

[89] L.C. Simon, J. Dupont, R.F. de Souza, *Appl.Catal. A*, 175 (1998) 215.

[90] Y. Chauvin, L. Mußman, H. Olivier, *Angew. Chem. Int. Ed. Engl.*, 34 (1995) 2698.

[91] A.L. Monteiro, F.K. Zinn, R.F. DeSouza, J. Dupont, *Tet.: Asym.*, 8 (1997) 177.

[92] D.B Zhao, M. Wu, Y. Kou Y, *Catal. Today*, 74 (2002) 157.

[93] T.S. Snowden, E.V. Anslyn, *Curr. Opin. Chem. Biol*, 3 (1999) 740.

[94] D. Schmidtchen, G. Berger, *Chem. Rev.*, 97 (1997) 1609.

[95] A. Bianchi, K. Bowman-James, E. García-España (Eds.), 'Supramolecular Chemistry of Anions', Wiley-VCH (1997).

[96] P.M. Quinton, *FASEB J.*, 4 (1990) 2709.

[97] K. Renkawek, *Pollution: Causes, Effects and Control*, RSC, London (1983).

[98] F.P. Schmidtchen, *Angew. Chem. Int.. Ed. Engl.*, 16 (1977) 751.

[99] F.P. Schmidtchen, *Chem Ber*, 113 (1980) 864.

[100] F.P. Schmidtchen, *Chem Ber*, 114 (1981) 597.

[101] F.P. Schmidtchen, G. Muller, *J. Chem . Soc., Chem. Commun.*, (1984) 1115.

[102] K. Worm, F.P. Schmidtchen, A. Schier, A. Schäfer, M. Hesse, *Angew. Chem. Int. Ed. Engl.*, 33 (1994) 327.

[103] K. Worm, F.P. Schmidtchen, *Angew. Chem. Int. Ed. Engl.*, 34 (1995) 65.

[104] R.A. Pascal, J. Spergel, D. Van Engen, *Tet. Lett.*, 27 (1986) 4099.

[105] P.D. Beer, P.A. Gale, *Angew. Chem. Int. Ed. Engl.*, 40 (2001) 486.

[106] Y. Azuma, M. Newcomb, *Organometallics*, 3 (1984) 9.

[107] A. Elaiwi, P.B. Hitchcock, K.R. Seddon, N. Srinivasan, Y. Tan, T. Welton, J.A. Zola, *J. Chem. Soc., Dalton Trans.*, (1993) 3467.

[108] K. Sato, A. Arai, T. Yamagishi, *Tet. Lett.*, 40 (1999) 5219.

[109] J. Howarth, N.A. Al-Hashimy, *Tet. Lett.*, 42 (2001) 5777.

[110] E. Alcalde, C. Alavarez-Rúa, S. García-Granda, E. García-Rodriguez, N. Mesquida, L. Pérez-García, *Chem. Commun.*, (1999) 295.

[111] Y. Yuan, G. Gao, Z.-L. Jiang, J.-S. You, Z.-Y, Zhou, D.-Q. Yuan, R.-G. Xie, *Tetrahedron*, 58 (2002) 8993.

[112] P.D. Beer, A.D. Keefe, *J. Organomet. Chem.*, 375 (1989) C40.

[113] P.D. Beer, *J. Chem. Soc., Chem. Commun.*, (1996) 689.

[114] P.D. Beer, D. Hesek, J.E. Kingston, D.K. Smith, S.E. Stokes, *Organometallics*, 14 (1995) 3288.

[115] P.D. Beer, M.G.B. Drew, D. Hesek, M. Shade, F. Szemes, *J. Chem. Soc., Chem. Commun.*, (1996) 2161.

[116] P.D. Beer, M.G.B. Drew, D. Hesek, K.C. Nam, *J. Chem. Soc., Chem. Commun.*, (1997) 107.

[117] P.D. Beer, M.G.B. Drew, D. Hesek, M. Shade, F. Szemes, *J. Chem. Soc., Chem. Commun.*, (1996) 2161.

[118] P.D. Beer, M.G.B. Drew, D. Hesek, K.C. Nam, *Organometallics*, 18 (1999) 3933.

[119] P.D. Beer, A.R. Graydon, A.O.M. Johnson, D.K. Smith, *Inorg. Chem.*, 36 (1997) 2112.

[120] P.D. Beer, Z. Chen, M.G.B. Drew, J. Kingston, M. Ogden, P. Spencer, *J. Chem. Soc., Chem. Commun.*, (1993) 1046.

[121] P.D. Beer, Z. Chen, M.G.B. Drew, A.O.M. Johnson, D.K. Smith, P. Spencer, *Inorg. Chim Acta,* 246 (1996) 143.

[122] P.D. Beer, J. Cadman, J.M. Llioris, R. Martinez-Manez, M.E. Padilla-Tosta, T. Pardo, D.K. Smith, J. Soto, *J. Chem. Soc., Dalton Trans.*, (1999) 127.

[123] C. Dusemund, K.R.A.S. Sandanayake, S. Shinkai, *J. Chem. Soc., Chem. Commun.*, (1995) 333.

[124] A. Ori, S. Shinkai, *J. Chem. Soc., Chem. Commun.*, (1995) 1771.

[125] J.L. Thomas, J. Howarth, K. Hanlon, D. McGuirk, *Tet. Lett.*, 41 (2000) 413.

[126] K. Hanlon, *Ph.D. Thesis*, Dublin City University, Ireland (2000).

[127] A. Benito, R Martínez-Máñez, J. Payá, J. Soto, M.J.L. Tendero, E. Sinn, *J. Organomet. Chem.*, 503 (1995) 259.

[128] L.V. Snegur, V.I. Boev, V.N. Babin, *Russ. Chem. Bull.*, 3 (1995) 537.

[129] V.V. Gumenyuk, Z.V. Zhilina, Y.S. Nekrasov, *Russ. Chem. Bull.*, 46 (1997) 168.

[130] L.V. Snegur, V.I. Boev, Y.S. Nekrasov, *J. Organomet. Chem.*, 580 (1999) 26.

[131] B. Bildstein, M. Malaun, H. Kopacka, K.-H. Ongania, K. Wurst, *J. Organomet. Chem.*, 552 (1998) 45.

[132] B. Bildstein, M. Malaun, H. Kopacka, K. Wurst, M. Mitterbock, K.-H. Ongania, G. Opromolla, P. Zanello, *Organometallics*, 18 (1999) 4325.

[133] B. Bildstein, M. Malaun, H. Kopacka, K. Wurst, K.-H. Ongania, G. Opromolla, P. Zanello, *Organometallics*, 18 (1999) 4325.

[134] E. Rijnberg, B. Richter, K.-H. Thiele, J. Boersma, N. Veldman, A.L. Spek, G. Van Loten, *Inorg. Chem.*, 37 (1998) 56.

[135] A.A. Simenel, E.A. Morozova, Y.V. Kuzmenko, L.V. Snegur, *J. Organomet. Chem.*, 665 (2003) 13.

[136] B. Bildstien, *J. Organomet. Chem.*, 617–618 (2001) 28.

[137] L. Xu, W. Chen, J. Xaio, *Organometallics*, 19 (2000) 1123.

[138] C.J. Matthews, P.J. Smith, T. Welton, A.J.P. White, D.J. Williams, *Organometallics*, 20 (2001) 3848.

[139] D. Redmore, *Chem. Rev.*, 71 (1971) 315.

[140] N.J. Curtis, R.S. Browne, *J. Org. Chem.*, 45 (1980) 403.

[141] S.S. Moore, G.M. Whitesides, *J. Org. Chem.*, 47 (1982) 1489.

[142] H. Sleblocka-Tilk, J.L. Cocho, Z. Frakman, R.S. Brown, *J. Am. Chem. Soc.*, 106 (1984) 2421.

[143] C. Klimblin, G. Parkin, *Inorg. Chem.*, 35 (1996) 6912.

[144] C. Klimbin, V.J. Murphy, G. Parkin, *J. Chem. Soc., Chem. Commun.*, (1996) 235.

[145] W.E. Lynch, D.M. Kurtz, Jr., S. Wang, R.A. Scott, *J. Am. Chem. Soc.*, 116 (1994) 11030.

[146] F.-J. Wu, D.M. Kurtz, K.S. Hagen, P.D. Nyman, P.G. Debrunner, V.A. Vanki, *Inorg. Chem.*, 29 (1990) 5174.

[147] A. Antiñolo, F. Carrillo-Hermosila, E. Diez-Barra, J. Rernandez-Baeza, A. Fernández-Lopez, A. Lara-sanchez, A. Moreno, A. Otero, A.M. Rodríguez, J. Tejeda, *J. Chem. Soc., Dalton Trans.*, (1998) 3737.

[148] D.J. Brauer, K.W. Kottsieper, C. Like, O. Stelzer, H. Waffenschmidt, P. Wasserscheid, *J. Organomet. Chem.*, 630 (2001) 177.

[149] M.A. Jalil, T. Yamada, S. Fujinami, T. Honjo, H. Nishikawa, *Polyhedron*, 20 (2001) 627.

[150] K.W. Kottsieper, O. Stelzer, P. Wasserscheid, *J. Mol. Cat. A.*, 175 (2001) 285.

[151] T. Hayashi, M. Konishi, M. Kumada, *Tet. Lett.*, 174 (1979) 321.

[152] T. Hayashi, M. Konishi, M. Kumada, *J. Organomet. Chem.*, 186 (1980) C1.

[153] W.-Y. Yeh, Y.-J. Cheng, M.Y. Chiang, *Organometallics*, 16 (1997) 918.

[154] M.C. Gimeno, P.G. Jones, A. Laguna, C. Sarroca, *J. Chem. Soc., Dalton Trans.*, 9 (1995) 1473.

[155] G.Y. Zheng, D.P. Rillema, J.H. Reibenspies, *Inorg. Chem.*, 38 (1999) 794.

[156] J.-F. Mai, Y. Yamamoto, *J. Organomet. Chem.*, 560 (1998) 223.

[157] T. Naota, A. Tanna, S.-I. Murahashi, *J. Am. Chem. Soc.*, 122 (2000) 2960.

[158] J.J. Bishop, A. Davison, M.L. Katcher, D.W. Lichtenburg, R.E. Merrill, J.C. Smart, *J. Organomet. Chem.*, 27 (1971) 241.

[159] V. Rautenstrauch, K.P.M. Vanhessche, J. Genet, J. Lenoir, Patent Application (1997) WO 9718894.

[160] I.R. Butler, W.R. Cullen, T.J. Kim, *Synth. React. Inorg. Met-Org. Chem.*, 15 (1985) 109.

[161] W.R. Cullen, T.J. Kim, F.W.B. Einstein, T. Jones, *Organometallics*, 2 (1983) 714.

[162] D. Seyferth, H.P. Withers, *J. Organomet. Chem.*, (1980) C1.

[163] H. Stoeckli-Evans, A.G. Osborne, R.H. Whiteley, *J. Organomet. Chem.*, 194 (1980) 91.

[164] T. Hayashi, K. Yamamoto, M. Kumada, *Tet. Lett.*, 49–50 (1974) 4405.

[165] T. Hayashi, M. Konishi, M. Kumada, *Tet. Lett.*, (1979) 1871.

[166] M. Kawatsura, J.F. Hartwig, *J. Am. Chem. Soc.*, 122 (2000) 9546.

[167] E. Yoshikawa, K.V. Radhakrishnan, Y. Yamamoto, *J. Am. Chem. Soc.*, 122 (2000) 7280.

[168] W.-J. Xiao, G. Vasapollo, H. Alper, *J. Org. Chem.*, 65 (2000) 4138.

[169] M. Murata, T. Oyama, S. Watanabe, Y. Masuda, *J. Org. Chem.*, 65 (2000) 164.

[170] K. Ueda, Y. Sato, M. Mori, *J. Am. Chem. Soc.*, 122 (2000) 10722.

[171] M. Ueda, N. Miyaura, *J. Org. Chem.*, 65 (2000) 4450; A. Takezawa, K. Yamaguchi, T. Ohmura, Y. Yamamoto, N. Miyaura, *Synlett*, 10 (2002) 1730.

[172] M. Beller, W. Magerlein, A.F. Indolese, C. Fischer, *Synthesis*, 7 (2001) 1098–.

[173] J. McGarrity, F. Spindler, R. Fuchs, M. Eyer, *Chem. Abstr.*, 122 (1995) P81369q.

[174] T. Ireland, G. Grossheimann, C. Wieser-Jeunesse, P. Knochel, *Angew. Chem., Int. Ed.*, 38 (1999) 3212.

[175] M. Lautens, K. Fagnou, T. Rovis, *J. Am. Chem. Soc.*, 122 (2000) 5650.

[176] T. Hayashi, M, Tajika, K. Tamao, M. Kumada, *J. Am. Chem. Soc.*, 98 (1976) 3718.

[177] W.A. Herrmann, L.J. Goossen, G.R.J. Artus, C. Kocher, *Organometallics*, 16 (1997) 2472.

[178] A.J. Arduengo, R. Krafczyk, R. Schmultzler, *Tetrahedron*, 55 (1999) 14523.

[179] V.C.O. Njar, *Synthesis*, 14 (2000) 2019.

[180] C. Glidewell, B.J.L. Royles, D.M. Smith, *J. Organometal. Chem.*, 527 (1997) 259.

[181] J.R. Dimmock et al., *J. Pharm. Sci.*, 72 (1983) 887.

[182] A.A. Gridnev, I.M. Mihaltseva, *Syn. Commun.*, 24(11) (1994) 1547.

[183] J. Lindley, *Tetrahedron*, 40(9) (1984) 1433.

[184] M. Sato, S. Ebine, *Synthesis*, (1981) 472.

[185] N. Montserrat, A.W. Parkins, A.R. Tomkins, *J. Chem. Res. (S)*, (1995) 336.

[186] G.P. Newsoroff, S. Sternhell, *Aust. J. Chem.*, 21 (1986) 747.

[187] A. Spencer, *J. Organometal. Chem.*, 258 (1983) 101.

[188] P.B.D. De La Mare, *J. Chem. Soc., Perkin Trans.*, 2 (1973) 1480.

[189] H. Benhaoua, J.C. Piet, R. Danion-Bougot, L. Toupet, R. Carrie, *Bull. Soc. Chem. Fr.*, (1987) 325.

[190] J. Castells, *J. Chem. Soc., Perkin Trans.*, 1 (1979) 1.

[191] P.S. Stewart, J.W. Costerton, *Lancet, 358* (2001) 135.

[192] P.A. Suci, B.J. Tyler, *J. Microbiol. Methods*, 53 (1998) 313.

[193] B.H. Iglewski, C. Van Delden, *Emerg. Infect. Dis.*, 4 (1998) 551.

[194] S.F. Fridkin, W.R. Jarvis, *Clin. Microbiol. Rev.*, 9 (1996) 499.

[195] G.S. Baillie, L.J. Douglas, *Antimicrob. Agents Chemother.*, 42 (1998) 1900.

[196] G.S. Baillie, L.J. Douglas, *Antimicrob. Agents Chemother.*, 42 (1998) 2146.

[197] J. Chandra, P.K. Mukherjee, S.D. Leidich, F.F. Faddoul, L.L. Hoyer, L.J. Doulgas, M.A. Channoum, *J. Dent. Res.*, 80 (2001) 903.

[198] S.P. Hawser, L.J. Douglas, 62 (1994) 915.

[199] K.M. Smith, Y. Bu, H. Suga, *Chem. Biol.*, 10 (2003) 81.

[200] D. Seyferth, H.P. Withers, Jr., *Organometallics*, 1 (1982) 1275.

[201] J.K.F. Geirsson, B.O. Gudmundsson, J.F. Johannesdottir, J.T. Njardarson, V.G. Skulason, *Acta Chem. Scand.*, 49 (1995) 423.

[202] Gilbertson, Xie, Fu, *J. Org. Chem.*, 66 (2001) 7240.

[203] G. Marr, T. Hunt, *J. Chem. Soc., C*, (1969) 1070.

[204] T. Hayashi, *Bull. Chem. Soc. Jpn.*, 53 (1980) 1138.

[205] P. Braunstein, J. Pietsch, Y. Chauvin, A. DeCian, J. Fischer, *J. Organomet. Chem.*, 529 (1997) 387.

[206] P. Štěpnička, T. Baše, *Inorg. Chem. Commun.*, 4 (2001) 682.

[207] O.-Y. Kwon, J.-S. Kim, U.-H. Paek, *J. Kor. Chem.*, 435 (2001) 264.

Appendix I

Table 1. Bond lengths (Å) and angles (°) for 211.

Fe(1)–C(21)	2.011(2)	C(15)–H(15)	0.9300
Fe(1)–C(11)	2.0223(17)	C(21)–C(22)	1.401(4)
Fe(1)–C(25)	2.025(2)	C(21)–C(25)	1.407(4)
Fe(1)–C(22)	2.030(2)	C(22)–C(23)	1.386(4)
Fe(1)–C(15)	2.0333(19)	C(22)–H(22)	0.9300
Fe(1)–C(12)	2.0354(18)	C(23)–C(24)	1.373(3)
Fe(1)–C(23)	2.043(2)	C(23)–H(23)	0.9300
Fe(1)–C(24)	2.045(2)	C(24)–C(25)	1.384(4)
Fe(1)–C(14)	2.0489(18)	C(24)–H(24)	0.9300
Fe(1)–C(13)	2.0506(18)	C(25)–H(25)	0.9300
P(1)–C(1)	1.8257(18)	C(31)–C(36)	1.388(3)
P(1)–C(31)	1.8302(18)	C(31)–C(32)	1.391(3)
P(1)–C(41)	1.8364(17)	C(32)–C(33)	1.385(3)
N(1)–C(1)	1.325(2)	C(32)–H(32)	0.9300
N(1)–C(4)	1.363(3)	C(33)–C(34)	1.379(3)
N(2)–C(3)	1.364(2)	C(33)–H(33)	0.9300
N(2)–C(1)	1.370(2)	C(34)–C(35)	1.369(3)
N(2)–C(2)	1.477(2)	C(34)–H(34)	0.9300
C(2)–C(11)	1.498(2)	C(35)–C(36)	1.387(3)
C(2)–H(1A)	0.9700	C(35)–H(35)	0.9300
C(2)–H(1B)	0.9700	C(36)–H(36)	0.9300
C(3)–C(4)	1.355(3)	C(41)–C(46)	1.381(3)
C(3)–H(3)	0.9300	C(41)–C(42)	1.391(3)
C(4)–H(4)	0.9300	C(42)–C(43)	1.387(3)
C(11)–C(15)	1.422(2)	C(42)–H(42)	0.9300
C(11)–C(12)	1.429(3)	C(43)–C(44)	1.369(3)
C(12)–C(13)	1.418(3)	C(43)–H(43)	0.9300
C(12)–H(12)	0.9300	C(44)–C(45)	1.374(3)
C(13)–C(14)	1.410(3)	C(44)–H(44)	0.9300
C(13)–H(13)	0.9300	C(45)–C(46)	1.393(3)
C(14)–C(15)	1.420(3)	C(45)–H(45)	0.9300
C(14)–H(14)	0.9300	C(46)–H(46)	0.9300
		C(21)–H(21)	0.9300

C(21)–Fe(1)–C(11)	106.11(9)	C(14)–C(13)–H(13)	125.9
C(21)–Fe(1)–C(25)	40.80(13)	C(12)–C(13)–H(13)	125.9
C(11)–Fe(1)–C(25)	122.45(10)	Fe(1)–C(13)–H(13)	126.8
C(21)–Fe(1)–C(22)	40.55(13)	C(13)–C(14)–C(15)	108.22(16)
C(11)–Fe(1)–C(22)	121.89(9)	C(13)–C(14)–Fe(1)	69.95(11)
C(25)–Fe(1)–C(22)	67.98(12)	C(15)–C(14)–Fe(1)	69.05(10)
C(21)–Fe(1)–C(15)	122.60(11)	C(13)–C(14)–H(14)	125.9
C(11)–Fe(1)–C(15)	41.05(7)	C(15)–C(14)–H(14)	125.9
C(25)–Fe(1)–C(15)	108.01(10)	Fe(1)–C(14)–H(14)	126.7
C(22)–Fe(1)–C(15)	158.57(10)	C(14)–C(15)–C(11)	108.09(16)
C(21)–Fe(1)–C(12)	121.82(12)	C(14)–C(15)–Fe(1)	70.23(11)
C(11)–Fe(1)–C(12)	41.24(7)	C(11)–C(15)–Fe(1)	69.06(10)
C(25)–Fe(1)–C(12)	158.63(12)	C(14)–C(15)–H(15)	126.0
C(22)–Fe(1)–C(12)	106.85(9)	C(11)–C(15)–H(15)	126.0
C(15)–Fe(1)–C(12)	68.79(8)	Fe(1)–C(15)–H(15)	126.3
C(21)–Fe(1)–C(23)	67.14(11)	C(22)–C(21)–C(25)	107.7(2)
C(11)–Fe(1)–C(23)	158.54(9)	C(22)–C(21)–Fe(1)	70.47(14)
C(25)–Fe(1)–C(23)	66.71(10)	C(25)–C(21)–Fe(1)	70.17(14)
C(22)–Fe(1)–C(23)	39.79(10)	C(22)–C(21)–H(21)	126.1
C(15)–Fe(1)–C(23)	159.83(9)	C(25)–C(21)–H(21)	126.1
C(12)–Fe(1)–C(23)	123.45(9)	Fe(1)–C(21)–H(21)	124.8
C(21)–Fe(1)–C(24)	67.40(11)	C(23)–C(22)–C(21)	107.1(2)
C(11)–Fe(1)–C(24)	159.11(9)	C(23)–C(22)–Fe(1)	70.58(13)

C(25)–Fe(1)–C(24)	39.75(12)	C(21)–C(22)–Fe(1)	68.97(14)
C(22)–Fe(1)–C(24)	67.00(10)	C(23)–C(22)–H(22)	126.4
C(15)–Fe(1)–C(24)	124.29(9)	C(21)–C(22)–H(22)	126.4
C(12)–Fe(1)–C(24)	159.20(9)	Fe(1)–C(22)–H(22)	125.6
C(23)–Fe(1)–C(24)	39.25(9)	C(24)–C(23)–C(22)	109.2(2)
C(21)–Fe(1)–C(14)	159.52(14)	C(24)–C(23)–Fe(1)	70.48(12)
C(11)–Fe(1)–C(14)	68.81(7)	C(22)–C(23)–Fe(1)	69.63(13)
C(25)–Fe(1)–C(14)	123.98(12)	C(24)–C(23)–H(23)	125.4
C(22)–Fe(1)–C(14)	158.98(12)	C(22)–C(23)–H(23)	125.4
C(15)–Fe(1)–C(14)	40.71(7)	Fe(1)–C(23)–H(23)	126.1
C(12)–Fe(1)–C(14)	68.26(8)	C(23)–C(24)–C(25)	108.4(2)
C(23)–Fe(1)–C(14)	124.59(9)	C(23)–C(24)–Fe(1)	70.26(12)
C(24)–Fe(1)–C(14)	109.89(9)	C(25)–C(24)–Fe(1)	69.35(13)
C(21)–Fe(1)–C(13)	158.28(14)	C(23)–C(24)–H(24)	125.8
C(11)–Fe(1)–C(13)	68.85(7)	C(25)–C(24)–H(24)	125.8
C(25)–Fe(1)–C(13)	159.62(13)	Fe(1)–C(24)–H(24)	126.2
C(22)–Fe(1)–C(13)	122.88(11)	C(24)–C(25)–C(21)	107.5(2)
C(15)–Fe(1)–C(13)	68.31(8)	C(24)–C(25)–Fe(1)	70.90(13)
C(12)–Fe(1)–C(13)	40.60(7)	C(21)–C(25)–Fe(1)	69.03(14)
C(23)–Fe(1)–C(13)	109.41(9)	C(24)–C(25)–H(25)	126.3
C(24)–Fe(1)–C(13)	124.54(9)	C(21)–C(25)–H(25)	126.3
C(14)–Fe(1)–C(13)	40.23(8)	Fe(1)–C(25)–H(25)	125.4
C(1)–P(1)–C(31)	104.06(8)	C(36)–C(31)–C(32)	118.36(18)
C(1)–P(1)–C(41)	101.22(8)	C(36)–C(31)–P(1)	117.87(14)
C(31)–P(1)–C(41)	101.01(8)	C(32)–C(31)–P(1)	123.67(14)
C(1)–N(1)–C(4)	106.94(15)	C(33)–C(32)–C(31)	120.4(2)
C(3)–N(2)–C(2)	124.97(15)	C(33)–C(32)–H(32)	119.8
C(1)–N(2)–C(2)	128.01(14)	C(31)–C(32)–H(32)	119.8
N(1)–C(1)–N(2)	110.56(16)	C(34)–C(33)–C(32)	120.3(2)
N(1)–C(1)–P(1)	127.80(14)	C(34)–C(33)–H(33)	119.8
N(2)–C(1)–P(1)	121.63(12)	C(32)–C(33)–H(33)	119.8
N(2)–C(2)–C(11)	111.58(14)	C(35)–C(34)–C(33)	120.0(2)
N(2)–C(2)–H(1A)	109.3	C(35)–C(34)–H(34)	120.0
C(11)–C(2)–H(1A)	109.3	C(33)–C(34)–H(34)	120.0
N(2)–C(2)–H(1B)	109.3	C(34)–C(35)–C(36)	120.1(2)
C(11)–C(2)–H(1B)	109.3	C(34)–C(35)–H(35)	120.0
H(1A)–C(2)–H(1B)	108.0	C(36)–C(35)–H(35)	120.0
C(4)–C(3)–N(2)	106.25(16)	C(35)–C(36)–C(31)	120.90(19)
C(4)–C(3)–H(3)	126.9	C(35)–C(36)–H(36)	119.6
N(2)–C(3)–H(3)	126.9	C(31)–C(36)–H(36)	119.6
C(3)–C(4)–N(1)	110.53(17)	C(46)–C(41)–C(42)	118.08(17)
C(3)–C(4)–H(4)	124.7	C(46)–C(41)–P(1)	123.73(14)
N(1)–C(4)–H(4)	124.7	C(42)–C(41)–P(1)	117.85(13)
C(15)–C(11)–C(12)	107.46(15)	C(43)–C(42)–C(41)	121.11(19)
C(15)–C(11)–C(2)	126.66(17)	C(43)–C(42)–H(42)	119.4
C(12)–C(11)–C(2)	125.88(17)	C(41)–C(42)–H(42)	119.4
C(15)–C(11)–Fe(1)	69.89(10)	C(44)–C(43)–C(42)	119.9(2)
C(12)–C(11)–Fe(1)	69.88(10)	C(44)–C(43)–H(43)	120.1
C(2)–C(11)–Fe(1)	125.31(12)	C(42)–C(43)–H(43)	120.1
C(13)–C(12)–C(11)	107.96(16)	C(43)–C(44)–C(45)	120.0(2)
C(13)–C(12)–Fe(1)	70.27(10)	C(43)–C(44)–H(44)	120.0
C(11)–C(12)–Fe(1)	68.89(10)	C(45)–C(44)–H(44)	120.0
C(13)–C(12)–H(12)	126.0	C(44)–C(45)–C(46)	120.0(2)
C(11)–C(12)–H(12)	126.0	C(44)–C(45)–H(45)	120.0
Fe(1)–C(12)–H(12)	126.4	C(46)–C(45)–H(45)	120.0
C(14)–C(13)–C(12)	108.27(16)	C(41)–C(46)–C(45)	120.8(2)
C(14)–C(13)–Fe(1)	69.82(11)	C(41)–C(46)–H(46)	119.6
C(12)–C(13)–Fe(1)	69.13(10)	C(45)–C(46)–H(46)	119.6

Table 2. Bond lengths (Å) and angles (°) for 218.

Fe(1)–C(25)	2.019(3)	C(15)–H(15)	0.9300
Fe(1)–C(14)	2.027(3)	C(21)–C(25)	1.382(6)
Fe(1)–C(21)	2.028(3)	C(21)–C(22)	1.389(5)
Fe(1)–C(15)	2.028(3)	C(21)–H(21)	0.9300
Fe(1)–C(11)	2.028(2)	C(22)–C(23)	1.394(5)
Fe(1)–C(24)	2.030(3)	C(22)–H(22)	0.9300
Fe(1)–C(23)	2.034(3)	C(23)–C(24)	1.400(6)
Fe(1)–C(22)	2.036(3)	C(23)–H(23)	0.9300
Fe(1)–C(13)	2.042(3)	C(24)–C(25)	1.422(6)
Fe(1)–C(12)	2.051(3)	C(24)–H(24)	0.9300
P(1)–O(1)	1.4825(19)	C(25)–H(25)	0.9300
P(1)–C(31)	1.803(2)	C(31)–C(36)	1.385(3)
P(1)–C(1)	1.804(2)	C(31)–C(32)	1.388(4)
P(1)–C(41)	1.808(2)	C(32)–C(33)	1.386(4)
N(1)–C(1)	1.330(3)	C(32)–H(32)	0.9300
N(1)–C(4)	1.367(4)	C(33)–C(34)	1.383(5)
N(2)–C(1)	1.360(3)	C(33)–H(33)	0.9300
N(2)–C(3)	1.364(3)	C(34)–C(35)	1.369(5)
N(2)–C(2)	1.478(3)	C(34)–H(34)	0.9300
C(2)–C(11)	1.504(4)	C(35)–C(36)	1.387(4)
C(2)–H(2A)	0.9700	C(35)–H(35)	0.9300
C(2)–H(2B)	0.9700	C(36)–H(36)	0.9300
C(3)–C(4)	1.359(4)	C(41)–C(42)	1.385(4)
C(3)–H(3)	0.9300	C(41)–C(46)	1.390(4)
C(4)–H(4)	0.9300	C(42)–C(43)	1.394(4)
C(11)–C(15)	1.422(4)	C(42)–H(42)	0.9300
C(11)–C(12)	1.424(4)	C(43)–C(44)	1.367(4)
C(12)–C(13)	1.418(4)	C(43)–H(43)	0.9300
C(12)–H(12)	0.9300	C(44)–C(45)	1.372(5)
C(13)–C(14)	1.416(4)	C(44)–H(44)	0.9300
C(13)–H(13)	0.9300	C(45)–C(46)	1.385(4)
C(14)–C(15)	1.418(4)	C(45)–H(45)	0.9300
C(14)–H(14)	0.9300	C(46)–H(46)	0.9300

C(25)–Fe(1)–C(14)	115.96(15)	C(12)–C(13)–H(13)	126.0
C(25)–Fe(1)–C(21)	39.95(16)	Fe(1)–C(13)–H(13)	126.5
C(14)–Fe(1)–C(21)	147.39(15)	C(13)–C(14)–C(15)	108.4(3)
C(25)–Fe(1)–C(15)	108.04(15)	C(13)–C(14)–Fe(1)	70.20(17)
C(14)–Fe(1)–C(15)	40.93(12)	C(15)–C(14)–Fe(1)	69.57(17)
C(21)–Fe(1)–C(15)	115.14(13)	C(13)–C(14)–H(14)	125.8
C(25)–Fe(1)–C(11)	130.58(16)	C(15)–C(14)–H(14)	125.8
C(14)–Fe(1)–C(11)	68.82(12)	Fe(1)–C(14)–H(14)	126.0
C(21)–Fe(1)–C(11)	108.34(13)	C(14)–C(15)–C(11)	107.6(2)
C(25)–Fe(1)–C(24)	41.12(18)	C(14)–C(15)–Fe(1)	69.50(16)
C(14)–Fe(1)–C(24)	109.50(15)	C(11)–C(15)–Fe(1)	69.49(14)
C(21)–Fe(1)–C(24)	67.80(17)	C(14)–C(15)–H(15)	126.2
C(15)–Fe(1)–C(24)	131.83(17)	C(11)–C(15)–H(15)	126.2
C(11)–Fe(1)–C(24)	170.66(18)	Fe(1)–C(15)–H(15)	126.4
C(25)–Fe(1)–C(23)	68.38(17)	C(25)–C(21)–C(22)	108.4(3)
C(14)–Fe(1)–C(23)	132.41(14)	C(25)–C(21)–Fe(1)	69.7(2)
C(21)–Fe(1)–C(23)	67.75(14)	C(22)–C(21)–Fe(1)	70.34(19)
C(15)–Fe(1)–C(23)	171.15(15)	C(25)–C(21)–H(21)	125.8
C(11)–Fe(1)–C(23)	147.37(15)	C(22)–C(21)–H(21)	125.8

C(24)–Fe(1)–C(23)	40.30(17)	Fe(1)–C(21)–H(21)	125.8
C(25)–Fe(1)–C(22)	67.35(16)	C(21)–C(22)–C(23)	108.9(3)
C(14)–Fe(1)–C(22)	171.37(13)	C(21)–C(22)–Fe(1)	69.68(19)
C(21)–Fe(1)–C(22)	39.98(14)	C(23)–C(22)–Fe(1)	69.87(19)
C(15)–Fe(1)–C(22)	147.15(13)	C(21)–C(22)–H(22)	125.6
C(11)–Fe(1)–C(22)	115.73(13)	C(23)–C(22)–H(22)	125.6
C(24)–Fe(1)–C(22)	67.26(16)	Fe(1)–C(22)–H(22)	126.5
C(23)–Fe(1)–C(22)	40.05(14)	C(22)–C(23)–C(24)	107.5(3)
C(25)–Fe(1)–C(13)	148.46(17)	C(22)–C(23)–Fe(1)	70.08(18)
C(14)–Fe(1)–C(13)	40.74(13)	C(24)–C(23)–Fe(1)	69.72(19)
C(21)–Fe(1)–C(13)	170.78(16)	C(22)–C(23)–H(23)	126.3
C(15)–Fe(1)–C(13)	68.79(12)	C(24)–C(23)–H(23)	126.3
C(11)–Fe(1)–C(13)	68.67(11)	Fe(1)–C(23)–H(23)	125.5
C(24)–Fe(1)–C(13)	116.49(16)	C(23)–C(24)–C(25)	107.6(3)
C(23)–Fe(1)–C(13)	109.71(14)	C(23)–C(24)–Fe(1)	69.98(19)
C(22)–Fe(1)–C(13)	132.54(14)	C(25)–C(24)–Fe(1)	69.03(19)
C(25)–Fe(1)–C(12)	169.85(17)	C(23)–C(24)–H(24)	126.2
C(14)–Fe(1)–C(12)	68.46(12)	C(25)–C(24)–H(24)	126.2
C(21)–Fe(1)–C(12)	131.69(14)	Fe(1)–C(24)–H(24)	126.4
C(15)–Fe(1)–C(12)	68.79(12)	C(21)–C(25)–C(24)	107.6(4)
C(11)–Fe(1)–C(12)	40.88(10)	C(21)–C(25)–Fe(1)	70.35(19)
C(24)–Fe(1)–C(12)	147.93(18)	C(24)–C(25)–Fe(1)	69.8(2)
C(23)–Fe(1)–C(12)	116.15(14)	C(21)–C(25)–H(25)	126.2
C(22)–Fe(1)–C(12)	109.70(13)	C(24)–C(25)–H(25)	126.2
C(13)–Fe(1)–C(12)	40.53(12)	Fe(1)–C(25)–H(25)	125.2
O(1)–P(1)–C(31)	112.20(11)	C(36)–C(31)–C(32)	119.9(2)
O(1)–P(1)–C(1)	113.90(11)	C(36)–C(31)–P(1)	118.6(2)
C(31)–P(1)–C(1)	104.90(11)	C(32)–C(31)–P(1)	121.44(19)
O(1)–P(1)–C(41)	113.34(12)	C(33)–C(32)–C(31)	120.0(3)
C(31)–P(1)–C(41)	108.82(11)	C(33)–C(32)–H(32)	120.0
C(1)–P(1)–C(41)	102.95(11)	C(31)–C(32)–H(32)	120.0
C(1)–N(1)–C(4)	104.9(2)	C(34)–C(33)–C(32)	119.6(3)
C(1)–N(2)–C(3)	106.9(2)	C(34)–C(33)–H(33)	120.2
C(1)–N(2)–C(2)	127.3(2)	C(32)–C(33)–H(33)	120.2
C(3)–N(2)–C(2)	125.8(2)	C(35)–C(34)–C(33)	120.6(3)
N(1)–C(1)–N(2)	111.4(2)	C(35)–C(34)–H(34)	119.7
N(1)–C(1)–P(1)	123.07(18)	C(33)–C(34)–H(34)	119.7
N(2)–C(1)–P(1)	125.47(17)	C(34)–C(35)–C(36)	120.2(3)
N(2)–C(2)–C(11)	111.8(2)	C(34)–C(35)–H(35)	119.9
N(2)–C(2)–H(2A)	109.2	C(36)–C(35)–H(35)	119.9
C(11)–C(2)–H(2A)	109.2	C(31)–C(36)–C(35)	119.7(3)
N(2)–C(2)–H(2B)	109.2	C(31)–C(36)–H(36)	120.1
C(11)–C(2)–H(2B)	109.2	C(35)–C(36)–H(36)	120.1
H(2A)–C(2)–H(2B)	107.9	C(42)–C(41)–C(46)	119.5(2)
C(4)–C(3)–N(2)	106.2(2)	C(42)–C(41)–P(1)	123.9(2)
C(4)–C(3)–H(3)	126.9	C(46)–C(41)–P(1)	116.5(2)
N(2)–C(3)–H(3)	126.9	C(41)–C(42)–C(43)	119.8(3)
C(3)–C(4)–N(1)	110.6(2)	C(41)–C(42)–H(42)	120.1
C(3)–C(4)–H(4)	124.7	C(43)–C(42)–H(42)	120.1
N(1)–C(4)–H(4) 1	24.7	C(44)–C(43)–C(42)	119.9(3)
C(15)–C(11)–C(12)	108.1(2)	C(44)–C(43)–H(43)	120.0
C(15)–C(11)–C(2)	126.9(2)	C(42)–C(43)–H(43)	120.0
C(12)–C(11)–C(2)	124.9(2)	C(43)–C(44)–C(45)	120.8(3)
C(15)–C(11)–Fe(1)	69.47(15)	C(43)–C(44)–H(44)	119.6
C(12)–C(11)–Fe(1)	70.41(14)	C(45)–C(44)–H(44)	119.6
C(2)–C(11)–Fe(1)	124.14(19)	C(44)–C(45)–C(46)	119.9(3)
C(13)–C(12)–C(11)	107.8(3)	C(44)–C(45)–H(45)	120.0
C(13)–C(12)–Fe(1)	69.41(16)	C(46)–C(45)–H(45)	120.0
C(14)–C(13)–C(12)	108.1(3)	C(45)–C(46)–C(41)	120.0(3)
C(14)–C(13)–Fe(1)	69.06(17)	C(45)–C(46)–H(46)	120.0

C(12)–C(13)–Fe(1)	70.06(16)	C(41)–C(46)–H(46)	120.0
C(14)–C(13)–H(13)	126.0		

Table 3. *Atomic coordinates ($\times 10^4$) and equivalent isotropic displacement parameters ($Å^2 \times 10^3$) for* ***211****.*[a]

Atom	*x*	*y*	*z*	U_{eq}
Fe(1)	9125(1)	7798(1)	2465(1)	31(1)
P(1)	7337(1)	2780(1)	–82(1)	33(1)
N(1)	9017(1)	1514(2)	–36(1)	46(1)
N(2)	8999(1)	3847(2)	661(1)	36(1)
C(1)	8513(1)	2658(2)	187(1)	35(1)
C(2)	8696(1)	5367(3)	1010(1)	45(1)
C(3)	9844(1)	3424(3)	725(1)	44(1)
C(4)	9841(1)	1993(3)	299(1)	46(1)
C(11)	9304(1)	5860(2)	1764(1)	35(1)
C(12)	9997(1)	7044(2)	1842(1)	39(1)
C(13)	10405(1)	7162(3)	2652(1)	42(1)
C(14)	9978(1)	6064(3)	3074(1)	42(1)
C(15)	9299(1)	5252(2)	2529(1)	39(1)
C(21)	7995(2)	8867(4)	1940(2)	88(1)
C(22)	8657(2)	10066(3)	2019(2)	71(1)
C(23)	9017(2)	10234(3)	2816(2)	56(1)
C(24)	8597(2)	9176(3)	3230(1)	58(1)
C(25)	7962(2)	8317(3)	2699(2)	79(1)
C(31)	6987(1)	582(2)	–53(1)	34(1)
C(32)	7297(1)	–733(3)	–440(1)	45(1)
C(33)	6969(2)	–2350(3)	–425(1)	54(1)
C(34)	6331(2)	–2673(3)	–26(1)	56(1)
C(35)	6018(1)	–1392(3)	356(1)	55(1)
C(36)	6342(1)	232(3)	343(1)	43(1)
C(41)	7144(1)	3132(2)	–1148(1)	32(1)
C(42)	6328(1)	2766(3)	–1603(1)	46(1)
C(43)	6104(1)	3180(4)	–2396(1)	59(1)
C(44)	6688(2)	3980(3)	–2739(1)	61(1)
C(45)	7503(2)	4329(3)	–2304(1)	62(1)
C(46)	7732(1)	3897(3)	–1510(1)	50(1)

[a] U_{eq} is defined as one third of the trace of the orthogonalized.

Table 4. *Atomic coordinates ($\times 10^3$) and equivalent isotropic displacement parameters ($Å^2 \times 10^3$) for* ***218****.*[a]

Atom	*x*	*y*	*z*	U_{eq}
Fe(1)	5448(1)	6690(1)	1849(1)	38(1)
P(1)	1111(1)	3225(1)	1193(1)	31(1)
O(1)	1554(2)	2326(2)	1718(1)	45(1)
N(1)	–215(2)	6157(3)	1035(1)	43(1)
N(2)	1534(2)	6536(3)	1588(1)	36(1)
C(1)	786(2)	5417(3)	1285(1)	33(1)
C(2)	2729(2)	6195(4)	1917(1)	45(1)
C(3)	977(2)	8062(3)	1528(1)	46(1)
C(4)	–87(2)	7808(3)	1187(1)	49(1)
C(11)	3682(2)	7297(3)	1744(1)	38(1)
C(12)	4361(2)	8520(3)	2087(1)	43(1)
C(13)	5202(3)	9229(4)	1783(1)	52(1)
C(14)	5035(3)	8464(4)	1253(1)	53(1)
C(15)	4094(2)	7273(4)	1225(1)	45(1)

C(21)	5619(3)	4210(4)	2037(2)	68(1)
C(22)	6048(3)	5162(4)	2505(1)	60(1)
C(23)	6978(3)	6183(5)	2390(2)	68(1)
C(24)	7140(3)	5838(6)	1846(2)	90(2)
C(25)	6275(4)	4611(5)	1626(2)	80(1)
C(31)	2191(2)	3214(3)	727(1)	33(1)
C(32)	2025(2)	4176(4)	246(1)	47(1)
C(33)	2898(3)	4194(4)	–91(1)	60(1)
C(34)	3942(3)	3280(4)	62(2)	60(1)
C(35)	4104(3)	2319(4)	533(2)	58(1)
C(36)	3228(2)	2273(4)	868(1)	43(1)
C(41)	–299(2)	2417(3)	830(1)	35(1)
C(42)	–486(2)	1917(3)	280(1)	44(1)
C(43)	–1586(3)	1225(4)	44(1)	55(1)
C(44)	–2474(3)	1037(4)	357(2)	58(1)
C(45)	–2296(3)	1514(4)	903(2)	55(1)
C(46)	–1214(2)	2225(4)	1141(1)	45(1)

[a] U_{eq} is defined as one third of the trace of the orthogonalized.

Appendix 2